Biodegradability assessment of engineered model polymeric microparticles

Amna Khatun

Submitted in accordance with the requirements for the degree of Doctor of Philosophy

The University of Leeds

School of Chemical and Process Engineering

August, 2024

The candidate confirms that the work submitted is his/her own, except where work which has formed part of jointly-authored publications has been included. The contribution of the candidate and the other authors to this work has been explicitly indicated below. The candidate confirms that appropriate credit has been given within the thesis where reference has been made to the work of others. Details of the jointly-authored publications and contribution of each authors are outlined on the next page.

This copy has been supplied on the understanding that it is copyright material and that no quotation from the thesis may be published without proper acknowledgement.

The right of Amna Khatun to be identified as Author of this work has been asserted by her in accordance with the Copyright, Designs and Patents Act 1988.

© 2020 The University of Leeds and Amna Khatun

List of accepted conference abstracts

Poster presentation:

Khatun, A., Sarkar, A., Connell, S.D.A., Cayre, O.J. Testing the biodegradation of engineered polymeric microparticles. 1st EPSRC Centre for Doctoral Training in Molecules to Product - Annual Conference, July 2021 – Leeds, UK.

Khatun, A., Sarkar, A., Connell, S.D.A., Cayre, O.J Assessment of biodegradability of engineered polymeric microparticles using a simulated model, Food Science & Nutrition PGR conference, Dec 2021 – Leeds, UK.

Khatun, A., Sarkar, A., Connell, S.D.A., Cayre, O.J Assessment of biodegradability of engineered polymeric microparticles using a simulated model. June 2022 - 11th International Colloids Conference, Lisbon, Portugal.

Khatun, A., Sarkar, A., Connell, S.D.A., Cayre, O.J. Biodegradability assessment of engineered model polymeric microparticles. 2nd EPSRC Centre for Doctoral Training in Molecules to Product - Annual Conference, July 2022 – Leeds, UK.

Khatun, A., Sarkar, A., Connell, S.D.A., Cayre, O.J. Biodegradability assessment of engineered model polymeric microparticles. CDT REAL conference, August 2022 – Leeds, UK.

Khatun, A., Sarkar, A., Connell, S.D.A., Cayre, O.J. Biodegradability assessment of engineered model polymeric microparticles. SCI Formulation Forum 4th Annual Event, January 2023 – London, UK.

Khatun, A., Sarkar, A., Connell, S.D.A., Cayre, O.J. Biodegradability assessment of engineered model polymeric microparticles. 3rd EPSRC Centre for Doctoral Training in Molecules to Product - Annual Conference, July, 2023 – Leeds, UK.

Khatun, A., Sarkar, A., Connell, S.D.A., Cayre, O.J. Biodegradability assessment of engineered model polymeric microparticles. 4th UK Colloids Conference, July, 2023 – Liverpool, UK.

Oral presentations:

Khatun, A., Sarkar, A., Connell, S.D.A., Cayre, O.J. Testing the biodegradation of engineered polymeric microparticles. Food symposium 3 – Food microstructure, microgels and gels, Dec, 2020 – Leeds, UK.

Khatun, A., Sarkar, A., Connell, S.D.A., Cayre, O.J. Testing the biodegradation of engineered polymeric microparticles. 1st EPSRC Centre for Doctoral Training in Molecules to Product - Annual Conference, July 2021 – Leeds, UK.

Khatun, A., Sarkar, A., Connell, S.D.A., Cayre, O.J. Biodegradability assessment of engineered model polymeric microparticles. 2nd EPSRC Centre for Doctoral Training in Molecules to Product - Annual Conference, July 2022 – Leeds, UK.

Khatun, A., Sarkar, A., Connell, S.D.A., Cayre, O.J. Biodegradability assessment of engineered model polymeric microparticles. Food symposium 5 – Design of biopolymers, fragments & conjugates, March, 2023 – Leeds, UK.

Khatun, A., Sarkar, A., Connell, S.D.A., Cayre, O.J. Biodegradability assessment of engineered model polymeric microparticles. 3rd EPSRC Centre for Doctoral Training in Molecules to Product - Annual Conference, July, 2023 – Leeds, UK.

Acknowledgements

First and foremost, I would like to sincerely thank my main supervisor Dr. Olivier Cayre for all his guidance, persistent help, tolerance and consistent support as well as motivation throughout my PhD. I would also like to thank my co supervisors, Prof Anwesha Sarkar and Dr Simon Connell. Their office door was always open whenever I had a question and their support was truly crucial from the start up to the submission of my thesis. Thanks for being excellent supervisors, I truly think I was very lucky to have you in this process and I am deeply grateful to have conducted my research project with such an incredible and supportive team. Thanks for helping me follow my dreams and for boosting up my confidence.

I would also like to acknowledge Engineering and Physical Sciences Research Council (EPSRC) and Centre of Doctoral Training (CDT) in Molecules to Product for the financial support during my studies. I would like to extend my thanks to all staff in the School of Chemical and Process Engineering and School of Food Science and Nutrition, who helped me directly or indirectly throughout my research, Dr Ben Douglas, Dr Ben Lobel, Miles Ratcliff, Dr. Nataricha Phisarnchananan and Neil Rigby, many thanks for always being there to help and offer valuable technical support during my PhD.

Even though it is not possible to mention every single person in here, I would like to thank all my friends for all the meals, parties and laughs we shared together through my time as a PhD student.

I would also like to thank my family members, my brothers and sisters, nieces and nephews. Thank you so much for your support, understanding and patience when they had to bear my moments of stress and frustration and made it possible to overcome the hardship over the years. Thank you all for being an inspiration and role model through my life, thank you for all the sacrifice and selflessness care you always give me and thanks for your support and caring.

And finally, I would like to thank my mum and dad. My endless gratitude goes to my parents, who would be proud if they were here with me. May Allah grant them paradise. I know they would be here to love, support, encourage and comfort me all these years. None of this would have been possible without them. I love you both.

Thanks

Abstract

Non-biodegradable polymeric microparticles (PMP) with a diameter < 5 mm are a serious threat to the environment and human health due to their increased prevalence. Biodegradable polymers such as polylactic acid (PLA), polybutylene succinate (PBS), and polycaprolactone (PCL) have been developed in the last decade as alternatives. These polymers have shown various degrees of biodegradation as films. Only a limited number of studies have examined whether they retain their degradation properties when converted into PMP, despite the upcoming changes in regulation for formulated products containing such PMP. The biodegradation of polymers consists of three important steps: (1) Biodeterioration, which is the modification of mechanical, chemical, and physical properties of the polymer due to the growth of microorganisms on or inside the surface of the polymers. (2) Biofragmentation, which is the conversion of polymers to oligomers and monomers and (3) Assimilation, where microorganisms are supplied by necessary carbon from the fragmentation of polymers and converted to CO_2, water and biomass. This study aims to develop an in-vitro method for characterising the degradation of PMP using an enzyme, which can be applied to different systems to understand the ability of PMP to degrade in specific environments. PMPs, engineered using a solvent extraction method, were used as a model system and placed within an environment containing a microbial enzyme (lipase). PMPs have been engineered using three types of biodegradable polymers: polycaprolactone (PCL), poly (D, L-lactide-co-glycolide) – (PLGA), and poly[(R)-3-hydroxybutyric acid] – (PHB). An array of characterisation techniques (e.g. particle size distribution, transmitted light microscopy, and scanning electron microscopy imaging) is used to monitor the PMP's physical and biological degradation characteristics as a function of time when placed within an environment containing a microbial enzyme. The PMPs were degraded using two methods by: 1) monitoring the release of fatty acid during degradation using a pH stat (related to stage 2 of the biodegradation process). The hypothesis is that at this stage, we can monitor the breakdown of hydrolysable bonds and expect to observe an increase in the amount of acid released as a function of time. Although the pH stat is widely used to for digestion studies (Mat et al., 2016), it is not used/seldom used in measuring

biodegradability. 2) To study the production of carbon dioxide during degradation by measuring pressure, which is then used to calculate the amount of CO_2 removed by the base in the instrument sleeve. This will allow to understand the secondary products of the biodegradation process, representing the final stage 3 of biodegradation i.e. the conversion of PMPs into CO_2, water and biomass (Emadian et al., 2017). The hypothesis is that at this stage we expect to observe an increase of CO_2 production as a function of time. By combining both acid release and CO_2 production studies, a more complete understanding of the degradation behaviour of polymeric PMPs can be obtained.

Table of Contents

Biodegradability assessment of engineered model polymeric microparticles i

Amna Khatun i

Acknowledgements v

Abstract vi

Table of Contents viii

List of Tables xii

List of Figures xiv

List of Abbreviations xxiii

List of Symbols xxv

Chapter 1 Introduction 1

1.1 Introduction 1

1.2 Overall research aim 2

1.3 Thesis structure 3

1.4 References 6

Chapter 2 Literature review 8

2.1 Principles of biodegradation and literature review 8

2.2 Introduction to non-biodegradable microparticles currently used in formulated products 8

2.3 Polymer biodegradation process and biodegradable polymers 12

2.3.1 Are particles made with biodegradable polymers actually degradable – film vs particles? 14

2.4 Standard biodegradation test methods 23

2.4.1 Factors affecting biodegradation rate 30

2.4.2 Identified gaps 34

2.5 Methods of engineered polymeric microparticles 35

2.5.1 Solid particles 35

2.5.2 Core shell structures 40

2.6 Conclusion 45

2.7 References 46

Chapter 3 Preparation of polymeric microparticles 54

3.1 Introduction 54

3.2 Materials and Methods....55
3.2.1 Materials....55
3.2.2 Biodegradable polymers....56
3.3 Methods....60
3.4 Preparation of polymeric microparticles (PMPs)....60
3.5 Characterisation methods....61
3.5.1 Light diffraction measurements (LD)....61
3.5.2 Optical light microscope....63
3.5.3 Scanning Electron Microscopy (SEM)....64
3.6 Calculations....66
3.6.1 Total surface area of particles....66
3.7 Results and Discussion....68
3.8 Reproducibility of the solvent extraction method using Polycaprolactone....68
3.8.1 Light diffraction measurements of PCL PMPs – repeatability study....69
3.8.2 Droplet to PCL PMPs evolution as a function of time....71
3.8.3 Scanning electron microscopy of PCL PMPs....74
3.8.4 Preparation and characterisation of PMPs using alternative biodegradable polymers....75
3.9 PLGA – poly (D, L-lactide-co-glycolide) (75:25) PMPs....76
3.9.1 Light diffraction measurements of PLGA PMPs....76
3.9.2 Droplet to PLGA particle evolution as a function of time....78
3.9.3 Scanning electron microscopy of PLGA PMPs....79
3.10 Poly [(R)-3-hydroxybutyric acid] – (PHB) PMPs....80
3.10.1 Light diffraction measurement of PHB PMPs....80
3.10.2 Droplet to particle evolution as a function of time of PHB PMPs 82
3.10.3 Scanning electron microscopy of PHB PMPs....85
3.11 Calculated total surface area of PCL, PLGA and PHB microparticles 87
3.12 Preparation of PCL PMPs of varying sizes....88
3.12.1 Laser diffraction measurements of PCL PMPs....89
3.12.2 Optical light microscopy and scanning electron microscopy of PCL particles prepared at varying homogenisation speed....91
3.13 Effect of solvent extraction matrix material concentration on microparticle properties....92
3.14 Conclusion....93

3.15 References 94

Chapter 4 Biodegradation of PCL PMPs 99

4.1 Introduction 99

4.2 Materials and Methods 104

4.2.1 Materials 104

4.2.2 Methods 104

4.3 Results and Discussion 120

4.4 Release of acid upon PCL PMPs degradation by lipase 120

4.4.1 The effect of Ratio PCL: Lipase and rate of degradation – acid release 127

4.4.2 Scanning electron microscopy of degraded PCL particles at varying ratio 130

4.5 Production of CO_2 upon PCL PMPs degradation by lipase 135

4.5.1 Control tests with 30 mM HEPES buffer as control substrate 135

4.5.2 Mean production of CO_2 as a function of time and Rate % degradation as a function enzyme-substrate 138

4.5.3 Rate of pressure difference 138

4.5.4 Rate of CO_2 production % degradation as a function of time 141

4.5.5 Scanning electron microscopy of PCL particles after degradation using pressure measurement – production of CO_2 145

4.6 Conclusion 147

4.7 References 149

Chapter 5 Effect of varying surface area of PCL PMPs biodegradation Biodegradation 157

5.1 Introduction 157

5.2 Materials and Methods 161

5.2.1 Materials 161

5.2.2 Free fatty acid release 162

5.2.3 Pressure measurement 162

5.2.4 Statistical Analysis 162

5.3 Results and Discussion 163

5.3.1 Effect of varying surface area of PCL PMPs biodegradation – Acid release 163

5.3.2 Effect of varying surface area of PCL PMPs biodegradation - Production CO_2 166

5.4 Conclusion 170

5.5 References 171

Chapter 6 Biodegradation effect of PCL, PLGA and PHB PMPs.....174
6.1 Introduction 174
6.2 Materials and Methods.....179
6.2.1 Materials 179
6.2.2 Free fatty acid release 180
6.2.3 Pressure measurement.....180
6.3 Results and Discussion.....181
6.3.1 Biodegradation effect of PCL, PLGA and PHB PMPs - Acid release 182
6.3.2 Biodegradation effect of PCL, PLGA and PHB PMPs – Production CO_2 185
6.3.3 Scanning electron Microscopy 188
6.4 Conclusion 195
6.5 References 196
Chapter 7 212
7.1 General discussion 212
Future direction.....217
Appendix A 219
Supporting information of Chapter 4 219
Appendix B 223
Supporting information of Chapter 5 223
Appendix C 226
Supporting information of Chapter 6 226

List of Tables

Table 2:1 Non-biodegradable microparticles currently used in formulated products (adapted from European Chemicals Agency 2020 (European Union, 2019).....11

Table 2:2 - Biodegradation of biodegradable polymers in different environments 16

Table 2:3 - Currently active biodegradability standards and test methods for all plastic materials in soil, marine and waste water environments (Adapted from Harrison et al. (2018).....25

Table 3:1 –Particle size distribution at D_{10}, D_{50} and D_{90} of PCL PMPs (six repeat batches) 70

Table 3:2 – Mean Particle size distribution at D_{10}, D_{50} and D_{90} of PLGA particles.....76

Table 3:3 – Mean Particle size distribution at D_{10}, D_{50} and D_{90} of PCL particles.....80

Table 3:4 – calculated total surface area of PCL, PLGA and PHB PMPs based on the size distribution 87

Table 3:5 – Effect of stirring speed in the emulsification process onto the final particle size 89

Table 4:1 - Biodegradation of polycaprolactone in different environments, adapted from Bartnikowski et al. (2019).....103

Table 4:2 - Calculated PCL PMPs: lipase ratio based on mass of PCL PMPs and lipase activity 109

Table 4:3 – Calculated PCL PMPs: lipase ratio based on mass of PCL PMPs and lipase activity 116

Table 4:4 – Normality test 118

Table 4:5 - Pairwise comparisons using Conover's all-pairs test 127

Table 4:6 - Friedman rank sum test.....128

Table 4:7 – Mean and median % FFA 128

Table 4:8 - The influence of PCL PMPs - lipase ratio on the degree and rate of CO_2 production - statistical analysis using the Tukey Method and 95% Confidence 143

Table 5:1 – Effect of surface area of PCL PMPs on the rate of biodegradation - statistical analysis using the Tukey Method and 95% Confidence 164

Table 5:2 - The influence of surface area of PCL PMPs on the degree and rate of CO_2 production - statistical analysis using the Tukey Method and 95% Confidence 167

Table 6:1 - Biodegradation of Poly[(R)-3-hydroxybutyric acid] – (PHB) in different environments.....177

Table 6:2 - Biodegradation of poly (D, L-lactide-co-glycolide) – (PLGA) in different environments.....178

Table 6:3 – depolymerisation of polymer and molecular weight used to calculate FFA and CO_2 production.....181

Table 6:4 – Biodegradation effect of PCL, PLGA and PHB PMPs – rate acid release 183

Table 6:5 - Biodegradation effect of PCL, PLGA and PHB PMPs – rate CO_2 production (% day^{-1}) 186

Table C 1- calculated surface area of PCL, PLGA and PHB PMPs based on the size distribution.....226

List of Figures

Figure 1:1 Schematic framework of the thesis.....5

Figure 2:1 - Schematic illustration of general biodegradation process of polymeric microparticles (PMPs). 1) bio-deterioration - surface degradation caused by exposure to microorganisms such as bacteria, fungi and yeast resulting in loss of polymer mechanical integrity, with erosion subsequently initiating from the surface. 2) bio-fragmentation - breakdown of hydrolysable bonds in the polymer to oligomers of different chain lengths by enzymes (example given as lipase for PCL) and 3) bio-assimilation - oligomers are broken down into smaller molecules, which can be assimilated by the microbial organisms into carbon dioxide and water. 13

Figure 2:2 - Crystallinity of PLA PMPs as function of degradation time (red – pH 8 NaOH solution) and (black – seawater) showing faster crystallisation rate in pH 8 NaOH when compared to the PLA PMPs in seawaters suggesting faster cleavage of ester bonds in the polymer in an alkaline environment (Nam and Park, 2020).....33

Figure 2:3 - Steps involved in preparing polymer particles from a solvent extraction method (Katou et al., 2008): a) two phase system, aqueous phase with surfactant and suitable organic solvent to disperse the polymer b) emulsification of polymer solution in aqueous phase to produce emulsion droplets c) the solvent is extracted into the continuous phase evaporates from the aqueous phase resulting in smaller solid particles.....37

Figure 2:4 – Dispersion polymerisation in a solvent 1) initial reaction mixture (homogeneous phase) 2) oligomer precipitation and oligomer coagulation into particle nuclei. Coagulation of these oligomer chains continues until steric stabilisation of the latex particles is fully achieved when enough stabiliser chains cover the particle surface. 3) particle stabilisation by polymer adsorption and particle growth (particle size increase) 4) continuation of particle growth until all the monomer is consumed (Richez et al., 2013)...39

Figure 2:5 - Illustration of a typical spray drying process. The main sections include (1) feed emulsion entry point (2) homogeniser (3) pre-heated air (4) drying vessel (5) microcapsule collection vessels (6) cyclone separator (7) air-filter. Adapted from BUCHI (downloaded Nov 2023).....43

Figure 3:1 Chemical structure of polycaprolactone (PCL) and its resulting monomer after biodegradation (Bartnikowski et al., 2019) 57

Figure 3:2 - Chemical structure of poly (D, L-lactide-co-glycolide) (x, number of lactic acid units; y, number of glycolic acid units) and its monomers (Ferrari et al., 2013; Gentile et al., 2014) 58

Figure 3:3 – Chemical structure of poly [(R)-3-hydroxybutyric acid] and its monomers (Yu et al., 2005; Gebauer and Jendrossek, 2006; Ariffin et al., 2010) 59

Figure 3:4 - Process of preparation of polymeric microparticles (PMPs) using the solvent extraction method where the various steps consist of a) to b) emulsification of a dispersed phase (polymer in DCM) into an aqueous continuous phase containing a rheology modifier and a non-ionic surfactant via high shear homogenisation, b to c/d) complete extraction and evaporation of the dispersed phase solvent from the emulsion droplets to obtain solid polymer particles characterised with c) Scanning Electron Micrograph and d) – and with light diffraction measurements to obtain average particle size distributions. 60

Figure 3:5 - Major components of a scanning electron microscope (Amelinckx et al., 2008). 65

Figure 3:6 - Particle size distribution measured using light diffraction for six batches of PCL PMPs prepared using the same conditions to test repeatability of the particle preparation method. 69

Figure 3:7 - optical micrograph of the evolution of PCL PMPs from emulsion droplets (PCL and dichloromethane) to 1 hr, 3 hr and final PMPs (assuming complete evaporation) in aqueous suspension. Images of emulsion taken after 10 minutes after 1 min homogenisation using UltraTurrax at 8000 rpm (of batch #6). Images taken across varying positions on glass slide to ensure good representation of the sample. Polymer concentration in the disperse phase was 2.44 wt%, the ratio of dispersed phase to continuous phase was 0.25 wt%. 72

Figure 3:8 - Scanning Electron Micrograph of polycaprolactone PMPs showing spherical particles at A) 500x, B) 1000x, C) 2000 and D) 5000x magnification and a voltage at 20 kV. The sample was coated with platinum with a thickness of 20 nm using Leica EM ACE600 before analysis. 74

Figure 3:9 – Particle size distribution measured using light diffraction of PLGA PMPs stabilised with 0.05 wt% surfactant in the aqueous phase with a gelatine concentration of 0.5 wt%. The polymer concentration (0.5 g) in the disperse phase was 2.44 wt% (2.83 v%) in DCM, the ratio of dispersed phase to continuous phase was 0.25 wt%. 76

Figure 3:10 – optical micrograph of the evolution of PLGA PMPs from emulsion droplets (PLGA and dichloromethane) to final PMPs (assuming complete evaporation) in aqueous suspension. Images of emulsion taken after 10 minutes after 1 min homogenisation using UltraTurrax at 8000 rpm. Images taken across varying positions on glass slide to ensure good representation of the sample. Polymer concentration in the disperse phase was 2.44 wt%. The ratio of dispersed phase to continuous phase was 0.25 wt% 78

Figure 3:11 - Scanning Electron Micrograph of PLGA PMPs at clockwise 2000x, and 5000x magnification and a voltage at 20 kV. The sample was coated with platinum with a thickness of 20 nm using Leica EM ACE600 before analysis.....79

Figure 3:12 – Particle size distribution measured using light diffraction of PHB PMPs stabilised with 0.05 wt% surfactant in the aqueous phase with a gelatine concentration of 0.5 wt%. The polymer concentration (0.5 g) in the disperse phase was 2.44 wt% (2.83 v%) in chloroform, the ratio of dispersed phase to continuous phase was 0.25 wt%.....80

Figure 3:13 - optical micrograph of emulsion droplets (PHB and chloroform) in aqueous suspension taken after 10 minutes after 1 min homogenisation using UltraTurrax at 8000 rpm. Images taken across varying positions on glass slide to ensure good representation of the sample. Polymer concentration in the disperse phase was 2.44 wt%, the volume ratio of dispersed phase to continuous phase was 0.25 wt%. All scale bar at 10 µm. 83

Figure 3:14 - Scanning Electron Micrograph of PHB PMPs at clockwise 2000x, 5000x 2000x and 5000x magnification and a voltage at 20 kV. The sample was coated with platinum with a thickness of 20 nm using Leica EM ACE600 before analysis.....85

Figure 3:15 – Effect of stirring speed in the emulsification process onto the final particle size prepared at varying homogenisation speed (4000 rpm, black), (8000 rpm, red), and (12000 rpm, blue) during the emulsification stage 90

Figure 3:16 - Optical light microscopy (inset: particle size distribution) and corresponding scanning electron microscopy of PCL PMPs prepared at varying homogenisation speed A) 4000 rpm, B) 8000 rpm and C) 12000 rpm showing the differences in particle size ...91

Figure 4:1 - Enzymatic degradation of PCL showing the hydrolysis of the ester bond into 6-hydroxylcaproic acid under specified conditions (Funabashi et al., 2006; Bartnikowski et al., 2019).....101

Figure 4:2 - Schematic illustration of a pH-stat device, equipped with a thermostat reaction vessel, in which the substrate emulsion is formed by mechanical stirring; a pH-electrode connected to a pH-meter and a control unit for the automated delivery of NaOH by a burette. Every time the pH decreases due to the release of free fatty acids (FFAs), NaOH is delivered to keep the pH constant at a pre-determined endpoint value. 106

Figure 4:3 - Theoretical illustration of a typical titration curve of formation of product in an enzyme-catalysed reaction plotted against time showing initial velocity and enzyme saturation point (Robinson, 2015).....107

Figure 4:4 Assembly of OxiTop©-IDS heads screwed to 250mL glass bottles with nozzles on a stirrer platform.....114

Figure 4:5 – Q-Q plot, model assumption of normality of residuals ...117

Figure 4:6 - Mean change in volume of NaOH as a function of time of enzymatic reaction during PCL degradation at varying concentration of enzyme at pH 7.4 and 37 °C. The black data are blank control tests showing limited acid release. Standard deviation shows error bars for three independent readings for triplicate samples (n = 3 x 3).....121

Figure 4:7 - Titration curve showing the % degradation of PCL PMPs at pH 7.4, 37°C at varying lipase dosages with a pH stat device. The percent degradation is related to the free fatty acid released from the ester functional groups of polycaprolactone (6-hydroxylcaproic acid) as they are hydrolysed in the course of a lipase assay. Data presented are of three independent experiments. All experiment with PCL PMPs 45 kDa molecular weight (10 mg particles) – Ratio of PCL: Lipase (mg per unit) (green – 0.005), (red – 0.009), (blue – 0.014), (olive – 0.040), (purple – 0.09), (yellow – 0.166), (dark cyan – 0.282).....124

Figure 4:8 - Enzymatic degradation of PCL PMPs at 37°C and pH 7.4. Boxplot distribution of the saturation results showing percentage of free fatty acid (% FFA available based on 10 mg PCL) released at different time points (solid black circles). The mean values for each sample (1-7) are shown as a thicker solid black lines. Proportion of FFA released (% rate acid release) after 2 h of exposure to lipase enzyme at varying concentration. Data presented are mean with standard deviation of three independent experiments. Different letters indicate significant differences. Ratio PCL; Lipase (mg/U) 1= 0.005, 2=0.009, 3=0.014, 4=0.040, 5=0.093, 6=0.166, 7=0.282.....127

Figure 4:9 – Scanning electron microscopy of PCL particles after degradation using pH stat at varying PCL PMPs: Lipase ratio (mg per unit). Showing significant differences in the morphology of the particles compared to the control (no lipase), a) Blank, no lipase (after pH stat run), b) Ratio 0.005 - PCL (45K) + Lipase (10 mg: 2130 units), c) Ratio 0.009 - PCL (45K) + Lipase (10 mg: 1065 units), d) Ratio 0.040 - PCL (45K) + Lipase (10 mg: 249 units) 133

Figure 4:10 - Pressure difference (∆hPa) as a function of time. a) No significant pressure change of the blank tests, indicating minimal CO_2 gas absorbed and recorded as expected b) Mean pressure difference of all blank tests combined.....136

Figure 4:11 – Mean pressure difference as a function of time of enzymatic reaction during PCL PMP degradation at varying concentration of enzyme at pH 7.4 and 37 °C in 30 mM HEPES buffer. Standard deviation shows error bars for three independent readings for triplicate samples (n = 3). Individual PCL/ lipase experiments can be found in the Appendix, Figure A:3. Ratio of PCL: Lipase (mg per unit) - (red – 0.009), (blue – 0.014), (olive – 0.040), (teal – 0.042), (purple – 0.090), (cyan – 0.28), (wine – 0.352) 139

Figure 4:12 – Mean rate of pressure difference hPa day^{-1} as a function of time of enzymatic reaction during PCL PMPs degradation at varying concentration of enzyme at pH 7.4 and 37 °C in HEPES buffer. The slope constants k are taken from the pressure difference (CO_2 PCL PMPs) rates (hPa day^{-1}) from Figure 4:11. Standard deviation shows error bars for three independent readings for triplicate samples (n = 3). Individual PCL/ lipase experiment can be found in the Appendix, Figure A:3.....140

Figure 4:13 – Mean CO_2 production as a function of time of enzymatic reaction during PCL degradation at varying concentration of enzyme at pH 7.4 and 37 °C in 30 mM HEPES buffer. The CO_2 production (%) was calculated from the pressure difference using the gas law equation as described using equation 4:5 (Funabashi et al., 2006; Kunioka et al., 2009; Chinaglia et al., 2018; Gartiser, 2018b). Standard deviation shows error bars for three independent readings for triplicate samples (n = 3 x 3). Individual PCL/ lipase experiment can be found in the Appendix, Figure A:4. Ratio of PCL: Lipase (mg per unit) - (red – 0.009), (blue – 0.014), (olive – 0.040), (teal – 0.042), (purple – 0.090), (cyan – 0.28), (wine – 0.352) 142

Figure 4:14 - CO_2 production rate resulting from the biodegradation of PCL PMPs of varying surface areas. Experiments are conducted at pH 7.4 in 30 mM HEPES buffer and a PCL/lipase ratio of 0.040. The biodegradation percentage is the ratio between the calculated CO_2 (%) (Figure 4:13) and the total possible CO_2 i.e. the amount of CO_2 expected in case of total oxidation of the carbon present in the PCL PMPs introduced in the vessel (Ahn et al., 2008; Gómez and Michel, 2013; Chinaglia et al., 2018). Error bars are standard deviation for three independent readings for triplicate samples (n = 3). Individual PCL/ lipase experiment can be found in the Appendix, Figure A:4. 143

Figure 4:15 - Scanning electron microscopy of PCL particles after degradation using pressure measurement – production of CO_2 at 0.040 PCL: Lipase ratio (mg per unit). A) HEPES + PCL only, B) 1 hr HEPES + PCL + lipase (0.040), C) 2 hr HEPES + PCL + lipase (0.040), D) Overnight HEPES + PCL + lipase (0.040). All images with scale bar at 10 µm.....146

Figure 5:1- Enzymatic degradation of PCL PMPs at 37°C and pH 7.4 for varying initial total particle surface area. 6-hydroxycaproic acid (6-HCA) released (% rate acid release) after 2 h of exposure to lipase enzyme. Data presented are given as the mean of three independent experiments with the corresponding standard deviation. The quoted surface area of particles is calculated based on mass (10 mg PCL PMPs)/250 units lipase = 0.040 ratio (PCL PMPs:lipase mg/unit).....164

Figure 5:2 - CO_2 production rate resulting from the biodegradation of PCL PMPs of varying total surface areas (tested in each sample). Experiments are conducted at pH 7.4 in 30 mM HEPES buffer (N-(2-Hydroxyethyl)piperazine-N′-(2-ethanesulfonic acid). The reason for using a buffer system to maintain the pH at 7.4 is to avoid changes in hydrogen ion concentrations Pastorino et al. (2004); (Adhikari et al., 2016; Fang et al., 2020; Oh et al., 2022). When the enzyme attacks the surface of the PCL PMP, acid is released and therefore a pH decrease is observed which results in the denaturing of the enzyme, leading to insufficient degradation capacity and inaccurate data and a PCL/lipase ratio of 0.040. The biodegradation percentage is the ratio between the measured CO_2 and the total possible CO_2 i.e. the amount of CO_2 expected in case of total oxidation of the carbon present in the PCL PMPs introduced in the vessel. (Ahn et al., 2011; Gómez and Michel, 2013; Chinaglia et al., 2018). Error bars are standard deviation for three independent readings for triplicate samples (n = 3). 166

Figure 6:1- Effect of the polymer type on the initial rate of acid release from enzymatic degradation of PCL, PLGA and PHB PMPs at 37°C and pH 7.4 (mean ± SD, n=3 from independent experiments). The rate of acid release is calculated using over the first 2 h of exposure to lipase enzyme in a pH stat instrument. Data presented are the mean rate over the 2h with standard deviation of three independent experiments (Figure C 1 and Figure C 2). The mass of particle was kept constant (10 mg). 250 units lipase = 0.040 ratio (PMPs:lipase mg/unit). Inset: (images of PMPs before degradation), highlighting the variations in particle size and surface texture). 183

Figure 6:2 – Effect of the polymer type on the rate of production CO_2 during the first 2 days from enzymatic degradation of PCL, PLGA and PHB PMPs at 37°C and pH 7.4). The CO_2 production was calculated as described previously in equation 4:6. Data presented are the mean rate over 2 days with standard deviation of three independent experiments. The mass of particle was kept constant (25 mg). 625 units lipase = 0.040 ratio (PMPs:lipase mg/unit). Inset: (images of PMPs after degradation, highlighting the variations in particle size and surface texture). Individual experiment can be found in the Appendix, Figure C 3 (PLGA) and Figure C 4 (PHB).186

Figure 6:3 - Scanning electron microscopy of PCL PMPs after degradation using pH stat and pressure measurements at Ratio 0.040 - PCL PMP (45 kDa) + Lipase. Showing significant differences in the morphology of the particles compared to the control (no lipase), a) Blank, no lipase (after pH stat run), b) Ratio 0.040 - PCL (45 kDa) + Lipase (10 mg: 249 units) – experiment conducted in pH stat to monitor acid release, c) Ratio 0.040 - PCL (45 kDa) + Lipase (25 mg: 625 units) – experiment conducted in closed respiromter (pressure measrements) to monitor CO_2 production. All images at 10 µm scalebar. 190

Figure 6:4 - Scanning electron microscopy of PLGA PMPs after degradation using pH stat and pressure measurements at Ratio 0.040 – PLGA PMP + Lipase. Showing significant differences in the morphology of the particles compared to the control (no lipase), a) Blank, before degradation, b) Ratio 0.040 – PLGA PMP + Lipase (10 mg: 249 units) – experiment conducted in pH stat to monitor acid release, c) Ratio 0.040 – PLGA PMP + Lipase (25 mg: 625 units) – experiment conducted in closed respiromter (pressure measurements) to monitor CO_2 production 192

Figure 6:5 - Scanning electron microscopy of PHB PMPs after degradation using pH stat and pressure measurements at Ratio 0.040 – PHB PMP + Lipase. Showing significant differences in the morphology of the particles compared to the control (no lipase), a) Blank, before degradation, b) Ratio 0.040 – PHB PMP + Lipase (10 mg: 249 units) – experiment conducted in pH stat to monitor acid release, c) Ratio 0.040 – PHB PMP + Lipase (25 mg: 625 units) – experiment conducted in closed respiromter (pressure measrements) to monitor CO_2 production 194

Figure A:0:1 – Enzyme activity standard curve showing the volume of NaOH added as function of using 50µL @ 1 mg/mL lipase enzyme solution. The hydrolysis reaction takes place between the enzyme and the surface ester-bonds of tributyrin. The free fatty acids released by the lipase are titrated at a constant pH by sodium hydroxide (NaOH, 0.1N) during the course of the hydrolysis. 219

Figure A:0:2 - the initial rate of degradation – acid release as a function of time over 2 h can be determined by the gradient (rate constant *k*) for each of the lipase concentrations. The percent degradation is related to the free fatty acid released from the ester functional groups of polycaprolactone (6-hydroxylcaproic acid) as they are hydrolysed in the course of a lipase assay. Data presented are mean with standard deviation of three independent experiments All experiment with PCL PMPs 45 kDa molecular weight (10 mg particles) – Ratio of PCL: Lipase (mg per unit) (green – 0.005), (red – 0.009), (blue – 0.014), (olive – 0.040), (purple – 0.09), (yellow – 0.166), (dark cyan – 0.282). 220

Figure A:0:3 – Normalised pressure difference as a function of time of PCL particles at varying ratio of PCL: Lipase (mg per unit). The carbon dioxide produced during degradation of PMPs is absorbed by the NaOH and is neutralised i.e. removes the carbon dioxide from the atmosphere and the pressure drops (as carbon dioxide forms, the pressure will decrease because the oxygen is being removed) resulting in less pressure (negative pressure). All experiment with polycaprolactone - 45 kDa molecular weight (25 mg particles) at pH 7.4, 37°C in HEPES buffer – Ratio of PCL: Lipase (mg per unit) - (red – 0.009), (blue – 0.014), (olive – 0.040), (teal – 0.042), (purple – 0.090), (cyan – 0.28), (wine – 0.352) 221

Figure A:0:4 – CO_2 production as a function of time of PCL particles at varying ratio of PCL: Lipase (mg per unit) in triplicates. All experiment with polycaprolactone - 45 kDa molecular weight (25 mg particles) at pH 7.4, 37°C in HEPES buffer – Ratio of PCL: Lipase (mg per unit) - (red – 0.009), (blue – 0.014), (olive – 0.040), (teal – 0.042), (purple – 0.090), (dark cyan – 0.28), (wine – 0.352) 222

Figure B 1 Titration curve showing the % degradation of PCL PMPs with varying surface area at pH 7.4, 37°C at varying lipase dosages with a pH stat device. The percent degradation is related to the free fatty acid released from the ester functional groups of polycaprolactone (6-hydroxylcaproic acid) as they are hydrolysed in the course of a lipase assay. Data presented are of three independent experiments. All experiment with PCL PMPs 45 kDa molecular weight (10 mg particles) – Ratio of PCL: Lipase (mg per unit) at 0.040 (red – SA 0.0054 m^2), (blue – SA 0.099 m^2), (green – 0.0301 m^2) 223

Figure B 2 Pressure difference as a function of time of enzymatic reaction during PCL PMPs degradation at varying surface at pH 7.4 and 37 °C in HEPES buffer. All experiment with PCL PMPs 45 kDa molecular weight (25 mg particles) – Ratio of PCL: Lipase (mg per unit) at 0.040 (red – SA 0.0135 m^2), (blue – SA 0.0248 m^2), (green – 0.0753 m^2) 224

Figure B 3 CO_2 production as a function of time of enzymatic reaction during PCL PMPs degradation at varying surface area at pH 7.4 and 37 °C in HEPES buffer. The CO_2 production was calculated as described previously $\Delta p\ O2\ \times Vtot - V1V1 = nRT$ (Ahn et al., 2011; Gómez and Michel, 2013; Chinaglia et al., 2018). Three independent readings for each sample (n = 3). All experiment with PCL PMPs 45 kDa molecular weight (25 mg particles) – Ratio of PCL: Lipase (mg per unit) at 0.040 (red – SA 0.0135 m^2), (blue – SA 0.0248 m^2), (green – 0.0753 m^2) 225

Figure C 1 Titration curve showing the % degradation i.e. acid release of PLGA PMPs at pH 7.4, 37°C at PLGA:lipase ratio 0.040 with a pH stat device. The percent degradation is related to the free fatty acid released from the ester functional groups of PLGA (lactic acid) as they are hydrolysed in the course of a lipase assay. Data presented are of three independent experiments. All experiment with PLGA PMPs 66-107 kDa molecular weight (10 mg particles).....227

Figure C 2 Titration curve showing the % degradation i.e. acid release of PHB PMPs at pH 7.4, 37°C at PHB PMPs:lipase ratio 0.040 with a pH stat device. The percent degradation is related to the free fatty acid released from the ester functional groups of PHB (3-hyroxybutaric acid) as they are hydrolysed in the course of a lipase assay. Data presented are of three independent experiments. All experiment with PHB PMPs (10 mg particles) ..228

Figure C 3 CO_2 production as a function of time of enzymatic reaction during PLGA PMPs degradation at pH 7.4 and 37 °C in HEPES buffer. Three independent readings for triplicate samples (n = 3). The percent degradation is related to the conversion of organic carbon to CO_2 biomass (5 CO_2 for PLGA). Respirometer methods are normally used to record the quantitative formation of CO_2. Data presented are of three independent experiments. All experiment with PLGA PMPs (25 mg particles). 229

Figure C 4 CO_2 production as a function of time of enzymatic reaction during PHB PMPs degradation at pH 7.4 and 37 °C in HEPES buffer. Three independent readings for triplicate samples (n = 3). The percent degradation is related to the conversion of organic carbon to CO_2 (4 CO_2 for PHB). Respirometer methods are normally used to record the quantitative formation of CO_2. Data presented are of three independent experiments. All experiment with PHB PMPs (25 mg particles).....230

List of Abbreviations

ANOVA	Analysis of variance
ASTM	American Society for Testing and Materials
BOD	Biological Oxygen Demand
BS: EN	British standard: European standard
CO_2	Carbon dioxide
EU	European Union
d_{32}	De Broukere mean
d_{43}	Sauter mean
DCM	Dichloromethane
DIC	Dissolved inorganic carbon
DP	Dispersion polymerisation
DSC	Differential scanning calorimeter
CA	Cellulose acetate
CAB	Cellulose acetate butyrate
LD	Light diffraction
FFA	Free fatty acids
FTIR	Fourier Transform Infrared Spectroscopy
HSP	Hansen solubility parameters
HPLC	High-performance liquid chromatography
ISO	International Organisation for Standardisation
NPK	Fertiliser
MW	Molecular weight
PBSA	poly(butylene succinate-co-adipate)

PBS	Polybutylene sebacate
PCL	Polycaprolactone
PHA	Polyhyroxyalkanoate
PHB	Poly [(R)-3-hydroxybutyric acid]
PHBV	Poly(3-hyroxybutyrate-co-3-hydroxycalerate)
PLA	Polylactic acid
PLGA	Poly (D, L-lactide-co-glycolide)
PMP	Polymeric microparticles
PMMA	Poly methyl methacrylate
PPP	Poly(p-phenylene)
OECD	Organization for Economic Cooperation and Development
O/W	Oil-in-water
RSD	Relative standard deviation
RPM	Revolutions per minute
SE	Solvent extraction
TGA	Thermal gravimetric analysis

List of Symbols

M	Molar
mm	millimetre
µm	micrometre
n	Number of moles
α	Bunsen absorption coefficient
hPa	hectopascal
Δp	Differential pressure
R	Gas constant
T	Temperature
V	Volume
V_{tot}	Bottle volume [mL]
V_1	Sample volume [mL]

Chapter 1 Introduction

1.1 Introduction

Plastic products are an essential part of global economy, yet their waste can have serious effects on our health and environment. In the EU alone, 25 million tons of plastic waste is generated per year (European Union, 2019). The natural and artificial breakdown of plastics generate a form of microparticles (MPs) which travel up the food chain mostly via aquatic animals like fish and mussels *etc.* and have been demonstrated to accumulate in human bodies (Ragusa et al., 2021; Yang, X. et al., 2022). These can be unintentionally formed when larger pieces of plastic, specifically polymer, breakdown or they can be manufactured to specific sizes and included in consumer products for specific benefits. Polymeric microparticles (PMPs) are particulate materials that have specific performance properties and can be prepared from various polymers. Characteristics such as low density, good mechanical properties and low cost allow for successful use of PMPs in industries and everyday life but the high durability leads to persistence of the synthetic polymers in the marine environment where they cause harm to a great variety of organisms (Andrady, 2015; Scudo et al., 2017). PMPs are all polymer particles <5 mm in diameter (Hartmann et al., 2019). For example, polyurethane, polystyrene, polyacrylics and melamine formaldehyde are considered to form PMPs generally of diameter of < 5 mm (Li et al., 2020; Dey et al., 2021). Due to lack of uniformity in legislation and definition of PMPs by the governing bodies, there can be confusion regarding what can be classed as PMPs (Hartmann et al., 2019). It is therefore sensible to define what PMPs are for the purpose of this work. PMPs can be described as polymeric MPs of a certain size and shape that are made of polymers and therefore we will term them under the umbrella term of as polymeric microparticles (PMPs). This definition encompasses microgel particles, microbeads and microcapsules. Most of these polymers, and consequently the generated PMPs, are polyolefin, polyethylene (PE), polyethylene terephthalate (PET), polyurathanes and acrylates. These high

molar mass polymers with a very stable carbon–carbon or C-heteroatom backbone persist in the environment for a very long time spanning several tens and hundreds of years and mostly insoluble. (Dey et al., 2021; Ragusa et al., 2021). Polymeric microparticles (PMPs) can be manufactured to specific sizes and be included in consumer products such as personal care, (Ammala, 2013), food, (Sarkar et al., 2017; Valencia et al., 2019), paints, (Borthakur et al., 2010; Nguyen et al., 2016) and pharmaceutical, (Zhang, H. et al., 2018) for various functionalities such as encapsulation and abrasives. Their small size allows them to have a high surface area to volume ratio, which may minimise the quantity of product required and increase performance, such as in sunscreen. Due to their size, they may be included in formulations with relative ease, as they may be more conveniently suspended in products and more easily applied (or spread), compared with bulk material (Hartmann et al., 2019). Manufactured microparticles have distinct morphologies that are determined by their respective manufacturing methods. These manufacturing methods provide industry and researchers with options of preparing PMPs that vary significantly in their properties and key characteristics. Depending on the synthesis process used to produce microparticles, they can range from 0.05 µm to 5000 µm, which provides properties such as size and shape (Hartmann et al., 2019). These are explained in detail in the following Chapter.

1.2 Overall research aim

Biodegradable polymers have been studied for the past two decades as an alternative solution and largely consist of ester, amide and other functional groups that are easily cleaved and broken down into biomass in the natural environment (Nair and Laurencin, 2007). Biodegradable polymers used to design microparticles have already been researched and concluded as being biodegradable. However, these might not have been tested fully for their biodegradation fate in simulated or aqueous systems after turning the polymers or monomers into polymer microparticles (PMPs) with specific functionalities used in consumer products, which could potentially identify false claims in the literature. The presence and persistence of microplastics in the environment resulting from the breakdown of consumer polyester products is considered. The focus of this study is therefore on sustainable polyester microparticles. Polyester

microparticles are chosen for analysis due to their biodegradability through ester cleavage.

Thesis objective: The overarching goal of this thesis was to develop *in vitro* biodegradation test methods for studying the degradation of polyester PMPs using an enzyme. In order to do this, PMPs were engineered from a polyester polymer typically described as biodegradable, with a method that is simple and reasonably fast and that produces particles akin to those manufactured in industry. The solvent extraction method was chosen to prepare microparticles of varying sizes as it is very simple and can be related to industry where a polydisperse system is produced for inclusion in formulated products. Polycaprolactone (PCL), poly (D, L-lactide-co-glycolide) (75:25) (PLGA) and poly [(R)-3-hydroxybutyric acid] (PHB), were the chosen polyester polymers for biodegradation studies as these are highly cited and published in many review papers as being biodegradable and they are readily available (Nair and Laurencin, 2007; Ammala, 2013; Iwata, 2015; Bagheri et al., 2017; Kjelsden et al., 2019; Albright and Chai, 2021; Samir et al., 2022) . Next, we developed an *in vitro* method for accurately analysing the degradation of model microparticles using an enzyme that can potentially be used to identify the particle characteristics that influence the degradation the most. We developed a robust method to precisely measure the degradation of model systems at every step of the process based on physio-chemical factors such as surface area/size and polymer type.

Thesis hypothesis: The hypothesis was that by creating PMPs with different surface areas and types of polymers, it would be possible to gain a deeper understanding of the biodegradation process. This would be achieved by monitoring the increase of acid and production of carbon dioxide over time using a variety of characterisation techniques to track the physical and biological degradation of the PMPs in the presence of a microbial enzyme.

1.3 Thesis structure

This thesis starts with a literature review on the principles of biodegradation and the introduction of non-biodegradable engineered polymeric microparticles currently used in formulated products. It continues with the biodegradation process and introduces biodegradable polymers as alternatives which then leads onto the regulations and standard test methods to measure biodegradability. The

thesis then introduces the manufacturing methods of engineered microparticles design and characterisation, the influence of surface area and polymer type. The outline of this thesis is highlighted in **Figure 1:1** and follows four main lines of investigation.

Chapter 2 includes a **literature review** to understand the key factors that influence biodegradation. A summary of types of microparticles, their processing, and different types of biodegradation test method approaches that have been used in recent years is discussed. In this chapter, a knowledge gap was identified on model systems and build a picture of the fundamental process of degradation to set the scene for the experimental studies.

Chapter 3 discusses the **preparation and properties of engineered polymeric microparticles** using solvent extraction method. The influence of mixing speed to obtain particles of varying particle size was studied and characterised. Further particles were prepared using alternative biodegradable polymers using the same preparation technique and characterised.

In **Chapter 4**, the **influence of enzyme-substrate ratio on the degree and rate biodegradation was evaluated of polycaprolactone microparticles (PCL PMPs).** Biodegradation was carried out in the presence of lipase enzyme. The free fatty acid release and production of CO_2 were monitored and scanning electron microscopy was used to characterise the particles to compare the images before and after degradation. In this chapter, the optimal enzyme: substrate concentration was identified.

In **Chapter 5**, the **influence of the degree of degradation of PCL PMPs with varying surface area/particle size** was examined by monitoring the free fatty acid release and production of CO_2. The formation of PCL PMPs was achieved by adjusting the mixing speed during the emulsification stage of the solvent extraction process.

Chapter 6 presents the **biodegradation of PMPs using alternative polymers** by monitoring the free fatty acid release and production of CO_2.

The final **Chapter 7** includes a **general summary** and discussion of the main results of this PhD project. Areas for future studies are also included in this chapter.

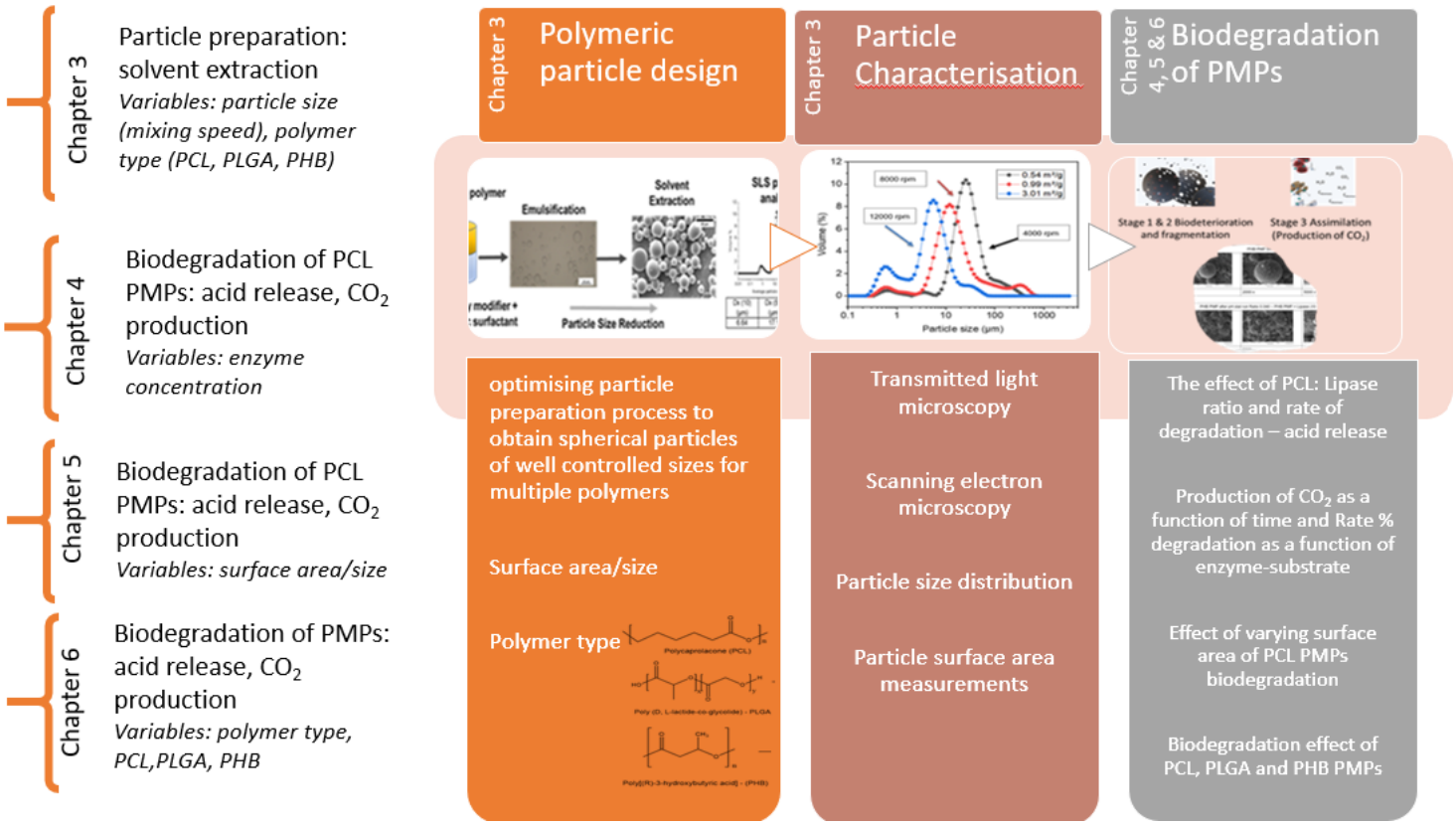


Figure 1:1 Schematic framework of the thesis

1.4 References

Albright, V.C., 3rd and Chai, Y. 2021. Knowledge Gaps in Polymer Biodegradation Research. *Environ Sci Technol.* **55**(17), pp.11476-11488.

Ammala, A. 2013. Biodegradable polymers as encapsulation materials for cosmetics and personal care markets. *Int J Cosmet Sci.* **35**(2), pp.113-124.

Andrady, A.L. 2015. Persistence of Plastic Litter in the Oceans. *Marine Anthropogenic Litter.* pp.57-72.

Bagheri, A.R., Laforsch, C., Greiner, A. and Agarwal, S. 2017. Fate of So-Called Biodegradable Polymers in Seawater and Freshwater. *Glob Chall.* **1**(4), p1700048.

Borthakur, L.J., Jana, T. and Dolui, S.K. 2010. Preparation of core–shell latex particles by emulsion co-polymerization of styrene and butyl acrylate, and evaluation of their pigment properties in emulsion paints. *Journal of Coatings Technology and Research.* **7**(6), pp.765-772.

Dey, T.K., Uddin, M.E. and Jamal, M. 2021. Detection and removal of microplastics in wastewater: evolution and impact. *Environ Sci Pollut Res Int.* **28**(14), pp.16925-16947.

European Union. 2020. *European Chemicals Agency.* [Online Accessed 19/07/2019]. Available from: https://echa.europa.eu/

Hartmann, N.B., Huffer, T., Thompson, R.C., Hassellov, M., Verschoor, A., Daugaard, A.E., Rist, S., Karlsson, T., Brennholt, N., Cole, M., Herrling, M.P., Hess, M.C., Ivleva, N.P., Lusher, A.L. and Wagner, M. 2019. Are We Speaking the Same Language? Recommendations for a Definition and Categorization Framework for Plastic Debris. *Environ Sci Technol.* **53**(3), pp.1039-1047.

Iwata, T. 2015. Biodegradable and bio-based polymers: future prospects of eco-friendly plastics. *Angew Chem Int Ed Engl.* **54**(11), pp.3210-3215.

Kjelsden, A.P., M. Lilley, C. Guznicak, E. Archer, I. 2019. A Review of Standards for Biodegradable Plastics. *Industrial Biotechnology Innovation Centre.*

Li, R.J., Liu, Y., Sheng, Y.F., Xiang, Q.Q., Zhou, Y. and Cizdziel, J.V. 2020. Effect of prothioconazole on the degradation of microplastics derived from mulching plastic film: Apparent change and interaction with heavy metals in soil. *Environmental Pollution.* **260**, article no: 113988 [no pagination].

Nair, L.S. and Laurencin, C.T. 2007. Biodegradable polymers as biomaterials. *Progress in Polymer Science.* **32**(8-9), pp.762-798.

Nguyen, T.V., Nguyen Tri, P., Nguyen, T.D., El Aidani, R., Trinh, V.T. and Decker, C. 2016. Accelerated degradation of water borne acrylic nanocomposites used in outdoor protective coatings. *Polymer Degradation and Stability.* **128**, pp.65-76.

Ragusa, A., Svelato, A., Santacroce, C., Catalano, P., Notarstefano, V., Carnevali, O., Papa, F., Rongioletti, M.C.A., Baiocco, F., Draghi, S., D'Amore, E., Rinaldo, D., Matta, M. and Giorgini, E. 2021. Plasticenta: First evidence of microplastics in human placenta. *Environment International.* **146**, p106274.

Samir, A., Ashour, F.H., Hakim, A.A.A. and Bassyouni, M. 2022. Recent advances in biodegradable polymers for sustainable applications. *npj Materials Degradation.* **6**(1).

Sarkar, A., Zhang, S., Murray, B., Russell, J.A. and Boxal, S. 2017. Modulating in vitro gastric digestion of emulsions using composite whey protein-cellulose nanocrystal interfaces. *Colloids Surf B Biointerfaces.* **158**, pp.137-146.

Valencia, G.A., Zare, E.N., Makvandi, P. and Gutiérrez, T.J. 2019. Self-Assembled Carbohydrate Polymers for Food Applications: A Review. *Comprehensive Reviews in Food Science and Food Safety.* **18**(6), pp.2009-2024.

Yang, X., Man, Y.B., Wong, M.H., Owen, R.B. and Chow, K.L. 2022. Environmental health impacts of microplastics exposure on structural organization levels in the human body. *Science of The Total Environment.* **825**, p154025.

Zhang, H., Wang, X., Wang, P., Liu, R., Hou, X., Cao, W., Zhong, R., Liu, X. and Zhang, Y. 2018. One-pot synthesis of biodegradable polydopamine-doped mesoporous silica nanocomposites (PMSNs) as pH-sensitive targeting drug nanocarriers for synergistic chemo-photothermal therapy. *RSC Advances.* **8**(65), pp.37433-37440.

Chapter 2 Literature review

2.1 Principles of biodegradation and literature review

In this Chapter, non-biodegradable microparticles that are used in formulated products are reviewed and the problems associated with their use is discussed. Then, we detail the biodegradation process chemistry and factors affecting biodegradation, giving examples of some biodegradable polymers as well as polymeric microparticles (PMPs) that have demonstrated efficient biodegradability in the aqueous systems. Next, we highlight the few current methodologies that have been used to develop biodegradable PMPs. We also highlight the complexity and disparity of the simulated environments used to understand the fate of PMPs in real aqueous systems.

2.2 Introduction to non-biodegradable microparticles currently used in formulated products

Synthetic polymers are formed by linking organic monomers with strong covalent bonds. The initial fully synthetic polymer, Bakelite, was created in the early 1900s, with mass production of polymers starting in the 1950s (Geyer. R et al., 2017). Global manufacturing of polymers has since grown, reaching 380 Mt $year^{-1}$ in 2015. Most of the polymers, and consequently the generated polymeric microparticles (PMPs), are non-biodegradable and thus, tend to remain in the environment for a very long time (Dey et al., 2021; Ragusa et al., 2021). microplastics can be classified as either primary or secondary. Primary plastics are large microplastics are still in their original form, such as cigarette butts, plastic bottlesbottle caps, as well as plastic pellets and microparticles used in various products. Secondary plastics are smaller items that have been formed by the disintegration of primary plastics (Rhodes, 2018). The Council approved the conclusions of 24 March 2017 regarding "International ocean governance: a plan for the future of our oceans" on 3 April 2017. This decision expanded the Commission's directive to incorporate a suggestion for prohibiting "micro-plastic particles in items such as personal care products and detergents, as well as recommendations for tackling other products that contribute to marine litter as

necessary" (Hann, 2018). Additionally, concerns about the potential environmental and human health impacts of polymeric microparticles found in consumer products have led to bans and restrictions in various countries, including Member States of the European Union and worldwide. In 2018, Canada implemented the Microbeads in Toiletries Regulation, prohibiting the use of polymeric microparticles in shower gels, toothpaste, and facial scrubs. France, Italy, and the US have also banned exfoliating or cleansing rinse-off cosmetic products containing these materials. In October 2017, the European Commission defined polymeric microparticles as man-made plastic items smaller than 5 mm, highlighting their particular threat to marine and inland aquatic environments (Scudo et al., 2017; Hann, 2018). The most common non-biodegradable polymers that are specifically designed as microparticles and formulated in a wide range of consumer products are polyamide, polyacrylics, such as methacrylate co-polymers and polystyrene amongst others (European Union, 2019; Kjelsden et al., 2019). PMPs are used in a variety of formulated products such as cosmetics, home and personal care products and pharmaceuticals, summarised in **Table 2:1**. Scudo et al. (2017) reported that there are significant gaps in literature, particularly regarding estimates of the quantities of microplastics used in the EU. The main uses of microplastics is personal care, paints/coating, detergents, oil and gas, agriculture and industrial abrasives. They found that personal care products have the highest confirmed tonnage of plastic microbeads (<5mm) used for exfoliation and cleansing in rinse-off products in the EU, with 714-793 tonnes per year, whereas, 220 tonnes of solid non-biodegradable polymeric particle with physical dimensions between 1µm - 5 mm is used in paints (Scudo et al., 2017). Additionally, around 540- 1120 tonnes of microplastics (<5mm) are used in leave-on products. It is important to mention that the use of microparticles in rinse-off products has decreased in recent years and is expected to continue to decline due to voluntary industry initiatives. It has been estimated that approximately 190-200 tonnes of microplastics are used in the detergent industry. The authors examined product information from manufacturers including BASF, Dow Chemicals, AkzoNobel, Polysciences, and SNF, focusing primarily on polymers for which general literature was lacking in sufficient detail (Scudo et al., 2017; van den Oever et al., 2017). The numbers mentioned above, underscore the significant demand for polymeric microparticles in formulated products, as well as the issue of waste management associated with them.

Industrial companies like Givaudan, for example, specialise in fragrance encapsulation with delivery systems for capsules used in personal/home care products. Another major player in the market is Clariant, whom produce polymer particles for use in coatings/paints.

Table 2:1 Non-biodegradable microparticles currently used in formulated products (adapted from European Chemicals Agency 2020 (European Union, 2019)

Polymer	Trade name, brief product description and manufacturer
Polyamide	Vestosint polyamide (PA12) coating and fine powders with d50 from 6 to 100 µm – Evonik (DE) – https://www.vestosint.com
	Orgasol ultrafine industrial polyamide (PA12 and or/PA6) powders from 5 to 60 µm – Arkema (FR) - https://www.orgasolpowders.com/en/
	Organsol cosmetics ultrafine multi-functional polyamide powders 5 to 20 µm (spherical shape) for anhydrous, oil and water-based systems – Arkema (FR) - cosmetics https://www.orgasolcosmetics.com
	Rilsan polyamide (PA11) fine powders – Arkema (FR) - https://www.rilsanfinepowders.com
Polyacrylics (PMMA, acrylate and methacrylate copolymers) – typically cross-linked	Acronal® A 508 is an aqueous, fine particle size (0.07 µm)dispersion of a straight acrylic copolymer. https://myindustryworld.basf.com/emea/en/products/30149979
	Altuglas BS spherical solid methacrylate beads (between 20 and 300 µm - Arkema (FR) - https://www.altuglas.com/en/resins/acrylics-beads/
	Lubrasil micro emulsions are clathrates of glyceryl acrylate and polyacrylic acid that enclose water molecules. https://www.ashland.com/industries/personal-and-home-care/skin-and-sun-care/lubrasil-microemulsions Lubrasil* microemulsions are manufactured for Ashland Inc. by Guardian Laboratories
	Caché CA cross-liked PMMA for cosmetics and toiletry applications 50 µm – Microbeads AS (NO) - http://www.micro-beads.com Lamberti corporate
Polystyrene	Spheromers CS spherical beads 6 to 40 µm – Microbeads AS (NO) - http://www.micro-beads.com (lamberti corporate)
	Dynoseeds TS spherical beads 10 to 500 µm – Microbeads AS (NO) - http://www.micro-beads.com (lamberti corporate)
	Calibre CS calibration standards in aqueous solutions 1 to 160 µm Techpolymer 6 to 12 µm – Sekisui (JP) - http://www.tech-p.com/en/
Polyurethane	Decosoft d50 of 7 to 60 µm – Microchem (CH) - http://www.microchemonline.com/en/microbeads.html
Melamine-formaldehyde	SADUREN 163 is a melamine-formaldehyde cross-linking agent for nonwoven applications.

2.3 Polymer biodegradation process and biodegradable polymers

Polymer biodegradation can be described as the process of biological breakdown of polymer chains into smaller molecules. The process of biodegradation is first initiated by the natural environment, which consists of both aerobic and anaerobic conditions, the smaller molecules generated are further broken down into monomers through the biological activity of microorganisms. Several reviews are available describing the process of biodegradation in detail (Scudo et al., 2017; Harrison et al., 2018; Kumar, G.A. et al., 2020; Qi et al., 2020; Zhao, L. et al., 2020). Most microparticles are made up of hydrophobic polymers which must be broken down into constituent parts for utilisation by microorganisms (Tokiwa et al., 2009; Agarwal, 2020; Nam and Park, 2020). Hydrolysis is the process of adding a water molecule to enable the splitting of a particular bond, which results into smaller molecules results in faster dissolution of the system. Heat, moisture, sunlight and/or enzymes can shorten and weaken polymer chains (fragmentation), resulting in shorter polymer chains (Song et al., 2009). Therefore, hydrolysis or oxidation of these high-molecular-weight polymeric components is the necessary first step in anaerobic or aerobic biodegradation. Oxidative degradation involves the breakdown of molecules through oxidation and thus only relevant to aerobic organisms. Oxidative breakdown is a significant chemical reaction that can occur in various biological and environmental systems. This chemical reaction can lead to the formation of free radicals and other reactive species that can cause damage to cells and tissues (Yang, X. et al., 2022). Through hydrolysis or oxidation or a combination thereof, the polymers can be converted from long chains to simple monomers and further into carbon dioxide (aerobically), methane gas (anaerobically), water and metabolic biomass as elaborated in **Figure 2:1**.

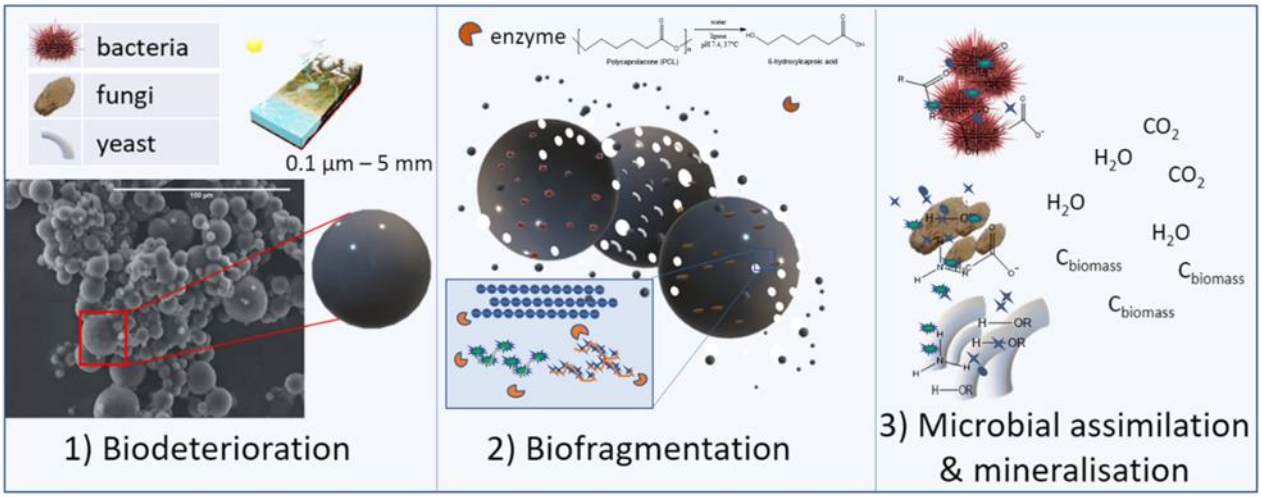


Figure 2:1 - Schematic illustration of general biodegradation process of polymeric microparticles (PMPs). 1) bio-deterioration - surface degradation caused by exposure to microorganisms such as bacteria, fungi and yeast resulting in loss of polymer mechanical integrity, with erosion subsequently initiating from the surface. 2) bio-fragmentation - breakdown of hydrolysable bonds in the polymer to oligomers of different chain lengths by enzymes (example given as lipase for PCL) and 3) bio-assimilation - oligomers are broken down into smaller molecules, which can be assimilated by the microbial organisms into carbon dioxide and water.

Figure 2:1 shows a schematic illustration of the general biodegradation process of PMPs, however, it should be noted that this biodegradation applies to all kind of polymers irrespective of form. Briefly, it includes three steps 1) bio-deterioration, 2) bio-fragmentation and 3) bio-assimilation. During the bio-deterioration step, the surfaces of the PMPs are exposed to microorganisms, such as fungi, bacteria or yeast from the natural environment. These surfaces degrade first, resulting in the PMPs losing their mechanical integrity, with erosion subsequently initiating from the surface. Polymers can be degraded by microorganisms primarily by their secreted enzymes (Adhikari et al., 2016; Siracusa, 2019; Qin et al., 2020; Rosato et al., 2020; Zhao, L. et al., 2020; Zhu and Wang, 2020) such as lipase, caseinase, gelatinase, amylase, carboxymethyl cellulase, and esterase. The fragmentation step corresponds to the breakdown of hydrolysable bonds in the polymer to result in water soluble oligomers of different chain length. This occurs when the microorganisms in the environment release enzymes such as lipase which hydrolyse the ester or amide bonds of the polymers into oligomers that are more readily degraded in the environment (Adhikari et al., 2016; Rosato et al., 2020). In the final biodegradation step, the bio-assimilation stage, oligomers are broken down into smaller molecules, which

can be assimilated by the microbial organisms into biomass. The basic driving force of biodegradation is the use of the carbon (C) bound in the polymer as a feedstock for microorganisms such as bacteria, fungi and yeast to grow resulting in the production of carbon dioxide, water and biomass (Kjelsden et al., 2019).

The three stages of biodegradation depends greatly on a range of intrinsic and extrinsic factors including the polymer type, available surface area, residuals from polymer like additives and by products, and environmental factors such as exposure (heat, light, air), and interactions with microorganisms (Adhikari et al., 2016; Kjelsden et al., 2019).

The proportion of biodegradable polymers used globally is still relatively small when compared to conventional polymers (Song et al., 2009). Current commercially available MPs are not degradable, as a result there is a new impetus to reformulate using products that contain engineered microparticles using biodegradable polymers instead (McDonough et al., 2017; Kozlowska et al., 2019; Lengyel et al., 2019). The challenge is therefore to maintain the key PMP performances in these products whilst improving the overall biodegradability. However, there is a shortage of systematic studies that report the biodegradation of polymers when they are converted into PMPs. The following section explores the factors affecting the biodegradability of PMPs.

2.3.1 Are particles made with biodegradable polymers actually degradable – film vs particles?

In the last decade, significant advances have been made in the development of biodegradable polymeric materials for a range of applications such as foods, cosmetics, detergents, and personal care products (Nair and Laurencin, 2007; Kumar, G.A. et al., 2020). The polymers used for this purpose include polylactic acid (PLA), polyhydroxy butyrate (PHB), polycaprolactone (PCL), and poly (D, L-lactide-co-glycolide) (PLGA). **Table 2:2** summarises results from the literature obtained from some of the degree of degradation studies under varying environmental conditions ranging from municipal wastewater treatment plant, compost, soil, seawater, river water, marine water and activated sludge . It is important to note that the majority of the tests are evaluated on polymeric films and not PMPs. The degradation of polymeric films are not representative of PMP degradation due to the difference in the available surface area for which is discussed in detail in **Chapter 5** which justifies the novelty of this project and

there is a need for harmonised testing protocol. The results in **Table 2:2** demonstrates the complications associated with biodegradation testing. Not all so called biodegradable polymers or polymeric microparticles are actually degradable, it very much depends on the environment in which they are placed. For instance, pure PLA film (polylactic acid) was found to completely biodegrade (100%) in 28 days (Ahn et al., 2011) and also 13% in 60 days (Arrieta et al., 2014) in compost (as inTable 2.2). The environment in which these polymers were tested must also be considered as it is not standardised, which further complicates the understanding of biodegradation studies. Some samples were tested for their biodegradability in simulated environments while others were tested in sea water with varying pH and temperature conditions, thus making it difficult to compare the biodegradation kinetics between these various polymers-based structures and the different testing methodologies (Pagga et al., 2000; Bagheri et al., 2017; Harrison et al., 2018; Wang, G.X. et al., 2020). Overall, the findings from **Table 2:2** underscore the importance of developing a harmonised testing protocol for evaluating the biodegradability of polymers.

Table 2:2 - Biodegradation of biodegradable polymers in different environments

Name of biodegradable polymer	Type of environment	Form	Conditions	Method used to quantify biodegradation	Biodegradability (%)	Length of time (days)	Ref
PLA	Compost	film - 0.5 cm square pieces	Aerobic, 58 °C	Produced CO_2	13	60	(Ahn et al., 2011)
PLA	Compost	film - 0.2 cm height and 0.065 m diameter	Aerobic, 58 °C, pH8.5, 63% humidity	Produced CO_2	84	58	(Kale et al., 2007)
PLA	Compost	film - thickness to 35 µm	Aerobic, 70% moisture, 55 °C	Produced CO_2	~70	28	(Tabasi and Ajji, 2015)
PLA	Compost	film - 3 x 4 cm	Aerobic 58 °C, 60% humidity	Weight loss	60	30	(Mihai et al., 2014)
PLA	Synthetic material containing compost	film - 25 x 25 x 3mm sheets	Aerobic, 58 °C	Weight loss	63.6	90	(Sarasa et al., 2009)
PLA	Synthetic material containing compost	film - 200 µm thickness	Aerobic, 58 °C	Weight loss	100	28	(Arrieta et al., 2014)
PLA	Soil	film - 30 x 30 x 1 mm	Aerobic, 30% moisture	Weight loss	10	98	(Wu, C.S., 2011)
PLA	Inoculum from a municipal wastewater treatment plant	film - 2 x 2 cm pieces and 20 µm thick	Aerobic, 30 °C	Weight loss	39	28	(Massardier-Nageotte et al., 2006)
PLA (powdered)	Soil	particles - 250 µm diameter	Anaerobic, 25 °C, 60% humidity	Weight loss	13.8	28	(Adhikari et al., 2016)
PLA/PPP/starch (80/5/15%)	Compost	film - 0.5 cm square pieces	Anaerobic, 58 °C	Produced CO_2	53	60	(Ahn et al., 2011)

Table 2:2 continued **-** Biodegradation of biodegradable polymers in different environments

Name of biodegradable polymer	Type of environment	Form	Conditions	Method used to quantify biodegradation	Biodegradability (%)	Length of time (days)	Ref
PLA/NPK (63.5/37.5%)	Soil	film - 150 x 150 x 1mm	Anaerobic, 30 °C, 80% humidity	Weight loss	37.4	56	(Harmaen et al., 2014)
PLA/NPK fertiliser/EFB (25/37.5/37.5%)	Soil	film - 150 x 150 x 1mm	Anaerobic, 30 °C, 80% humidity	Weight loss	43	56	(Harmaen et al., 2014)
PLA/Soft wood (70/30%)	Compost	film - 3 x 4 cm	Aerobic, 58 °C, 60% humidity	Weight loss	40	30	(Mihai et al., 2014)
PLA/corn (90/10%)	Synthetic material containing compost	film - 25 x 25 x 3mm sheets	Aerobic 58 °C	Weight loss	79.7	90	(Sarasa et al., 2009)
PLA/sisal fibre (SF) (60-40%)	Soil	film - 30 x 30 x 1 mm	Aerobic, 30% moisture	Weight loss	>60	98	(Wu, C.S., 2011)
PLA/PHB (75-25%)	Synthetic material containing compost	film - 200 µm thickness	Aerobic,58 °C	Weight loss	100	35	(Arrieta et al., 2014)
PHB	Soil	film	Aerobic, 30°C	Weight loss	64.3	180	(Jain and Tiwari, 2015)
PHB	Microbial culture from soil	film - 8 x 8 200 µm thick	Conditions not specified	Weight loss	~18	18	(Woolnough et al., 2008)
PHB	Soil	film - 30 mm in diameter and 0.1 mm thick	Real conditions, temperature and humidity were measured regularly	Weight loss	98	300	(Boyandin et al., 2013)
PHA	Soil	film - 50 x 30 x 1 mm	35 °C	Weight loss	35	60	(Wu, C.-S., 2014)

Table 2:2 continued **-** Biodegradation of biodegradable polymers in different environments

Name of biodegradable polymer	Type of environment	Form	Conditions	Method used to quantify biodegradation	Biodegradability (%)	Length of time (days)	Ref
PHA	Soil/compost (90/10%)	film 135 x 22 x 0.06mm thick	25 °C, 65% humidity	Produced CO_2	40*50	15	(Arcos-Hernandez et al., 2012)
PHA	Soil	film - 1 x1 cm, 0.3 - 3 mm thickness	60% moisture, 20 °C	Produced CO_2	48.5	280	(Gómez and Michel, 2013)
PHB	Compost	film - 90 µm thick	58 °C	Produced CO_2	79.9	110	(Weng et al., 2011)
PHB	Compost	film - thickness to 35 µm	70% moisture, 55 °C	Produced CO_2	~80	28	(Tabasi and Ajji, 2015)
PHB	Sea water	film - 8 x 12 x 50 mm thick.	25 °C	BOD degradability	80	14	(Tachibana et al., 2013)
PHB	Sea water	film - 152 to 190 µm thickness	Static incubation, 21 °C	Weight loss	99	49	(Thellen et al., 2008)
PHB	Sea water	film - 152 to 190 µm thickness	Dynamic incubation 12-22 °C, pH 7.9-8.1	Weight loss	30	90	(Thellen et al., 2008)
PHBV	Sea water	film - 152 to 190 µm thickness	Static incubation, 21 °C	Weight loss	99	49	(Thellen et al., 2008)
PHBV	Sea water	film - 152 to 190 µm thickness	Dynamic incubation 12-22 °C, pH 7.9-8.1	Weight loss	30	90	(Thellen et al., 2008)
PHB	River water	film - 5.507 mm thickness	Real conditions ~20 °C	Weight loss	43.5	42	(Volova et al., 2010)

Table 2:2 continued **-** Biodegradation of biodegradable polymers in different environments

Name of biodegradable polymer	Type of environment	Form	Conditions	Method used to quantify biodegradation	Biodegradability (%)	Length of time (days)	Ref
PHB	Brackish water sediment	film - 1 x 1 cm	32 °C, pH 7.06	Weight loss	100	56	(Sridewi et al., 2006)
PHB	Marine water	film - 5.507 mm thickness	28.75 °C (average temperature, pH 7-7.5)	Weight loss	58	160	(Volova et al., 2010)
PHB/CAB (50/50%)	Soil	film	-	Weight loss	31.5	180	(Jain and Tiwari, 2015)
PHBV	Microbial culture from soil	film - 8 x 8 200 µm thick	-	Weight loss	~41	18	(Woolnough et al., 2008)
PHA/Rice husk (60/40%)	Soil	film - 50 x 30 x 1 mm	35 °C	Weight loss	>90	60	(Wu, C.-S., 2014)
Bioplastic (made from potato almidon)	Compost	film - 25 x 25 x 3mm sheets	Aerobic, 58 °C	Weight loss	~85	90	(Sarasa et al., 2009)
Starch-based	Soil	film - 1 x1 cm, 0.3 - 3 mm thickness	60% moisture, 20 °C	Produced CO_2	14.2	110	(Gómez and Michel, 2013)
Mater-Bi bioplastic	Marine water with sediment	film 20µm thick	Room temperature	BOD biodegradability	68.9	236	(Tosin et al., 2019)
Mater-bi bioplastic (60% starch 40% resin)	Compost	film - 0.25 to 0.50 cm	55% moisture, aerobic, 23 °C	weight loss	26.9	72	(Mohee et al., 2008)

Table 2:2 continued **-** Biodegradation of biodegradable polymers in different environments

Name of biodegradable polymer	Type of environment	Form	Conditions	Method used to quantify biodegradation	Biodegradability (%)	Length of time (days)	Ref
CA (from fibre flax)	Municipal solid waste mixture	fibre	-	weight loss	44	14	(Mostafa et al., 2018)
CA (from cotton linters)	Municipal solid waste mixture	fibre	-	weight loss	35	14	(Mostafa et al., 2018)
Sponge cloth (cellulose-based)	Synthetic material containing compost	sponge pieces 25 mm × 25 mm	Aerobic, 58 °C	weight loss	>80	154	(Vaverková and Adamcová, 2015)
Nylon 4 (polyamides, bio-based)	Sea water	film - 8 x 12 x 50 mm thick.	25 °C	BOD biodegradability/weight loss	80/30	25/21	(Tachibana et al., 2013)
Nylon 4 (polyamides, bio-based)	Composted soil	film - 50–70 µm thickness.	25 °C, 80% humidity, pH 7.5-7.6	Weight loss	100	120	(Hashimoto et al., 2002)
PBS	Compost	films	Aerobic, pH 7-8, 58-65 °C, 50-55% moisture	Produced CO_2	90	160	(Anstey et al., 2014)
PBS (films)	Soil	films (3 cm × 3 cm)	25 °C, 60% humidity	weight loss	1	28	(Adhikari et al., 2016)
PBS (powdered)	Soil	particles - 250 µm diameter	25 °C, 60% humidity	weight loss	16.8	28	(Adhikari et al., 2016)
PBS/soy meal (75/25%)	Compost	films	Aerobic, pH 7-8, 58-65 °C, 50-55% moisture	Produced CO_2	90	100	(Anstey et al., 2014)

Table 2:2 continued **-** Biodegradation of biodegradable polymers in different environments

Name of biodegradable polymer	Type of environment	Form	Conditions	Method used to quantify biodegradation	Biodegradability (%)	Length of time (days)	Ref
PBS/canola meal (75/25%)	Compost	films	Aerobic, pH 7-8, 58-65 °C, 50-55% moisture	Produced CO_2	90	100	(Anstey et al., 2014)
PBS/switch grass (75/25%)	Compost	films	Aerobic, pH 7-8, 58-65 °C, 50-55% moisture	Produced CO_2	90	170	(Anstey et al., 2014)
PBS/starch (films)	Soil	films (3 cm × 3 cm)	25 °C, 60% humidity	weight loss	7	28	(Adhikari et al., 2016)
PBS/starch (powdered)	Soil	particles - 250 µm diameter	25 °C, 60% humidity	weight loss	24.4	28	(Adhikari et al., 2016)
PCL	Inoculum from a municipal wastewater treatment plant	film - 2 x 2 cm pieces and 20 µm thick	30 °C, aerobic	weight loss	7.6	28	(Massardier-Nageotte et al., 2006)
Starch/PCL	Inoculum from a municipal wastewater treatment plant	film - 2 x 2 cm pieces and 20 µm thick	30 °C aerobic	weight loss	53	28	(Massardier-Nageotte et al., 2006)
PCL	compost	particles - 63 to 250 mm	55 °C	Produced CO_2	38	6	(Nakasaki et al., 2006)
PCL	activated sludge	particle 125–250 µm	58°C	weight loss	90	47	(Funabashi et al., 2006)
PCL	compost	particle - 246.3 µm	58°C	weight loss	80	30	(Funabashi et al., 2006)
PCL	compost	Particle - 157.8 µm	58°C	Produced CO_2	80	20	(Kunioka et al., 2009)

Table 2:2 continued **-** Biodegradation of biodegradable polymers in different environments

Name of biodegradable polymer	Type of environment	Form	Conditions	Method used to quantify biodegradation	Biodegradability (%)	Length of time (days)	Ref
PLGA	water	Nanoparticles ~68.6 nm	Aerobic, 50°C	Monitor pH (acid release)	< 2	3 hrs	(Ferrari et al., 2013;;
PLGA	Film	Film 1.2 x 1.2 cm and average thickness: 320 ± 20 µm	Aerobic 25 °C	Mass loss	100	270	Bagheri et al., 2017
PLGA	Film	Thickness 83 ± 7 µm	Aerobic, 37 ◦C	SEM	visual	5 weeks	Abid et al., 2019)

PLA = polylactic acid; PPP = poly(p-phenylene); NPK = fertiliser; PHA = polyhyroxyalkanoate; PHB = polyhydroxybutyrate; PHBV = poly(3-hyroxybutyrate-co-3-hydroxycalerate); CAB = cellulose acetate butyrate; CA = cellulose acetate; PBS = polybutylene succinate; PCL = polycaprolactone; PLGA = Poly (D, L-lactide-co-glycolide); NPK: fertilizer; EFB: empty fruit bunch.

2.4 Standard biodegradation test methods

The definition for different biodegradation processes can be found in several standard Test Guidelines (Harrison et al., 2011). The 2022 OECD (Organization for Economic Cooperation and Development) reports predict that plastic pollution in the environment will worsen significantly in the future (Scudo et al., 2017; European Union, 2019; Martin, 2022). It is expected that the amount of plastic leakage into the environment will double to 44 million tons per year (Barrowclough and Birkbeck, 2022), and the build-up of plastic waste in waterways is projected to increase by more than threefold, from 353 million tons in 2019 to over 1000 million tons by 2060 (European Union, 2019). The International Standards ISO 14851 (1999) and ISO 14852 (1999) are specifically created to assess the aerobic biodegradability of polymeric and plastic materials, including any additives used in their formulation. These tests involve exposing the material to a diverse range of microorganisms in either activated sludge or compost suspension, under controlled laboratory conditions in an aqueous medium (Pagga et al., 2000).

Many of the experimental approaches described in biodegradability standards and test methods (**Table 2:3**) have been used in research. While a number of standards and test methods for measuring polymer biodegradability within aqueous environments have been developed, several issues can limit their reliability when attempting to predict *in situ* rates of biodegradation i.e. how quickly a substance (e.g. pollution in a river) will break down and be eliminated from the environment in which they are placed (Massardier-Nageotte et al., 2006). In general, biodegradation testing is based on measuring oxygen consumption or biogas generation by monitoring differences in pressure between the test flasks and carbon dioxide production (Massardier-Nageotte et al., 2006). Biological oxygen demand (BOD) is a crucial and commonly utilised indicator for assessing the breakdown of organic materials through biodegradation (Roppola et al., 2007). BOD quantifies the oxygen required for the oxidation of organic matter. When it comes to measuring the degradation of microparticles, there are specific challenges and considerations that need to be taken into account. The small size of microparticles (as compared to polymer films) makes it difficult to accurately measure their degradation, and traditional testing methods may not be suitable for these materials. For example, weight loss is commonly used for

biodegradation of a broad range of materials, including polymer films; however, this method can be problematic, as degrading materials can absorb moisture, which alters their weight, or the materials could disintegrate into smaller fragments, causing difficulty in recovering the materials to determine the weight loss. The most common standard to biodegradability relied upon in industry are issued by the International Organisation for Standardisation (ISO) and the American Society for Testing and Materials (ASTM). However, often academic and industrial studies have changed parameters to suit their requirements or facilities, which could lead to false claims (Pagga et al., 2000; Kjelsden et al., 2019). Furthermore, different studies may use varying methods to quantify the degradation of plastic materials, leading to difficulties in comparing results. Some testing methods also necessitate a more rigorous laboratory setup, making it challenging to accurately replicate a natural environment (Kjelsden et al., 2019). According to OECD, the “ready biodegradable” chemicals have to reach 60% of the theoretical carbon dioxide in a 10-day window within a 28-day period of the test (see **Table 2:3**). The standard duration of the test is 28 days, but it may be terminated earlier if the biodegradation curve reaches a plateau for at least three consecutive determinations. Conversely, tests may be extended beyond 28 days if the curve indicates that biodegradation has begun but the plateau has not been reached by day 28. However, in these instances, the chemical would not be considered readily biodegradable (Pagga et al., 2000; O’Malley, 2006; Gartiser, 2018b).

Efforts to standardise conditions often involve closely monitoring temperature, humidity, and other variables to regulate the environment in which the rate of biodegradation is assessed (Kjelsden et al., 2019). Many of the biodegradability standards developed for aqueous environments are either characterised by a lack of information on the level of statistical replication required, or involve measurements performed in duplicate (**Table 2:3**). A minimum of three measurements is required to ensure statistical validity and reproducibility as part of a given biodegradability standard (Harrison et al., 2018).

Table 2:3 - Currently active biodegradability standards and test methods for all plastic materials in soil, marine and waste water environments (Adapted from Harrison et al. (2018).

Environment	Standard or test method	Inoculum	Medium	Temp (°C)	Measurement Type	Test Duration	Number of replicates	Validity criteria
Wastewater and sewage sludge	BS EN ISO 14851:2004	Sludge, compost and/or soil	Synthetic; aerobic	20-25 (±1)	BOD; static test conditions	Max. 6 months	Min. 2	Greater than 60% degradation of reference material; BOD of negative control must not exceed a specified upper limit.
	BS EN ISO 14852:2018	Sludge, compost and/or soil	Synthetic; aerobic	20-25 (±1)	CO_2 evolution; static test conditions	Max. 6 months	Min. 2	Greater than 60% degradation of reference material; CARBON DIOXIDE evolved from negative control must not exceed a specified upper limit.
	BS ISO 13975:2012	Sludge, livestock faeces or other organic waste	Direct exposure to inoculum; anaerobic	35 ±3 or 55 ±5	CO_2 and CH_4 evolution, DIC; static test conditions	Max. 3 months	2	Greater than 70% degradation of reference material after 15 days; Extent of degradation (%) must differ by <20% between replicates.
	BS EN ISO 14853:2016	Sludge, livestock faeces or other organic waste	Synthetic; anaerobic	35 ±2	CO_2 and CH_4 evolution, DIC; static test conditions	Max. 3 months	Min. 3	Greater than 70% degradation of reference material; pH of the medium must remain between 6 and 8
	ISO 18830:2016	Sediment or sediment and seawater	Synthetic or natural seawater	15-28 (±2)	BOD; static test conditions	Max. 24 months	3	Greater than 60% degradation of reference material; BOD of negative control must not exceed a specified upper limit.

Table 2:3 continued - Currently active biodegradability standards and test methods for all plastic materials in soil, marine and waste water environments (Adapted from Harrison et al. (2018).

Environment	Standard or test method	Inoculum	Medium	Temp (°C)	Measurement Type	Test Duration	Number of replicates	Validity criteria
Marine	ISO 19679:2016	Sediment or sediment and seawater	Synthetic or natural seawater	Synthetic or natural seawater	CO_2 evolution; static test conditions	Max. 24 months	3	Greater than 60% degradation of reference material; CO_2 evolved from negative control must not exceed a specified upper limit.
	ASTM D6691-09	Preselected strains or seawater	Synthetic; aerobic	30 (±1)	CO_2 evolution; static test conditions	Max. 3 months	Not specified	≥70% degradation of reference material
	ASTM D7473-12	Seawater or combination of seawater and sediment	Direct exposure to inoculum; aerobic	Varies depending on *in situ* conditions	Visual evidence for degradation; loss of dry mass	Max. 6 months	3	Not specified
	ASTM D7991-15	Sediment and seawater	Direct exposure to inoculum; aerobic	15-28 (±2)	CO_2 evolution; static test conditions	Max. 24 months	3	≥60% degradation of reference material
	ISO 17556:2012	Adapted or non-adapted soil	Natural Soil; aerobic	20-28 (±2)	BOD; CO_2 evolution	Max. 6 months	Not specified	≥60% degradation of reference material. The measured CO_2 or the BOD values from the blanks at the end of the test are within 20% of the mean.

Table 2:3 continued - Currently active biodegradability standards and test methods for all plastic materials in soil, marine and waste water environments (Adapted from Harrison et al. (2018).

Environment	Standard or test method	Inoculum	Medium	Temp (°C)	Measurement Type	Test Duration	Number of replicates	Validity criteria
Soil*	ASTM D5988-12	Adapted or non-adapted soil	Natural Soil; aerobic	20-28 (±2)	CO_2 evolution	Max. 6 months	Not specified	≥70% degradation of reference material. The measured CO_2 or the BOD values from the blanks at the end of the test are within 20% of the mean.
	NF U52-001	non-adapted soil	Natural Soil; aerobic	Not specified	Visual evidence for degradation	Max. 6 months	Not specified	≥70% degradation of reference material. Standard deviation of replicates <20%.
	UNI 11462:2012	non-adapted soil	Natural Soil; aerobic	21-28	CO_2 evolution	Max. 3 months	Not specified	≥60% degradation of reference material. Standard deviation of replicates <10%..

BOD= Biological oxygen demand; DIC = Dissolved inorganic carbon; * = information derived from Kjelsden et al. (2019)

As mentioned above, the biodegradation extent of polymers is typically followed by measuring the oxygen demand or carbon dioxide (CO_2) production, or the amount of CO_2 and methane (CH_4) produced when the plastic material is either aerobically or anaerobically biodegraded (Garcia-Depraect et al., 2022). The process typically involves placing a known mass of polymer in a controlled environment with microorganisms present which secrete enzymes and monitoring the amount of carbon dioxide released over a specified period of time. The amount of carbon dioxide produced is then compared to the theoretical maximum carbon dioxide that could be produced if the polymer was completely degraded.

Anstey et al. (2014) evaluated the biodegradation of poly(butylene succinate) PBS (as a film) in compost soil by analysing the conversion of organic carbon into carbon dioxide according to the ASTM D6400 standard. These authors found that PBS films showed 90% biodegradability in 160 days in terms of produced CO_2 under aerobic conditions (Anstey et al., 2014). The biodegradation percentage are calculated by the ratio between the produced CO_2 (or pressure decrease) and the theoretical CO_2 ($ThCO_2$/pressure) i.e. the amount of CO_2 expected in case of total oxidation of the carbon present in the polymer sample (Cpolymer) introduced in the vessel (Chinaglia et al., 2018) based on the amount of carbon dioxide produced compared to the theoretical maximum. The theoretical carbon dioxide ($ThCO_2$) is the expected maximum amount of carbon dioxide that can be produced from a polymer as a result of biodegradation based on the stoichiometry. In this case, the PBS produced 90% of the theoretical maximum amount of carbon dioxide, therefore, it would be considered 90% biodegradable. Gómez and Michel (2013) studied particle size effects on biodegradation by monitoring the amount of CO_2 produced of a co-polyester plus corn-based polymer in a soil incubation by comparing the rates of degradation of 1 cm square films (0.23−2.74 mm thick) and ground samples, however, no particle size was given. They found that polymer in film form was more degradable (55%) than the powder form (40%) after 660 days. However, as the particle size of the ground samples were unknown, the influence of particle size or sample surface area cannot be extracted from these data.

Ahn et al. (2011) evaluated the biodegradability of a PLA polymer as a film (0.5 cm square pieces) by measuring carbon dioxide produced in a compost environment which resulted in 13% biodegradability over 60 days. On the other

hand, Tabasi and Ajji (2015) also studied the degradation of PLA polymer films in a compost environment but found 70% degradation over 28 days. However many other factors differ when comparing the two: the source of soil differed (temperature and moisture content) and the mass, thickness and size of the films differed (see **Table 2:2**)**.** Funabashi et al; evaluated produced CO_2 during degradation of PCL particles (125–250 μm) in compost and found 90% biodegradability over 47 days (Funabashi et al., 2006). They found that the size of PCL particles affected the biodegradation rate (i.e., smaller size samples degraded faster due to higher surface area exposure to microorganisms attack) (Funabashi et al., 2006). The enzymatic degradation of PCL was also interesting, since the degradation can be easily measured with a small amount of polymer samples in the laboratory. An enzyme of Lipase PS from *Pseudomonas cepacia* is known to degrade PCL (Funabashi et al., 2006; Nakasaki et al., 2006). Based on a previous study, PCL can be considered biodegradable under aerobic composting conditions (Funabashi et al., 2006). Once more, the discrepancies and differences identified in all these examples of biodegradation characterisation highlight several issues in interpreting the standards available for the Industry to use and rely on. While these methods exist, they lack proper regulation. For instance, in intricate settings such as seawater or soil, much of the research is centred on polymer films rather than particles. This means that there is a need for conducting simple tests with which the degradation of a wide range of samples can be compared before using the standards taking into account the environments in which engineered microparticles found themselves degrading in.

2.4.1 Factors affecting biodegradation rate

There are many factors that can influence the mechanisms behind the biodegradation processes of PMPs, mostly divided into the properties of the polymer particles being degraded and the degradation environment. Here we look at both of these series of factors separately.

2.4.1.1 Characteristics of the MPs.

As mentioned earlier, biodegradation occurs first at the surface of the polymer particles by the process of surface erosion (**Figure 2:1**). The ratio of surface area to volume is thus a significant factor that determines the rate of surface erosion, the higher the surface area to volume ratio, the higher the biodegradation kinetics (Chinaglia et al., 2018). In addition, where degradation is driven by an enzyme, the high surface area enables the enzymes to quickly penetrate through pores and attack an increased surface area of the PMPs (Funabashi et al., 2006). However, the overall CO_2 production (stage 3 of the biodegradation process) has no influence on the available surface area at this stage as the rate of the degradation process may initially be limited by the surface area, but once the polymer chains have been broken down into smaller dissolvable molecules (acids) into solution, the rate of CO_2 production exerts its own influence in the final stages. Chinaglia et al. (2018) compared the degradation rate of different physical forms of polybutylene sebacate (PBS) in soil, and found that smaller sized particles (~ 60 µm) have a faster degradation rate as more surface area for a given mass is available for enzymatic activity and is only limited by the saturation of the enzyme. This point is referred to as the saturation point, where the addition of more enzyme does not enhance the enzymatic reaction any further. One common cause for the decrease in reaction speed is the depletion of substrate within the mixture, leading to the degradation of particles (Pastorino et al., 2004; Robinson, 2015). Another possible explanation is that the enzyme may be unstable or saturated, resulting in denaturation during the course of the experiment. In this study, the researchers obtained pellets of the polymer and then ground them into powders in three different size ranges: 50−75 µm, 200−355 µm, and 500−700 µm. The biodegradation of these powders and pellets was tested in an agricultural soil enriched with compost. The results showed that after 138 days, the pellets were only around 55% degraded, with degradation still ongoing. On the other hand, all

three powder forms achieved over 89% degradation. It was noted that the particle size had a significant impact on the degradation rate, with the 50−75 μm and 200−355 μm powder fractions degrading at similar rates, while the 500−700 μm powder fraction degraded at a slower pace. The degradation of polymer films of poly(3-hydroxybutyrate) (PHB) with a thickness of 0.2–0.3 mm and powder forms with dimeter of ≥100 μm in a soil environment have been investigated by Modelli et al. (1999). The authors reported that the powdered polymers exhibited very high initial degradation rate (90% in 65 days) but slowed down rapidly following the relatively faster degradation of small particles which left behind a wide size distribution of larger particles. These larger particle mixture had inherently slower degradation rates due to reduced surface area to volume ratio. Conversely, the polymer films had a virtually constant reaction rate, attributed to the constant available surface area between the polymer and the microorganisms present in the soil (26% degradation 210 days).

The molecular weight of the monomer is also an important factor that affects the biodegradability of PMPs because it determines the physicochemical properties of the polymer. The hypothesis is that longer polymer chains often take longer to degrade and do not degrade as completely as smaller polymers chains (Albright and Chai, 2021). A study by Tokiwa et al. (2009) showed that PCL film with higher molecular weight (M_w > 4,000 Da) were degraded slower by *Rhizopus delemar* lipase than those with lower molecular weight (M_w < 2,220 Da) because the initial smaller chain length results in smaller oligomers for the same number of ester bonds being cleaved. The PCL film with lower M_w (<2,200 Da) also had lower melting temperature (T_m < 60°C) which is related to the M_w and the crystallinity. In another study by Tokiwa and Suzuki (2014) showed that the melting temperature (T_m) of polyesters had a strong correlation to the enzymatic degradation of the polymer. They found that the higher the T_m (>60°C) of the polymer, the lower the biodegradation of the polymer. They claim that polyesters with lower T_m have less crystalline parts than those with high T_m and therefore undergo faster enzymatic hydrolysis. The degree of crystallinity of a polymer is therefore a crucial factor affecting biodegradability since enzymes mainly attack the amorphous domains of a polymer (Tokiwa and Suzuki, 2014). This is because molecules in the amorphous region are loosely packed, and thus more susceptible to degradation than molecules in crystalline regions. In a study by Chen et al. (1999), the change in the level of crystallinity after degradation of PCL

PMPs was investigated using X-ray diffraction. PCL PMPs were immersed in pH 7.4 phosphate-buffered saline medium and incubated at 37 °C with lipase enzyme. The test-tube was shaken at regular intervals and the buffer medium was renewed every 3 days due to pH drop. After predetermined periods of time, the sample was recovered via centrifugation from the buffer, then washed with distilled water and dried in vacuum at room temperature for analysis (Chen et al., 1999). A decrease in the molecular weight of PCL was observed from 30 kDa to 27 kDa after 9 weeks, although this difference is very small. The results showed an increase in crystallinity from 51% to 62% when compared to a control sample without the presence of lipase after 9 weeks. This observed change in crystallinity was due to the degradation of the amorphous regions of PCL PMPs resulting in an increase in overall sample crystallinity (Chen et al., 1999). In a study by Nam and Park (2020) the degree of crystallisation over time (%c) of PLA PMPs were analysed during biodegradation in two different aqueous environments (seawater and NaOH solution at pH 11). Thermal analysis was conducted using a differential scanning calorimeter (DSC 6000, PerkinElmer, USA) with a heating rate of 10 °C/min from 25 to 200 °C. After rapid cooling to 25 °C, the sample was re-heated at the same heating rate to observe its crystallisation behaviour. The results of PLA PMPs clearly show an increase in crystallinity as a function of time, indicating hydrolytic degradation. The rate of crystallinity growth is accelerated in NaOH solution shown in **Figure 2:2**, due to changes in pH which is related to ionic strength, making it more difficult to biodegrade over time.

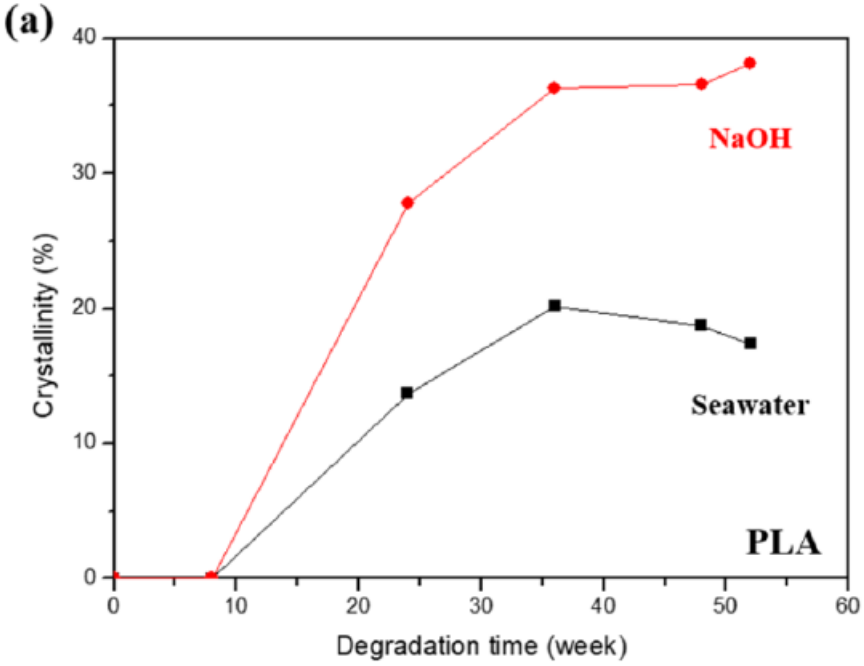


Figure 2:2 - Crystallinity of PLA PMPs as function of degradation time (red – pH 8 NaOH solution) and (black – seawater) showing faster crystallisation rate in pH 8 NaOH when compared to the PLA PMPs in seawaters suggesting faster cleavage of ester bonds in the polymer in an alkaline environment (Nam and Park, 2020).

2.4.1.2 Characteristics of biodegradation environment.

The environmental conditions in which the biodegradation takes place are an important aspect since the biodegradability of a material differs from one environment to another as summarised in **Table 2:2**. For instance, PLA films (thickness 100 and 350 µm) was reported to break down at a slower rate (with varying times reported) in landfills or natural soil at room temperature, but can fully biodegrade within 6-9 months in industrial composting facilities due to the differences in temperature, humidity and pH (Pranamuda et al., 1997; Karamanlioglu and Robson, 2013). The temperature within industrial composts is elevated (58-65 °C) and near its glass transition temperature (Tg), leading to higher hydrolysis rates (Laycock et al., 2017). Pastorino et al. (2004) studied the degradation of polycaprolactone using an enzyme at varying temperatures (40, 50 60 and 70 °C) and found that the optimum condition was 40 °C, whereas no degradation was observed at 70 °C due to the denaturing of the enzyme at that temperature (Pastorino et al., 2004). The kinetics of each biodegradation step is dependent on environmental factors such as, microbial activity, humidity, temperature and pH. The rate of deterioration (stages 1 and 2) will differ from the rate of assimilation (stage 3). The current standards framework places emphasis

on the rate of polymer assimilation (stage 3) rather than the rate of surface erosion (stages 1 and 2).

2.4.2 Identified gaps

The review of literature identified gaps in research on the biodegradation of microparticles in the European Union (EU). Microparticles are commonly used in personal care, paints/coatings, detergents, oil and gas, agriculture, and industrial abrasives. The study found that personal care products accounted for the highest amount of microparticles used for exfoliation and cleansing in rinse-off products in the EU, with an estimated 714-793 tonnes per year. Paints used around 220 tonnes of solid non-biodegradable polymeric particles, while leave-on products contained approximately 540-1120 tonnes of microplastics. The use of microparticles in rinse-off products has been decreasing and is expected to continue to decline. The detergent industry was estimated to use around 190-200 tonnes of microplastics. The researchers analysed product information from manufacturers like BASF, Dow Chemicals, AkzoNobel, Polysciences, and SNF, focusing on polymers with limited available literature. These findings highlight the high demand for polymeric microparticles in products and the challenges of waste management. The study also noted inconsistencies in biodegradation characterisation, indicating challenges in understanding industry standards. Environmental conditions and particle characteristics show limitations in relying on standard test methods for biodegradation. Basic tests should be conducted to compare degradation of different samples before relying on standards, especially in challenging environments like seawater or soil. More research is needed on model systems to better understand the degradation process.

2.5 Methods of engineered polymeric microparticles

In this section, examples of a few manufacturing techniques to prepare microparticles are discussed. Firstly examples of manufacturing techniques to produce solid particles are mentioned and then secondly the manufacturing techniques to produce core shell structures are discussed.

2.5.1 Solid particles

2.5.1.1 Solvent extraction

Solvent extraction (SE) is a technique where a solution of polymer in an organic solvent is emulsified into an aqueous extraction phase, resulting in finely dispersed emulsion droplets containing the polymer and solvent. As the solvent is extracted from the droplets and eventually evaporated, the polymer's solubility within the droplet decreases, which forces it to precipitate out (**Figure 2:3**) into what eventually forms a solid particle once all the solvent is removed. Precipitation of the particles is influenced by how fast the solvent is removed from the initial droplets, which in turn can vary the porosity of the resulting particles, while particle size is influenced by the stirring rate during the emulsification process and the concentration of polymer in the droplets (Makadia and Siegel, 2011). In this technique, controlling the extraction rate of the solvent allows for manipulating the characteristics of the PMPs (Katou et al., 2008). Examples of some emulsifiers are polysorbate, polyvinyl alcohol or gelatine (Katou et al., 2008; Heiskanen et al., 2012a; Heiskanen et al., 2012b; Staff et al., 2013a; Staff et al., 2013b). The challenge is to find a suitable polar solvent with a low boiling point that can solubilise the polymer (Staff et al., 2013a). However, the solvents need to be relatively soluble in water, to be easily extracted from the droplets but at the same time they need to have a solubility that is low enough to enable formation of droplets. There is a need to keep the droplets well suspended over a long period of time to facilitate the extraction of the co-solvent from the droplets and thus the need for an increased viscosity in the continuous phase. The particles can then be collected by centrifugation or filtration if required and are typically washed with distilled water. The reason for washing the particles is to remove excess materials such as solvent and rheology modifier.

The limitations of this method result from the different hydrophilic / lipophilic nature and level of crystallinity of the polymers (Gentile et al., 2014). For example, pure poly lactic acid (PLA) is less water soluble than the copolymer poly (D, L-lactide-co-glycolide) (PLGA) which in turn is more hydrophobic than pure poly glycolic acid (PGA) and therefore the same solvent cannot be used for all three polymers (Gentile et al., 2014). This also adversely affects the performance in formulations such as control drug delivery where poor mechanical strength, weak wall-formation, and easy rupture on reaction to osmotic change have been reported (Lengyel et al., 2019). Another disadvantage of this technique is that it is difficult to control the process to achieve monodispersed particles (54). This is because the initial emulsion droplets are used as templates for the final particles. As emulsion droplets are typically made from stochastic processes, they are polydisperse, which then influences the dispersity of the final particles. However, in industry, dispersity is not controlled unless heterogeneous polymerisation methods such as dispersion or emulsion polymerisation is used, which is often used in paints and coatings applications. For this reason, the solvent extraction is best suited for this PhD to prepare microparticles.

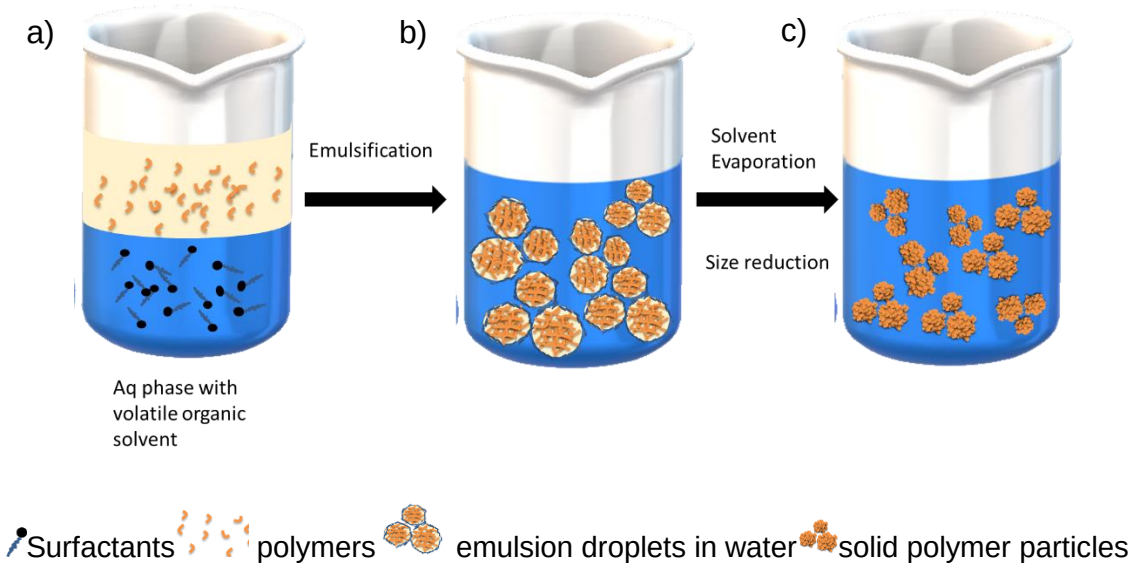


Figure 2:3 - Steps involved in preparing polymer particles from a solvent extraction method (Katou et al., 2008): a) two phase system, aqueous phase with surfactant and suitable organic solvent to disperse the polymer b) emulsification of polymer solution in aqueous phase to produce emulsion droplets c) the solvent is extracted into the continuous phase evaporates from the aqueous phase resulting in smaller solid particles

2.5.1.2 Heterogeneous polymerisations

Heterogeneous polymerisations are polymerisation processes with two or more phases where the monomer and the continuous phase are immiscible. Polymerisation results in the precipitation of polymer chains into particulates within the reaction continuous phase at the surface or interface. An example of a heterogeneous polymerisation is dispersion polymerisation (DP). DP is a heterogeneous polymerisation process carried out in the presence of a (generally polymeric) stabiliser in the reaction medium (Wang, X. et al., 2018; Zhong and Pan, 2022). DP refers to a process in which an initial reaction mixture comprises a monomer, an initiator of polymerisation and a stabiliser which are all initially soluble in the solvent used for the reaction. Over time, as the polymerisation proceeds and the monomer turns into a growing polymer, the solubility of the polymer chains decrease and above a certain length, the polymer precipitates out of the solvent and forms a particle nucleus (Richez et al., 2013). The growing polymer chains and monomers swell and grow the particle nuclei until all the monomers are consumed and the final particle size is reached (**Figure 2:4**). Applications for DP are in coatings formulations in paints for potential use at different temperatures (e.g., paints applied in cold climates or coatings applied in drying ovens) and pressures (Richez et al., 2013). This method offers many advantages such as control of particle size, it is also relatively simple to perform at an industrial scale with low processing costs. The disadvantage of this technique is that it is difficult to control the polymerisation to develop particle properties in terms of size and size distribution (Jiang et al., 2008). This is because there are many variables to consider such as the concentration of monomer and solvent, initiator type, emulsifier, rate of polymerisation, temperature, pH etc. for example, in a study by Jiang et al. (2008), the effect of the concentration of monomer and solvent on the kinetics of dispersion polymerization of methyl methacrylate was investigated. They found that that increasing the monomer concentration increased the reaction rate which in turn resulted in broader molecular weight distribution with increasing monomer concentration, hence increasing particle size. Narrow particle size distributions were achieved at the lower monomer concentrations.

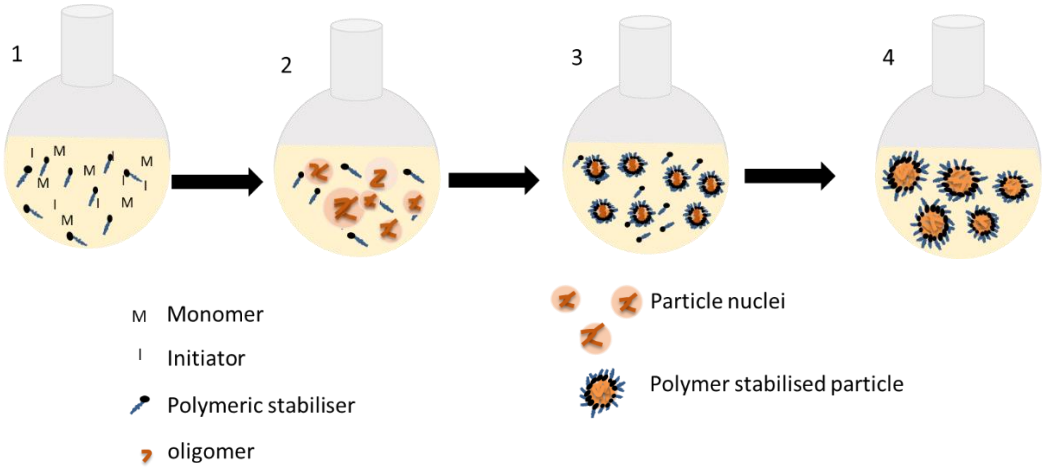


Figure 2:4 – Dispersion polymerisation in a solvent 1) initial reaction mixture (homogeneous phase) 2) oligomer precipitation and oligomer coagulation into particle nuclei. Coagulation of these oligomer chains continues until steric stabilisation of the latex particles is fully achieved when enough stabiliser chains cover the particle surface. 3) particle stabilisation by polymer adsorption and particle growth (particle size increase) 4) continuation of particle growth until all the monomer is consumed (Richez et al., 2013)

2.5.2 Core shell structures

2.5.2.1 Coacervation

Coacervation is a process where a single phase polymer mixture separates into two immiscible polymer liquid phases with a concentrated and dilute phase (Lengyel et al., 2019). The phase with more concentrated polymer component is known as the coacervate and the dilute phase is known as the equilibrium solution. The separation is designed to occur upon a change in solvency for the polymer(s) involved as a result of an engineered variation in pH, temperature or solvent composition. For example the use of a single polymer dissolved in water which loses its solubility as a function of a pH change. Another example is electrostatic attraction between two oppositely charged polymers used to initiate the phase separation of these two polymers from the water phase (Xiao et al., 2014).

Coacervation can be defined as either simple or complex. Simple coacervation is a phenomenon where a single polymer separates from a colloidal solution with the addition of a salt that is incompatible with the polymer due to the decrease in solubility or changes in pH and temperature (Lengyel et al., 2019). On the other hand, complex coacervation involves the interaction of two oppositely charged polymers resulting in a liquid-liquid separation, where the two interacting polymers concentrate in one phase and are only present in very small concentrations in the other (Zhao, W.W. and Wang, 2017; Eghbal and Choudhary, 2018; Lengyel et al., 2019). An example of a simple coacervation is by Mauguet et al. (2002) in which they encapsulated hexadecane (food oil). Hexadecane was emulsified by a gliadin solution and the coacervation was induced by adding a salt-solution in the continuous phase of the emulsion containing gliadin. In complex coaceravtion, coacervates form particles around the core material (positively charged gelatine and negatively charged gum Arabic) deposit around the oil particles/droplets to form shells on particulate. The pH is gradually lowered to 4.5 and the core material is added. The microcapsules are cooled which hardens the deposited shell, which is typically further cross-linked with, for example with glutaraldehyde (Ammala, 2013; Corrêa-Filho et al., 2019).

The main uses of the coacervation technique are to encapsulate essential oils, pigments and dyes (Eghbal and Choudhary, 2018; Corrêa-Filho et al., 2019). The coacervation process has its disadvantages when encapsulating fragrances and low molecular weight oils, due to loss of the volatile fragrance during coacervation (Gouin, 2004). In addition, capsules formed from this process have poor barrier properties resulting in poor retention and leaching of the active ingredient and therefore reduced performance and make them prone to bacterial growth and hence reduced shelf life. Also, harmful residual of the crosslinking agent such as glutaraldehyde can be present (Eghbal and Choudhary, 2018; Corrêa-Filho et al., 2019). The inclusion of residual materials will affect the biodegradation process and cross-linking will likely reduce degradability quite drastically.

.

2.5.2.2 Interfacial polymerisation

Interfacial polymerisation is a phenomenon where reactants such as urea or amines dissolved in the continuous phase react with a different reactant in the dispersed phase (Mezhuev et al., 2020). As the polymerisation proceeds, a thin shell forms at the interface of the dispersed and continuous phases, which slows down the diffusion of the reactants towards each other resulting in the reaction rate decreasing over time (Lee et al., 2013; Perignon et al., 2015). The polymerisation causes the resulting polymer to precipitate out of solution at the interface. For example, (Nair and Laurencin, 2007) demonstrated interfacial polymerisation of diamine monomers dissolved in water and aqueous phase dispersed in the oil phase. The second monomer (oil soluble) diacid chloride was then added, which reacted at the interface with the first monomer diamine forming a membrane.

2.5.2.3 Spray drying

Spray-drying is the most well established and technologically mature technique currently available in the industry for the purpose of producing particles/globules as a dry powder from a solution/emulsion (Schuck et al., 2016). The emulsion or solution is sprayed into a chamber as droplets through a nozzle, where warm air dries the droplets (**Figure 2:5**). In general is used to produce dried powders of a range of formulation, some of which (but not the majority) aim to produce encapsulated active ingredients. Most of the applications basically process a solution mixture of various components into dry particles. Several types of particles can be produced from this drying process. Their morphology include dense, hollow, porous composite or encapsulated structures with spherical, wrinkled, collapsed or doughnut-like shapes. This processing technique requires the wall material to be form a film and dry with minimum energy requirements. The capsule material may be selected from a wide range of polymers, tailored to the desired properties of the final product (BUCHI, downloaded Nov 2023). Spray-drying presents several advantages such as low-cost, ease of scaling up in industry and high encapsulation efficiency (Schuck et al., 2016; Lengyel et al., 2019). Furthermore, it is not well suited for producing microparticles in the low micrometre size range (Freitas et al., 2005).

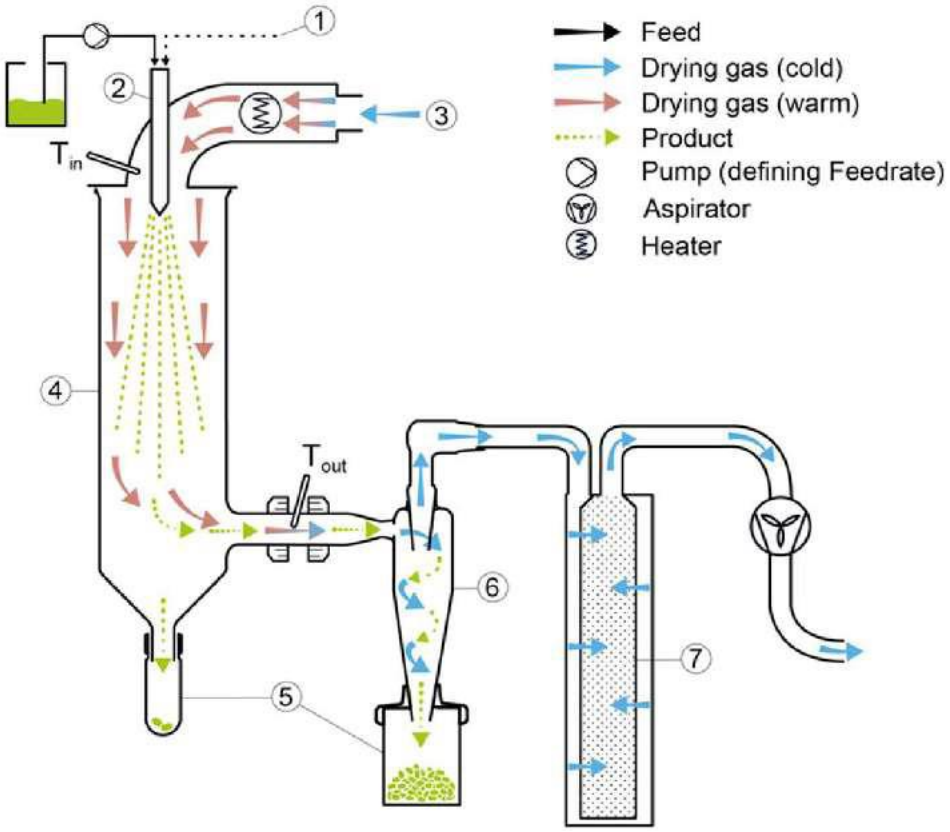


Figure 2:5 - Illustration of a typical spray drying process. The main sections include (1) feed emulsion entry point (2) homogeniser (3) pre-heated air (4) drying vessel (5) microcapsule collection vessels (6) cyclone separator (7) air-filter. Adapted from BUCHI (downloaded Nov 2023).

Other PMPs manufacturing processes are summarised in **Table 2:**

Table 2:4. Manufacturing methods for polymeric microparticles

Method	Description	Scalability	Typical solvents	Size range reported	Temperature	Uses	Ref
Coacervation	polymers in solution from a single colloidal coaceravate solution facilitated through changes in pH	continuous	aqueous to organic solvent	2 - 1200 µm	ambient	encapsulate essential oils containing pigments and dyes	(Xiao et al., 2014; Sing and Perry, 2020)
Electrospray	atomisation of two liquids phases via electrostatic interactions to create fine mist aerosol of droplets containing polymer and encapsulates	continuous	aqueous to organic solvent	0.6 - 2000 µm	ambient	cosmetic, toothpaste and soap additives	(Jaworek, 2006; Bae et al., 2019)
Emulsion - solvent extraction	two immiscible liquid phases are mixed with stabilisers to form colloidal suspension	Semi-continuous	aqueous to organic solvent	0.5 - 1000 µm	ambient	polymeric nanocarriers i.e. drug delivery, agriculture pesticide control, cosmetic, toothpaste and soap additives	(Freitas et al., 2005; Kumar, A. et al., 2019)
Ionotropic gelation process	two liquid solutions form a gel due to ionic interactions	continuous	Aqueous	50 - 300 µm	ambient	polymeric nanocarriers i.e. drug delivery, agriculture pesticide control	(Leong et al., 2016; Gadzinski et al., 2022)
Heterogeneous Polymerisation	reaction of monomers in solution with encapsulates to form polymeric particles	batch	aqueous to organic solvent	0.05 - 10 µm	varies	cosmetic, toothpaste and soap additives, polymeric nanocarriers i.e. drug delivery, agriculture pesticide control	(Chern, 2006)
Spray drying	a liquid or slurry is rapidly dried with hot gas phase	continuous	organic solvent	5 - 5000 µm	elevated	encapsulate food ingredients such as flavours and lipids	(Schuck et al., 2016)

2.6 Conclusion

Manufactured polymeric microparticles (PMPs) are an integral part of our life and will continue to serve a wide range of important functions in areas such as pharmaceuticals, cosmetics and cleaning products where they provide significant improvement to our quality of life. The literature review identified gaps in research on microparticle usage in the EU, with personal care products being the largest consumer. Paints, leave-on products, and detergents also utilise significant amounts of microparticles. The use of microparticles in rinse-off products is decreasing, and industry initiatives are expected to further reduce their usage. These findings highlight the demand for polymeric microparticles in formulated products and the challenges of waste management. To reduce its negative impact on the environment, a complete shift to sustainable and biodegradable alternatives is imperative. This review has highlighted the limitations of PMP degradation studies carried out in so called real simulations systems that introduce process gaps which undermine the lifecycle and impact of PMPs on the environment. This review further explored areas such as the mechanisms of biodegradation, factors that affect the biodegradation of PMPs and the scientific basis of current biodegradation test methods. Overall, it was found that biodegradation consists of multiple steps occurring in series, each with their exclusive kinetics. The kinetics of each biodegradation step is dependent on factors such as, available surface area, chemical composition (such as chemical cross-linking), microbial activity and environmental conditions (temperature, pH, salinity). It was very challenging to measure biodegradation rate as a function of surface area across multiple studies due to multiple variations between studies such as different soil types, sample processing and experimental setup. Establishing and adhering to standardised testing methods for determining the biodegradability of engineered PMPs will provide the confidence in industry necessary to innovate new PMPs that will lead to a more sustainable future. It is thought that these studies contribute to a better understanding of the biodegradation mechanism of polyesters and possibly may lead to novel engineered polymers with tailor made properties and biodegradation characteristics.

2.7 References

Adhikari, D., Mukai, M., Kubota, K., Kai, T., Kaneko, N., Araki, K.S. and Kubo, M. 2016. Degradation of Bioplastics in Soil and Their Degradation Effects on Environmental Microorganisms. *Journal of Agricultural Chemistry and Environment.* **05**(01), pp.23-34.

Agarwal, S. 2020. Biodegradable Polymers: Present Opportunities and Challenges in Providing a Microplastic-Free Environment. *Macromolecular Chemistry and Physics.* **221**(6), article no: 2000017 [no pagination].

Ahn, H.K., Huda, M.S., Smith, M.C., Mulbry, W., Schmidt, W.F. and Reeves, J.B., 3rd. 2011. Biodegradability of injection molded bioplastic pots containing polylactic acid and poultry feather fiber. *Bioresour Technol.* **102**(7), pp.4930-4933.

Albright, V.C., 3rd and Chai, Y. 2021. Knowledge Gaps in Polymer Biodegradation Research. *Environ Sci Technol.* **55**(17), pp.11476-11488.

Ammala, A. 2013. Biodegradable polymers as encapsulation materials for cosmetics and personal care markets. *Int J Cosmet Sci.* **35**(2), pp.113-124.

Anstey, A., Muniyasamy, S., Reddy, M.M., Misra, M. and Mohanty, A. 2014. Processability and Biodegradability Evaluation of Composites from Poly(butylene succinate) (PBS) Bioplastic and Biofuel Co-products from Ontario. *Journal of Polymers and the Environment.* **22**(2), pp.209-218.

Arcos-Hernandez, M.V., Laycock, B., Pratt, S., Donose, B.C., Nikolić, M.A.L., Luckman, P., Werker, A. and Lant, P.A. 2012. Biodegradation in a soil environment of activated sludge derived polyhydroxyalkanoate (PHBV). *Polymer Degradation and Stability.* **97**(11), pp.2301-2312.

Arrieta, M.P., López, J., Rayón, E. and Jiménez, A. 2014. Disintegrability under composting conditions of plasticized PLA–PHB blends. *Polymer Degradation and Stability.* **108**, pp.307-318.

Bae, S.B., Nam, H.C. and Park, W.H. 2019. Electrospraying of environmentally sustainable alginate microbeads for cosmetic additives. *International Journal of Biological Macromolecules.* **133**, pp.278-283.

Bagheri, A.R., Laforsch, C., Greiner, A. and Agarwal, S. 2017. Fate of So-Called Biodegradable Polymers in Seawater and Freshwater. *Glob Chall.* **1**(4), p1700048.

Boyandin, A.N., Prudnikova, S.V., Karpov, V.A., Ivonin, V.N., Đỗ, N.L., Nguyễn, T.H., Lê, T.M.H., Filichev, N.L., Levin, A.L., Filipenko, M.L., Volova, T.G. and Gitelson, I.I. 2013. Microbial degradation of polyhydroxyalkanoates in tropical soils. *International Biodeterioration & Biodegradation.* **83**, pp.77-84.

BUCHI. downloaded Nov 2023. *Spray Drying Basic theory applications, BUCHI,* [Exhibition catalogue]. BUCHI UK Ltd, Unit 6, Goodwin Business Park, Willie Snaith Road, Newmarket Suffolk, CB8 7SQ.

Chen, D.R., Bei, J.Z. and Wang, S.G. 1999. Polycaprolactone microparticles and their biodegradation. *Polymer Degradation and Stability.* **67**, pp.455-459.
Chern, C.S. 2006. Emulsion polymerization mechanisms and kinetics. *Progress in Polymer Science.* **31**(5), pp.443-486.

Chinaglia, S., Tosin, M. and Degli-Innocenti, F. 2018. Biodegradation rate of biodegradable plastics at molecular level. *Polymer Degradation and Stability.* **147**, pp.237-244.

Corrêa-Filho, L., Moldão-Martins, M. and Alves, V. 2019. Advances in the Application of Microcapsules as Carriers of Functional Compounds for Food Products. *Applied Sciences.* **9**(3).

Dey, T.K., Uddin, M.E. and Jamal, M. 2021. Detection and removal of microplastics in wastewater: evolution and impact. *Environ Sci Pollut Res Int.* **28**(14), pp.16925-16947.

Eghbal, N. and Choudhary, R. 2018. Complex coacervation: coacervation: Encapsulation and controlled release of active agents in food systems. *Lwt-Food Science and Technology.* **90**, pp.254-264.

European Union. 2020. *European Chemicals Agency.* [Online Date accessed 19/07/2019]. Available from: https://echa.europa.eu/

Freitas, S., Merkle, H.P. and Gander, B. 2005. Microencapsulation by solvent extraction/evaporation: reviewing the state of the art of microsphere preparation process technology. *J Control Release.* **102**(2), pp.313-332.

Funabashi, M., Ninomiya, F. and Kunioka, M. 2006. Biodegradation of Polycaprolactone Powders Proposed as Reference Test Materials for International Standard of Biodegradation Evaluation Method. *Journal of Polymers and the Environment.* **15**(1), pp.7-17.

Gadzinski, P., Froelich, A., Jadach, B., Wojtylko, M., Tatarek, A., Bialek, A., Krysztofiak, J., Gackowski, M., Otto, F. and Osmalek, T. 2022. Ionotropic Gelation and Chemical Crosslinking as Methods for Fabrication of Modified-Release Gellan Gum-Based Drug Delivery Systems. *Pharmaceutics.* **15**(1).

Garcia-Depraect, O., Lebrero, R., Rodriguez-Vega, S., Bordel, S., Santos-Beneit, F., Martinez-Mendoza, L.J., Aragao Borner, R., Borner, T. and Munoz, R. 2022. Biodegradation of bioplastics under aerobic and anaerobic aqueous conditions: Kinetics, carbon fate and particle size effect. *Bioresource Technology.* **344**, pp.126-265.

Gentile, P., Chiono, V., Carmagnola, I. and Hatton, P.V. 2014. An overview of poly(lactic-co-glycolic) acid (PLGA)-based biomaterials for bone tissue engineering. *Int J Mol Sci.* **15**(3), pp.3640-3659.

Geyer. R, Jambeck. R and Law. K.L. 2017. Production, use, and fate of all plastics ever made. *Science Advances.*

Gómez, E.F. and Michel, F.C. 2013. Biodegradability of conventional and bio-based plastics and natural fiber composites during composting, anaerobic digestion and long-term soil incubation. *Polymer Degradation and Stability.* **98**(12), pp.2583-2591.

Gouin, S. 2004. Microencapsulation. *Trends in Food Science & Technology.* **15**(7-8), pp.330-347.

Harmaen, A.S., Khalina, A., Azowa, I., Hassan, M.A., Tarmian, A. and Jawaid, M. 2014. Thermal and biodegradation properties of poly(lactic acid)/fertilizer/oil palm fibers blends biocomposites. *Polymer Composites.* **36**(3), pp.576-583.

Harrison, J.P., Boardman, C., O'Callaghan, K., Delort, A.M. and Song, J. 2018. Biodegradability standards for carrier bags and plastic films in aquatic environments: a critical review. *R Soc Open Sci.* **5**(5), p171792.

Harrison, J.P., Sapp, M., Schratzberger, M. and Mark Osborn, A. 2011. Interactions between Microorganisms and marine micro plastics: A call for research. *Marine Technology Society Journal.* **45**(2), pp.12-20.

Hashimoto, K., Sudo, M., Ohta, K., Sugimura, T., Yamada, H. and Aoki, T. 2002. Biodegradation of nylon4 and its blend with nylon6. *Journal of Applied Polymer Science.* **86**(9), pp.2307-2311.

Heiskanen, H., Denifl, P., Hurme, M., Pitkänen, P. and Oksman, M. 2012. Effect of Physical Properties and Emulsification Conditions on the Microsphere Size Prepared Using a Solvent Extraction Process. *Journal of Dispersion Science and Technology.* **33**(2), pp.234-244.

Jain, R. and Tiwari, A. 2015. Biosynthesis of planet friendly bioplastics using renewable carbon source. *J Environ Health Sci Eng.* **13**, p11.

Jaworek, A. 2006. Electrospray droplet sources for thin film deposition. *Journal of Materials Science.* **42**(1), pp.266-297.

Jiang, S., Sudol, E.D., Dimonie, V.L. and El-Aasser, M.S. 2008. Kinetics of dispersion polymerization: Effect of medium composition. *Journal of Polymer Science Part A: Polymer Chemistry.* **46**(11), pp.3638-3647.

Kale, G., Auras, R., Singh, S.P. and Narayan, R. 2007. Biodegradability of polylactide bottles in real and simulated composting conditions. *Polymer Testing.* **26**(8), pp.1049-1061.

Katou, H., Wandrey, A.J. and Gander, B. 2008. Kinetics of solvent extraction/evaporation process for PLGA microparticle fabrication. *Int J Pharm.* **364**(1), pp.45-53.

Kjelsden, A.P., M. Lilley, C. Guznicak, E. Archer, I. 2019. A Review of Standards for Biodegradable Plastics. *Industrial Biotechnology Innovation Centre.*

Kozlowska, J., Prus, W. and Stachowiak, N. 2019. Microparticles based on natural and synthetic polymers for cosmetic applications. *International Journal of Biological Macromolecules.* **129**, pp.952-956.

Kumar, A., Thakur, A. and Panesar, P.S. 2019. Recent developments on sustainable solvents for emulsion liquid membrane processes. *Journal of Cleaner Production.* **240**.

Kumar, G.A., Anjana, K., Hinduja, M., Sujitha, K. and Dharani, G. 2020. Review on plastic wastes in marine environment – Biodegradation and biotechnological solutions. *Marine Pollution Bulletin.* **150**, article no: 110733 [no pagination].

Kunioka, M., Ninomiya, F. and Funabashi, M. 2009. Biodegradation of poly(butylene succinate) powder in a controlled compost at 58 degrees C evaluated by naturally-occurring carbon 14 amounts in evolved CO(2) based on the ISO 14855-2 method. *Int J Mol Sci.* **10**(10), pp.4267-4283.

Lee, J., Hill, A. and Kentish, S. 2013. Formation of a thick aromatic polyamide membrane by interfacial polymerisation. *Separation and Purification Technology.* **104**, pp.276-283.

Lengyel, M., Kállai-Szabó, N., Antal, V., Laki, A.J. and Antal, I. 2019. Microparticles, Microspheres, and Microcapsules for Advanced Drug Delivery. *Scientia Pharmaceutica.* **87**(3).

Leong, J.-Y., Lam, W.-H., Ho, K.-W., Voo, W.-P., Lee, M.F.-X., Lim, H.-P., Lim, S.-L., Tey, B.-T., Poncelet, D. and Chan, E.-S. 2016. Advances in fabricating spherical alginate hydrogels with controlled particle designs by ionotropic gelation as encapsulation systems. *Particuology.* **24**, pp.44-60.

Makadia, H.K. and Siegel, S.J. 2011. Poly Lactic-co-Glycolic Acid (PLGA) as Biodegradable Controlled Drug Delivery Carrier. *Polymers (Basel).* **3**(3), pp.1377-1397.

Massardier-Nageotte, V., Pestre, C., Cruard-Pradet, T. and Bayard, R. 2006. Aerobic and anaerobic biodegradability of polymer films and physico-chemical characterization. *Polymer Degradation and Stability.* **91**(3), pp.620-627.

Mauguet, M.C., Legrand, J., Brujes, L., Carnelle, G., Larre, C. and Popineau, Y. 2002. Gliadin matrices for microencapsulation processes by simple coacervation method. *J Microencapsul.* **19**(3), pp.377-384.

McDonough, K., Itrich, N., Casteel, K., Menzies, J., Williams, T., Krivos, K. and Price, J. 2017. Assessing the biodegradability of microparticles disposed down the drain. *Chemosphere.* **175**, pp.452-458.

Mezhuev, Y.O., Motyakin, M.V., Plyushchii, I.V., Alekperov, R.A., Luss, A.L., Kovarskii, A.L., Degtyarev, Y.N., Ionova, I.S., Dyatlov, V.A., Vorobev, I.Y., Vagramyan, T.A., Abrashov, A.A., Tsatsakis, A.M., Shtilman, M.I. and Korshak, Y.V. 2020. Interfacial oxidative polymerization of aniline on silica gel's surface. *Polymer.* **203**, p122808.

Mihai, M., Legros, N. and Alemdar, A. 2014. Formulation-properties versatility of wood fiber biocomposites based on polylactide and polylactide/thermoplastic starch blends. *Polymer Engineering & Science.* **54**(6), pp.1325-1340.

Modelli, A., Calcagno, B. and Scandola, M. 1999. Kinetics of Aerobic Polymer Degradation in Soil by Means of the ASTM D 5988-96 Standard Method. *Journal of Environmental Polymer Degradation.* **7**(2), pp.109-116.

Mohee, R., Unmar, G.D., Mudhoo, A. and Khadoo, P. 2008. Biodegradability of biodegradable/degradable plastic materials under aerobic and anaerobic conditions. *Waste Manag.* **28**(9), pp.1624-1629.

Mostafa, N.A., Farag, A.A., Abo-dief, H.M. and Tayeb, A.M. 2018. Production of biodegradable plastic from agricultural wastes. *Arabian Journal of Chemistry.* **11**(4), pp.546-553.
Nair, L.S. and Laurencin, C.T. 2007. Biodegradable polymers as biomaterials. *Progress in Polymer Science.* **32**(8-9), pp.762-798.

Nakasaki, K., Matsuura, H., Tanaka, H. and Sakai, T. 2006. Synergy of two thermophiles enables decomposition of poly-epsilon-caprolactone under composting conditions. *FEMS Microbiol Ecol.* **58**(3), pp.373-383.

Nam, H.C. and Park, W.H. 2020. Aliphatic Polyester-Based Biodegradable Microbeads for Sustainable Cosmetics. *Acs Biomaterials Science & Engineering.* **6**(4), pp.2440-2449.

Pagga, U., Schafer, A., Muller, R.J. and Pantke, M. 2000. Determination of the aerobic biodegradability of polymeric material in aquatic batch tests. *Chemosphere.* **42**, pp.319-331.

Pastorino, L., Pioli, F., Zilli, M., Converti, A. and Nicolini, C. 2004. Lipase-catalyzed degradation of poly(ε-caprolactone). *Enzyme and Microbial Technology.* **35**(4), pp.321-326.

Perignon, C., Ongmayeb, G., Neufeld, R., Frere, Y. and Poncelet, D. 2015. Microencapsulation by interfacial polymerisation: membrane formation and structure. *Journal of Microencapsulation.* **32**(1), pp.1-15.

Qi, R., Jones, D.L., Li, Z., Liu, Q. and Yan, C. 2020. Behavior of microplastics and plastic film residues in the soil environment: A critical review. *Science of the Total Environment.* **703**, article no: 134722 [no pagination].

Qin, R., Su, C., Liu, W., Tang, L., Li, X., Deng, X., Wang, A. and Chen, Z. 2020. Effects of exposure to polyether sulfone microplastic on the nitrifying process and microbial community structure in aerobic granular sludge. *Bioresource Technology.* **302**, article no: 122827 [no pagination].

Ragusa, A., Svelato, A., Santacroce, C., Catalano, P., Notarstefano, V., Carnevali, O., Papa, F., Rongioletti, M.C.A., Baiocco, F., Draghi, S., D'Amore, E., Rinaldo, D., Matta, M. and Giorgini, E. 2021. Plasticenta: First evidence of microplastics in human placenta. *Environment International.* **146**, p106274.

Rana, S., Chaudhary, H., Arora, V., Kholi, K. and Kumar, D. 2013. Effect of Physicochemical Properties of Biodegradable Polymers on Nano Drug Delivery. *Polymer Reviews.* **53**.

Reul, R., Renette, T., Bege, N. and Kissel, T. 2011. Nanoparticles for paclitaxel delivery: a comparative study of different types of dendritic polyesters and their degradation behavior. *Int J Pharm.* **407**(1-2), pp.190-196.

Richez, A.P., Yow, H.N., Biggs, S. and Cayre, O.J. 2013. Dispersion polymerization in non-polar solvent: Evolution toward emerging applications. *Progress in Polymer Science.* **38**(6), pp.897-931.

Rosato, A., Barone, M., Negroni, A., Brigidi, P., Fava, F., Xu, P., Candela, M. and Zanaroli, G. 2020. Microbial colonization of different microplastic types and biotransformation of sorbed PCBs by a marine anaerobic bacterial community. *Science of the Total Environment.* **705**, article no: 135790 [no pagination].

Sarasa, J., Gracia, J.M. and Javierre, C. 2009. Study of the biodisintegration of a bioplastic material waste. *Bioresour Technol.* **100**(15), pp.3764-3768.

Schuck, P., Jeantet, R., Bhandari, B., Chen, X.D., Perrone, Í.T., de Carvalho, A.F., Fenelon, M. and Kelly, P. 2016. Recent advances in spray drying relevant to the dairy industry: A comprehensive critical review. *Drying Technology.* **34**(15), pp.1773-1790.

Scudo, A., Liebmann, B., Corden, C., Tyler, D., Kreissing, J. and Warwick, O. 2017. *Intentionally added microplastics in products.* UK: Amec Foster Wheeler Environment & Infrastructure UK Limited.

Sing, C.E. and Perry, S.L. 2020. Recent progress in the science of complex coacervation. *Soft Matter.* **16**(12), pp.2885-2914.

Siracusa, V. 2019. Microbial Degradation of Synthetic Biopolymers Waste. *Polymers (Basel).* **11**(6).

Song, J.H., Murphy, R.J., Narayan, R. and Davies, G.B. 2009. Biodegradable and compostable alternatives to conventional plastics. *Philos Trans R Soc Lond B Biol Sci.* **364**(1526), pp.2127-2139.

Song, P.P., Wu, Y.Y., Zhang, X.M., Yan, Z.Y., Wang, M. and Xu, F. 2018. Preparation of Covalently Crosslinked Sodium Alginate/Hydroxypropyl Methylcellulose pH-Sensitive Microspheres for Controlled Drug Release. *Bioresources.* **13**(4), pp.8614-8628.

Sridewi, N., Bhubalan, K. and Sudesh, K. 2006. Degradation of commercially important polyhydroxyalkanoates in tropical mangrove ecosystem. *Polymer Degradation and Stability.* **91**(12), pp.2931-2940.

Staff, R.H., Landfester, K. and Crespy, D. 2013. Recent Advances in the Emulsion Solvent Evaporation Technique for the Preparation of Nanoparticles

and Nanocapsules. *Hierarchical Macromolecular Structures: 60 Years after the Staudinger Nobel Prize II.* pp.329-344.

Staff, R.H., Schaeffel, D., Turshatov, A., Donadio, D., Butt, H.J., Landfester, K., Koynov, K. and Crespy, D. 2013. Particle formation in the emulsion-solvent evaporation process. *Small.* **9**(20), pp.3514-3522.

Tabasi, R.Y. and Ajji, A. 2015. Selective degradation of biodegradable blends in simulated laboratory composting. *Polymer Degradation and Stability.* **120**, pp.435-442.

Tachibana, K., Urano, Y. and Numata, K. 2013. Biodegradability of nylon 4 film in a marine environment. *Polymer Degradation and Stability.* **98**(9), pp.1847-1851.

Thellen, C., Coyne, M., Froio, D., Auerbach, M., Wirsen, C. and Ratto, J.A. 2008. A Processing, Characterization and Marine Biodegradation Study of Melt-Extruded Polyhydroxyalkanoate (PHA) Films. *Journal of Polymers and the Environment.* **16**(1), pp.1-11.

Tokiwa, Y., Calabia, B.P., Ugwu, C.U. and Aiba, S. 2009. Biodegradability of plastics. *Int J Mol Sci.* **10**(9), pp.3722-3742.

Tokiwa, Y. and Suzuki, T. 2014. Hydrolysis of Polyesters byRhizopus delemarLipase. *Agricultural and Biological Chemistry.* **42**(5), pp.1071-1072.

Tosin, M., Pischedda, A. and Degli-Innocenti, F. 2019. Biodegradation kinetics in soil of a multi-constituent biodegradable plastic. *Polymer Degradation and Stability.* **166**, pp.213-218.

Vaverková, M. and Adamcová, D. 2015. Biodegrability of Bioplastic Materials in a Controlled Composting Environment. *Journal of Ecological Engineering.* **16**, pp.155-160.

Vogel, C. and Siesler, H.W. 2008. Thermal Degradation of Poly(ε-caprolactone), Poly(L-lactic acid) and their Blends with Poly(3-hydroxy-butyrate) Studied by TGA/FT-IR Spectroscopy. *Macromolecular Symposia.* **265**(1), pp.183-194.

Volova, T.G., Boyandin, A.N., Vasiliev, A.D., Karpov, V.A., Prudnikova, S.V., Mishukova, O.V., Boyarskikh, U.A., Filipenko, M.L., Rudnev, V.P., Bá Xuân, B., Việt Dũng, V. and Gitelson, I.I. 2010. Biodegradation of polyhydroxyalkanoates (PHAs) in tropical coastal waters and identification of PHA-degrading bacteria. *Polymer Degradation and Stability.* **95**(12), pp.2350-2359.

Wang, G.X., Huang, D., Ji, J.H., Völker, C. and Wurm, F.R. 2020. Seawater-Degradable Polymers—Fighting the Marine Plastic Pollution. *Advanced Science.*
Wang, X., Shen, L.L. and An, Z.S. 2018. Dispersion polymerization in environmentally benign solvents via reversible deactivation radical polymerization. *Progress in Polymer Science.* **83**, pp.1-27.

Weng, Y.-X., Wang, X.-L. and Wang, Y.-Z. 2011. Biodegradation behavior of PHAs with different chemical structures under controlled composting conditions. *Polymer Testing.* **30**(4), pp.372-380.

Woolnough, C.A., Charlton, T., Yee, L.H., Sarris, M. and Foster, L.J.R. 2008. Surface changes in polyhydroxyalkanoate films during biodegradation and biofouling. *Polymer International.* **57**(9), pp.1042-1051.

Wu, C.-S. 2014. Preparation and Characterization of Polyhydroxyalkanoate Bioplastic-Based Green Renewable Composites from Rice Husk. *Journal of Polymers and the Environment.* **22**(3), pp.384-392.

Wu, C.S. 2011. Preparation, characterization, and biodegradability of renewable resource-based composites from recycled polylactide bioplastic and sisal fibers. *Journal of Applied Polymer Science.* **123**(1), pp.347-355.

Wu, W.N., Gao, J.M., Shen, Q., Yao, L.F. and An, L.H. 2019. Comparison of microplastic extraction methods from organisms. *Zhongguo Huanjing Kexue/China Environmental Science.* **39**(10), pp.4343-4349.

Xiao, Z., Liu, W., Zhu, G., Zhou, R. and Niu, Y. 2014. A review of the preparation and application of flavour and essential oils microcapsules based on complex coacervation technology. *J Sci Food Agric.* **94**(8), pp.1482-1494.

Zhang, S., Wang, J., Liu, X., Qu, F., Wang, X., Wang, X., Li, Y. and Sun, Y. 2019. Microplastics in the environment: A review of analytical methods, distribution, and biological effects. *TrAC Trends in Analytical Chemistry.* **111**, pp.62-72.

Zhao, L., Su, C., Liu, W., Qin, R., Tang, L., Deng, X., Wu, S. and Chen, M. 2020. Exposure to polyamide 66 microplastic leads to effects performance and microbial community structure of aerobic granular sludge. *Ecotoxicology and Environmental Safety.* **190**, article no: 110070 [no pagination].

Zhao, W.W. and Wang, Y.L. 2017. Coacervation with surfactants: From single-chain surfactants to gemini surfactants. *Advances in Colloid and Interface Science.* **239**, pp.199-212.

Zhong, F. and Pan, C.-Y. 2022. Dispersion Polymerization versus Emulsifier-Free Emulsion Polymerization for Nano-Object Fabrication: A Comprehensive Comparison. **43**(3), p2100566.

Chapter 3 Preparation of polymeric microparticles

3.1 Introduction

The objective of this chapter was to synthesize polymer microparticles (PMPs) using a biodegradable polymer through a simple and efficient method to produce particles similar to those used in industry. Among the various methods discussed in Chapter 2, the solvent extraction method was selected for its simplicity and relevance to industrial applications.

.

3.2 Materials and Methods

3.2.1 Materials

Polycaprolactone**,** Mn (45 kDa polydispersity 1.2 - 1.8, PLGA – poly (D, L-lactide-co-glycolide) (75:25), mol wt 66 kDa – 107 kDa, no data for polydispersity. PHB - Poly [(R)-3-hydroxybutyric acid], natural origin, no molecular weight data available, Tween 80 (non-ionic surfactant), >50% purity and Dichloromethane (DCM), >99/8% purity and chloroform, > 99.5% purity were purchased from Sigma Aldrich. Gelatine from procine skin (viscosifier), Type A, 78-80 millimoles of free carboxyl groups per 100 g of protein, isoelectric point of 7.0-9.5, CAS# 9000-70-8 was purchased from BioServ, UK. All solutions were prepared using Milli-Q water which was purified by a Milli-Q apparatus (Merck Milli-Q EQ7008, UK) with an ionic purity of 18.2 MΩ·cm at 25°C.

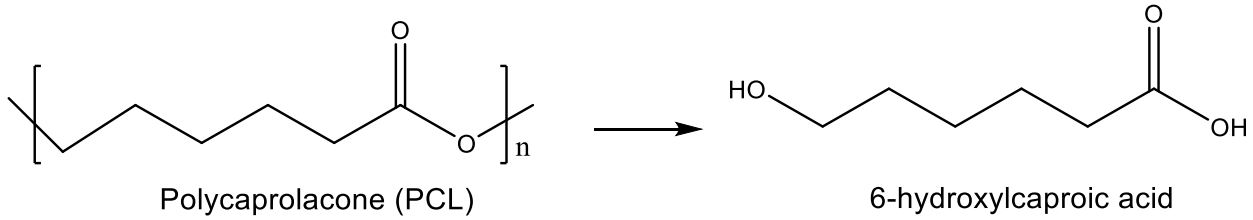
3.2.2 Biodegradable polymers

The following section provides information of the biodegradable polymers used for the preparation of microparticles.

3.2.2.1 Polycaprolactone (PCL)

PCL is a synthetic polymer that can be degraded by microorganisms and is derived from the chemical synthesis of crude petroleum (Labet and Thielemans, 2009; Bartnikowski et al., 2019). It is a partially-crystalline aliphatic polyester with a low melting point (60°C) and a glass transition temperature of -60 °C. In addition, PCL is a thermoplastic polymer, which has chemical resistance to water, oil and chlorine. The low melting point of PCL makes it suitable for composting, which will help in the disposal of this polymer. Moreover, PCL has low viscosity and it is easy to process because it can be soluble in a wide range of organic solvents (Funabashi et al., 2006; Nair and Laurencin, 2007). The molecular formula of PCL is $(C_6H_{10}O_2)_n$ and it is synthesized by ring-opening polymerization of the cyclic monomer Ɛ-caprolactone (Tokiwa et al., 2009). There are many applications of PCL or example PCL can be used as sutures, anchors and scaffold for tissue engineering. This polymer is composed of a 6-hydroxyhexanoate backbone, which can be attacked by microorganisms and undergo biodegradation (Bartnikowski et al., 2019). During the degradation of PCL, enzymes from the microorganisms break down complex polymers to yield shorter chains or new molecules entirely. These short-chain molecules are then mineralised into final respiratory products, which are utilised as carbon and energy sources and may be quantified similarly to respirometric analysis (Shah et al., 2008). Enzymatic degradation of polymers is a two-step process. First, the enzyme binds to the polymer substrate, the second is the catalysis of a hydrolytic cleavage, breaking apart the polymer chain as shown in **Figure 3:1** (Bartnikowski et al., 2019). During degradation, enzymes from the microorganisms break down complex polymers to yield shorter chains or new molecules entirely. These short-chain molecules are then mineralised into final respiratory products, which are utilised as carbon and energy sources and may be quantified similarly to respirometric analysis (Shah et al., 2008). An enzymatic degradation test of polycaprolactone (PCL) powders was reported using an amino lipase enzyme from *Pseudomonas cepacia* which is known to be the degradation enzyme for

PCL PMPs (63 to 250 µm) by Funabashi et al. (2006). Fragmentation of the biodegradable polymers into oligomers of smaller molecular weights results in larger surface to volume ratio for the enzymes to act upon. Enzymatic depolymerisation of the polymers releases oligomers and/or monomers that can be easily assimilated by the microorganisms as a carbon source resulting to increase in microbial biomass (Kumar, G.A. et al., 2020). The degradation of PCL is shown below:



Polycaprolacone (PCL) 6-hydroxylcaproic acid

Figure 3:1 Chemical structure of polycaprolactone (PCL) and its resulting monomer after biodegradation (Bartnikowski et al., 2019)

3.2.2.2 Poly (D, L-lactide-co-glycolide) (75:25) – (PLGA)

This class of polymer includes polyglycolide (PGA), poly (L-lactide) (PLA), and poly (D, L-lactide-co-glycolide) (PLGA). Poly (D, L-lactide-co-glycolide) (PLGA) is more hydrophilic than the other polyesters widely used for biomedical applications, such as poly(lactic acid) and poly(ε-caprolactone) (Ferrari et al., 2013). PGA is a hydrophilic and highly crystalline polymer with a relatively fast degradation rate. Although structurally very similar to PGA, PLA exhibits different chemical, physical, and mechanical properties because of the presence of a pendant methyl group on the alpha carbon. Generally, the co-polymer PLGA is preferred compared with its constituent homopolymers for the fabrication of bone substitute constructs, as PLGA offers superior control compared with degradation properties by varying the ratio between its monomers (Gentile et al., 2014). PLGA, for instance, has a wide range of degradation rates, governed by the composition of chains, both hydrophobic/hydrophilic balance and crystallinity. These polymers are able to undergo degradation via hydrolytic cleavage of the ester linkages that make up the polymer backbone. For PGA, PLA and PLGA, the degradation by-products, lactic acid and glycolic acid as shown in **Figure 3:2**, are water- soluble and non-toxic products of normal metabolism with the rate of degradation dependent on the chain length (molecular weight) and the lactide/glycolide ratio (Ammala, 2013). In cosmetic applications, the use of PLA has been recently reported to encapsulate retinyl retinoate as an anti-wrinkle treatment (Ammala, 2013). The degradation process of PLGA is shown below:

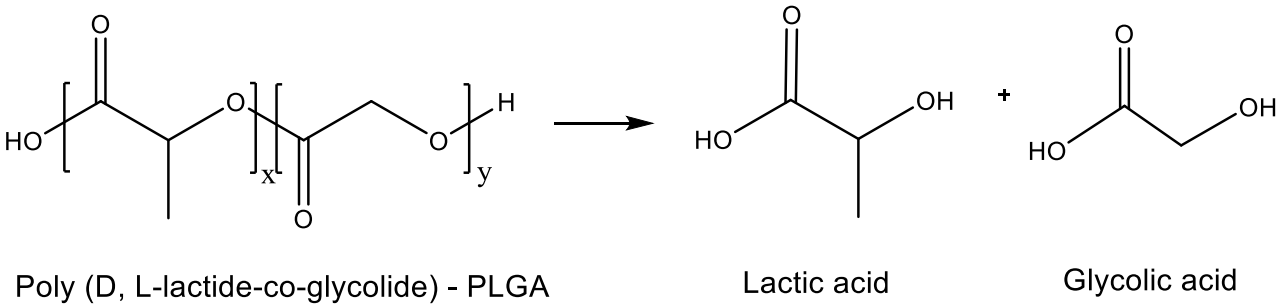
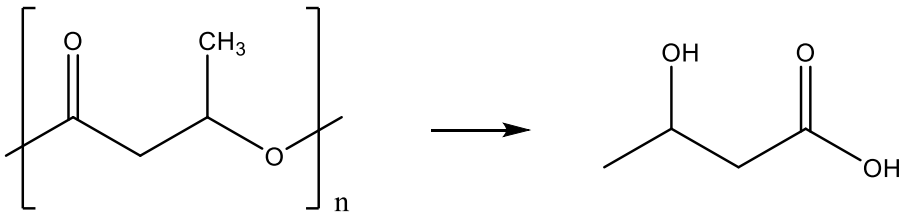


Figure 3:2 - Chemical structure of poly (D, L-lactide-co-glycolide) (x, number of lactic acid units; y, number of glycolic acid units) and its monomers (Ferrari et al., 2013; Gentile et al., 2014)

3.2.2.3 Poly [(R)-3-hydroxybutyric acid] – (PHB)

PHB is a bacterial polyester that is highly crystalline with a melting temperature of 180°C and a Tg ~5°C. PHB is a polyester that occurs naturally and accumulates in bacterial cells as a reservoir of carbon and energy (Laycock et al., 2017). It can be produced from other types of substrates including renewable resources like starch, cellulose and sucrose or from fossil resources like methane, mineral oil and hard coal. There are a number of potential applications of PHB in different disciplines such as example in medicine where PHB can be used as sutures, surgical mesh and many other applications (Leja and Lewandowicz, 2010). Other applications of PHB are in pharmacology where it can be used as microcapsules in drug treatment and for controlled drug release (Gonzalez-Pleiter et al., 2019). PHB can be used in the food industry and this includes bottles, laminated foil and one-use cups (Govindasamy et al., 2019). PHB can be fully degraded and converted to carbon dioxide and energy by the action of microorganisms such as bacteria and fungi (Volova et al., 2010; Volova et al., 2011; Boyandin et al., 2013). Gebauer and Jendrossek (2006) investigated the degradation of poly(3-hydroxybutyrate) (PHB) using a pH stat to monitor the NaOH consumption to neutralise 3-hyroxybutaric acid (3HB). The degradation process of PHB is shown below in **Figure 3:3**:



Poly[(R)-3-hydroxybutyric acid] - (PHB) 3-hydroxybutyric acid

Figure 3:3 – Chemical structure of poly [(R)-3-hydroxybutyric acid] and its monomers (Yu et al., 2005; Gebauer and Jendrossek, 2006; Ariffin et al., 2010)

3.3 Methods

3.4 Preparation of polymeric microparticles (PMPs)

PCL/PLGA and PHB PMPs were prepared by an emulsification-solvent extraction technique (Cao et al., 2015). The solvent phase (also the emulsion dispersed phase) was prepared using a known mass of polymer (0.5 g) dissolved in 20 ml of dichloromethane (for PHB, chloroform was used). This solution was added into 200 mL of a pre-prepared aqueous solution (emulsion continuous phase) containing 0.5% gelatine and 0.05% of Tween-80 in a 250 mL glass beaker. The solvent/W emulsion was then formed using an UltraTurrax (180 mm head diameter) homogeniser operated at varying speed (4000, 8000 and 12000 rpm) for 1 min. The emulsion system was then continuously stirred overnight to allow for complete evaporation of the solvent extracted into the water continuous phase in a 250 mL glass beaker at 350 rpm on a magnetic stirrer in the fume hood. Finally, the produced PMPs were washed 3 times with centrifugation force of 9000 rpm for 5 mins with the supernatant replaced with fresh Milli-Q water to remove gelatine, excess surfactant and any remaining solvent from the sample (**Figure 3:4**).

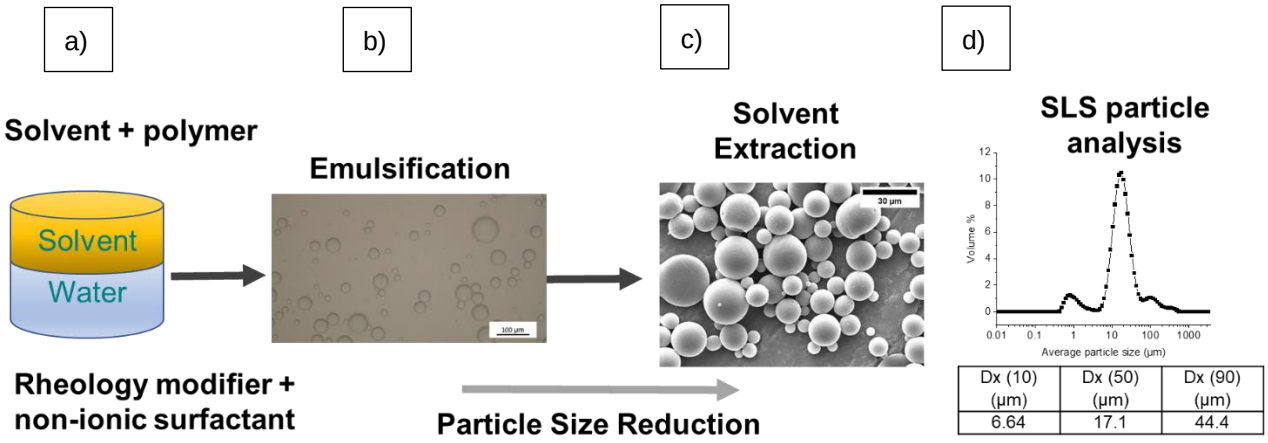


Figure 3:4 - Process of preparation of polymeric microparticles (PMPs) using the solvent extraction method where the various steps consist of a) to b) emulsification of a dispersed phase (polymer in DCM) into an aqueous continuous phase containing a rheology modifier and a non-ionic surfactant via high shear homogenisation, b to c/d) complete extraction and evaporation of the dispersed phase solvent from the emulsion droplets to obtain solid polymer particles characterised with c) Scanning Electron Micrograph and d) – and with light diffraction measurements to obtain average particle size distributions.

3.5 Characterisation methods

3.5.1 Light diffraction measurements (LD)

Light diffraction (LD) is a technique used to measure the size distribution of droplets dispersed in a medium in the order of 100 nm -1000 μm size range. LS uses typically a He-Ne or Ar, where the laser is focused on an optically clear cylindrical cell containing the sample. Most of the light passes directly through the sample but a small portion of the light is scattered. This scattered light intensity is detected at an angle, typically from about 15 – 180^{o} from the incident beam by a photomultiplier or photodiode. The angle and intensity of the scattered light detected by the photodiode is then input into an algorithm that uses the “Mie theory”, which converts the intensity of scattered light into particle size distribution data. The “Mie theory” makes certain assumptions such as the particle is spherical and dispersed in an homogeneous solution, and that the refractive index of the particle and the dispersed medium is known. The most common approach for expressing LS results is to report the d43 (De Brouckere mean diameter) and d32 (Sauter mean diameter) values based on a volume and surface area distribution (equation **3:1** and **3:2**), respectively. The d32 is most sensitive to the presence of fine particulates, whereas the d43 is most sensitive to the presence of large particulates in the size distribution.

For this project, particle size distributions were determined at 25^{o}C using a Malvern Mastersizer 3000 (Malvern Instruments Ltd, Malvern, Worcestershire, UK) in conjunction with a Malvern Hydro MV dispersion unit. The samples were diluted in Milli-Q water to give an obscuration of between 4 and 6%. The stirring speed was 2500 rpm. The refractive index of polymeric particles (PCL, PLGA and PHB) were set at 1.46 and the refractive index for the dispersion phase was set at 1.33. The light absorbance value used for the emulsion droplets was 0.01. The mean particle size distribution was reported as volume mean diameter d43 (De Brouckere mean diameter) and surface mean d32 (Sauter mean diameter). The d43 refers to the mean diameter of a sphere with the same volume, whereas the d32 is the diameter of a sphere that has the same volume/surface area ratio as the sphere of interest.

$d_{43} = \frac{\sum_1^n d_i^4 v_i}{\sum_1^n d_i^3 v_i}$	**3:1** De Brouckere mean diameter
$d_{32} = \frac{\sum_1^n d_i^3 v_i}{\sum_1^n d_i^2 v_i}$	**3:2** Sauter mean diameter

where *d* is the diameter and *v* the volume of the *ith* particle.

3.5.2 Optical light microscope

A light microscope uses light to view an image. Brightfield light microscopes produces a dark image on a light background. The light is reflected or refracted from the particle that is being viewed, resulting in a lighter image of the particle. Light passes through the condenser lens to focus the light on the particle. The level of light can be adjusted from the diaphragm. The particle sample is placed on a microscope slide and placed on a stage, light will be reflected, refracted, or/and absorbed by the particle sample. The objective lens and the eyepiece (ocular lens) are used to achieve total magnification. The revolving nosepiece allows the objective lens to be rotated to view under different magnification. Typically, the objective lens consists of 4, 10- and 40-times magnification. The eyepiece lens also consists of magnification lens of typically, 10 times. The total magnification can then calculate as eyepiece lens times by the objective lens. For example, if using eyepiece lens at 10X magnification and objective lens at 4X magnification, the total magnification will be 40X. The coarse focus and fine focus both rise and lower the stage which helps with focusing, the coarse focus moves dramatically whereas the fine focus moves the stage at a slower rate to aid with visualisation, (Hochleitner et al., 2003)

For this project, the emulsions and polymer PMPs were visualised using an Olympus BX51 optical microscope with a digital camera at 10x, 20x and 50x magnification. The optical images of the formation of the particles were viewed as a function of time where a decrease in size is expected as the DCM is progressively extracted from the droplet phase.

3.5.3 Scanning Electron Microscopy (SEM)

Scanning electron microscopes are used to increase magnification and resolution abilities to view particle size ranges at >50 nm. Electron microscope use electron beams to create an image of the sample and to perform chemical analysis of it. The electron beam hits the observed particle and scans its surface. SEM is ideal for visualising a 3D image of a particle surface. The SEM works on the principle of the scattering of secondary electrons on the surface of a particle. In SEM the image is scanned meaning the electrons are reflected from the particles. The particles are scanned from side to side and so a 3D image can be constructed, (Amelinckx et al., 2008).

An electron is the negatively charged particle of an atom orbiting around the nucleus, it is released by an electric field. Electrons are 2000 times lighter than the smallest atom and therefore easily be stopped or diverted when hitting materials. The column of the electron microscope consists of the same parts as the optical microscope, but the source of light is replaced by the electron guns and the glass lenses by electromagnetic ones. The electron beam is produced by the electron gun in which for example Tungsten filament can be placed as the electron source. The beam is produced by heating the filament up to 2700ºC and connected to high voltage, the higher the voltage the higher the energy of the electrons. A schematic illustration is provided in **Figure 3:5**.

Since electrons move freely in a vacuum, there must be only vacuum in the column. To achieve this, vacuum pumps are used, various levels of vacuum are needed, and the highest is around the electron gun. The samples must withstand vacuum and irradiation with electrons. The samples must be conductive and dry.

The SEM was used to obtain information about the morphology of PMPs (size and shape), the surface structure, roughness, and porosity of the particles, which has a significant effect on biodegradation. Visual observation during biodegradation as a function of time can be compared to the PMPs before degradation.

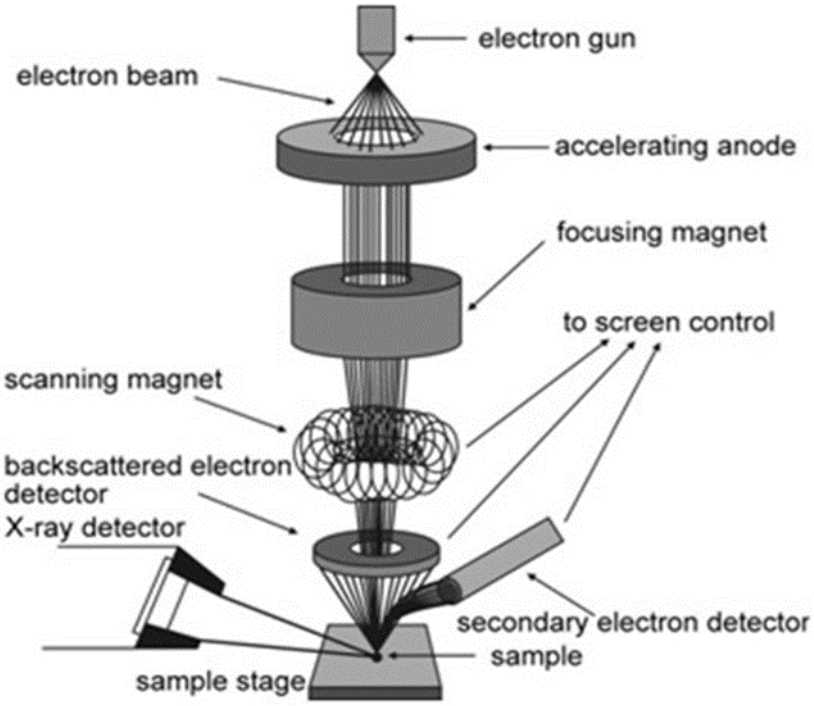


Figure 3:5 - Major components of a scanning electron microscope (Amelinckx et al., 2008).

For this project, the morphological properties of particles were characterised using a Zeiss Evo10 Environmental Scanning Electron Microscope at 20 kV. The samples for SEM analysis were prepared by adding a pipette drop of the suspension onto a stub and left to air dry overnight in a clean environment to avoid any dust contamination. The sample was then coated with platinum with a thickness of 20 nm using Leica EM ACE600 before analysis.

3.6 Calculations

3.6.1 Total surface area of particles

The purpose of measuring the surface area of PMPs is that the ratio of surface area to volume is a significant factor to determine the rate of degradation; the higher the surface area, the higher the biodegradation kinetics (Chinaglia et al., 2018). Additionally, if the degradation is driven by an enzyme, then the enzymes can penetrate through pores of the PMPs and attack more of the available surface area (Funabashi et al., 2006).

The surface area of the particles is calculated from the total surface area which is based on the bin limits of the particle size distribution obtained from the mastersizer, from which a mean size for each bin limit and the surface area is calculated. The total number of PMPs in the system can be calculated from the density and mass of the polymer.

To calculate the total surface area of PCL, PLGA and PHB PMPs, the following equation was applied (equation **3:3**). Example here given with PCL PMPs.

$$S_{tot} = S_{PCL}\ x\ N$$

$$S_{PCL} = 4\pi r^2$$

$$V_{PCL} = \frac{4}{3}\pi r^3$$

$$N = \left(\frac{VT_{PCL}}{V_{PCL}}\right) \qquad \textbf{3:3}$$

Where:

S_{tot}= Total surface area of PCL particles

S_{PCL}= Surface area of single PCL particle

N = Number of PCL particles

V_{PCL}= Volume of single PCL particle

r = Radius of PCL particle

VT_{PCL}= Volume of total PCL particles

$$Volume\ of\ Polycaprolactone = \frac{Mass\ of\ polycaprolactone,\ g}{Density\ of\ polycaprolactone,\ g/cm^3} = \frac{0.50}{1.14}$$
$$= 0.44\ cm^3$$

$$Volume\ of\ 1\ particle\ in\ each\ bin = \frac{4}{3}\ \pi r^3 = \frac{4}{3}\ \pi\ x\ radius\ of\ particle\ in\ each\ bin(\mu m^3)$$
$$= \mu m^3 = m^3$$

$$Total\ volume\ for\ each\ bin\ (m^3) = 0.44 \times volume\ \%$$

$$Number\ of\ particles\ in\ each\ bin\ N$$
$$= Total\ volume\ for\ each\ bin/Volume\ of\ 1\ particle\ in\ each\ bin$$

$$Suface\ area\ of\ particle\ in\ each\ bin\ (m^3)$$
$$= Number\ of\ particles\ in\ sample\ N$$
$$\times Surface\ area\ for\ 1\ particle\ in\ each\ bin\ (m^3)$$

$$The\ total\ surface\ area\ S_{tot}$$
$$= sum\ of\ Total\ suface\ area\ of\ particle\ based\ on\ each\ bin\ (\mu m^2)$$

The total surface area is based on one bin limit and is repeated for all bin limits to get the sum of total surface area based on bin limits.

$$Bin\ limit\ 1 = S_{tot}\ x\ \frac{Volume\ \%}{100}$$

$$Total\ surface\ area\ (bin\ limits) = Sum\ of\ bin\ limits\ Surface\ area$$

3.7 Results and Discussion

3.8 Reproducibility of the solvent extraction method using Polycaprolactone

The aim of this experiment was to test the reproducibility of the solvent extraction production method. A reliable and robust method to develop PMPs is essential to minimise any error in the production of PMPs. The solvent extraction method described in section **3.4** is used for all the PMPs produced throughout this project. For this work, the same conditions are applied to all six batches of PCL PMPs.

3.8.1 Light diffraction measurements of PCL PMPs – repeatability study

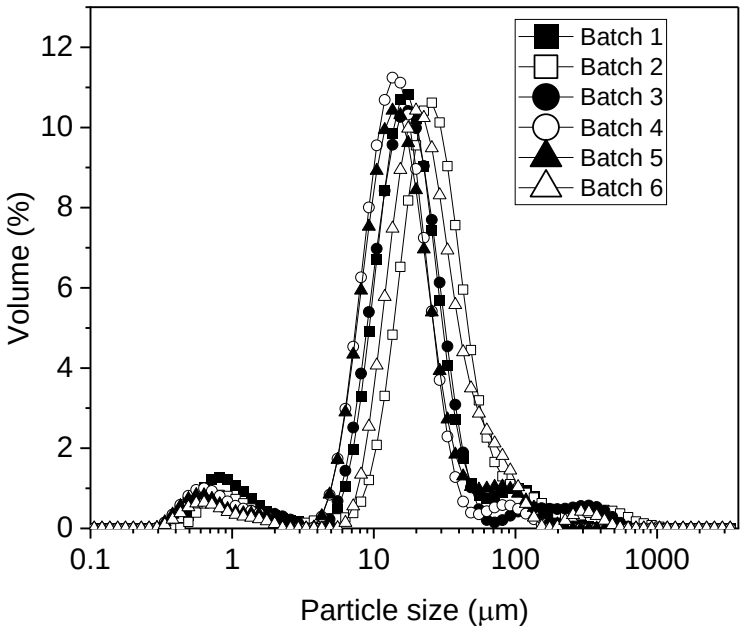


Figure 3:6 - Particle size distribution measured using light diffraction for six batches of PCL PMPs prepared using the same conditions to test repeatability of the particle preparation method.

Table 3:1 –Particle size distribution at D_{10}, D_{50} and D_{90} of PCL PMPs (six repeat batches)

Batch #	**D_{10} (µm)**	**D_{50} (µm)**	**D_{90} (µm)**
1	6.64	17.10	44.40
2	10.90	24.70	53.90
3	7.00	16.80	38.00
4	6.00	13.70	27.30
5	8.50	23.80	69.40
6	10.50	22.10	58.40
Mean	8.26	19.70	48.57
Standard deviation	2.07	4.44	15.10

In **Figure 3:6** it can be observed that the polycaprolactone particles are polydisperse where smaller particles at < 1 µm are observed and the presence of aggregation or larger particles >100 µm is also detected. There is a higher volume contribution of particles between 10-50 µm. The d32 is reported as 8.1 µm and span at 2.36 (**Table 3:4**). The results in **Table 3:1** are promising in that they conclude that the solvent extraction method is repeatable and robust and can be used to prepare further particles under the same conditions. Consequently, one batch was prepared for subsequent PMPs using different polymers (PLGA and PHB) and/or changes in speed to obtain varying particle size.

3.8.2 Droplet to PCL PMPs evolution as a function of time

The emulsions and PCL PMPs were visualised using an Olympus BX51 optical microscope with a digital camera at 10x, 20x and 50x magnification to monitor the evolution from droplet to PCL particles. It is expected that a decrease in droplet size will be observed as the DCM is progressively evaporated (Katou et al., 2008; Staff et al., 2013b). The images of the evolution from droplet to particle as a function of time was conducted by taking a small amount of sample of the emulsion system from the beaker which is continuously stirred and a drop placed on a glass slide and immediately covered with a cover glass. Several images were taken across varying positions on the glass slide to ensure good representation of the sample shown in **Figure 3:7**. CellSens standard was used to record the images.

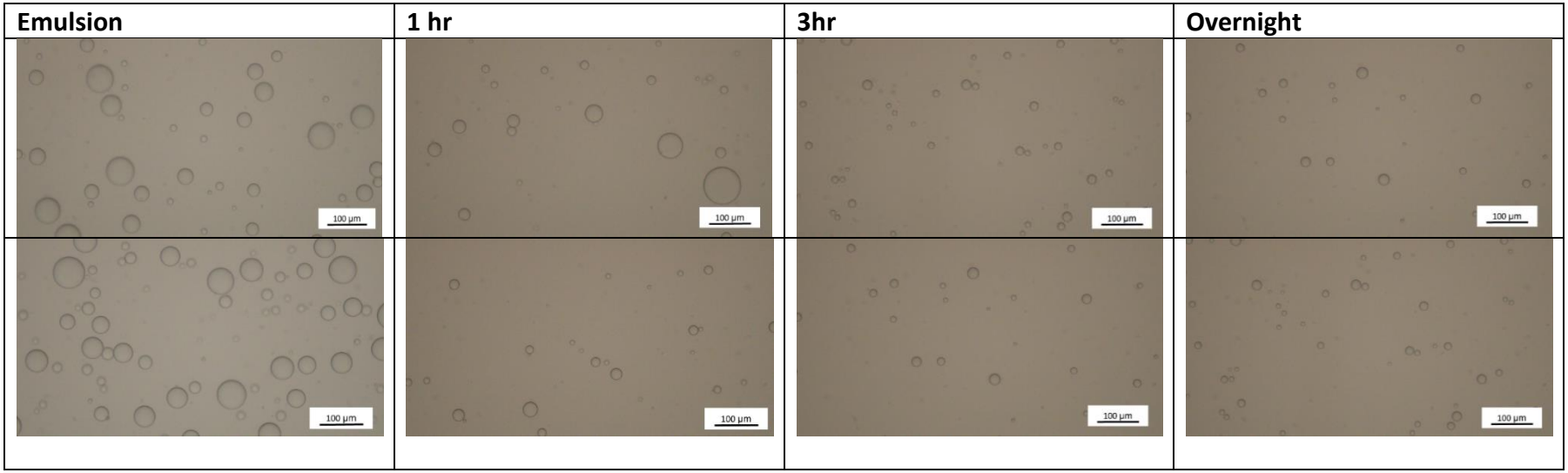


Figure 3:7 - optical micrograph of the evolution of PCL PMPs from emulsion droplets (PCL and dichloromethane) to 1 hr, 3 hr and final PMPs (assuming complete evaporation) in aqueous suspension. Images of emulsion taken after 10 minutes after 1 min homogenisation using UltraTurrax at 8000 rpm (of batch #6). Images taken across varying positions on glass slide to ensure good representation of the sample. Polymer concentration in the disperse phase was 2.44 wt%, the ratio of dispersed phase to continuous phase was 0.25 wt%.

The optical micrographs **Figure 3:7** shows the evolution of PCL PMPs from emulsion droplets (PCL and DCM) observed 10 minutes after the emulsification step. After 1 hour, a reduction in droplet size is observed as the DCM is being extracted from the droplets and evaporated from the emulsion. This is followed by images of PCL PMPs after 3 h and overnight respectively. It is assumed that all the DCM is evaporated overnight as evidenced by the clear reduction in size compared to the initial emulsion droplets. Further confirmation of complete evaporation comes from the washing stage of the particles, where fresh Milli-Q water is replaced three times to ensure removal of excess solvent. It is expected that a change in refractive index between a droplet and solid particles would occur because DCM and polymer do not have the same refractive index thus mixtures of them at different ratios (effectively what the droplets contain at various times in the process) have different refractive indices. This is evident as the images during transition from droplets to particles appear to be darker although this is not very well captured by the microscope images. Several attempts were made to analyse the particle size distribution in optical images taken at different time points using ImageJ. However, this task was found to be infeasible due to the limitations of the software. One major challenge was the inability of ImageJ to accurately detect and measure particles in the images. Additionally, the complexity of the particle size distribution in the images posed difficulties in obtaining reliable results. Overall, the analysis of particle size distribution in optical images using ImageJ was hindered by software limitations and the complexity of the images. One possible solution is to utilise a white filter with confocal EVOS technology. This approach could potentially enhance the accuracy of particle size analysis in optical images. The reduction in particle size is in agreement with the findings from Staff et al. (2013b) where they run a solvent extraction process reported a decrease of the diameter of emulsion droplets (PLA and chloroform) in aqueous continuous phase with time until a plateau was reached (Staff et al., 2013b). The images show spherical particles which are well suspended in the continuous phase, no aggregation or instability is observed throughout the process.

3.8.3 Scanning electron microscopy of PCL PMPs

The PCL PMPs were characterised using scanning electron microscopy to obtain information about the surface structure, roughness, and porosity of PCL PMPs. This information can be used to compare the images before, during and after degradation (Nam and Park, 2020).

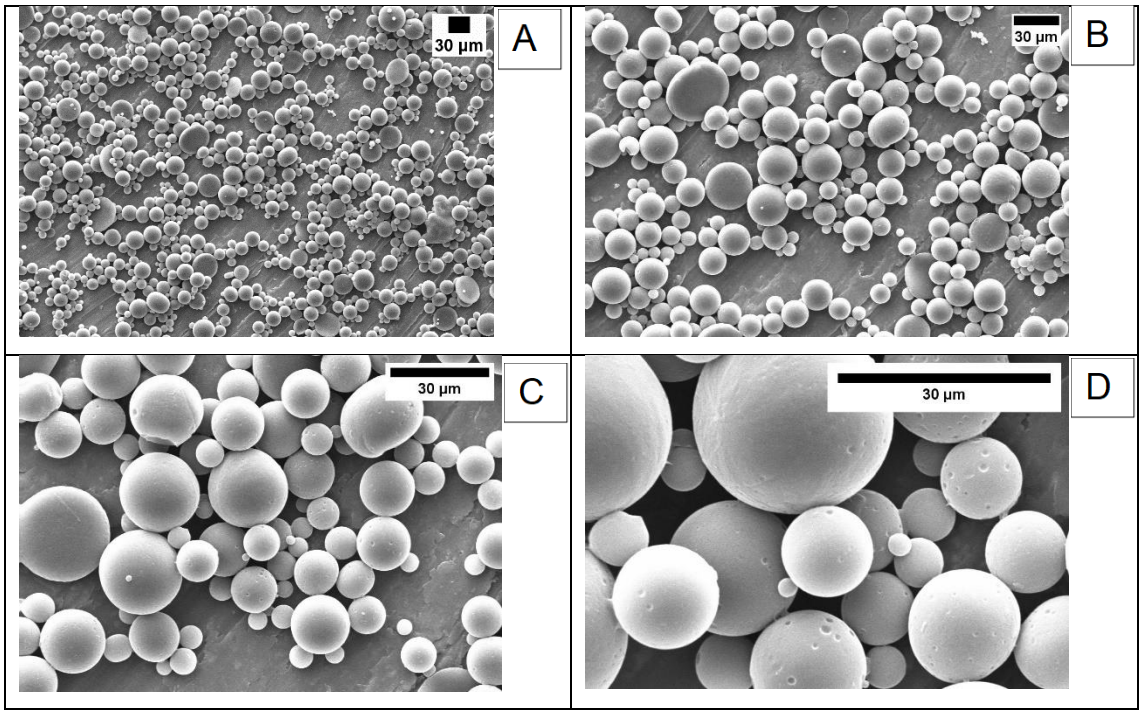


Figure 3:8 - Scanning Electron Micrograph of polycaprolactone PMPs showing spherical particles at A) 500x, B) 1000x, C) 2000 and D) 5000x magnification and a voltage at 20 kV. The sample was coated with platinum with a thickness of 20 nm using Leica EM ACE600 before analysis.

The morphological properties of PCL particles were characterised using Zeiss Evo10 Environmental Scanning Electron Microscope at 20 kV at varying magnifications and depicted in **Figure 3:8.** The PCL PMPs show mostly spherical particles with a smooth surface and range of sizes, these agree with the particle size distribution data from the Mastersizer, further particle size analysis was not conducted. Overall, the particles are in line with the expected outcome in terms of size distribution, surface area and morphology suitable for biodegradation studies as previously reported by several authors (Gonzalez-Pleiter et al., 2019; Qiao et al., 2019; Nam and Park, 2020). Further PMPs are prepared using biodegradable polymers namely poly (D, L-lactide-co-glycolide) (75:25) (PLGA) and poly [(R)-3-hydroxybutyric acid] (PHB) and are discussed in the following section.

3.8.4 Preparation and characterisation of PMPs using alternative biodegradable polymers

The aim of this section was to prepare further PMPs using the same method as for the PCL PMPs reported in section **3.4** so that alternative polymer particles could be tested for biodegradation. Here, we present data using poly (D, L-lactide-co-glycolide) (75:25) (PLGA) and poly [(R)-3-hydroxybutyric acid] (PHB).

In order to test the biodegradation using other polymer type, poly (D, L-lactide-co-glycolide) (75:25) (PLGA) and poly[(R)-3-hydroxybutyric acid] (PHB), were also chosen for biodegradation studies as these are highly cited as being biodegradable and are readily available. Bagheri et al. (2017) conducted a study aimed specifically at determining if the so-called biodegradable polymers can degrade in simulated seawater and freshwater. In this study, PLGA was reported to show 100% degradation as determined by weight loss and change in molar mass with time over 270 days. In comparison PHB showed about 8% mass loss with no change in molar mass at day 365. This demonstrates the uncertainty of biodegradability claims of polymers and in some cases, significant chemical modifications are needed for these polymers to be developed into PMPs, which in turn affects their biodegradability (McDonough et al., 2017).

3.9 PLGA – poly (D, L-lactide-co-glycolide) (75:25) PMPs

For this work, the same conditions to prepare PLGA PMPs are applied as previously mentioned in section **3.4**. When the Hansen solubility parameters (HSP) of both polymers (PCL and PLGA) were investigated by Pawlik et al. (2019) they found that PLGA was more soluble in DCM than PCL, thus DCM was used to dissolve PLGA polymer.

3.9.1 Light diffraction measurements of PLGA PMPs

In the previous section, light diffraction was used to determine the particle size distribution of the PCL PMPs and showed a polydisperse system. Similar method is used to determine the size distribution of PLGA PMPs.

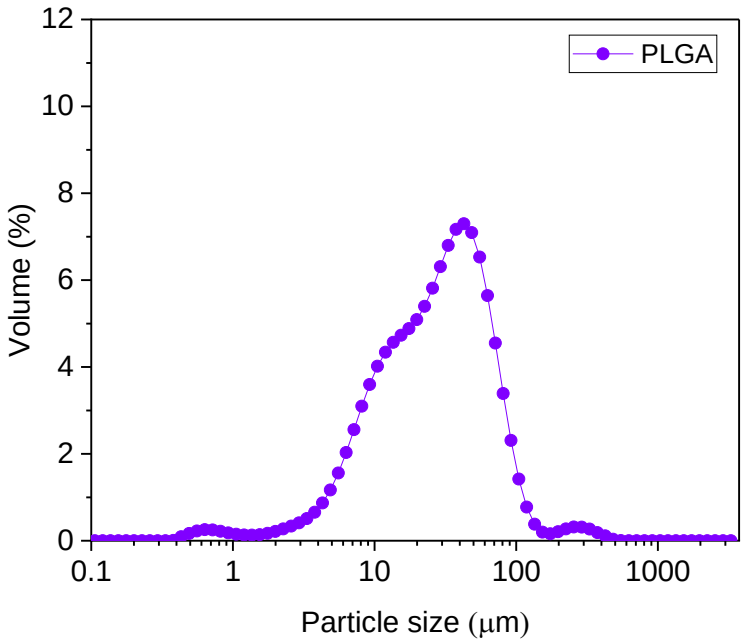


Figure 3:9 – Particle size distribution measured using light diffraction of PLGA PMPs stabilised with 0.05 wt% surfactant in the aqueous phase with a gelatine concentration of 0.5 wt%. The polymer concentration (0.5 g) in the disperse phase was 2.44 wt% (2.83 v%) in DCM, the ratio of dispersed phase to continuous phase was 0.25 wt%.

Table 3:2 – Mean Particle size distribution at D_{10}, D_{50} and D_{90} of PLGA particles

	D_{10} (µm)	D_{50} (µm)	D_{90} (µm)
Mean	7.39	28.4	72.4
Standard Deviation	0.03	0.20	1.04
RSD (%)	0.36	0.72	1.44

As expected, the PLGA particle size distribution shown in **Figure 3:9** shows a polydisperse system with d32 reported as 12.5 µm and span at 2.22 **(Table 3:4).** These differ from the PCL PMPs where d32 was reported as 10.1 µm and span at 2.36. A number of factors can be related to the differences. The polymer molecular weight can play a significant role in the initial size of the droplets developed during the solvent extraction process, which in turn affects the viscosity of the dispersed phase. In this case, the PCL polymer has a molecular weight of 45,000 kDa, whereas, the molecular weight of PLGA is higher at 66-107 kDa. Generally, the higher the molecular weight, the higher the viscosity in a solution. Increased viscosity of the dispersed phase yields larger microparticles because higher shear forces are necessary to break up the droplets (Heiskanen et al., 2012a). However, as the same method parameters are applied as the PCL PMPs preparation, the speed was unchanged which contributed to the larger particles seen here. Consequently, this is supported by the optical images in **Figure 3:10** and the SEM images in **Figure 3:11**. The size distribution for the PLGA PMPs are broader when compared to the size distribution of PCL PMPs using the same conditions depicted in **Figure 3:6**. Although repeatability tests confirmed a robust method for preparing microparticles was achieved with PCL polymer, in this case, the polymer (PLGA) was different. The difference in the particle size distribution could be due to several factors such as the change in viscosity of the dispersed and continuous phases when changing the polymer, the solubility of the different chemicals, the different interfacial tensions of the system, and the coefficient of diffusion of the droplets (Staff et al., 2013b).

3.9.2 Droplet to PLGA particle evolution as a function of time

The emulsions and particles were visualised using an Olympus BX51 optical microscope with a digital camera at 10x, 20x and 50x magnification to monitor the evolution from droplet to PLGA particles.

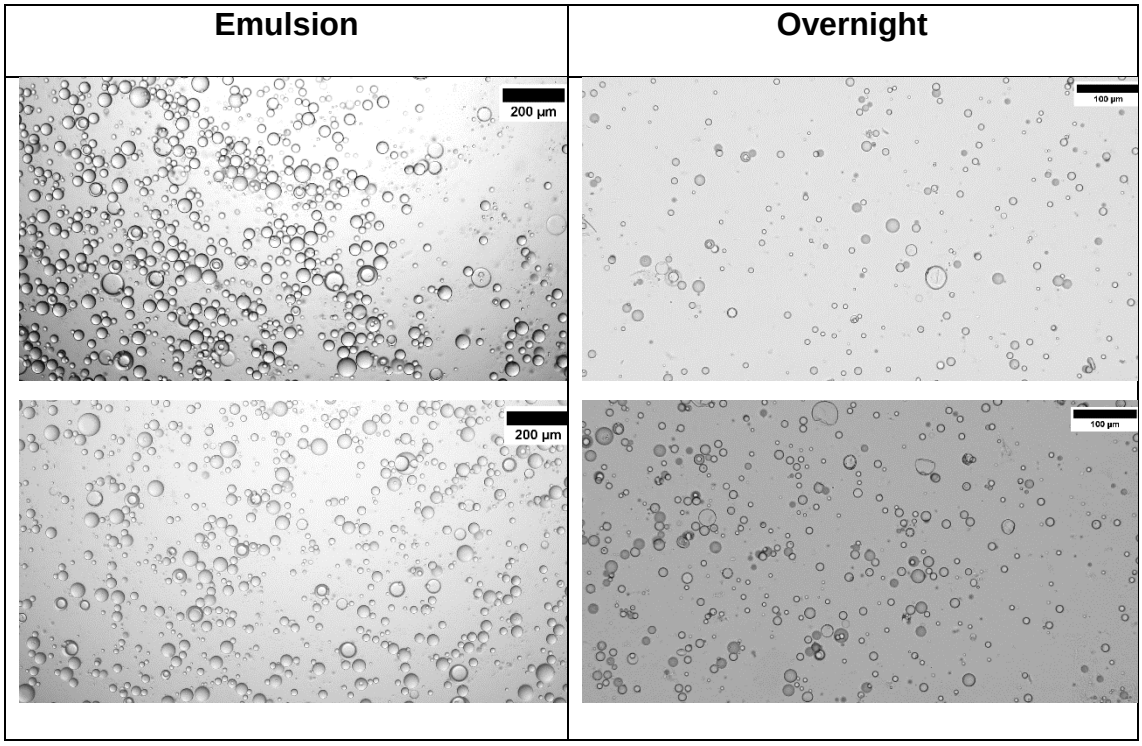


Figure 3:10 – optical micrograph of the evolution of PLGA PMPs from emulsion droplets (PLGA and dichloromethane) to final PMPs (assuming complete evaporation) in aqueous suspension. Images of emulsion taken after 10 minutes after 1 min homogenisation using UltraTurrax at 8000 rpm. Images taken across varying positions on glass slide to ensure good representation of the sample. Polymer concentration in the disperse phase was 2.44 wt%. The ratio of dispersed phase to continuous phase was 0.25 wt%

3.9.3 Scanning electron microscopy of PLGA PMPs

The PLGA PMPs were characterised using scanning electron microscopy to obtain information about the surface structure, roughness, and porosity of PLGA PMPs. This information can be used to compare the images before, during and after degradation (Nam and Park, 2020).

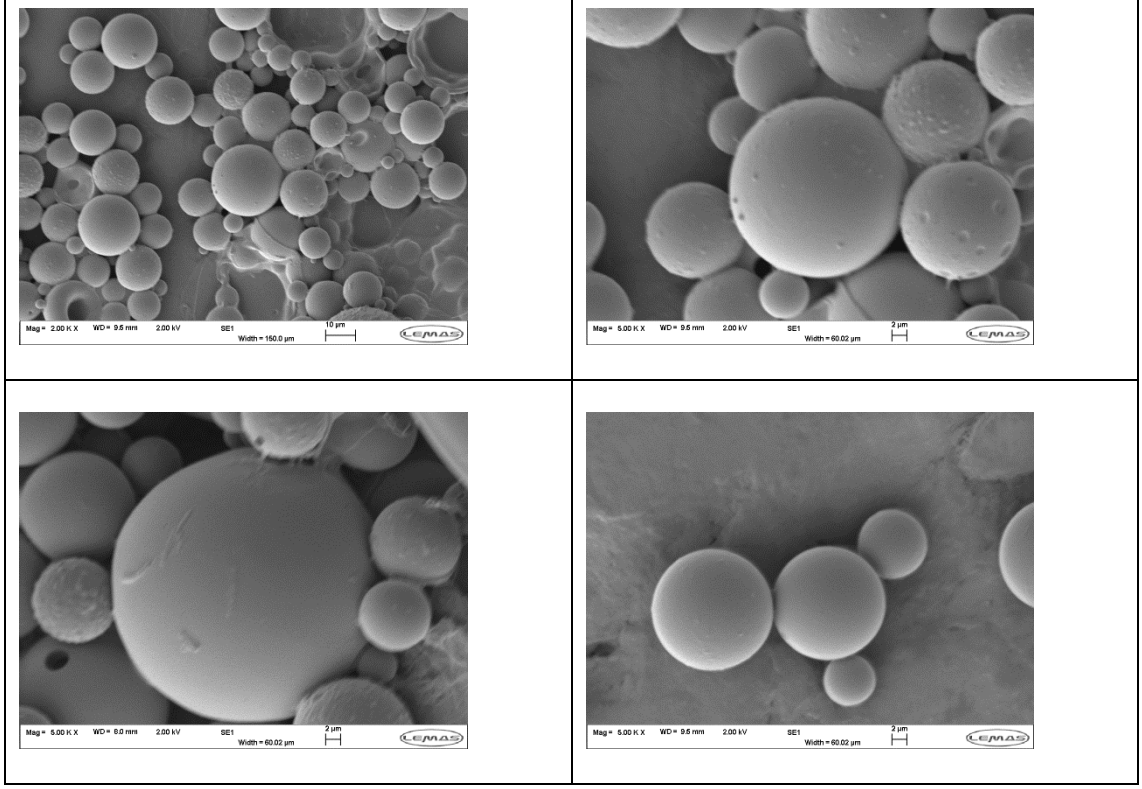


Figure 3:11 - Scanning Electron Micrograph of PLGA PMPs at clockwise 2000x, and 5000x magnification and a voltage at 20 kV. The sample was coated with platinum with a thickness of 20 nm using Leica EM ACE600 before analysis.

3.10 Poly [(R)-3-hydroxybutyric acid] – (PHB) PMPs

3.10.1 Light diffraction measurement of PHB PMPs

In this work, the same conditions used to prepare PCL and PLGA PMPs are applied as previously mentioned with the exception that the solvent used was chloroform instead of dichloromethane previously used. This is due to the change in solubility between the polymer (PHB) and solvent.

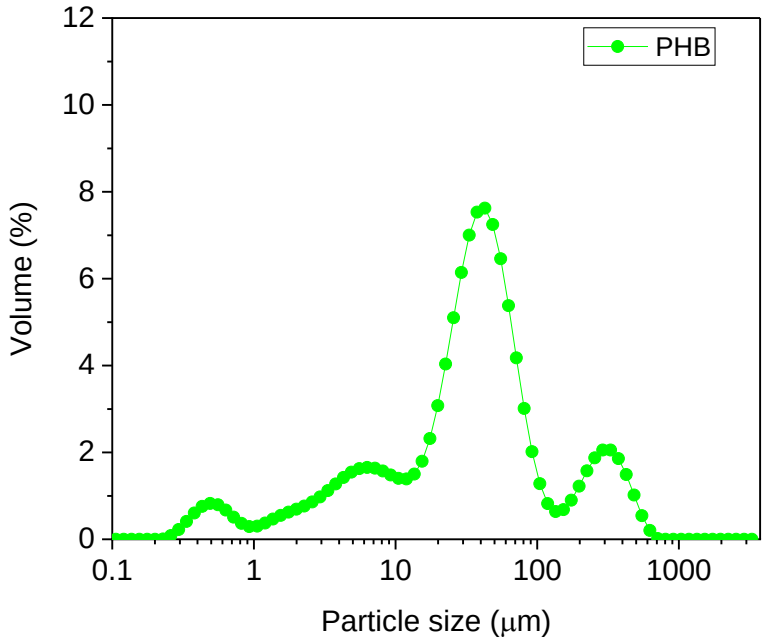


Figure 3:12 – Particle size distribution measured using light diffraction of PHB PMPs stabilised with 0.05 wt% surfactant in the aqueous phase with a gelatine concentration of 0.5 wt%. The polymer concentration (0.5 g) in the disperse phase was 2.44 wt% (2.83 v%) in chloroform, the ratio of dispersed phase to continuous phase was 0.25 wt%.

Table 3:3 – Mean Particle size distribution at D_{10}, D_{50} and D_{90} of PCL particles

	D_{10} (μm)	D_{50} (μm)	D_{90} (μm)
Mean	3.44	36.4	222
Std Dev	0.11	0.82	44.4
RSD (%)	3.07	2.24	20

In **Figure 3:12** we can see that the PHB particles are more polydisperse compared to the previous samples made with PCL and PLGA (**Figure 3:6** and **Figure 3:9** respectively) where smaller particles at < 1 μm is observed and

aggregation or larger particles >100 µm is detected. However, for these PMPs a larger span is observed at 7.38 and a d32 of 6.42 µm (**Table 3:4**). This could be due to the challenges faced when selecting a suitable solvent to dissolve PHB polymer. Several solvents were investigated to dissolve PHB using the same recipe as consistently used for all the microparticles at ~ 2.5 wt%, however the same solvent (DCM) could not be used at the same concentration with PHB. Further studies needed to find a suitable solvent can be achieved based on the Hansen solubility parameters (Abbott, 2018). The Hansen Solubility Parameters determines the best match between solutes (polymers, crystalline solids, nanoparticles, pigments etc. and solvents by providing three numbers for each solute or solvent which describe the van der Waals, polar and H-bonding capabilities. Finally, from literature a suitable solvent was sought namely chloroform without making any changes to the recipe (Makio, 1999). A 2.5% (w/w) solution of PHB in chloroform was prepared and heated to 50 ± 5 °C for 3 hours under stirring in order to solubilise the polymer. During this stage, some of the solvent could have evaporated as this step was not carried out under reflux. Therefore, possibly reducing the polymer concentration in the disperse phase resulting in increased viscosity of the droplets where more energy would be required to form droplets resulting in larger droplet size which in turn would increase the likelihood of coalescence and therefore larger particles as is well document by several authors (Dalgleish et al., 1996; McClements and Gumus, 2016; Abbott, 2018).

3.10.2 Droplet to particle evolution as a function of time of PHB PMPs

The emulsions and particles were visualised using an Olympus BX51 optical microscope with a digital camera at 10x, 20x and 50x magnification to monitor the evolution from droplet to PHB particles.

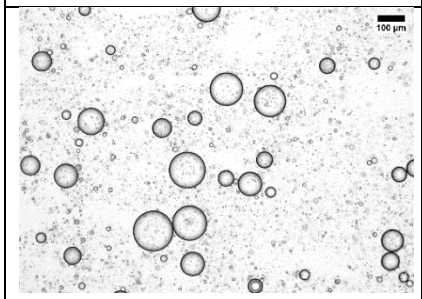
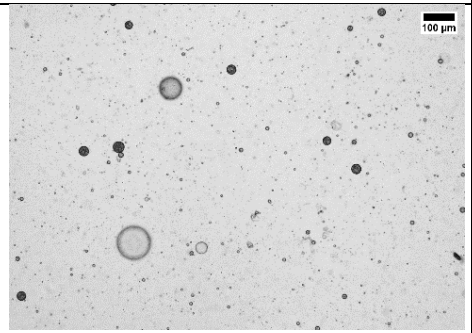
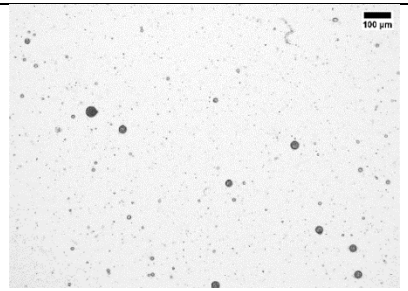
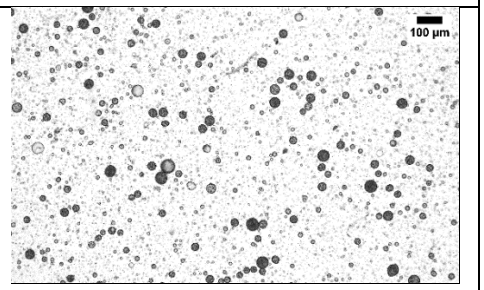
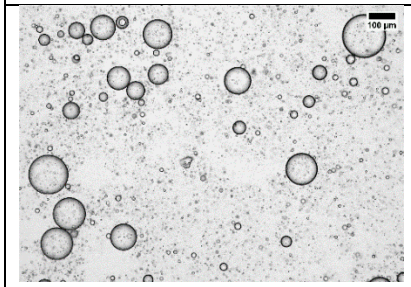
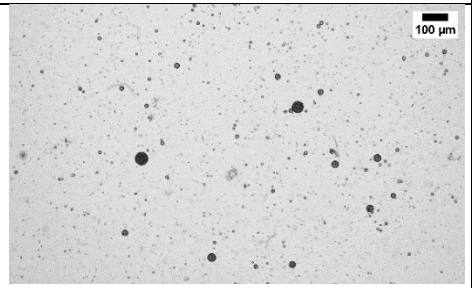
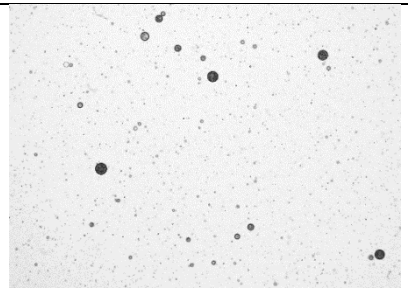
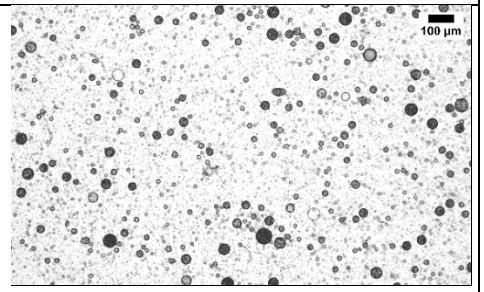
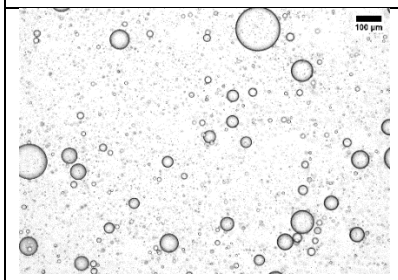
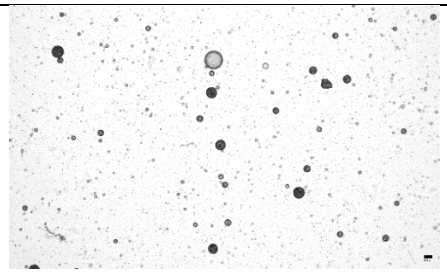
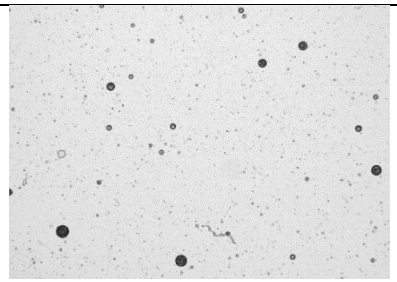
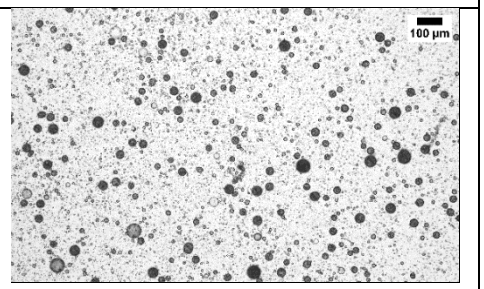
Emulsion	2 h	4 h	Overnight
			
			
			

Figure 3:13 - optical micrograph of emulsion droplets (PHB and chloroform) in aqueous suspension taken after 10 minutes after 1 min homogenisation using UltraTurrax at 8000 rpm. Images taken across varying positions on glass slide to ensure good representation of the sample. Polymer concentration in the disperse phase was 2.44 wt%, the volume ratio of dispersed phase to continuous phase was 0.25 wt%. All scale bar at 10 µm.

Figure 3:13 demonstrates the development of PHB PMPs from the initial emulsion droplets to final solvent (chloroform) extraction at the same magnification at 10x. All the droplets and particles remain stable and no aggregation is seen. Furthermore, a larger concentration of smaller particles are seen compared to the images with PCL and PLGA particles when left to stir overnight, assuming complete solvent evaporation. This is in line and reflected with the particle size distribution seen in **Figure 3:12** where a 2 volume % of particles <2 µm is seen as well as 2 volume% of particles >100-1000 µm is observed.

3.10.3 Scanning electron microscopy of PHB PMPs

The PHB PMPs were characterised using scanning electron microscopy to obtain information about the surface structure, roughness, and porosity of PHB PMPs. This information can be used to compare the images before, during and after degradation (Nam and Park, 2020).

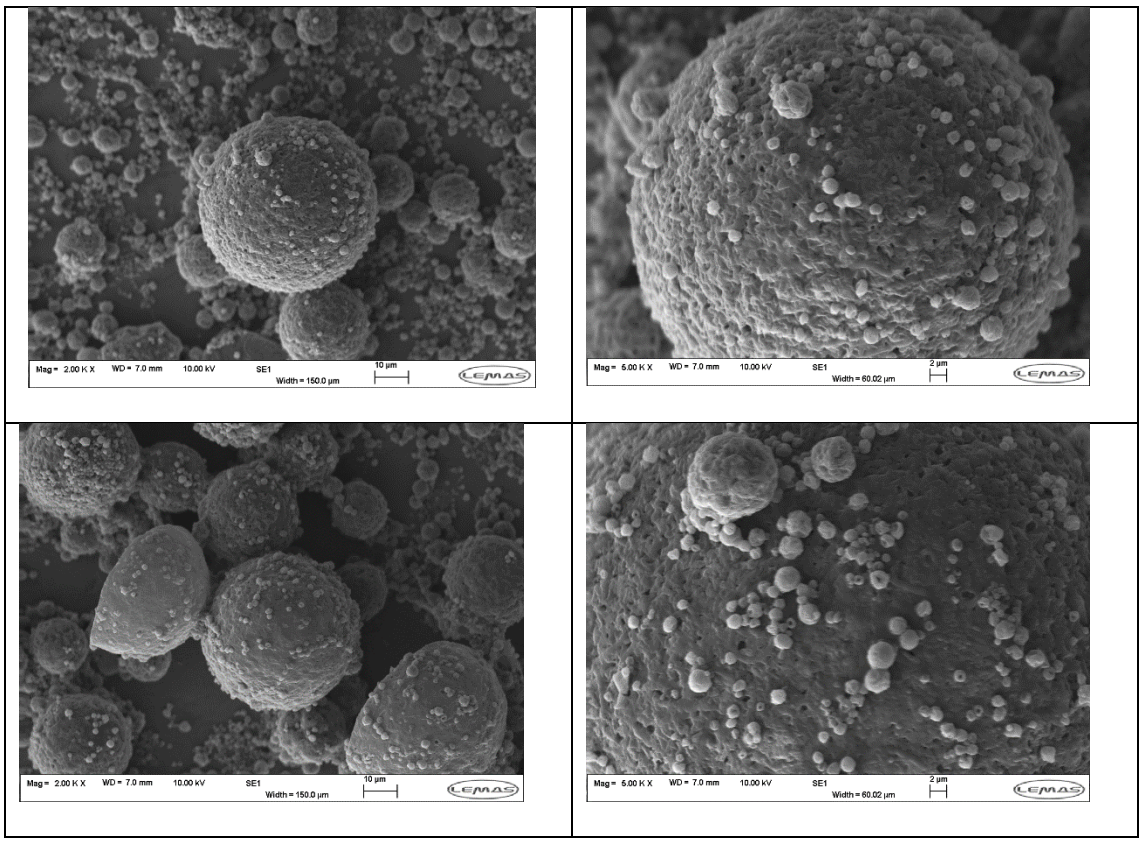


Figure 3:14 - Scanning Electron Micrograph of PHB PMPs at clockwise 2000x, 5000x 2000x and 5000x magnification and a voltage at 20 kV. The sample was coated with platinum with a thickness of 20 nm using Leica EM ACE600 before analysis.

Interestingly, the PHB PMPs show a very rough porous surface but spherical particles and a range of sizes. They are heterogeneous in their shape which are in line with the particle size distribution data from the Mastersizer (**Figure 3:12**) and the optical imaging where larger particles are seen compared to PCL and PLGA PMPs as well as smaller particles. This further confirms the complications faced with the preparation of PHB particles using the same conditions as applied throughout. However, several authors reported similar

structure of PHB particles with size ranging from 0.3 to 0.6 µm, 8 to 56 µm, 10.1 to 140 µm (Shah et al., 2008; Murueva et al., 2013; Govindasamy et al., 2019). The unique morphology of PHB may be influenced by its interactions with cellular components like fatty acids/glycerides and proteins.

Overall, the engineered PMPs produced in this work of all three polymers (PCL, PLGA and PHB) are suitable for biodegradation studies and would be interesting to investigate the influence on biodegradation with varying surface area and polymer type. The following section will explore the effect of varying surface area.

3.11 Calculated total surface area of PCL, PLGA and PHB microparticles

From the previous sections, it was demonstrated that polymeric PMPs were produced using three types of polymers (PCL, PLGA and PHB) using the solvent extraction process with the same method preparation conditions. The average Sauter mean diameter, d32, of PCL PMPs batches produced under the same conditions was 8.1 µm with standard deviation 1.3 µm indicating that the experiments were repeatable. The average Sauter mean diameter, d32, of PLGA and PHB was 12.5 µm and 6.42 µm respectively. The d43 refers to the mean diameter of a sphere with the same volume, whereas the d32 is the diameter of a sphere that has the same volume/surface area ratio. The ratio of surface area to volume is a significant factor to determine the rate of degradation, the higher the surface area, the higher the biodegradation kinetics (Chinaglia et al., 2018). In this section, the surface area of the particles has been calculated from the total surface area which is based on the bin limits of the particle size distribution, from which a mean size is obtained for each bin limit and the surface area is calculated at each bin limit (**Table 3:4**). The total number of PMPs in the system can be calculated from the density and mass of the polymer.

Table 3:4 – calculated total surface area of PCL, PLGA and PHB PMPs based on the size distribution

Polymeric microparticle	**Total surface area (m^2/g)**	**D_{32} (µm)**	**D_{43} (µm)**	**Span**
PCL	0.90	8.1	33.4	2.36
PLGA	0.49	12.5	35.3	2.22
PHB	0.95	6.42	81.9	7.38

3.12 Preparation of PCL PMPs of varying sizes

The ratio of surface area to volume is a significant factor to determine the rate of degradation, the higher the surface area, the higher the biodegradation kinetics (Chinaglia et al., 2018). Biodegradation by an enzyme occurs at the surface of each particle therefore, particles with smaller diameter have a larger surface area and biodegrade more quickly by enzyme than particles with greater diameter which have a smaller surface area. (Funabashi et al., 2006).

In a recent study, Chinaglia et al. (2018) found that smaller particle sizes have a faster degradation rate as more surface area for a given mass is available for enzymatic activity. However, the polymer was milled into different sizes prior to degradation studies, which adds complications and interference in the study leading to potential inaccurate representation of the real biodegradation process in the natural environment.

Polymer films with powder forms of polycaprolactone (PCL), poly(butylene succinate-co-adipate) (PBSA), polylactic acid (PLA) and poly(butylene succinate) (PBS) in a soil environment has been compared by Modelli et al. (1999). The authors reported that the powdered polymers had a very high initial degradation rate but slowed down rapidly because the small particles degrade faster, but then leave behind the larger particles in mixtures with many sizes, whilst the polymer films had a virtually constant reaction rate, attributed to the same available surface area between the polymer and the microorganisms present in the soil.

Previous PCL PMPs for biodegradation studies have been made using the solvent extraction method. Additional PCL PMPs are required for biodegradation studies with varying surface area. The aim was to change the total surface area of the particles tested for biodegradation while keeping the total mass of polymer in the experiment constant by using particles of different sizes. Increasing the surface area of PCL PMPs was done by changing the homogenisation speed during the emulsion preparation stage which resulted in varying droplet size and finally the particle size. (Katou et al., 2008; Makadia and Siegel, 2011; Staff et al., 2013b). The homogenisation speeds used to prepare emulsion droplets were 4000 rpm, 8000 rpm and 12000 rpm.

3.12.1 Laser diffraction measurements of PCL PMPs

3.12.1.1 Calculated surface area of PCL microparticles

The surface area of the PCL particle is calculated from the total surface area which is based on the bin limits of the particle size distribution, from which a mean size is obtained for each bin limit and the surface area is calculated at each bin limit. The total number of PMPs in the system can be calculated from the density and mass of polycaprolactone:

Table 3:5 – Effect of stirring speed in the emulsification process onto the final particle size

Stirring speed (RPM)	Total surface area (m^2/g)	D_{10} (µm)	D_{50} (µm)	D_{90} (µm)	D_{32} (µm)
4000	0.54	12.4	26.8	75.8	12.9
8000	0.99	5.0	13.4	84.0	8.1
12000	3.01	0.66	4.92	12.9	2.1

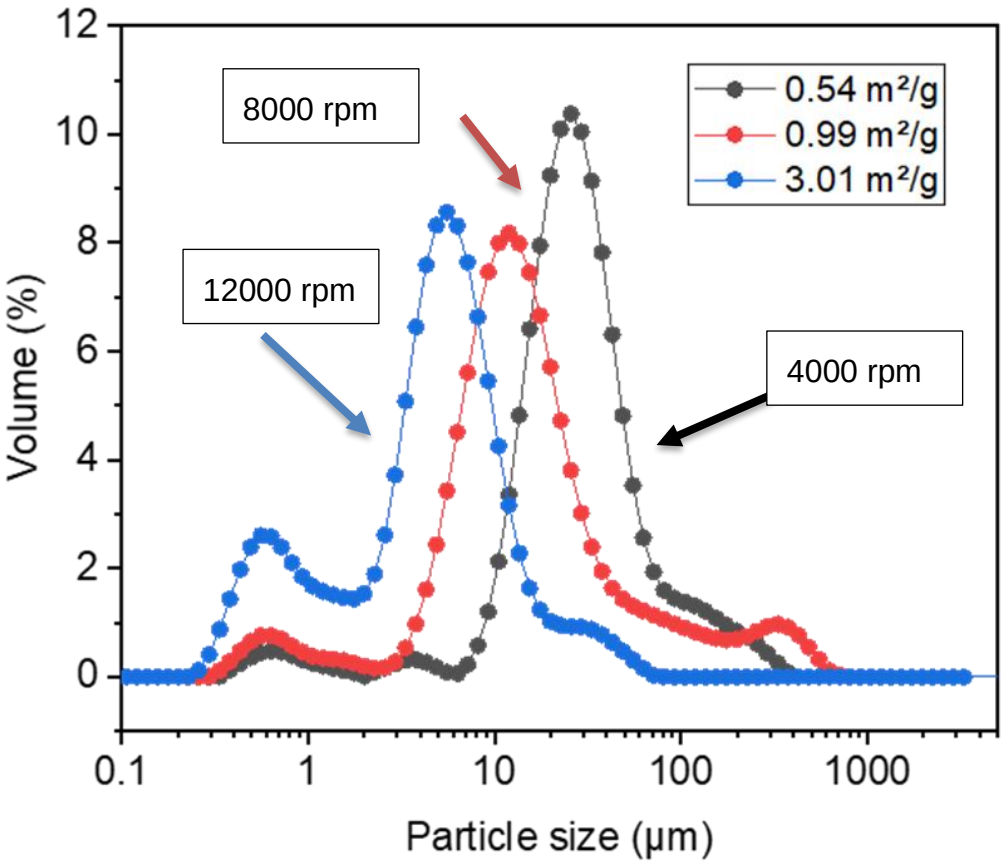


Figure 3:15 – Effect of stirring speed in the emulsification process onto the final particle size prepared at varying homogenisation speed (4000 rpm, black), (8000 rpm, red), and (12000 rpm, blue) during the emulsification stage

The particle size distributions of the various PCL PMPs prepared from emulsions emulsified with varying homogenisation speed show significant differences. Reports in the literature, showed that there have been many studies of the relationship between particle size and stirring speed (Baudonnet et al., 2002; Ibraheem et al., 2014). In **Figure 3:15**, it can be seen that particles <1 µm was increased as the stirring speed was increased, this is in line with the data as demonstrated by (Baudonnet et al., 2002) where they found this phenomenon could be explained by the fact that dispersed particles were primary particle aggregates. As is the case for suspensions of hard particles, these aggregates are broken down by the presence of considerable mechanical energy, this can be seen with particle size range >100 µm decreases as the stirring speed increases and depicted by the optical micrographs and scanning electron microscopy in **Figure 3:16**.

3.12.2 Optical light microscopy and scanning electron microscopy of PCL particles prepared at varying homogenisation speed

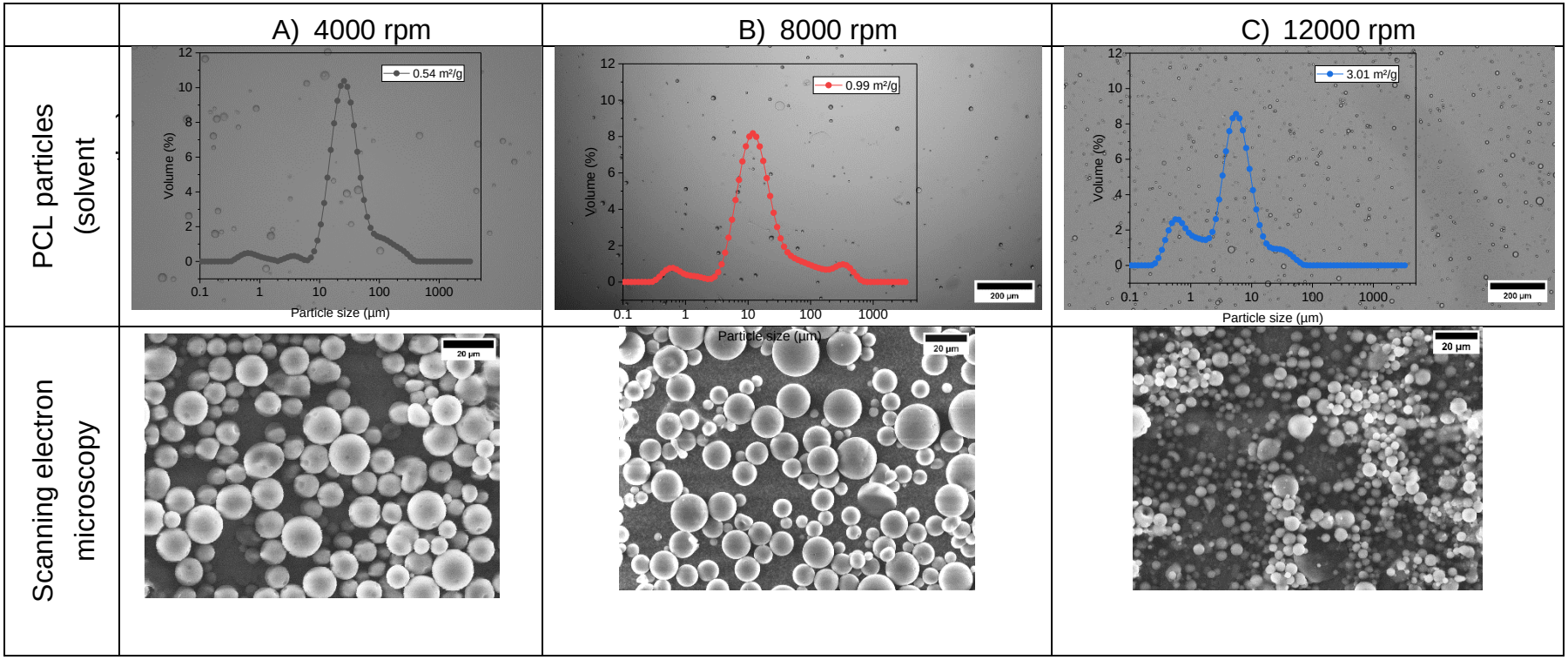


Figure 3:16 - Optical light microscopy (inset: particle size distribution) and corresponding scanning electron microscopy of PCL PMPs prepared at varying homogenisation speed A) 4000 rpm, B) 8000 rpm and C) 12000 rpm showing the differences in particle size

3.13 Effect of solvent extraction matrix material concentration on microparticle properties

As expected, the size of the solvent droplet decreases with time as the solvent is evaporated as evident from the optical micrographs depicted in sections **3.8.2**, **3.9.2** and **3.10.2**. Several attemps were made to quantify the decrease in droplet size using light diffraction measurements. However, this was not possible as the rate of extraction of the solvent was too rapid i.e. it was noticed that the solvent was extracting into the water continuous phase at t=0. To prevent this, the water continious phase used for the mastersizer measurements was saturated with DCM above the solubility in water. This would stop the loss of solvent from the droplets momentarily during the measurements. However despite this, the measurements were still not reproducible over time for the same sample in the same measurement series as loss of solvents was not prevented by this method, likely as a result of (also) fast evaporation of the solvent dissolved in the continuous phase, a process that therefore dragged more solvent from the droplets. This can be explained by the hypothesis involving the the diffusion coefficient of the solvent in polymer solution. The solvent of the polymer phase droplets is extracted into the surrounding aqueous continuous phase. The solvent extracted from the polymer droplet must eventually be removed from the continuous phase to obtain solid particles (Katou et al., 2008).

3.14 Conclusion

In this chapter, we have successfully produced polymeric PMPs using three types of biodegradable polymers (PCL, PLGA and PHB) using the solvent extraction process with the same method preparation conditions. We have demonstrated that the solvent extraction method is repeatable and robust and can be used to prepare further particles under the same conditions. All polymeric PMPs are polydisperse where smaller particles at < 1 µm is observed and larger particles >100 µm is detected. The PMPs appear to be well dispersed in suspension as seen by the optical micrographs and no aggregation is observed when dry as seen by scanning electron microscopy. We can manipulate the particle size/surface area by simply making changes to the stirring speed of the UltraTurrax during the emulsification stage.

The following chapter will focus on the biodegradation polycaprolactone (PCL) PMPs using an enzyme. The aim of this study is to understand the hydrolytic degradation of PCL PMPs by 1) monitoring the release of fatty acid during degradation using a pH stat (related to stage 2 of the biodegradation process). The hypothesis is that at this stage, we can monitor the breakdown of hydrolysable bonds in the PCL to produce 6-hydroxylcaproic acid (6-HCA) using an enzyme and expect to observe an increase in the amount of 6-HCA as a function of time. Although the pH stat is widely used to for digestion studies (Mat et al., 2016), it is not used/seldom used in measuring biodegradability. 2) To study the production of carbon dioxide during degradation by measuring pressure, which is then used to calculate the amount of CO_2 removed by the base in the instrument sleeve. This will allow to understand the secondary products of the biodegradation process, representing the final stage 3 of biodegradation i.e. the conversion of PCL into CO_2, water and biomass (Emadian et al., 2017). The hypothesis is that at this stage we expect to observe an increase of CO_2 as a function of time. By combining both acid release and CO_2 production studies, a more complete understanding of the degradation behaviour of polymeric PMPs can be obtained.

3.15 References

Abbott, S. 2018. *Solubility Science Principles and Practice.*

Albright, V.C., 3rd and Chai, Y. 2021. Knowledge Gaps in Polymer Biodegradation Research. *Environ Sci Technol.* **55**(17), pp.11476-11488.

Amelinckx, S., Dyck, D., Landuyt, V.J. and Tendeloo, V.G. 2008. *Electron microscopy: principles and fundamentals.* [Online]. John Wiley & Sons.

Ammala, A. 2013. Biodegradable polymers as encapsulation materials for cosmetics and personal care markets. *Int J Cosmet Sci.* **35**(2), pp.113-124.

Ariffin, H., Nishida, H., Shirai, Y. and Hassan, M.A. 2010. Highly selective transformation of poly[(R)-3-hydroxybutyric acid] into trans-crotonic acid by catalytic thermal degradation. *Polymer Degradation and Stability.* **95**(8), pp.1375-1381.

Bagheri, A.R., Laforsch, C., Greiner, A. and Agarwal, S. 2017. Fate of So-Called Biodegradable Polymers in Seawater and Freshwater. *Glob Chall.* **1**(4), p1700048.

Bartnikowski, M., Dargaville, T.R., Ivanovski, S. and Hutmacher, D.W. 2019. Degradation mechanisms of polycaprolactone in the context of chemistry, geometry and environment. *Progress in Polymer Science.* **96**, pp.1-20.

Baudonnet, L., Pere, D., Michaud, P., Grossiord, J.L. and Rodriguez, F. 2002. Effect of Dispersion Stirring Speed on the Particle Size Distribution and Rheological Properties of Carbomer Dispersions and Gels. *Journal of Dispersion Science and Technology.* **23**(4), pp.499-510.

Borthakur, L.J., Jana, T. and Dolui, S.K. 2010. Preparation of core–shell latex particles by emulsion co-polymerization of styrene and butyl acrylate, and evaluation of their pigment properties in emulsion paints. *Journal of Coatings Technology and Research.* **7**(6), pp.765-772.

Boyandin, A.N., Prudnikova, S.V., Karpov, V.A., Ivonin, V.N., Đỗ, N.L., Nguyễn, T.H., Lê, T.M.H., Filichev, N.L., Levin, A.L., Filipenko, M.L., Volova, T.G. and Gitelson, I.I. 2013. Microbial degradation of polyhydroxyalkanoates in tropical soils. *International Biodeterioration & Biodegradation.* **83**, pp.77-84.

Cao, J., Dang, G., Li, H., Li, T., Yue, Z., Li, N., Liu, Y., Liu, S. and Chen, L. 2015. Identification and Characterization of Lipase Activity and Immunogenicity of LipL from Mycobacterium tuberculosis. *PLoS One.* **10**(9), pe0138151.

Chinaglia, S., Tosin, M. and Degli-Innocenti, F. 2018. Biodegradation rate of biodegradable plastics at molecular level. *Polymer Degradation and Stability.* **147**, pp.237-244.

Dalgleish, D., West, J.S. and Hallett, F.R. 1996. The characterization of small emulsion droplets made from milk proteins and trigyceride oil. *Colloids and Surfaces.* pp.145-153.

Ellis, B. and Smith, M.C. 2009. *Polymers: A Property Database, Second Edition.* 2nd ed. US: Taylor & Francis.

Emadian, S.M., Onay, T.T. and Demirel, B. 2017. Biodegradation of bioplastics in natural environments. *Waste Manag.* **59**, pp.526-536.

Ferrari, R., Colombo, C., Dossi, M. and Moscatelli, D. 2013. Tunable PLGA-Based Nanoparticles Synthesized Through Free-Radical Polymerization. *Macromolecular Materials and Engineering.* **298**(7), pp.730-739.

Funabashi, M., Ninomiya, F. and Kunioka, M. 2006. Biodegradation of Polycaprolactone Powders Proposed as Reference Test Materials for International Standard of Biodegradation Evaluation Method. *Journal of Polymers and the Environment.* **15**(1), pp.7-17.

Gebauer, B. and Jendrossek, D. 2006. Assay of poly(3-hydroxybutyrate) depolymerase activity and product determination. *Appl Environ Microbiol.* **72**(9), pp.6094-6100.

Gentile, P., Chiono, V., Carmagnola, I. and Hatton, P.V. 2014. An overview of poly(lactic-co-glycolic) acid (PLGA)-based biomaterials for bone tissue engineering. *Int J Mol Sci.* **15**(3), pp.3640-3659.

Gonzalez-Pleiter, M., Tamayo-Belda, M., Pulido-Reyes, G., Amariei, G., Leganes, F., Rosal, R. and Fernandez-Pinas, F. 2019. Secondary nanoplastics released from a biodegradable microplastic severely impact freshwater environments. *Environmental Science-Nano.* **6**(5), pp.1382-1392.

Govindasamy, S., Syafiq, I.M., Amirul, A.A., Amin, R.M. and Bhubalan, K. 2019a. Dataset on controlled production of polyhydroxyalkanoate-based microbead using double emulsion solvent evaporation technique. *Data in Brief.* **23**, article no: Unsp 103675 [no pagination].

Heiskanen, H., Denifl, P., Hurme, M., Pitkänen, P. and Oksman, M. 2012. Effect of Physical Properties and Emulsification Conditions on the Microsphere Size Prepared Using a Solvent Extraction Process. *Journal of Dispersion Science and Technology.* **33**(2), pp.234-244.

Hochleitner, B., Schreiner, M., Drakopoulos, M., Snigireva, I. and Snivireg, A. 2003. Analysis of Paint Layers by Light Microscopy, Scanning Electron Microscopy and Synchrotron induced X-Ray Micro-Diffraction.

Ibraheem, D., Iqbal, M., Agusti, G., Fessi, H. and Elaissari, A. 2014. Effects of process parameters on the colloidal properties of polycaprolactone microparticles

prepared by double emulsion like process. *Colloids and Surfaces A: Physicochemical and Engineering Aspects.* **445**, pp.79-91.

Iwata, T. 2015. Biodegradable and bio-based polymers: future prospects of eco-friendly plastics. *Angew Chem Int Ed Engl.* **54**(11), pp.3210-3215.

Katarzyna Leja, G.L. 2010. Polymer Biodegradation and Biodegradable Polymers – a Review. *Polish J. of Environ. Stud.* **Vol. 19**(2), pp.255-266.

Katou, H., Wandrey, A.J. and Gander, B. 2008. Kinetics of solvent extraction/evaporation process for PLGA microparticle fabrication. *Int J Pharm.* **364**(1), pp.45-53.

Kumar, G.A., Anjana, K., Hinduja, M., Sujitha, K. and Dharani, G. 2020. Review on plastic wastes in marine environment – Biodegradation and biotechnological solutions. *Marine Pollution Bulletin.* **150**, article no: 110733 [no pagination].

Laycock, B., Nikolić, M., Colwell, J.M., Gauthier, E., Halley, P., Bottle, S. and George, G. 2017. Lifetime prediction of biodegradable polymers. *Progress in Polymer Science.* **71**, pp.144-189.

Makadia, H.K. and Siegel, S.J. 2011. Poly Lactic-co-Glycolic Acid (PLGA) as Biodegradable Controlled Drug Delivery Carrier. *Polymers (Basel).* **3**(3), pp.1377-1397.

Makio, T.R., H, Marchessault. 1999. Determination of solubility parameters for poly(3-hydroxyalkanoates). *International Journal of Biological Macromolecules.* **25**, pp.207-215.

Mat, D.J.L., Le Feunteun, S., Michon, C. and Souchon, I. 2016. In vitro digestion of foods using pH-stat and the INFOGEST protocol: Impact of matrix structure on digestion kinetics of macronutrients, proteins and lipids. *Food Research International.* **88**, pp.226-233.

McClements, D.J. and Gumus, C.E. 2016. Natural emulsifiers - Biosurfactants, phospholipids, biopolymers, and colloidal particles: Molecular and physicochemical basis of functional performance. *Adv Colloid Interface Sci.* **234**, pp.3-26.

McDonough, K., Itrich, N., Casteel, K., Menzies, J., Williams, T., Krivos, K. and Price, J. 2017. Assessing the biodegradability of microparticles disposed down the drain. *Chemosphere.* **175**, pp.452-458.

Modelli, A., Calcagno, B. and Scandola, M. 1999. Kinetics of Aerobic Polymer Degradation in Soil by Means of the ASTM D 5988-96 Standard Method. *Journal of Environmental Polymer Degradation.* **7**(2), pp.109-116.

Mohamed, F. and van der Walle, C.F. 2008. Engineering biodegradable polyester particles with specific drug targeting and drug release properties. *J Pharm Sci.* **97**(1), pp.71-87.

Murueva, A.V., Shishatskaya, E.I., Kuzmina, A.M., Volova, T.G. and Sinskey, A.J. 2013. Microparticles prepared from biodegradable polyhydroxyalkanoates as matrix for encapsulation of cytostatic drug. *J Mater Sci Mater Med.* **24**(8), pp.1905-1915.

Nair, L.S. and Laurencin, C.T. 2007. Biodegradable polymers as biomaterials. *Progress in Polymer Science.* **32**(8-9), pp.762-798.

Nam, H.C. and Park, W.H. 2020. Aliphatic Polyester-Based Biodegradable Microbeads for Sustainable Cosmetics. *Acs Biomaterials Science & Engineering.* **6**(4), pp.2440-2449.

Nguyen, T.V., Nguyen Tri, P., Nguyen, T.D., El Aidani, R., Trinh, V.T. and Decker, C. 2016. Accelerated degradation of water borne acrylic nanocomposites used in outdoor protective coatings. *Polymer Degradation and Stability.* **128**, pp.65-76.

Pawlik, J., Łukowicz, K., Cholewa-Kowalska, K. and Osyczka, A.M. 2019. New insights into the PLGA and PCL blending: physico-mechanical properties and cell response. *Materials Research Express.* **6**(8).

Qiao, T., Kim, S., Lee, W. and Lee, H. 2019. Biodegradable and Porous Poly(lactic-co-glycolic acid) Microbeads for In vitro Evaluation of Negatively Charged Fluorescent Bacteria. *Macromolecular Research.*

Samir, A., Ashour, F.H., Hakim, A.A.A. and Bassyouni, M. 2022. Recent advances in biodegradable polymers for sustainable applications. *npj Materials Degradation.* **6**(1).

Sarkar, A., Zhang, S., Murray, B., Russell, J.A. and Boxal, S. 2017. Modulating in vitro gastric digestion of emulsions using composite whey protein-cellulose nanocrystal interfaces. *Colloids Surf B Biointerfaces.* **158**, pp.137-146.

Shah, A.A., Hasan, F., Hameed, A. and Ahmed, S. 2008. Biological degradation of plastics: A comprehensive review. *Biotechnology Advances.* **26**(3), pp.246-265.

Staff, R.H., Schaeffel, D., Turshatov, A., Donadio, D., Butt, H.J., Landfester, K., Koynov, K. and Crespy, D. 2013. Particle formation in the emulsion-solvent evaporation process. *Small.* **9**(20), pp.3514-3522.

Tokiwa, Y., Calabia, B.P., Ugwu, C.U. and Aiba, S. 2009. Biodegradability of plastics. *Int J Mol Sci.* **10**(9), pp.3722-3742.

Valencia, G.A., Zare, E.N., Makvandi, P. and Gutiérrez, T.J. 2019. Self-Assembled Carbohydrate Polymers for Food Applications: A Review. *Comprehensive Reviews in Food Science and Food Safety.* **18**(6), pp.2009-2024.

Yu, J., Plackett, D. and Chen, L.X.L. 2005. Kinetics and mechanism of the monomeric products from abiotic hydrolysis of poly[(R)-3-hydroxybutyrate] under acidic and alkaline conditions. *Polymer Degradation and Stability.* **89**(2), pp.289-299.

Zhang, H., Wang, X., Wang, P., Liu, R., Hou, X., Cao, W., Zhong, R., Liu, X. and Zhang, Y. 2018. One-pot synthesis of biodegradable polydopamine-doped mesoporous silica nanocomposites (PMSNs) as pH-sensitive targeting drug nanocarriers for synergistic chemo-photothermal therapy. *RSC Advances.* **8**(65), pp.37433-37440.

Chapter 4 Biodegradation of PCL PMPs

4.1 Introduction

In the literature review, we described what polymeric microparticles (PMPs) are and the issues associated with the accumulation of PMPs in the environment.

This chapter will focus on the biodegradation of model polycaprolactone microparticles (PCL PMPs), with d_{32} of 10.1 µm, that have been prepared in **Chapter 3**. The PCL PMPs will be degraded using lipase enzyme using two different methods. The aim of this study was to develop an *in vitro* method for describing the degradation of PCL PMPs using an enzyme that can potentially be used across many different systems. PCL was chosen for this study as there is significant data already available on the degradation of films but lack of data on PMPs, it is also well cited as being biodegradable and are readily available. **Table 4:1** summarises some of the environmental conditions used to degrade polycaprolactone polymer in either film or particle form and describes their degradation behaviour. This chapter is split into two parts. The degradation of PCL PMPs will be carried out by firstly, monitoring production of acid through the degradation process using a pH stat (related to stage 2 of the biodegradation process). The hypothesis is that at this stage, we can monitor the breakdown of hydrolysable bonds in the PCL to produce 6-hydroxylcaproic acid (6-HCA) using an enzyme and expect to observe an increase in the amount of 6-HCA as a function of time. Although the pH stat is widely used to for digestion studies (Mat et al., 2016), it is not used/seldom used in measuring biodegradability. Secondly, we study the production of carbon dioxide (CO_2) using pressure measurements to understand the secondary products of the biodegradation process, representing the final stage 3 of biodegradation i.e. the conversion of PCL into CO_2, water and biomass (Emadian et al., 2017). The hypothesis is that at this stage we expect to observe an increase of CO_2 as a function of time.

We studied the production of carbon dioxide using pressure measurements as described by others (Nakasaki et al., 2006; Ahn et al., 2008; Gómez and Michel, 2013; Anstey et al., 2014) to understand the secondary products of the

biodegradation process (3rd stage of the biodegradation process). From all the tests summarised in in the literature review (**Table 2:3**), the production of CO_2 measurements was chosen as it the most common test method used in industry and allows to manipulate simulations and test conditions easily. For simplicity, the biodegradation media will consist of the PMPs, water and enzyme. This method monitors the full extent of the degradation pathway and thus complements the pH stat method, which monitors the production of acid at the start of the degradation process. There is significant amount of available data available on films but lack of data on particles. As the issue of microparticle pollution becomes more prevalent, there is a growing need for updated and adapted standards for measuring the degradation of these small particles.

A range of lipase concentration has been studied to find the optimum PCL PMPs: lipase ratio, thus insight from this study will allow us to focus on other factors affecting biodegradation such as surface area at the optimum PCL PMPs: lipase ratio. By combining both acid release and CO_2 production studies, a more complete understanding of the degradation behaviour of polymeric PMPs can be obtained. A range of lipase concentration has been studied to find the optimum PCL PMPs: lipase ratio, thus insight from this study will allow us to focus on other factors affecting biodegradation such as surface area at the optimum PCL PMPs: lipase ratio.

Although enzymatic degradation of polycaprolactone powders and films has been reported using an amino lipase enzyme from *Pseudomonas cepacia,* which is well-established for *in vitro* biodegradation studies of polymers (Funabashi et al., 2006), such degradation studies on microparticles seems overlooked in literature to date. Fragmentation of the biodegradable polymers into oligomers of smaller molecular weights may be hypothesised to result in larger surface-to volume-ratio for the enzymes to act upon increasing the biodegradability. Enzymatic depolymerisation of the polymeric microparticles (PMPs) releasing oligomers and/or monomers can thus be easily assimilated by the microorganisms as a carbon source resulting in increase of microbial biomass, water and carbon dioxide (Kumar, G.A. et al., 2020)..

Enzymatic degradation of PCL: Enzymatic degradation of polymers is a two-step process. First, the enzyme binds to the polymer substrate, the second is the catalysis of a hydrolytic cleavage, breaking apart the polymer chain as

shown in **Figure 4:1** (Bartnikowski et al., 2019). During degradation, enzymes from the microorganisms break down complex polymers to yield shorter chains or new molecules entirely. These short-chain molecules are then mineralised into final respiratory products, which are utilised as carbon and energy sources and may be quantified similarly to respirometric analysis (Shah et al., 2008). An enzymatic degradation test of polycaprolactone (PCL) powders was reported using an amino lipase enzyme from *Pseudomonas cepacia* which is known to be the degradation enzyme for PCL PMPs (63 to 250 µm) by Funabashi et al. (2006). Fragmentation of the biodegradable polymers into oligomers of smaller molecular weights results in larger surface to volume ratio for the enzymes to act upon. Enzymatic depolymerisation of the polymers releases oligomers and/or monomers that can be easily assimilated by the microorganisms as a carbon source resulting to increase in microbial biomass (Kumar, G.A. et al., 2020). The enzymatic hydrolysis of polycaprolactone by lipase involves the cleavage of ester bonds in the polymer chain, leading to the formation of smaller molecules. Lipase enzymes serve as catalysts in this process, accelerating the degradation of polycaprolactone. The resulting hydrolysis products include hydroxyl and carboxyl end groups in the polymer. Understanding the mechanism of polycaprolactone hydrolysis by lipase is essential for biodegradation research and can aid in the design of eco-friendly materials and waste management approaches (Blackwell et al., 2018).

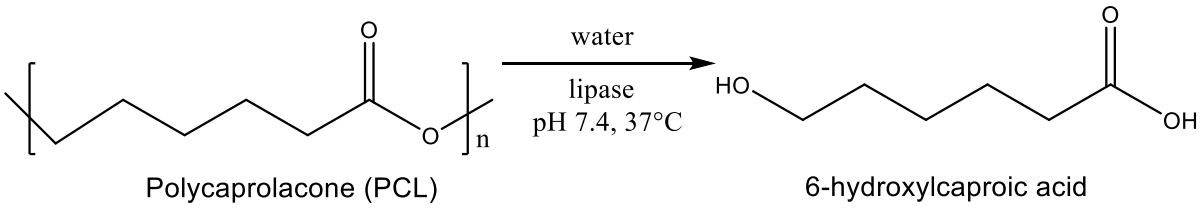


Figure 4:1 - Enzymatic degradation of PCL showing the hydrolysis of the ester bond into 6-hydroxylcaproic acid under specified conditions (Funabashi et al., 2006; Bartnikowski et al., 2019).

Biodegradability of polymers and PMPs is thus affected by both their chemical and physical properties such as molecular weight, crystallinity, melting temperature, particle size as well as environmental factors such as pH, enzymatic activity, temperature, ionic strength *etc.* By thoroughly analysing the characteristics of PMPs before and during biodegradation, a better understanding of the chemical and physical changes of the PMPs can be realised. Development

of robust and harmonized simulated methods and characterisation techniques to characterize biodegradation fate of both polymers and their MPs are needed. More importantly, there has been no study on PMP degradation and limited *in vitro* studies using an enzyme have been performed on those particles to study biodegradation.

Table 4:1 - Biodegradation of polycaprolactone in different environments, adapted from Bartnikowski et al. (2019)

Enzymatic system	Polymeric system	Observation	Ref
Lipase (unspecified)	PCL PMPs, PCL solvent-cast (chloroform) films	37°C, 7 weeks. Molecular weight decrease by 7.9 kDa (film, no lipase), 9.6 kDa (particles, no lipase), and 15 kDa (particles, lipase). Crystallinity unchanged with no lipase (51%), increased (51 – 62 %) with lipase over	(Chen et al., 1999)
Lipase: Pseudomonas (unspecified), porcine pancreatic, Candida cylindracea	PCL solvent-cast films	37°C, 4 days – 1 week. Mass loss of 100 % in 4 days, PCL was very effective, degrading both amorphous and crystalline regions of the polymer.	(Blackwell et al., 2018)
Pseudomonas fluorescens lipase	PCL solvent-cast films	37°C, 2 weeks (15 days). 100% mass loss with high concentration of lipase	(Ashton et al., 2011)
Pseudomonas lipase (unspecified)	PCL network polymer: photo-polymerisable polymer made by modifying ω-dihydroxy-terminated PCL (2 kDa Mw) with methacrylic anhydride	37°C, up to 65 weeks; lipase, 37°C, 14 weeks. Mass loss of 32 % (H_2O only), 18 % (PBS only), 60 weeks, and 20 % (lipase), 14 weeks. Easier to degrade than linear PCL. Enzymatic degradation appeared to proceed via surface erosion. Concentration much lower than Ashton et al. study.	(Castilla-Cortázar et al., 2012)
Degradation by Aspergillus fumigatus, compost, and in anaerobic sewage	PCL solvent-cast films	Assessed biodegradation of PCL for environmental applications. Found amorphous degradation was preferred by these enzymes/organisms.	(Eldsater et al., 2000)
Novozym 435 and Candida rugosa lipase	PCL solution (toluene)	Toluene solution at 60°C. Found that both enzymes were effective unless PCL was mixed with poly(vinyl acetate) (PVAc), where a significant drop in reaction rate for PCL was observed	(Sivalingam, G. et al., 2003)
Novozyme 435 and lipolase	PCL solution (various solvents)	Reaction rate decreased with increasing viscosity, and increased with increasing solvent polarity	(Sivalingam, G. et al., 2002)
Thermomyces lanuginosus lipase	Crosslinked PCL implants, directly synthesized into desired shape. Crosslinker was bis(trimethylene carbonate) (BTB)	Observed that surface erosion dominated. Higher amount of crosslinker resulted in slower degradation.	(Yang, L. et al., 2015)
Immobilised Candida rugosa lipase on amino-functionalized magnetic supports via crosslinked enzyme aggregates	PCL PMPd	30°C, 30 days. Looked at both free and immobilized lipase. Improved degradation from immobilized lipase, attributed to the stability of the enzyme over extended periods of time in this form. Observed a 6-fold increase in biodegradability of PCL with immobilized lipase compared with free lipase.	(Kim et al., 2010)
Pseudomonas cepacia lipase	PCL with various levels of crystallinity	37°C, 100 h. Found that higher molecular weight polymers had higher initial crystallinity, and noted that crystallinities increased around 5 % per group over the 100 h period. Mass loss was significantly higher in the lower molecular weight groups. Increased degradation with lower crystallinity overall. Attribute lower degradation in higher molecular weight polymer to higher inherent	(Jenkins and Harrison, 2008)

4.2 Materials and Methods

4.2.1 Materials

Lipase from *Pseudomonas cepacia* with measured enzymatic activity of 27.6 to 43.1 U/mg (**Figure A:0**:**1** in the appendix) was purchased from Sigma Aldrich, Dorset, UK (CAS#: 9001-62-1). Polycaprolactone (PCL), Mn (45 kDa polydispersity 1.2 - 1.8. Tween 80 (non-ionic surfactant), >50% purity and Dichloromethane (DCM), >99/8% purity and chloroform, > 99.5% purity were purchased from Sigma Aldrich. The PCL PMPs were prepared as previously described in **Chapter 3**. All solutions used were prepared using Milli-Q water which was purified by a Milli-Q apparatus (Merck Milli-Q EQ7008, UK) with an ionic purity of 18.2 MΩ·cm at 25°C. HEPES buffer, N-(2-Hydroxyethyl) piperazine-N′-(2-ethanesulfonic acid), CAS# 7364-45-9, mw = 238.31 g/mol was purchased from Sigma Aldrich, Dorset, UK. Sodium hydroxide pellets (CAS # 1310-73-2) was purchased from Sigma Aldrich, Dorset, UK. OxiTop©-IDS wireless measuring head was purchased from Xylem (Germany) with Bluetooth© LE technology for operation with Multi 3620 IDS or Multi 3630 IDS and was used to monitor changes in pressure.

4.2.2 Methods

4.2.2.1 Measurement of lipase activity

The hydrolytic activity of lipases was determined according to Carriere et al. (1993) and Erlanson and Borgström (2020). The substrate assay was prepared by dissolving 39 mg/L Tris-(hydroxymethyl)-aminomethane, electrolytes (9000 mg/L NaCl, 200 mg/L $CaCl_2$) and biliary salts (2080 mg/L Sodium taurodeoxycholate) in 200 mL purified water. The substrate assay was magnetically stirred (500 rpm) at 37°C and emulsified by adding 0.5 mL tributyrin. The hydrolysis was started by adding lipase into emulsified tributyrin and the pH was adjusted to 8.0 using 0.1M NaOH as shown in **Appendix**, **Figure A:0:1** . The amount of free fatty acids (FFAs) released by the lipase action was determined by titration with 0.1M NaOH. The measured enzyme activity was found to be

between 27.6 to 43.1 U/mg where the lipase activity is expressed in international units (U) with 1 U = 1 µmol butyric acid released per minute at 37°C and at pH 8.0. This in agreement with the reported enzyme activity by Sigma at $\geq$ 30.0 U/mg where 1 U corresponds to the amount of enzyme which liberates 1 umol oleic acid per minute at pH 8.0 and 40 °C (triolein, CAT. No. 62314 as substrate).

4.2.2.2 pH-stat-based free fatty acid release

The free fatty acids (FFAs) released from the depolymerisation of PCL PMPs were measured by using an automatic pH-stat titration unit (TIM 856 titration manager, Titralab, Radiometer analytical) (Tan et al., 2020) as shown below in **Figure 4:2.**

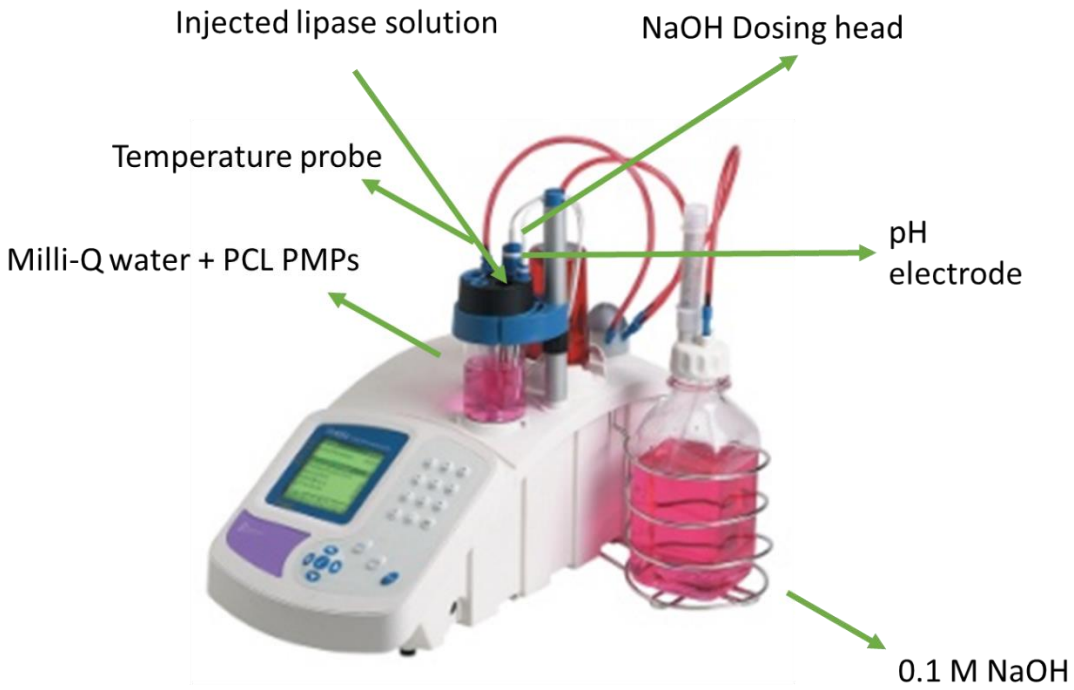


Figure 4:2 - Schematic illustration of a pH-stat device, equipped with a thermostat reaction vessel, in which the substrate emulsion is formed by mechanical stirring; a pH-electrode connected to a pH-meter and a control unit for the automated delivery of NaOH by a burette. Every time the pH decreases due to the release of free fatty acids (FFAs), NaOH is delivered to keep the pH constant at a pre-determined endpoint value.

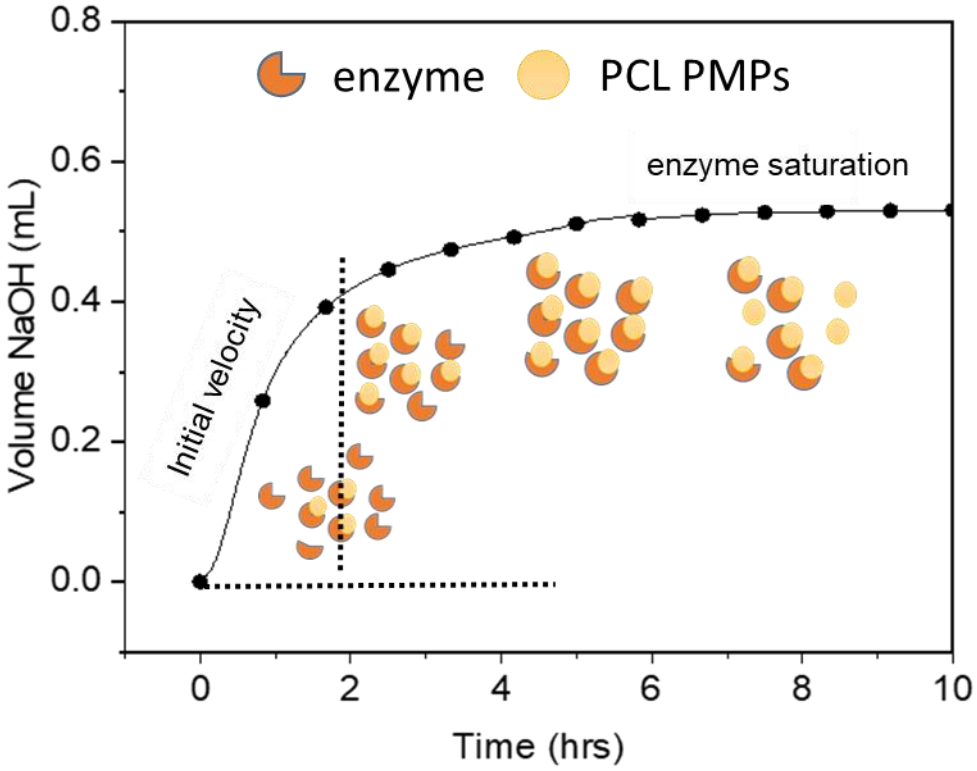


Figure 4:3 - Theoretical illustration of a typical titration curve of formation of product in an enzyme-catalysed reaction plotted against time showing initial velocity and enzyme saturation point (Robinson, 2015).

During the course of the experiment, the volume of NaOH (mL) is recorded as a function of time (hrs). Every time the pH decreases due to the release of FFAs, NaOH is delivered to keep the pH constant at a pre-determined endpoint value. **Figure 4:3** illustrates a typical titration curve where a linear gradient is initially observed followed by a slow almost as the reaction progresses, this is known as the saturation point where adding more enzyme does not promote any further enzymatic reaction. A common reason for this slowing down of the speed (rate) of the reaction is that the substrate within the mixture is being used up and thus the particles are being degraded (Pastorino et al., 2004; Robinson, 2015). Another explanation could be that the enzyme is unstable (or saturated) and is denaturing over the course of the experiment. Blank experiments were performed as a control, to measure pH fluctuation in the absence of enzymes or PCL particles as demonstrated by Pastorino et al. (2004) where they reported that no PCL degradation was observed in water or solvent mixtures in the absence of the enzyme. The volume of NaOH released during the control experiments was then

subtracted from the data recorded in the presence of PCL PMPs/lipase. Each blank and PCL/Lipase experiment was repeated at least four times. For the analysis of FFA release of PCL PMPs, the pH stat was used to monitor and control the pH for 23 hours. After addition of lipase at pH 7.4 at 37°C, the depolymerisation of PCL leads to one 6-hydroxylcaproic acid (6-HCA) as shown in **Figure 4:1**. By maintaining the pH at 7.4, the volume of sodium hydroxide (NaOH) titrated into the substrate to neutralise 6-HCA produced by depolymerisation can be recorded as a function of time (Ciuffreda et al., 2009; Pabois et al., 2020; Grundy et al., 2021). The volume of added NaOH (0.1 M) was assumed to be equal to the amount of free acids generated by the degradation of PCL. The amount of 6-HCA released was calculated from the titration curves as described by Sarkar et al. (2017). The percentage of FFAs released can then be calculated based on the assumption that one mole of NaOH is required to neutralise one mole of 6-hydroxylcaproic acid (6-HCA).

To calculate the percent degradation or FFA (6-HCA) release, the following equation **4:1** is applied

$$\%\, degradation\ = 100 \times \frac{V_{NaOH}\ (t) \times 0.1\ (NaOH) \times M_{CL}}{m_{PCL}} \qquad \textbf{4:1}$$

where V_{NaOH} is the volume of NaOH required to neutralise the FFA produced over time, [NaOH] the concentration of the NaOH solution used, M_{CL} the molecular weight of caprolactone (M_{CL}= 114.14 g/mol), and m_{PCL} the mass of PCL PMPs (10 mg) initially present in the digestion vessel (Pabois et al., 2020).

From the lipase activity and mass of PCL PMPs in the system, the ratio can be calculated **Table 4:2**. For all tests, a mass of PCL PMPs of 10 mg was used. The lipase activity was re-measured during the course of the PhD and the mass of enzyme used in each experiment was adjusted accordingly to ensure consistency of activity throughout all conducted tests.

Table 4:2 - Calculated PCL PMPs: lipase ratio based on mass of PCL PMPs and lipase activity

Lipase (mg)	Lipase activity in the reaction vessel (U/mg)	Ratio PCL PMPs:Lipase
60	2130	0.005
30	1065	0.009
20	710	0.014
7	249	0.040
3	107	0.094
1.7	60	0.17
1	35.5	0.282

A first order rate kinetics model was initially introduced by Ye et al. (2013) assuming that the adsorption kinetics of lipase onto a hard surface of the particle is very rapid. The biodegradation curves in the first part of the reaction are well described by linear regressions (Chinaglia et al., 2018). For this project, the rate of the amount of free fatty acids released (%FFA) was evaluated during the first 2 h as this was the best fits to the experimental data predicted using the mathematical model (Pearson correlation coefficient 0.998).

4.2.2.3 Pressure measurement

Biodegradation is the disintegration of materials by microorganisms such as bacteria, fungi or yeast. Biodegradation can be described as the process of breakdown of polymer chains into smaller molecules resulting from biological processes (microorganisms) initiated by the natural environment in aerobic (with oxygen) and anaerobic (without oxygen) conditions (Kjeldsen et al., 2019). Biological oxygen demand (BOD) is an important and widely used sum parameter to evaluate biodegradation of an organic material (Roppola et al., 2007). BOD is a measure of the amount of oxygen consumed for the oxidation of an organic matter. Roppola et al. (2007) studied the biological oxygen demand of wastewaters from various sources using three methods: the manometric respirometric test (WTW Weilheim, Germany), oxygen sensor determination, and iodometric titration. The authors found that the manometric respirometric method was suitable for the BOD determination of the wastewater of the pulp and paper mills. Through the years, a number of improvements have been made to an automated system to measure BOD. One of the widely used and reliable device is an OxiTop©. Measurement using OxiTop© is based on pressure measurement in a closed system. The test determines the biodegradability of organic substances in an aqueous medium by determining the oxygen consumption in a closed respirometer (Gartiser, 2018b).

Biodegradable polymers are a source of carbon and energy for microbes. In the final biodegradation step (bio-assimilation stage), oligomers are broken down into smaller molecules, which can be assimilated by the microbial organisms into biomass. The basic driving force of biodegradation is the use of the carbon (C) bound in the polymer as a feedstock for microorganisms such as bacteria, fungi and yeast to grow to produce carbon dioxide, water and biomass (Kjelsden et al., 2019)

In aerobic conditions, the biodegradation can be described as:

$$C_{polymer} + O_2 \longrightarrow CO_2 + H_2O + C_{biomass} \quad \textbf{4:2}$$

Microorganisms in the sample consume the oxygen and form CO_2. This is absorbed by NaOH, creating a vacuum. The measured negative pressure

is converted into the BOD (mg/L) value using the following equation as described by several authors (Funabashi et al., 2006; Kunioka et al., 2009; Gómez and Michel, 2013; Chinaglia et al., 2018).

$$BOD\ mg/l = \frac{M(O_2)}{R \times Tm} \times \left[\frac{Vtot - V1}{V1} + \alpha \frac{T_m}{T_0}\right] \times \Delta p\ (O_2) \qquad \textbf{4:3}$$

Where:

M (O_2) = Molecular weight of oxygen (32000mg/mol)

R = Gas constant (83,144 L·hPa/(mol·K))

T_0 = Temperature (273.15 K)

T_m = Measuring temperature (310 K) for BOD_n

V_{tot} = Bottle volume [mL]

V_1 = Sample volume [mL]

α = Bunsen absorption coefficient (0.03103)

Δp(O_2) = Difference of the partial oxygen pressure [hPa]

The equation can be simplified as the difference in pressure is equal to the amount of consumed oxygen and CO_2 produced. Example given below from the degradation of caprolactone monomer as described by the following mechanism (Chinaglia et al., 2018; Gartiser, 2018b)

$$C_6H_{10}O_2 + 6O_2 \longrightarrow 6CO_2 + XH_2O \qquad \textbf{4:4}$$

Using the gas law equation as described below, the pressure difference can be simplified using equation **4:5** (Funabashi et al., 2006; Kunioka et al., 2009; Chinaglia et al., 2018).

$$\Delta p\ (O_2) \times \left[\frac{Vtot - V1}{V1}\right] = nRT \qquad \textbf{4:5}$$

Δp(O_2) = Difference of the partial oxygen pressure [hPa]

V_{tot} = Bottle volume [mL]

V_1 = Sample volume [mL]

n = number of moles CO_2

R = Gas constant (83,144 L·hPa/(mol·K)

T = Measuring temperature (310 K)

The percent degradation can then be calculated according to the following formula:

$$\%\ degradation = \frac{CO_2\ produced\ from\ test\ (PMPs + lipase) - CO_2\ produced\ control\ test}{CO_2\ produced\ control\ test} \quad \textbf{4:6}$$

The total CO_2 production from the test materials (PMPs) was calculated by subtracting the average amount of CO_2 produced in the blank tests to the amount of CO_2 produced in the tests with PMPs + lipase (see section **4.5 Figure 4:10**). The biodegradation percentage is the ratio between the produced CO_2 (or pressure decrease) and the theoretical CO_2 ($ThCO_2$/pressure) i.e. the amount of CO_2 expected in case of total oxidation of the carbon present in the polymer sample (Cpolymer) introduced in the vessel (Chinaglia et al., 2018; Gartiser, 2018b). The theoretical carbon dioxide ($ThCO_2$) is the expected amount of carbon dioxide to be produced from a polymer as a result of biodegradation based on the stoichiometry and theoretical yield calculations.

A field report by WTW Xylem describes the methodology used to determine the 'ready biodegradability' of organic substances, while following the OECD Guidelines 301F or 92/69 EEC, C.4-D by means of oxygen consumption due to mineralisation under aerobic conditions (Gartiser, 2018a). The plastic material as the single carbon source is added to mineral dilution water. The CO_2 developing due to oxygen consumption is absorbed by concentrated NaOH and manometrically measured as a negative pressure. The standard test concentration used for this experiment was 100 mg/L, with a theoretical oxygen demand (ThOD) of 100 mg/L , for example For example, 10 g of sodium acetate produces 10.7 g of CO_2 (10 g x $2CO_2$ (44 x 2)/sodium acetate ($(C_2H_3NaO_2)_n$82), this is to ensure sufficient available amount of carbon is present to be able to be detected and improve the biodegradation of plastic materials. For example, 10 g of PLA produces 18.3 g of CO_2 (10 g x $3CO_2$ (44 x 3)/PLA $(C_3H_4O_2)_n$72), which is the theoretical amount for 100% biodegradation. Similarly, for example, 10 g of PCL produces 23.2 g of CO_2 (10 g x $6CO_2$ (44 x 6)/PCL $(C_6H_{10}O_2)_n$114), which is the theoretical amount in the case of 100% biodegradation. Another example is for PBS, 10 g of poly(butylene succinate) (PBS) produces 20.5 g of CO_2 (10 g × $8CO_2$ (44 × 8)/PBS $(C_8H_{12}O_4)_n$172). The dilution water consists of deionized water and four mineral nutrient solutions (cf. OECD 301 F in conjunction with

OECD 301 A). Activated sludge from a wastewater treatment plant with mainly municipal wastewater is used as the inoculum, corresponding to a concentration of 30 mg TSS/L. In every test series, a reference substance (sodium acetate or sodium benzoate) is tested in a parallel series with a concentration of 100 mg/L. The standard filling volume used for this experiment was 164 mL/bottle based on the mass of plastic material. This enables to determine BOD values up to 400 mg/L in the aqueous phase. Approx. 16.4 mg/bottle solid matter (TSS) is directly weighted into the bottles (corresponds to100 mg/L).

Following on from this methodology, similar experimental set-up was applied for biodegradation studies. HEPES buffer is used for these experiments in order to maintain the pH at 7.4. The reason for using a buffer system to maintain the pH at 7.4 is to avoid pH decrease. It is well documented (Pastorino et al., 2004; Adhikari et al., 2016; Fang et al., 2020; Oh et al., 2022) when the enzyme attacks the surface of the PCL PMP, acid is released and therefore a pH decrease is observed which results in the denaturing of the enzyme, leading to insufficient degradation capacity and inaccurate data.

OxiTop®-IDS measures carbon dioxide by monitoring the pressure changes in a closed vessel as microorganisms consume oxygen and produce CO_2. This process is based on respirometry, where the absorption of CO_2 by sodium hydroxide pellets in the sleeve leads to pressure changes that are detected by the OxiTop®-IDS system. The system is versatile and can be used for measuring BOD and respiration in both aerobic and anaerobic conditions. By utilising the OxiTop®-IDS measuring heads, users can easily backup and analyse data to track the production of CO_2 during microbial decomposition processes. Overall, OxiTop®-IDS provides a reliable and efficient method for measuring carbon dioxide production in various environmental samples



Figure 4:4 Assembly of OxiTop©-IDS heads screwed to 250mL glass bottles with nozzles on a stirrer platform

Preparation of HEPES buffer: 800 mL MilliQ water (MΩ·cm at 25°C) was poured into a 1.5 L glass beaker and heated to 37ºC. The required amount (7.15 g) of HEPES buffer (N-(2-Hydroxyethyl)piperazine-N′-(2-ethanesulfonic acid) was added and the pH was adjusted to 7.4 with 0.1 M NaOH and transferred into a 1 L volumetric flask and made up to 1 L to make a concentration of 30 mM. It should be noted alternative buffer systems were tested. When PCL PMPs were degraded in a different buffer solution (Tris(Hydroxymethyl)aminomethane (Tris) or phosphate-buffered saline (PBS), no pressure change was observed i.e., no produced CO_2 was detected, which suggests that that no gas is being generated. It could be possible that since the system is buffered, the CO_2 is dissolving in the liquid rather than as carbonate gas. The chemical structure for Tris is similar to monoethanolamine (solvent for carbon capture) used to capture carbon in wastewater treatment plants so it is thought the CO_2 reaction with Tris is likely to degrade the PCL. After several tests, HEPES buffer was chosen as this interacted less with the reaction mechanism and was proven to be suitable for these studies.

Biodegradation tests: The required volume of HEPES was added through the side arms of 250 mL bottles. PCL PMPs (2.5 g suspension at 1 wt%) was also added at this stage. The stirrer platform was placed into an incubator set at 37°C. A magnetic stirrer bar was added into each bottle. Two NaOH pallets were added into the rubber sleeve connected to the OxiTop©-IDS wireless measuring heads and sealed tightly. The amount of NaOH pellets (~468mg) was sufficient to absorb all the produced CO_2 expected (the mass of carbon present in the PCL PMPs of 25 mg and calculated based on the theoretical CO_2 ($ThCO_2$/pressure) as described above. The bottles were placed in the oven to reach ~37°C prior to the addition of lipase solution to allow the temperature to equilibrate. The Bluetooth© LE technology (data logger) for operation with Multi 3630 IDS wireless measuring head was started to record the changes in pressure (hPa). After allowing the system to equilibrate overnight, the lipase solution was added into the bottle via a syringe needle through the rubber stoppers of the side arms. The test was set up with control (without PCL PMPs) and with reference PCL PMPs (without enzyme). Three replicates were carried out for each PCL PMPs, for blank and for reference PCL PMPs, and incubated in the dark at 37 ± 2 °C.

From the lipase activity and mass of PCL PMPs in the system, the ratio can be calculated **Table 4:3**. For all tests, a mass of PCL PMPs of 25 mg was used. The lipase activity was re-measured during the course of the PhD and the mass of enzyme used in each experiment was adjusted accordingly to ensure consistency of activity throughout all conducted tests.

Table 4:3 – Calculated PCL PMPs: lipase ratio based on mass of PCL PMPs and lipase activity

Lipase (mg)	Lipase activity in the reaction vessel (U/mg)	Ratio PCL PMPs:lipase
82	2911	0.009
50	1065	0.014
27.7	625	0.040
16.9	600	0.042
12.3	277	0.090
2.5	88.8	0.282
2.1	71	0.352

4.2.2.4 Statistical analysis

To decide which statistical analysis to use or what is the appropriate statistical test to be employed for the analysis of the pH-stat (FFA) data , some pre-analysis checks were done. Among the pre-analysis checks are examination of the data type and some preliminary statistical test on the assumptions of parametric test to help decide whether parametric or non-parametric is suitable for the analysis. To compare the difference among the seven samples at different time points, the ANOVA is most suitable. Therefore, basic assumptions of the ANOVA needed to be satisfied before it could be used. They include normality of residuals and the consistency of the error variance among the samples (**Figure 4:5**).

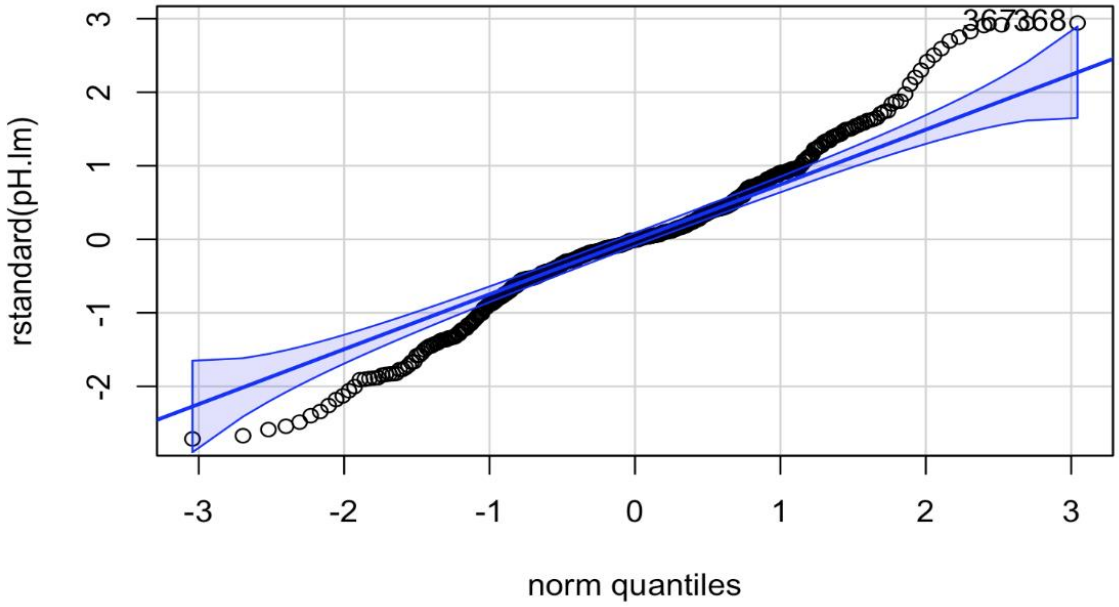


Figure 4:5 – Q-Q plot, model assumption of normality of residuals

The Q-Q plot seems to indicate a problem with the normality of residuals, as more than half of the residuals from each of the three separate groups of residuals deviate from the straight line, resulting in them being outside of the shaded area. To confirm that the residuals do not satisfy the normality assumption as indicated by the Q-Q plot shown in **Figure 4:5**, normality tests are conducted using Shapiro-Wilk test, the Lillifors (also known as the Kolmogorov-Smirnov test) and the Anderson-Darling test.

Table 4:4 – Normality test

Test	**Statistic**	p-value
Shapiro-Wilk	0.98008	$1.32e^{-05}$
Anderson-Darling	3.3241	$2.48e^{-08}$
Kolmogorov-Smirnov	0.07364	$8.59e^{-06}$
Breusch-Pagan	284.38	$2.2e^{-16}$

The Shapiro-Wilk test, the Kolmogorov-Smirnov test and the Anderson-Darling test all confirm that the residual do not satisfy the normality assumption (non-normality of the standardised residuals) as their p-values as shown in **Table 4:4** are all less than 0.05.

Model Assumption of Consistency of error variance.

Breusch-Pagan (BP) test is used to examine consistency of error variance. The result BP test as shown in **Table 4:4** has p-value of $2.2e^{-16}$, which is less than a significance of 0.05. Hence, we can conclude that there is no consistency in the error variance. Therefore, we should proceed directly to the step which tests our hypothesis with the Friedman two-way ANOVA.

Significant differences between samples were determined by Friedman rank sum test by two-way ANOVA using R studio software. The Friedman test is a non-parametric statistical test (Zimmerman and Zumbo, 1993) meaning in this case, that repeated measures of %FFA as a function of time are analysed for significant differences. Experiments were conducted at least in triplicate. Results in **Table 4:5** are expressed as mean ± standard deviation.

The mathematical model for the Freidman test is shown in equation **4:7**

$$T_1 = \frac{12}{bk(k+1)} \sum_{i=1}^{k} (R_i - b(k+1)/2)^2 \qquad \textbf{4:7}$$

where *k* is the number of ranked observations or measurements (columns), *b* is the number of subjects (rows), and R*i* is the sum of the ranked scores in each column. The numbers 12 and 2 are constants, not dependent on the number of subjects or experimental conditions

The results for the experimental data obtained for the pressure measurement tests, were carried out using Microsoft Excel. The statistical analyses were conducted using one-way ANOVA and the mathematical model Pearson correlation coefficient 0.998 using statistical functions of Excel Microsoft and the significant difference between samples were considered when $p < 0.05$. If the null hypothesis (H_0) is not rejected then no further analysis is required. On the other hand, if the null hypothesis is rejected then further analysis is required to identify significant differences. The level of significance are $p < 0.05$, therefore, the null hypothesis is rejected. The results were reported as mean and standard deviations of five measurements on triplicate samples ($n = 3 \times 3$).

4.3 Results and Discussion

The first part of the results and discussion focusses on the release of acid upon the degradation of PCL PMPs by lipase. The second part of the results and discussion then focusses on the production of carbon dioxide (CO_2) using pressure measurements to understand the secondary products of the biodegradation process.

4.4 Release of acid upon PCL PMPs degradation by lipase

The aim of this experiment was to understand whether the PCL PMPs (d_{32} 10.1 µm, surface area of 0.99 m^2) degrades using lipase enzyme and how enzyme-substrate ratio influence the rate and degree of free fatty acid (FFA) release.

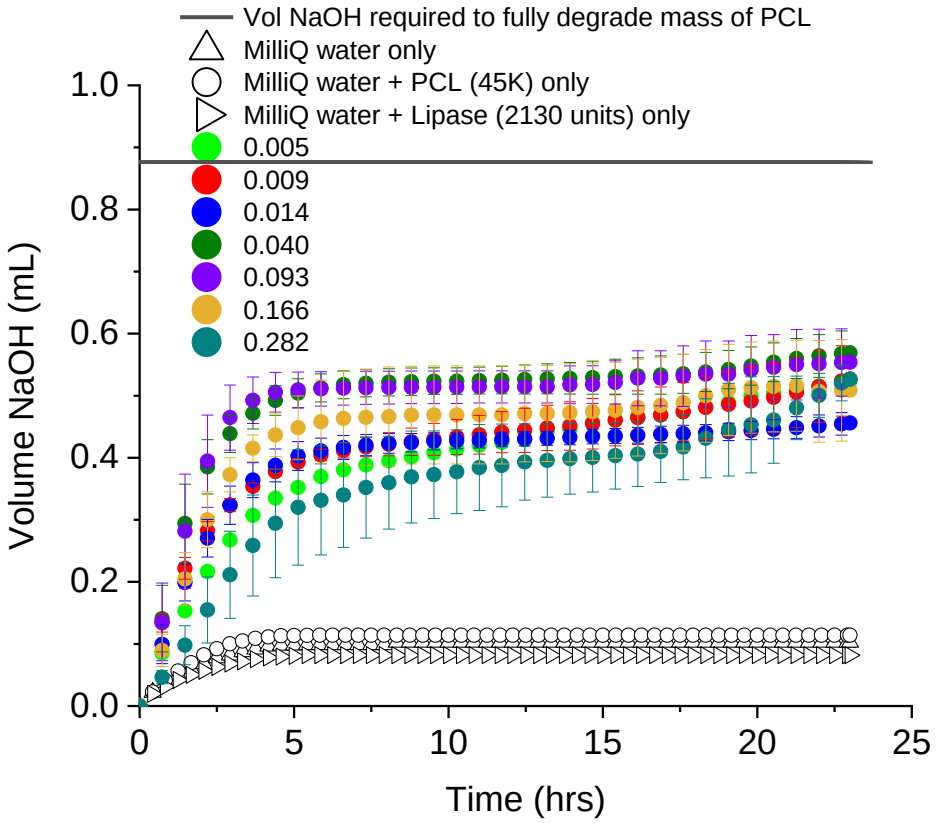
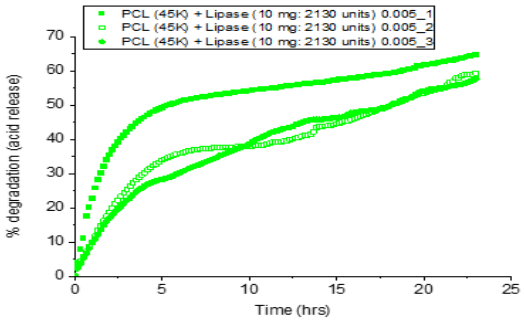


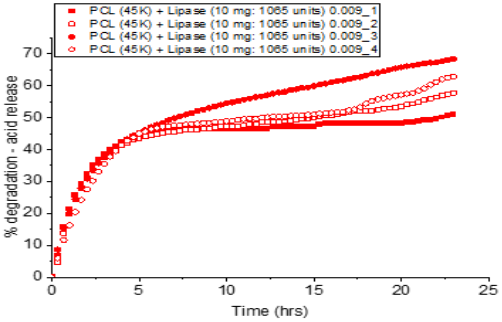
Figure 4:6 - Mean change in volume of NaOH as a function of time of enzymatic reaction during PCL degradation at varying concentration of enzyme at pH 7.4 and 37 °C. The black data are blank control tests showing limited acid release. Standard deviation shows error bars for three independent readings for triplicate samples (n = 3 x 3).

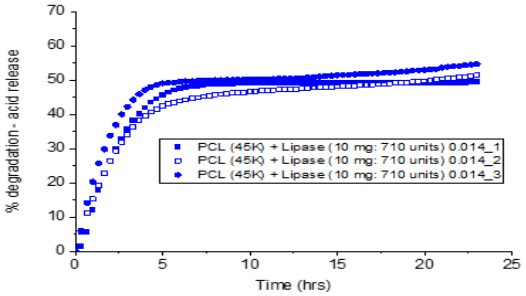
The free fatty acids (FFAs) released from the depolymerisation of PCL PMPs were measured by using an automatic pH-stat titration unit (TIM 856 titration manager, Titralab, Radiometer analytical) (Tan et al., 2020). The theoretical delivery of NaOH to fully degrade the mass of PCL PMPs (10 mg) is 0.876 mL (continuous black line) as shown in **Figure 4:6**. The results follow a typical titration curve as described in the previous section **Figure 4:3**. The results suggest that there is a limited degree of hydrolysis for PCL PMPs in the absence of lipase (hollow black circle, square and triangle) which is expected as the blank experiments were performed as a control, to measure pH fluctuation in the absence of enzymes or PCL PMPs as demonstrated by Pastorino et al. (2004) where they reported that no PCL degradation was observed in water or solvent mixtures in the absence of the enzyme. A dose-response relationship is observed in the degradation of PCL PMPs at 37 ºC over 24 hours when exposed to lipase, but it is uncertain if a dose-dependent trend in lipase activity can be identified.

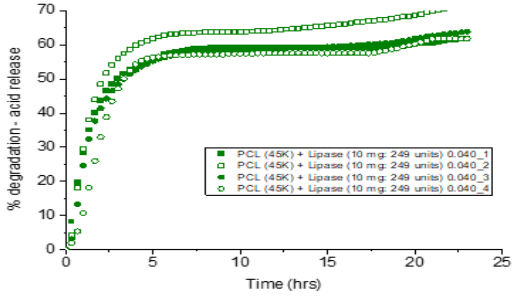
Another approach to examining this phenomenon is through rate kinetics analysis. Rate kinetics analysis may provide additional insights into the degradation of PCL PMPs when exposed to lipase at different doses. This method can help elucidate any potential dose-dependent trends in lipase activity that may not be readily apparent from the initial observations. FFA release

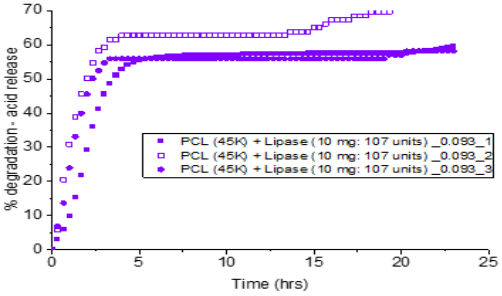
In order to investigate the degradation behaviour of PCL PMPs when induced by enzyme, a pH stat was used to monitor FFA release. The hydrolysis reaction takes place between the enzyme and the surface ester-bonds of PCL PMPs resulting in the generation of 6-hydroxylcaproic acid (6-HCA). For this, the enzyme penetrates the surface and bonds to a surface-ester group, where the hydrolytic step takes place as explained by **Figure 4:1** and **Figure 4:3** (Reul et al., 2011).

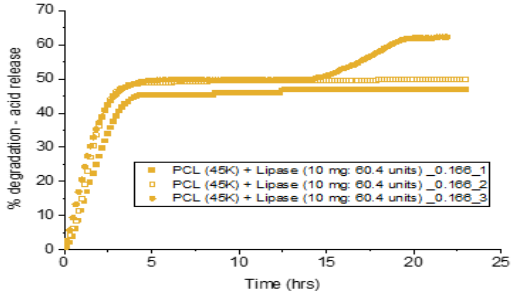

PCL (45K) + Lipase (10 mg: 2130 units) 0.005_1
PCL (45K) + Lipase (10 mg: 2130 units) 0.005_2
PCL (45K) + Lipase (10 mg: 2130 units) 0.005_3
% degradation (acid release)
Time (hrs)


PCL (45K) + Lipase (10 mg: 1065 units) 0.009_1
PCL (45K) + Lipase (10 mg: 1065 units) 0.009_2
PCL (45K) + Lipase (10 mg: 1065 units) 0.009_3
PCL (45K) + Lipase (10 mg: 1065 units) 0.009_4
% degradation - acid release
Time (hrs)


PCL (45K) + Lipase (10 mg: 710 units) 0.014_1
PCL (45K) + Lipase (10 mg: 710 units) 0.014_2
PCL (45K) + Lipase (10 mg: 710 units) 0.014_3
% degradation - acid release
Time (hrs)


PCL (45K) + Lipase (10 mg: 249 units) 0.040_1
PCL (45K) + Lipase (10 mg: 249 units) 0.040_2
PCL (45K) + Lipase (10 mg: 249 units) 0.040_3
PCL (45K) + Lipase (10 mg: 249 units) 0.040_4
% degradation - acid release
Time (hrs)


PCL (45K) + Lipase (10 mg: 107 units) _0.093_1
PCL (45K) + Lipase (10 mg: 107 units) _0.093_2
PCL (45K) + Lipase (10 mg: 107 units) _0.093_3
% degradation - acid release
Time (hrs)


PCL (45K) + Lipase (10 mg: 60.4 units) _0.166_1
PCL (45K) + Lipase (10 mg: 60.4 units) _0.166_2
PCL (45K) + Lipase (10 mg: 60.4 units) _0.166_3
% degradation - acid release
Time (hrs)

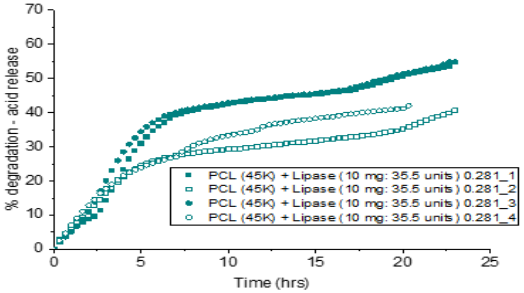

PCL (45K) + Lipase (10 mg: 35.5 units) 0.281_1
PCL (45K) + Lipase (10 mg: 35.5 units) 0.281_2
PCL (45K) + Lipase (10 mg: 35.5 units) 0.281_3
PCL (45K) + Lipase (10 mg: 35.5 units) 0.281_4
% degradation - acid release
Time (hrs)

Figure 4:7 - Titration curve showing the % degradation of PCL PMPs at pH 7.4, 37°C at varying lipase dosages with a pH stat device. The percent degradation is related to the free fatty acid released from the ester functional groups of polycaprolactone (6-hydroxylcaproic acid) as they are hydrolysed in the course of a lipase assay. Data presented are of three independent experiments. All experiment with PCL PMPs 45 kDa molecular weight (10 mg particles) – Ratio of PCL: Lipase (mg per unit) (green – 0.005), (red – 0.009), (blue – 0.014), (olive – 0.040), (purple – 0.09), (yellow – 0.166), (dark cyan – 0.282).

All PCL PMPs presented a steep increase in the amount of %FFA released within the first 2 h after exposure lipase enzyme (pH 7.4) as shown in **Figure 4:7.** It was followed by a more gradual increase at longer times, until a relatively constant final value of %FFA was reached. The initial rapid rate illustrated in **Figure 4:3** and seen in all the tests in **Figure 4:7** followed a linear gradient. This was followed by a slow almost plateauing trend at approx. 5 hours also known as the saturation point. This decrease in the rate of FFA release can be explained by the accumulation of 6-hydroxylcaproic acid (6-HCA) products at the PCL/water interface during the process of degradation (Sarkar et al., 2019; Fang et al., 2020). Another possible explanation is that the solubility of hydroxyhexanoic acid is influenced by various factors including temperature, pressure, and solvent chemistry. These factors can alter the interactions between the acid and solvent molecules, consequently affecting the acid's solubility. The similarity of the data has also been shown by Oh et al. (2022) where the production of 6-hydroxyhexanoic acid (6-HHA) from the degradation of PCL (form or mass not provided) with an enzyme was monitored at varying pH, temperature, enzyme concentration and enzyme addition times. The percent degradation achieved in the study was not explicitly mentioned in the provided data. The study focused on the efficient enzymatic depolymerization of polycaprolactone into 6-hydroxyhexanoic acid and the microbial conversion of 6-hydroxyhexanoic acid into adipic acid. Optimization of reaction conditions led to a titer of 114.9 g/L of 6-HHA and productivity of 2.87 g/L/h from 100 g/L PCL. The study sets the groundwork for eco-friendly recycling of waste PCL into a value-added chemical. Further research is ongoing to enhance the production of adipic acid from 6-HHA.. Pastorino et al. (2004) evaluated the degradation of PCL films with a molecular weight of 87 K Da with three sources of enzymes. The results of the degradation reaction showed that *M. miehei* lipase was able to degrade PCL with a maximum conversion degree of ~70% after 1 h, within the temperature range of 40–60°C, whereas the enzyme half-life was less than 2 h at 60°C. Reul et al. (2011) investigated the degradation of nanoparticles (diameter 70 to 170nm) of three different branched polyester nanoparticles (Boltron H40 (116 nm), Boltron U3000 (diameter 160 nm), Boltron W3000 (diameter 73 nm). They conducted pH

titration using a pH stat at pH 7.4 and 37 ºC and hypothesised that when the ester bonds of the branched polymer cleave, the resulting carboxylic acid can be titrated by NaOH. During pH titration, the pH value is maintained to pH 7.4 by constantly neutralizing the free acids being produced by the degradation process. The amount of required NaOH to maintain the pH constant results from the level of degradation in the sample. The results showed that the branched polyester namely, Boltorn H40 showed hydrolytic degradation of 6.95% of ester bonds were cleaved in 24 h. Degradation of the other two nanoparticles, Boltorn U3000 (2.39%) and Boltorn W3000 (1.50%), was slower, showing only very few cleaved ester bonds after titration. They concluded that this was probably caused by the presence of lipophilic fatty acid groups, which both polymers possess, as well as by the lower ester content. The ester degradation follows a first order kinetic and is therefore concentration dependent. Both dendritic polymers, Boltorn U3000 and Boltorn W3000, possess less ester in 2mg/ml compared to Boltorn H40 which does not contain any hydrophilic or lipophilic chains (Reul et al., 2011).

4.4.1 The effect of Ratio PCL: Lipase and rate of degradation – acid release

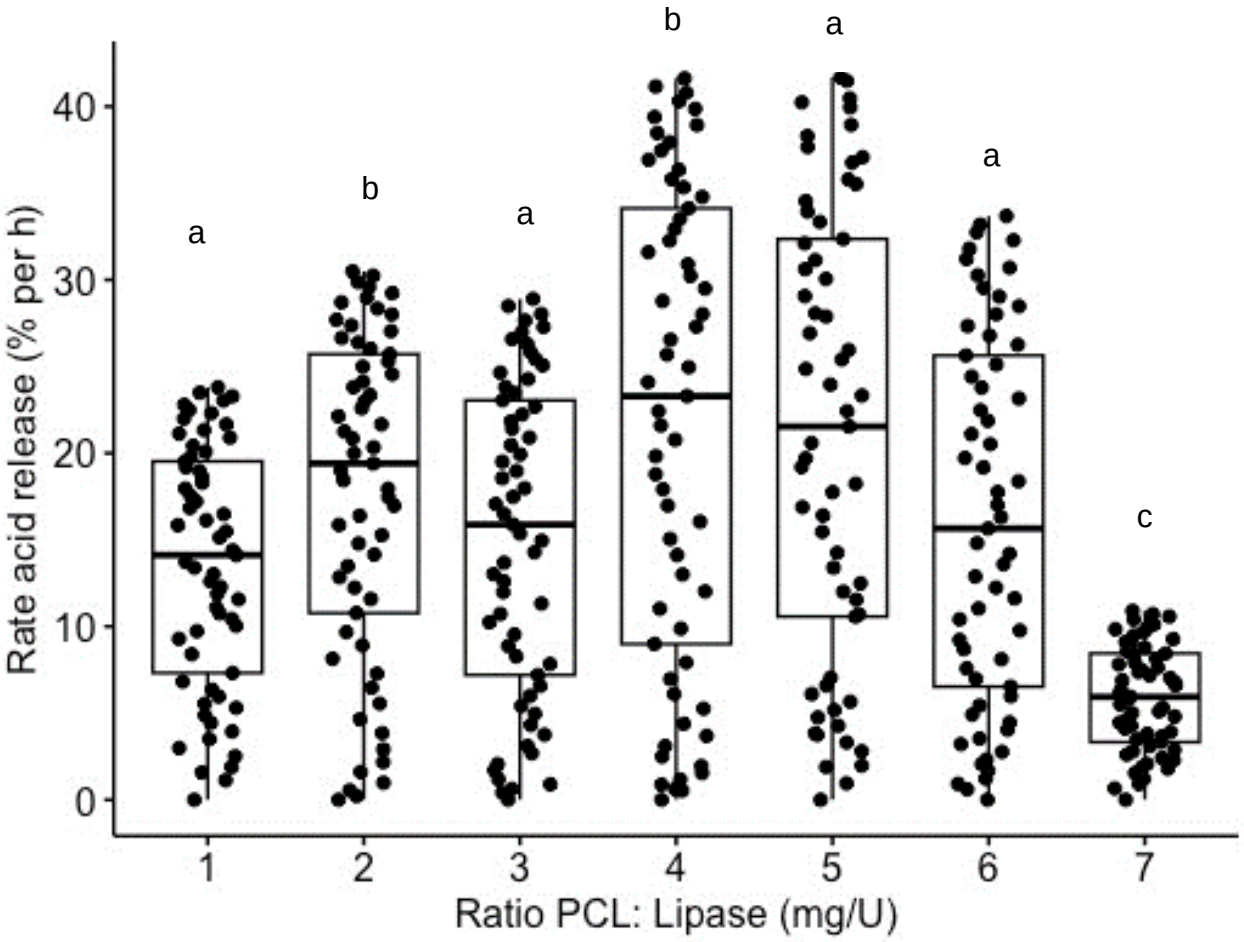


Figure 4:8 - Enzymatic degradation of PCL PMPs at 37°C and pH 7.4. Boxplot distribution of the saturation results showing percentage of free fatty acid (% FFA available based on 10 mg PCL) released at different time points (solid black circles). The mean values for each sample (1-7) are shown as a thicker solid black lines. Proportion of FFA released (% rate acid release) after 2 h of exposure to lipase enzyme at varying concentration. Data presented are mean with standard deviation of three independent experiments. Different letters indicate significant differences. Ratio PCL; Lipase (mg/U) 1= 0.005, 2=0.009, 3=0.014, 4=0.040, 5=0.093, 6=0.166, 7=0.282.

Table 4:5 - Pairwise comparisons using Conover's all-pairs test

		1	2	3	4	5	6
2		6.10E-05*	-	-	-	-	-
3		1	6.10E-05*	-	-	-	-
4		5.70E-10*	0.7207	5.70E-10*	-	-	-
5		1.30E-10*	0.3995	1.30E-10*	1	-	-
6		1	0.0071*	1	4.20E-07*	1.20E-07*	-
7		3.70E-05*	< 2e-16*	3.70E-05*	< 2e-16*	< 2e-16*	1.00E-07*

**p<0.05*

Table 4:6 - Friedman rank sum test

Chisq	**Df**	**p.chisq**	**F**	**DFerror**	**p.F**	**t.value**	**LSD**
228.37	6	0	99.56	360	0	1.97	28.78

The chi-square statistic was 228.37, which results in a p-value (for comparison with the chi-square statistics) of p.chisq < 0.001, which is much smaller than a 5% significance level. There is enough evidence to conclude there is at least one comparison, based on the rank sums, that is different. Furthermore, pairwise comparison test was employed to identify the samples are significantly different from the others and the result is presented in **Table 4:6** and **Figure 4:8**

Table 4:7 – Mean and median % FFA

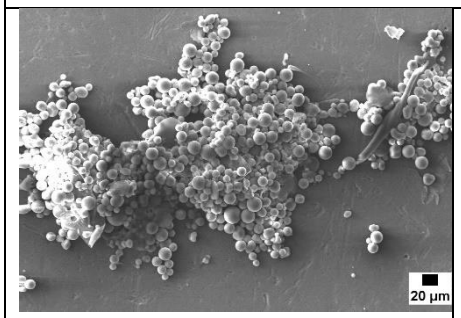
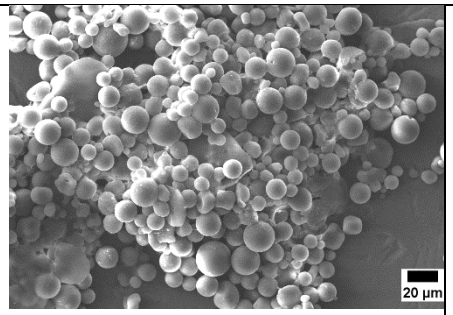
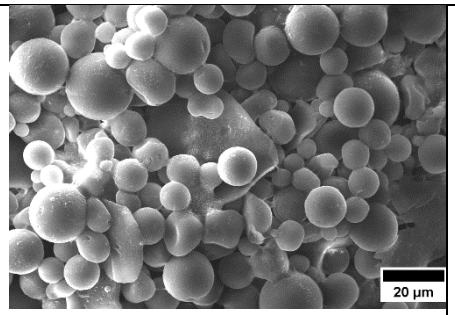
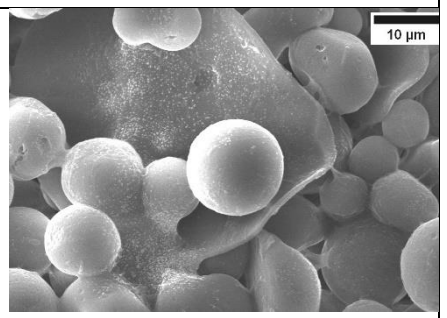
Sample	**n**	**Mean Rate acid release (% h^{-1})**	**Median Rate acid release (% h^{-1})**
1 – 0.005	61	13.5	14.1
2 – 0.009	61	17.7	19.4
3- -0.014	61	15.1	15.9
4 – 0.040	61	21.7	23.3
5 – 0.093	61	21.1	21.5
6 – 0.166	61	16.1	15.7
7 – 0.282	61	5.86	5.94

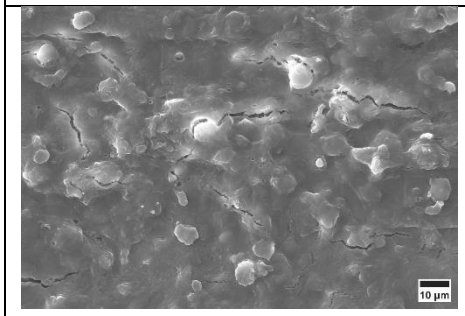
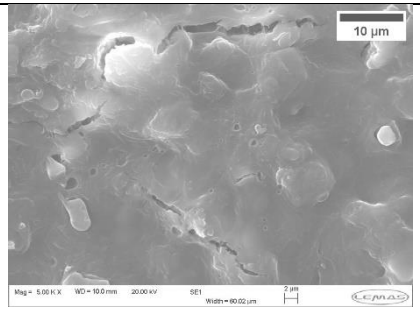
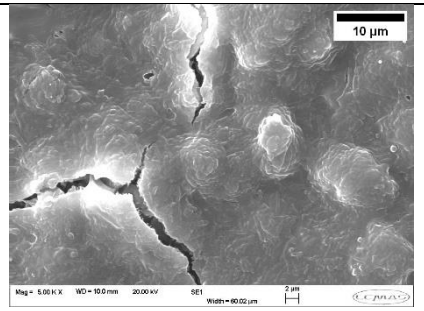
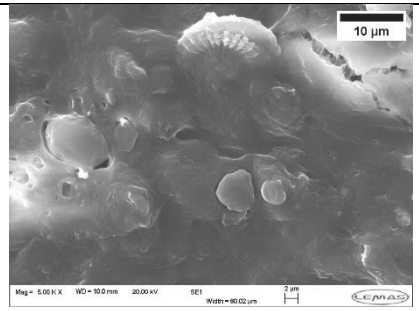
Sample 4 at PCL: Lipase ratio 0.040 has the highest rate of acid release (% per h) and sample 7 (0.005) the lowest rate. The mean values place the rate of acid release (% per h) at the category levels. The letters a, b and c identify significant differences by analysing multiple comparisons in which a set of group means are ranked from smallest to largest with letters to indicate significant differences and 95% confidence limit. Means that do not share a letter are significantly different (level of significance) $p<0.05$. Hence, we have rates ranging from 5.86 to 21.7 (**Table 4:7**). The results in **Figure 4:8** show that significant differences ($p<0.05$) in the rate of acid release are seen between high, mid and low levels of lipase dose, where a high peak is seen with ratio 0.040 (sample 4) and 0.093 (sample 5) PCL PMPs: lipase at 21.7% and 21.1% respectively. The ratio at 0.005 (sample 1) is where excess lipase dose is added at a ratio of 0.282 and sample 7 is the lowest lipase dose tested where only 5.86% is seen. This is supported by the explanation from authors Robinson (2015) and Sarkar et al. (2019) where the surface area available for lipase to bind is significantly reduced due to the presence of excess lipase/ and or excess PCL particle and not enough enzyme on the particle surface resulting in reduced kinetics. The results suggests that the maximum PCL to lipase concentration ratio is 0.040. Consequently, this ratio was chosen for subsequent degradation analysis in the following chapters.

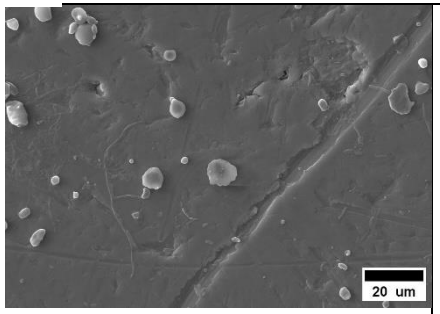
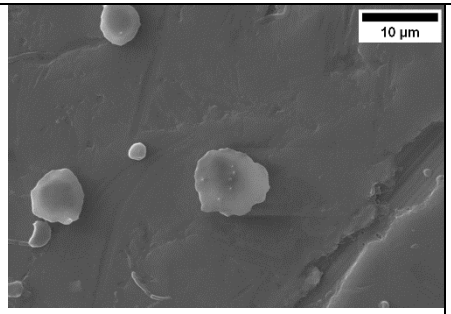
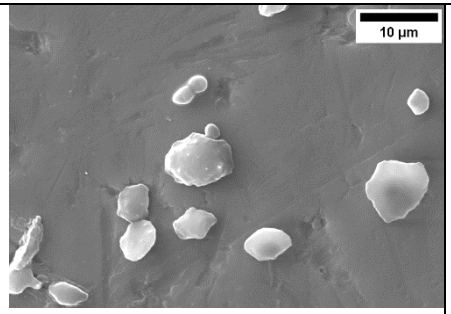
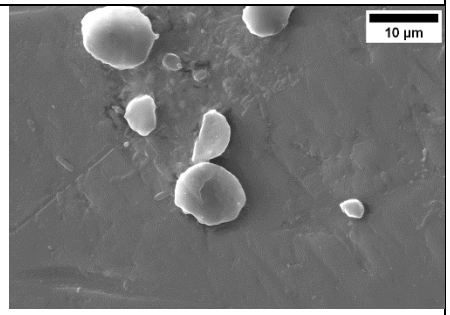
4.4.2 Scanning electron microscopy of degraded PCL particles at varying ratio

The aim of this study was to use scanning electron microscopy (SEM) to obtain information about the surface structure, roughness, and porosity of particles. This information can be used to compare the images before during and after degradation. The samples for the SEM analysis were prepared by adding a pipette drop of the suspension onto a stub and left to air dry overnight in a clean environment to avoid any dust contamination. The samples were coated with platinum with a thickness of 20 nm using Leica EM ACE600 before analysis. The images shown in **Figure 4:9** (a) show PCL PMPs blank tests in the absence of lipase after a pH stat run (24 h) and shows that the particles are not degraded although slightly aggregated compared to the images before degradation shown in Section **3.8.3**, but this could be due to the sample preparation for SEM analysis. This suggests that the PCL PMPs are not damaged during the pH-stat method and in agreement with the data seen in **Figure 4:6** where no degradation is observed further confirming the findings. The images shown in **Figure 4:9** (b) are of PCL PMPs: lipase ratio 0.005 (have the highest dose of lipase). The images appear to show a ‘coating’ like material over the PCL particles, this supports the information obtained from the reduced rate of FFA release mentioned earlier which could be caused by enzyme saturation (Robinson, 2015; Sarkar et al., 2019). **Figure 4:9** (c) shows the images of particles at PCL: lipase ratio at 0.009, where the fragmentation of the particles is observed, which supports the hypothesis of the biodegradation process that the hydrolysable bonds in the polymer chain are broken down to oligomers of different chain lengths (Adhikari et al., 2016; Rosato et al., 2020). Finally, **Figure 4:9** (d) shows the degradation of PCL PMPs at PCL PMPs: lipase ratio of 0.040 where the maximum concentration was found to be in terms of FFA release (%). The images show the PCL PMPs have been degraded on the surface of the particle which confirms the hypothesis of the stage 2 degradation process where surface erosion is initially observed, however not completely degraded as it is well documented that as the polymer degrades, biomass is formed which is associated with stage 3 of the

biodegradation process (Ruka et al., 2015; Chinaglia et al., 2018). It can be seen that the PCL PMPs have a rough surface with some cracks because of the polymer surface degradation.

a	Blank, no lipase (after pH stat run)		
			
500 x	1000 x	2000 x	5000 x

b	Ratio 0.005 - PCL (45K) + Lipase (10 mg: 2130 units)		
			
2000 x	5000x	5000 x	5000 x

c	Ratio 0.009 - PCL (45K) + Lipase (10 mg: 1065 units)		
			
2000 x	5000x	5000 x	5000 x

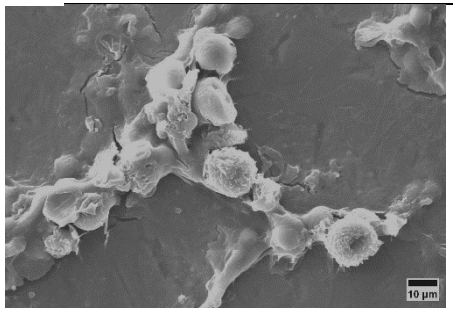
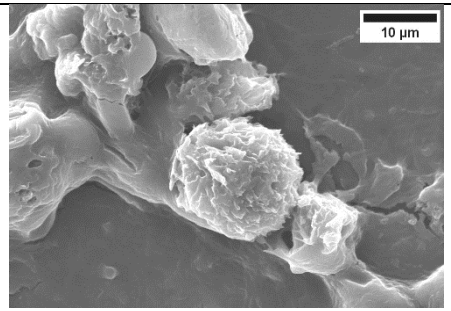
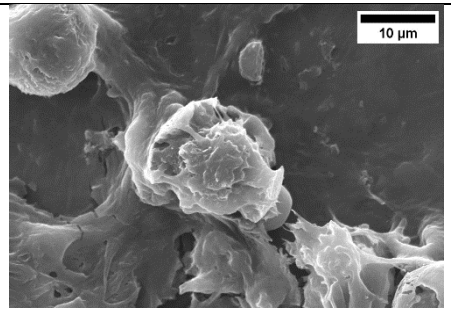
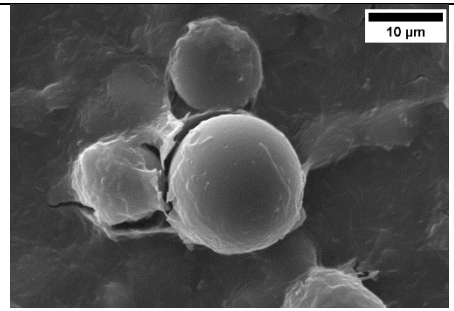
d	Ratio 0.040 - PCL (45K) + Lipase (10 mg: 249 units)		
			
2000 x	5000 x	5000 x	5000 x

Figure 4:9 – Scanning electron microscopy of PCL particles after degradation using pH stat at varying PCL PMPs: Lipase ratio (mg per unit). Showing significant differences in the morphology of the particles compared to the control (no lipase), a) Blank, no lipase (after pH stat run), b) Ratio 0.005 - PCL (45K) + Lipase (10 mg: 2130 units), c) Ratio 0.009 - PCL (45K) + Lipase (10 mg: 1065 units), d) Ratio 0.040 - PCL (45K) + Lipase (10 mg: 249 units)

4.5 Production of CO_2 upon PCL PMPs degradation by lipase

This section focusses on the production of carbon dioxide (CO_2) using pressure measurements to understand the secondary products of the biodegradation process. PCL PMPs (d32 10.1 µm, surface area of 0.99 m2) were degraded using lipase enzyme and varying enzyme-substrate ratio was used to understand the influence on the rate and degree of degradation.

4.5.1 Control tests with 30 mM HEPES buffer as control substrate

The aim of this experiment was to perform blank experiments as a control to measure CO_2 fluctuation in the absence of lipase or PCL PMPs (**Figure 4:10 a and b**). The difference in pressure produced during the control experiments, will then be subtracted from the data recorded obtained in the experiments conducted in the presence of PCL particles/lipase.

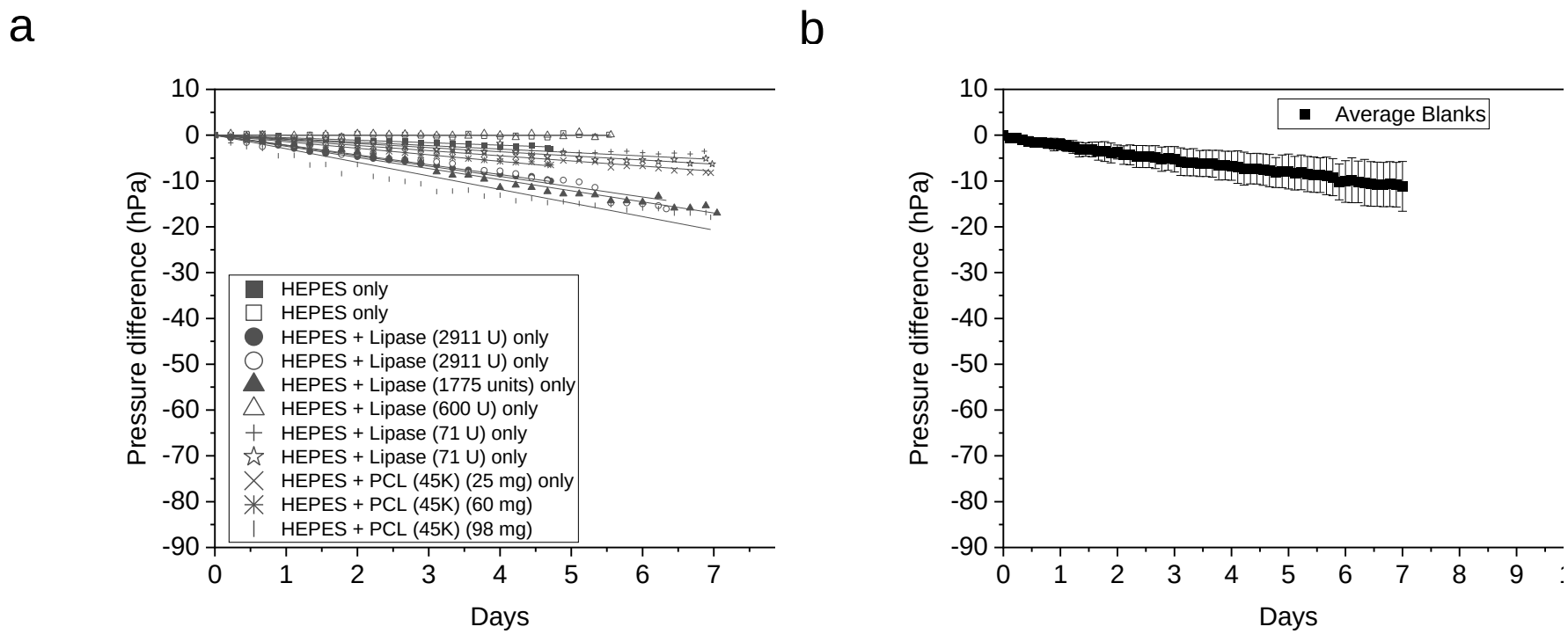


Figure 4:10 - Pressure difference (ΔhPa) as a function of time. a) No significant pressure change of the blank tests, indicating minimal CO_2 gas absorbed and recorded as expected b) Mean pressure difference of all blank tests combined.

The results in **Figure 4:10a**, suggest that there is a limited degree of CO_2 production for PCL PMPs in the absence of lipase which is expected as the blank experiments were performed as a control, to measure CO_2 fluctuation in the absence of enzymes or PCL particles. The average pressure difference (hPa) during the control experiments (**Figure 4:10b**) will be subtracted from the data recorded in the presence of PCL particles/lipase experiments. Each blank and PCL/Lipase experiment was repeated at least three times.

4.5.2 Mean production of CO_2 as a function of time and Rate % degradation as a function enzyme-substrate

The aim of this experiment was to degrade PCL PMPs using lipase enzyme and evaluate the influence of enzyme-substrate ratio on the degree and rate of CO_2 production. The purpose was to understand the degradation of PCL PMPs by monitoring the increase in production of CO_2 during the degradation process using pressure measurements to understand the secondary products of the biodegradation process (3rd stage). An explanation is given about how the data is converted from pressure measurement (hPa) into the percent CO_2 production (%) and rate of biodegradation (% day^{-1}). The pressure difference is measured first then this is turned into a calculation as a percent of how much CO_2 is removed by the NaOH in the instrument sleeve. Next, in order to determine the initial degradation rate, k (% day^{-1}), a simple linear regression analysis on the data over 2 days of the biodegradation phase of each sample is taken where the best fits to the experimental data predicted using the mathematical model Pearson correlation coefficient 0.998 using statistical functions of Excel (Microsoft) is performed.

4.5.3 Rate of pressure difference

The pressure difference (hPa) was determined by subtracting the total pressure (produced CO_2) of the blank tests (**Figure 4:10**) from the pressure of the experiment with PLC: lipase (CO_2 PCL) at $t=_0$ for each PCL: lipase ratio shown in **Figure 4:11** (Chinaglia et al., 2018).

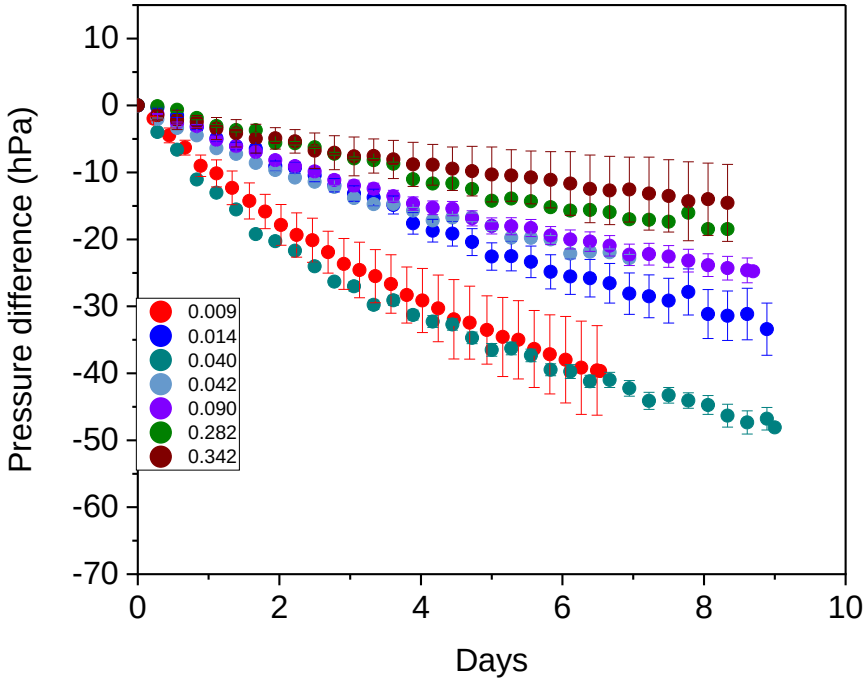


Figure 4:11 – Mean pressure difference as a function of time of enzymatic reaction during PCL PMP degradation at varying concentration of enzyme at pH 7.4 and 37 °C in 30 mM HEPES buffer. Standard deviation shows error bars for three independent readings for triplicate samples (n = 3). Individual PCL/ lipase experiments can be found in the Appendix, **Figure A:0:3.** Ratio of PCL: Lipase (mg per unit) - (red – 0.009), (blue – 0.014), (olive – 0.040), (teal – 0.042), (purple – 0.090), (cyan – 0.28), (wine – 0.352)

Figure 4:11 shows the decrease in pressure as the PCL PMP are exposed to lipase at varying concentrations. This behaviour is line with the hypothesis that as expected, the PCL PMPs consume oxygen and form CO_2 which is absorbed by NaOH, creating a vacuum resulting in measured negative pressure (hPa) as described by several authors (Funabashi et al., 2006; Kunioka et al., 2009; Gómez and Michel, 2013; Chinaglia et al., 2018). From this data, it is unclear of any trends in terms of varying lipase concentration and thus, the measured negative pressure for each sample can be analysed in terms of a rate kinetics as a linear regression plot as shown in **Figure 4:12.**

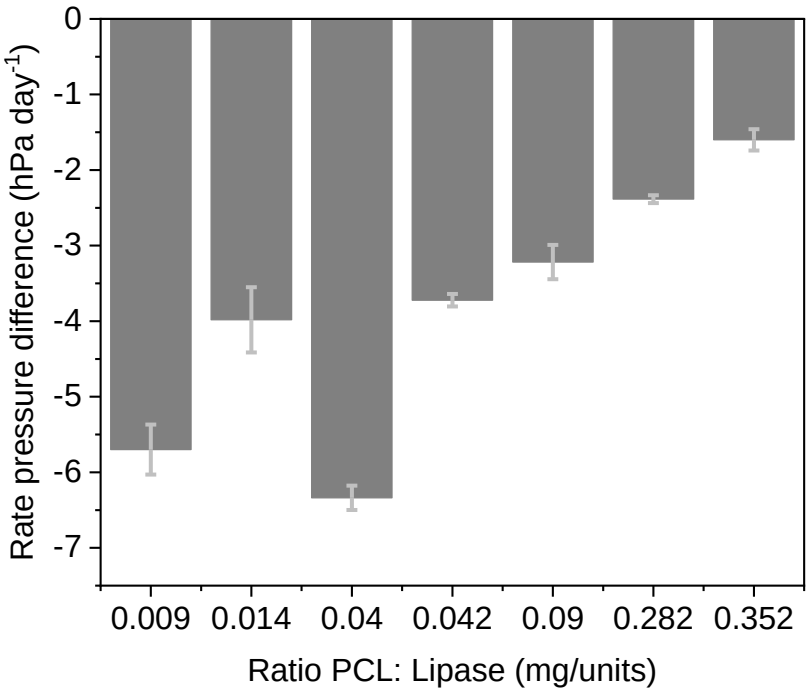


Figure 4:12 – Mean rate of pressure difference hPa day^{-1} as a function of time of enzymatic reaction during PCL PMPs degradation at varying concentration of enzyme at pH 7.4 and 37 °C in HEPES buffer. The slope constants k are taken from the pressure difference (CO_2 PCL PMPs) rates (hPa day^{-1}) from **Figure 4:11**. Standard deviation shows error bars for three independent readings for triplicate samples (n = 3). Individual PCL/ lipase experiment can be found in the Appendix, **Figure A:0:3**

The relationship between the pressure difference (hPa) rate and the PCL: lipase ratio has been explored using the regression analysis (simple regression) shown in **Figure 4:12** and based on the stoichiometry described in equation **4:4** as described by a few authors (Chinaglia et al., 2018; Tosin et al., 2019). In order to determine the initial degradation rate, k (hPa day^{-1}), a simple linear regression analysis on the data over 2 days of the biodegradation phase of each sample was taken where the best fits to the experimental data predicted using the mathematical model Pearson correlation coefficient 0.998 using statistical functions of Excel (Microsoft) was performed.

The results indicate that there is a trend in terms of the rate of degradation and the PCL: lipase ratio where an optimal rate is observed at ratio 0.040 PCL: lipase. Interestingly, this trend is also observed and in line with the pH stat data (see section **4.4.1**) where the optimal PCL; lipase ratio is also 0.040 of the degradation of PCL showing the hydrolysis of the ester bond into 6-hydroxycaproic acid (6-HCA) under similar conditions (pH 7.4, 37°C).

4.5.4 Rate of CO_2 production % degradation as a function of time

The percentages of biodegradation were calculated from the ratio between the total CO_2 production and the theoretical CO_2 production calculated on the basis of carbon content for PCL (equations **4:5** and **4**:**6**) shown in **Figure 4:13**. For example, 0.025 g of caprolactone produces 0.0579 g of CO_2 (0.025 g /Mw caprolactone ($C_6H_{10}O_2$) 114.14 g/mol^{-1}) = 2.19 x 10^{-4} moles caprolactone x 6CO_2 = 1.31 x 10^{-3} moles CO_2, using the gas law equation, PV=nRT, the theoretical pressure can be calculated which is the theoretical amount in the case of 100% biodegradation, (83.14 L.hPa.K^{-1}.mol^{-1} x 1.31 x 10^{-3} moles CO_2 x 310 K)/0.146 L = 231.9 hPa. Authors Tosin et al. (2019) and Chinaglia et al. (2018), applied the Lineweaver-Burk plot to determine the rate degradation. The data is described by a linear regression of the double reciprocal plot that can be used to estimate the theoretical maximum biodegradation. In this work, a linear regression analysis on the data over 2 days of the biodegradation phase of each sample was taken, where the best fits to the experimental data predicted using the mathematical model Pearson correlation coefficients 0.998 using statistical functions of excel was performed (**Figure 4:14** and **Table 4:8**). The slope constants k are the rate of CO_2 production rates (% day^{-1}).

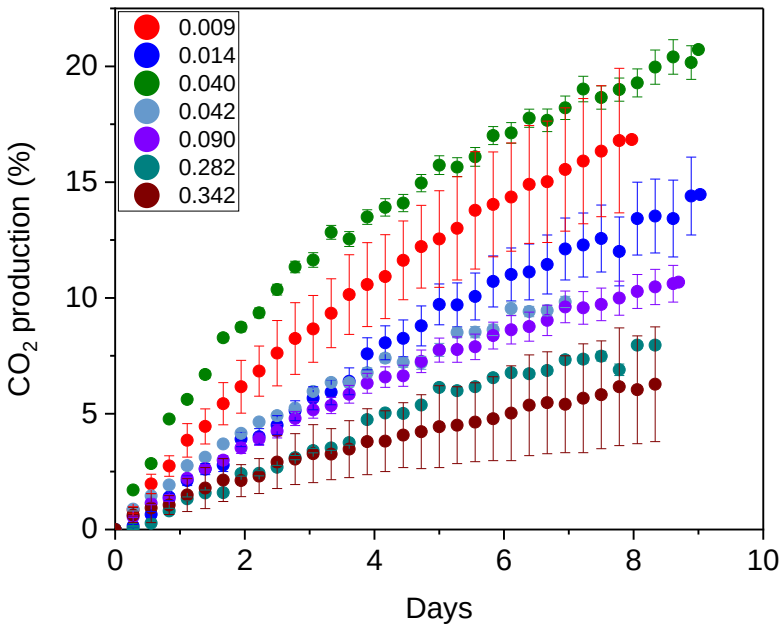


Figure 4:13 – Mean CO_2 production as a function of time of enzymatic reaction during PCL degradation at varying concentration of enzyme at pH 7.4 and 37 °C in 30 mM HEPES buffer. The CO_2 production (%) was calculated from the pressure difference using the gas law equation as described using **equation 4:5** (Funabashi et al., 2006; Kunioka et al., 2009; Chinaglia et al., 2018; Gartiser, 2018b). Standard deviation shows error bars for three independent readings for triplicate samples (n = 3 x 3). Individual PCL/ lipase experiment can be found in the **Appendix, Figure A:0:4.** Ratio of PCL: Lipase (mg per unit) - (red – 0.009), (blue – 0.014), (olive – 0.040), (teal – 0.042), (purple – 0.090), (cyan – 0.28), (wine – 0.352)

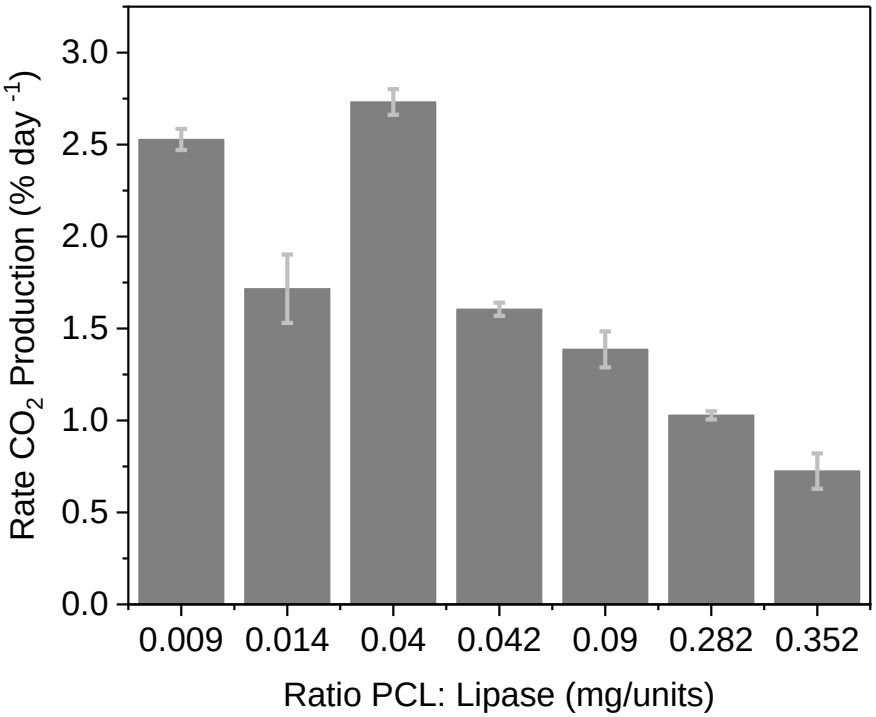


Figure 4:14 - CO_2 production rate resulting from the biodegradation of PCL PMPs of varying surface areas. Experiments are conducted at pH 7.4 in 30 mM HEPES buffer and a PCL/lipase ratio of 0.040. The biodegradation percentage is the ratio between the calculated CO_2 (%) (**Figure 4:13**) and the total possible CO_2 i.e. the amount of CO_2 expected in case of total oxidation of the carbon present in the PCL PMPs introduced in the vessel (Ahn et al., 2008; Gómez and Michel, 2013; Chinaglia et al., 2018). Error bars are standard deviation for three independent readings for triplicate samples (n = 3). Individual PCL/ lipase experiment can be found in the Appendix, **Figure A:0:4.**

Table 4:8 - The influence of PCL PMPs - lipase ratio on the degree and rate of CO_2 production - statistical analysis using the Tukey Method and 95% Confidence

Ratio PCL: lipase (mg/U)	**Rate CO_2 production (% day^{-1})**	**Pearson's r**	***p* value**	**CLD**
0.009	2.3	0.989	0.014	b
0.014	1.7	0.995	0.007	c
0.017	1.0	0.997	0.003	f
0.040	2.7	0.971	0.026	a
0.042	1.6	0.986	0.012	d
0.090	1.4	0.990	0.008	d
0.282	1.0	0.991	0.005	e
0.342	0.6	0.991	0.003	f

Compact Letter Display (CLD) - Means that do not share a letter are significantly different (level of significance) *p<0.05.*

As observed before, the results indicate that there is a trend in terms of the rate of degradation and the PCL: lipase ratio where an optimal rate is observed at ratio 0.040 PCL: lipase at 2.7 % day^{-1} (**Figure 4:14** and **Table 4:8**) and similar conclusions can be drawn as described previously that all the PCL PMPs presented a steep increase in the amount of % CO_2 production within the first 2 days after exposure lipase enzyme (pH 7.4) as shown in **Figure 4:13**. The sample at PCL: Lipase ratio 0.040 has the highest rate of CO_2 production (% day^{-1}) and 0.352 has the lowest rate.

4.5.5 Scanning electron microscopy of PCL particles after degradation using pressure measurement – production of CO_2

The PCL PMPs were characterised using scanning electron microscopy (SEM) to obtain information about the surface structure, roughness, and porosity of particles. This information can be used to compare the images before during and after degradation. The samples for the SEM analysis were prepared by adding a pipette drop of the suspension onto a stub and left to air dry overnight. The sample was coated with rhodium before analysis. The images shown in **Figure 4:15a** show PCL PMPs blank tests in the absence of lipase after a run (10 days) and shows that the particles are slightly damaged (flattened and aggregated) compared to the images before degradation shown in Section **3.8.3**, but this could be due between the interaction with PCL and HEPES buffer as this was not observed with the blank runs using the pH stat which was in MilliQ water another explanation could be the damaged caused by sample preparation for SEM analysis. The images shown in **Figure 4:15b** to **d** are of PCL PMPs: lipase ratio 0.040 as a function of time at 1 h, 2 h, and overnight (24 h) respectively. The images clearly appear to show fragmentation of the particles which supports the hypothesis of the biodegradation process that the hydrolysable bonds in the polymer chain are broken down to oligomers of different chain lengths (Adhikari et al., 2016; Rosato et al., 2020).

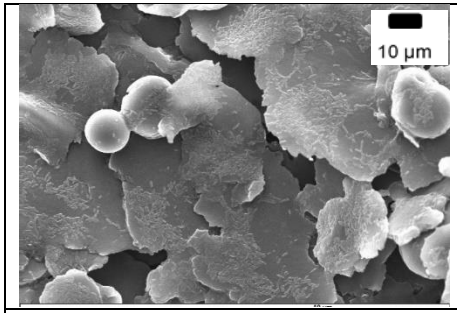
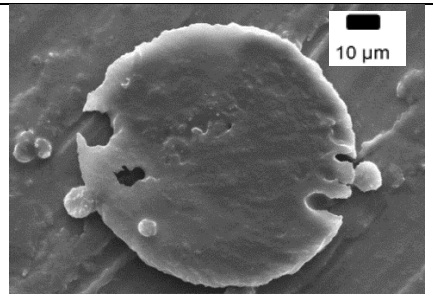
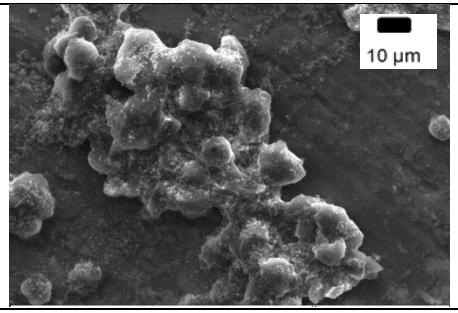
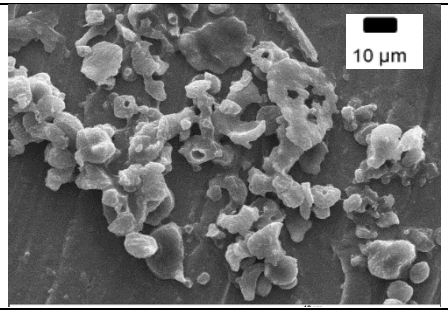
			
A) HEPES + PCL only	B) 1 hr HEPES + PCL + lipase (0.040)	C) 2 hr HEPES + PCL + lipase (0.040)	D) Overnight HEPES + PCL + lipase (0.040)

Figure 4:15 - Scanning electron microscopy of PCL particles after degradation using pressure measurement – production of CO_2 at 0.040 PCL: Lipase ratio (mg per unit). A) HEPES + PCL only, B) 1 hr HEPES + PCL + lipase (0.040), C) 2 hr HEPES + PCL + lipase (0.040), D) Overnight HEPES + PCL + lipase (0.040). All images with scale bar at 10 µm

4.6 Conclusion

Polycaprolactone microparticles (PCL PMPs) were degraded with lipase in different substrate-enzyme ratio to understand the hydrolytic biodegradation kinetics. All PCL PMPs that were tested at varying ratios of PCL PMPs: lipase presented a steep increase in the amount of %FFA (6-hydroxycaproic acid; 6-HCA) released within the first 2 h after exposure lipase enzyme at pH 7.4 and 37°C, indicating that the ester bonds on the surface of the particles were accessed by lipase immediately irrespective of the amount of lipase used leading to degradation (Reul et al., 2011). Furthermore, the scanning electron microscopy images support PCL PMPs degradation with the PCL PMPs showing rough surfaces with some cracks confirming degradation. Notably at a high lipase concentration (0.005 ratio PCL: lipase), enzyme saturation was observed with limited degradation in line with reduced amount of 6-HCA release. The maximum PCL to lipase concentration ratio was found to be 0.040 where 22% 6-HCA was observed. Furthermore, the maximum degradation rate measured via the production of carbon dioxide (CO2) was also with a ratio of 0.040 PCL PMPs: lipase, where 2.73% CO2 production per day was observed.

4.7 References

Adhikari, D., Mukai, M., Kubota, K., Kai, T., Kaneko, N., Araki, K.S. and Kubo, M. 2016. Degradation of Bioplastics in Soil and Their Degradation Effects on Environmental Microorganisms. *Journal of Agricultural Chemistry and Environment.* **05**(01), pp.23-34.

Agarwal, S. 2020. Biodegradable Polymers: Present Opportunities and Challenges in Providing a Microplastic-Free Environment. *Macromolecular Chemistry and Physics.* **221**(6), article no: 2000017 [no pagination].

Ahn, H.K., Huda, M.S., Smith, M.C., Mulbry, W., Schmidt, W.F. and Reeves, J.B., 3rd. 2011. Biodegradability of injection molded bioplastic pots containing polylactic acid and poultry feather fiber. *Bioresour Technol.* **102**(7), pp.4930-4933.

Albright, V.C., 3rd and Chai, Y. 2021. Knowledge Gaps in Polymer Biodegradation Research. *Environ Sci Technol.* **55**(17), pp.11476-11488.
Ammala, A. 2013. Biodegradable polymers as encapsulation materials for cosmetics and personal care markets. *Int J Cosmet Sci.* **35**(2), pp.113-124.

Anstey, A., Muniyasamy, S., Reddy, M.M., Misra, M. and Mohanty, A. 2014. Processability and Biodegradability Evaluation of Composites from Poly(butylene succinate) (PBS) Bioplastic and Biofuel Co-products from Ontario. *Journal of Polymers and the Environment.* **22**(2), pp.209-218.

Ashton, J.H., Mertz, J.A., Harper, J.L., Slepian, M.J., Mills, J.L., McGrath, D.V. and Vande Geest, J.P. 2011. Polymeric endoaortic paving: Mechanical, thermoforming, and degradation properties of polycaprolactone/polyurethane blends for cardiovascular applications. *Acta Biomater.* **7**(1), pp.287-294.

Bagheri, A.R., Laforsch, C., Greiner, A. and Agarwal, S. 2017. Fate of So-Called Biodegradable Polymers in Seawater and Freshwater. *Glob Chall.* **1**(4), p1700048.

Bartnikowski, M., Dargaville, T.R., Ivanovski, S. and Hutmacher, D.W. 2019. Degradation mechanisms of polycaprolactone in the context of chemistry, geometry and environment. *Progress in Polymer Science.* **96**, pp.1-20.

Blackwell, C.J., Haernvall, K., Guebitz, G.M., Groombridge, M., Gonzales, D. and Khosravi, E. 2018. Enzymatic Degradation of Star Poly(epsilon-Caprolactone) with Different Central Units. *Polymers (Basel).* **10**(11).

Borthakur, L.J., Jana, T. and Dolui, S.K. 2010. Preparation of core–shell latex particles by emulsion co-polymerization of styrene and butyl acrylate, and evaluation of their pigment properties in emulsion paints. *Journal of Coatings Technology and Research.* **7**(6), pp.765-772.

C. Eldsater, B.E., R. Renstad, A.-C. Albertsson, S. Karlsson. 2000. The biodegradation of amorphous and crystalline regions in film-blown poly(e-caprolactone). *Polymer.* **41**, pp.1297-1304.

Cao, J., Dang, G., Li, H., Li, T., Yue, Z., Li, N., Liu, Y., Liu, S. and Chen, L. 2015. Identification and Characterization of Lipase Activity and Immunogenicity of LipL from Mycobacterium tuberculosis. *PLoS One.* **10**(9), pe0138151.

Castilla-Cortázar, I., Más-Estellés, J., Meseguer-Dueñas, J.M., Escobar Ivirico, J.L., Marí, B. and Vidaurre, A. 2012. Hydrolytic and enzymatic degradation of a poly(ε-caprolactone) network. *Polymer Degradation and Stability.* **97**(8), pp.1241-1248.

Chen, D.R., Bei, J.Z. and Wang, S.G. 1999. Polycaprolactone microparticles and their biodegradation. *Polymer Degradation and Stability.* **67**, pp.455-459.
Chinaglia, S., Tosin, M. and Degli-Innocenti, F. 2018. Biodegradation rate of biodegradable plastics at molecular level. *Polymer Degradation and Stability.* **147**, pp.237-244.

Ciuffreda, P., Casati, S., Loseto, A. and Santaniello, E. 2009. Spectrophotometric Assay of Lipase Activity: A New 4-nitrophenyl Ester of a Dialkylglycerol Suitable as a Chromogenic Substrate of Pseudomonas cepacia Lipase. *Biocatalysis and Biotransformation.* **21**(3), pp.123-127.

Emadian, S.M., Onay, T.T. and Demirel, B. 2017. Biodegradation of bioplastics in natural environments. *Waste Manag.* **59**, pp.526-536.

Erlanson, C. and Borgström, B. 2020. Tributyrine as a Substrate for Determination of Lipase Activity of Pancreatic Juice and Small Intestinal Content. *Scandinavian Journal of Gastroenterology.* **5**(4), pp.293-295.

Fang, Z., Gao, Y., Wu, X., Xu, X., Sarmah, A.K., Bolan, N., Gao, B., Shaheen, S.M., Rinklebe, J., Ok, Y.S., Xu, S. and Wang, H. 2020. A critical review on remediation of bisphenol S (BPS) contaminated water: Efficacy and mechanisms. *Critical Reviews in Environmental Science and Technology.* **50**(5), pp.476-522.

Fredric. Carriere, James. A.Barrowman, Robert. Verger and Rene. Laugier. 1993. Secretion and Contribution to Lipolysis of Gastric and Pancreatic Lipases During a Test Meal in Humans. *SECRETION OF DIGESTIVE LIPASES AND LIPOLYSIS.* **105**, pp.876-888.

Funabashi, M., Ninomiya, F. and Kunioka, M. 2006. Biodegradation of Polycaprolactone Powders Proposed as Reference Test Materials for International Standard of Biodegradation Evaluation Method. *Journal of Polymers and the Environment.* **15**(1), pp.7-17.

G. Sivalingam, S.C., G. Madras. 2002. Solvent effects on the lipase catalyzed biodegradation of poly (e-caprolactone) in solution. *Polymer Degradation and Stability.* **79**, pp.413-418.

Gartiser, S. Manometric respiration tests according to OECD 301F with the OxiTop®Control measuring system under GLP conditions.

Gartiser, S. 2018. Manometric respiration tests according to OECD 301F with the OxiTop® Control measuring system under GLP conditions. **WTW Field Report**.

Ghimire, S., Flury, M., Scheenstra, E.J. and Miles, C.A. 2020. Sampling and degradation of biodegradable plastic and paper mulches in field after tillage incorporation. *Science of the Total Environment.* **703**, article no: 135577 [no pagination].

Gómez, E.F. and Michel, F.C. 2013. Biodegradability of conventional and bio-based plastics and natural fiber composites during composting, anaerobic digestion and long-term soil incubation. *Polymer Degradation and Stability.* **98**(12), pp.2583-2591.

Gonzalez-Pleiter, M., Tamayo-Belda, M., Pulido-Reyes, G., Amariei, G., Leganes, F., Rosal, R. and Fernandez-Pinas, F. 2019. Secondary nanoplastics released from a biodegradable microplastic severely impact freshwater environments. *Environmental Science-Nano.* **6**(5), pp.1382-1392.

Grundy, M.M.L., Abrahamse, E., Almgren, A., Alminger, M., Andres, A., Ariëns, R.M.C., Bastiaan-Net, S., Bourlieu-Lacanal, C., Brodkorb, A., Bronze, M.R., Comi, I., Couëdelo, L., Dupont, D., Durand, A., El, S.N., Grauwet, T., Heerup, C., Heredia, A., Infantes Garcia, M.R., Jungnickel, C., Kłosowska-Chomiczewska, I.E., Létisse, M., Macierzanka, A., Mackie, A.R., McClements, D.J., Menard, O., Meynier, A., Michalski, M.-C., Mulet-Cabero, A.-I., Mullertz, A., Payeras Perelló, F.M., Peinado, I., Robert, M., Secouard, S., Serra, A.T., Silva, S.D., Thomassen, G., Tullberg, C., Undeland, I., Vaysse, C., Vegarud, G.E., Verkempinck, S.H.E., Viau, M., Zahir, M., Zhang, R. and Carrière, F. 2021. INFOGEST inter-laboratory recommendations for assaying gastric and pancreatic lipases activities prior to in vitro digestion studies. *Journal of Functional Foods.* **82**.

Iwata, T. 2015. Biodegradable and bio-based polymers: future prospects of eco-friendly plastics. *Angew Chem Int Ed Engl.* **54**(11), pp.3210-3215.
Jenkins, M.J. and Harrison, K.L. 2008. The effect of crystalline morphology on the degradation of polycaprolactone in a solution of phosphate buffer and lipase. *Polymers for Advanced Technologies.* **19**(12), pp.1901-1906.

Kim, M., Park, J.M., Um, H.J., Lee, D.H., Lee, K.H., Kobayashi, F., Iwasaka, Y., Hong, C.S., Min, J. and Kim, Y.H. 2010. Immobilization of cross-linked lipase aggregates onto magnetic beads for enzymatic degradation of polycaprolactone. *J Basic Microbiol.* **50**(3), pp.218-226.

Kjeldsen, A., Price, M., Lilley, C. and Guzniczak, E. 2019. A Review of Standards for Biodegradable Plastics. *IBioIC.*

Kumar, G.A., Anjana, K., Hinduja, M., Sujitha, K. and Dharani, G. 2020. Review on plastic wastes in marine environment – Biodegradation and biotechnological solutions. *Marine Pollution Bulletin.* **150**, article no: 110733 [no pagination].

Kunioka, M., Ninomiya, F. and Funabashi, M. 2009. Biodegradation of poly(butylene succinate) powder in a controlled compost at 58 degrees C evaluated by naturally-occurring carbon 14 amounts in evolved CO(2) based on the ISO 14855-2 method. *Int J Mol Sci.* **10**(10), pp.4267-4283.

Magni, S., Bonasoro, F., Della Torre, C., Parenti, C.C., Maggioni, D. and Binelli, A. 2020. Plastics and biodegradable plastics: ecotoxicity comparison between polyvinylchloride and Mater-Bi (R) micro-debris in a freshwater biological model. *Science of the Total Environment.* **720**, article no: 137602 [no pagination].

Mat, D.J.L., Le Feunteun, S., Michon, C. and Souchon, I. 2016. In vitro digestion of foods using pH-stat and the INFOGEST protocol: Impact of matrix structure on digestion kinetics of macronutrients, proteins and lipids. *Food Research International.* **88**, pp.226-233.

Nair, L.S. and Laurencin, C.T. 2007. Biodegradable polymers as biomaterials. *Progress in Polymer Science.* **32**(8-9), pp.762-798.

Nakasaki, K., Matsuura, H., Tanaka, H. and Sakai, T. 2006. Synergy of two thermophiles enables decomposition of poly-epsilon-caprolactone under composting conditions. *FEMS Microbiol Ecol.* **58**(3), pp.373-383.

Nam, H.C. and Park, W.H. 2020. Aliphatic Polyester-Based Biodegradable Microbeads for Sustainable Cosmetics. *Acs Biomaterials Science & Engineering.* **6**(4), pp.2440-2449.

Nguyen, T.V., Nguyen Tri, P., Nguyen, T.D., El Aidani, R., Trinh, V.T. and Decker, C. 2016. Accelerated degradation of water borne acrylic nanocomposites used in outdoor protective coatings. *Polymer Degradation and Stability.* **128**, pp.65-76.

Oh, Y.-R., Jang, Y.-A., Song, J.K. and Eom, G.T. 2022. Efficient enzymatic depolymerization of polycaprolactone into 6-hydroxyhexanoic acid by optimizing reaction conditions and microbial conversion of 6-hydroxyhexanoic acid into adipic acid for eco-friendly upcycling of polycaprolactone. *Biochemical Engineering Journal.* **185**.

Pabois, O., Antoine-Michard, A., Zhao, X., Omar, J., Ahmed, F., Alexis, F., Harvey, R.D., Grillo, I., Gerelli, Y., Grundy, M.M., Bajka, B., Wilde, P.J. and Dreiss, C.A. 2020. Interactions of bile salts with a dietary fibre, methylcellulose, and impact on lipolysis. *Carbohydr Polym.* **231**, p115741.

Pastorino, L., Pioli, F., Zilli, M., Converti, A. and Nicolini, C. 2004. Lipase-catalyzed degradation of poly(ε-caprolactone). *Enzyme and Microbial Technology.* **35**(4), pp.321-326.

Qiao, T., Kim, S., Lee, W. and Lee, H. 2019. Biodegradable and Porous Poly(lactic-co-glycolic acid) Microbeads for In vitro Evaluation of Negatively Charged Fluorescent Bacteria. *Macromolecular Research.*

Reul, R., Renette, T., Bege, N. and Kissel, T. 2011. Nanoparticles for paclitaxel delivery: a comparative study of different types of dendritic polyesters and their degradation behavior. *Int J Pharm.* **407**(1-2), pp.190-196.

Robinson, P.K. 2015. Enzymes: principles and biotechnological applications. *Essays Biochem.* **59**, pp.1-41.

Roppola, K., Kuokkanen, T., Ramo, J., Prokkola, H. and Heiska, E. 2007. Comparison Study of Different BOD Tests in the Determination of BOD(7) Evaluated in a Model Domestic Sewage. *J Autom Methods Manag Chem.* **2007**, p39761.

Rosato, A., Barone, M., Negroni, A., Brigidi, P., Fava, F., Xu, P., Candela, M. and Zanaroli, G. 2020. Microbial colonization of different microplastic types and biotransformation of sorbed PCBs by a marine anaerobic bacterial community. *Science of the Total Environment.* **705**, article no: 135790 [no pagination].

Ruka, D.R., Sangwan, P., Garvey, C.J., Simon, G.P. and Dean, K.M. 2015. Biodegradability of Poly-3-hydroxybutyrate/Bacterial Cellulose Composites under Aerobic Conditions, Measured via Evolution of Carbon Dioxide and Spectroscopic and Diffraction Methods. *Environ Sci Technol.* **49**(16), pp.9979-9986.

Samir, A., Ashour, F.H., Hakim, A.A.A. and Bassyouni, M. 2022. Recent advances in biodegradable polymers for sustainable applications. *npj Materials Degradation.* **6**(1).

Sanchez-Hernandez, J.C., Capowiez, Y. and Ro, K.S. 2020. Potential Use of Earthworms to Enhance Decaying of Biodegradable Plastics. *ACS Sustainable Chemistry and Engineering.* **8**(11), pp.4292-4316.

Sánchez, C. 2020. Fungal potential for the degradation of petroleum-based polymers: An overview of macro- and microplastics biodegradation. *Biotechnology Advances.* **40**, article no: 107501 [no pagination].

Sarkar, A., Zhang, S., Holmes, M. and Ettelaie, R. 2019. Colloidal aspects of digestion of Pickering emulsions: Experiments and theoretical models of lipid digestion kinetics. *Adv Colloid Interface Sci.* **263**, pp.195-211.

Sarkar, A., Zhang, S., Murray, B., Russell, J.A. and Boxal, S. 2017. Modulating in vitro gastric digestion of emulsions using composite whey protein-cellulose nanocrystal interfaces. *Colloids Surf B Biointerfaces.* **158**, pp.137-146.

Shah, A.A., Hasan, F., Hameed, A. and Ahmed, S. 2008. Biological degradation of plastics: A comprehensive review. *Biotechnology Advances.* **26**(3), pp.246-265.

Sivalingam, G., Chattopadhyay, S. and Madras, G. 2003. Enzymatic degradation of poly (ε-caprolactone), poly (vinyl acetate) and their blends by lipases. *Chemical Engineering Science.* **58**(13), pp.2911-2919.

Tosin, M., Pischedda, A. and Degli-Innocenti, F. 2019. Biodegradation kinetics in soil of a multi-constituent biodegradable plastic. *Polymer Degradation and Stability.* **166**, pp.213-218.

Valencia, G.A., Zare, E.N., Makvandi, P. and Gutiérrez, T.J. 2019. Self-Assembled Carbohydrate Polymers for Food Applications: A Review. *Comprehensive Reviews in Food Science and Food Safety.* **18**(6), pp.2009-2024.

Yang, L., Li, J., Jin, Y., Li, M. and Gu, Z. 2015. In vitro enzymatic degradation of the cross-linked poly(ε-caprolactone) implants. *Polymer Degradation and Stability.* **112**, pp.10-19.

Ye, A., Cui, J., Zhu, X. and Singh, H. 2013. Effect of calcium on the kinetics of free fatty acid release during in vitro lipid digestion in model emulsions. *Food Chemistry.* **139**(1-4), pp.681-688.

Yunbing. Tan, Z.Z., Hualu. Zhou, Hang. Xiao, and David. Julian. McClements,. 2020. Factors impacting lipid digestion and β-carotene bioaccessibility assessed by standardized gastrointestinal model (INFOGEST): Oil droplet concentration. *Food & Function.*

Zhang, H., Wang, X., Wang, P., Liu, R., Hou, X., Cao, W., Zhong, R., Liu, X. and Zhang, Y. 2018. One-pot synthesis of biodegradable polydopamine-doped mesoporous silica nanocomposites (PMSNs) as pH-sensitive targeting drug nanocarriers for synergistic chemo-photothermal therapy. *RSC Advances.* **8**(65), pp.37433-37440.

Zimmerman, D.W. and Zumbo, B.D. 1993. Relative Power of the Wilcoxon Test, the Friedman Test, and Repeated-Measures ANOVA on Ranks. *The Journal of Experimental Education.* **62**(1), pp.75-86.

Anstey, A., Muniyasamy, S., Reddy, M.M., Misra, M. and Mohanty, A. Processability and Biodegradability Evaluation of Composites from Poly(butylene succinate) (PBS) Bioplastic and Biofuel Co-products from Ontario. *Journal of Polymers and the Environment.* 2014, **22**(2), pp.209-218.

Gómez, E.F. and Michel, F.C. Biodegradability of conventional and bio-based plastics and natural fiber composites during composting, anaerobic digestion and long-term soil incubation. *Polymer Degradation and Stability.* 2013, **98**(12), pp.2583-2591.

Ahn, H.K., Huda, M.S., Smith, M.C., Mulbry, W., Schmidt, W.F. and Reeves, J.B., 3rd. Biodegradability of injection molded bioplastic pots containing polylactic acid and poultry feather fiber. *Bioresour Technol.* 2011, **102**(7), pp.4930-4933.

Nakasaki, K., Matsuura, H., Tanaka, H. and Sakai, T. Synergy of two thermophiles enables decomposition of poly-epsilon-caprolactone under composting conditions. *FEMS Microbiol Ecol.* 2006, **58**(3), pp.373-383.

FRÉDÉRIC CARRIERE, J.A.B., ROBERT VERGER, and RENÉ LAUGIER. Secretion and Contribution to Lipolysis of Gastric and Pancreatic Lipases During a Test Meal in Humans. *SECRETION OF DIGESTIVE LIPASES AND LIPOLYSIS.* 1993, **105**, pp.876-888.

Erlanson, C. and Borgström, B. Tributyrine as a Substrate for Determination of Lipase Activity of Pancreatic Juice and Small Intestinal Content. *Scandinavian Journal of Gastroenterology.* 2020, **5**(4), pp.293-295.

Cao, J., Dang, G., Li, H., Li, T., Yue, Z., Li, N., Liu, Y., Liu, S. and Chen, L. Identification and Characterization of Lipase Activity and Immunogenicity of LipL from Mycobacterium tuberculosis. *Plos One.* 2015, **10**(9), p.e0138151.

Kjeldsen, A., Price, M., Lilley, C. and Guzniczak, E. A Review of Standards for Biodegradable Plastics. *IBioIC.* 2019.

Roppola, K., Kuokkanen, T., Ramo, J., Prokkola, H. and Heiska, E. Comparison Study of Different BOD Tests in the Determination of BOD(7) Evaluated in a Model Domestic Sewage. *J Autom Methods Manag Chem.* 2007, **2007**, p.39761.

Gartiser, S. Manometric respiration tests according to OECD 301F with the OxiTop® Control measuring system under GLP conditions. 2018, **WTW Field Report**.

Kunioka, M., Ninomiya, F. and Funabashi, M. Biodegradation of poly(butylene succinate) powder in a controlled compost at 58 degrees C evaluated by naturally-occurring carbon 14 amounts in evolved CO(2)

based on the ISO 14855-2 method. *Int J Mol Sci.* 2009, **10**(10), pp.4267-4283.

Funabashi, M., Ninomiya, F. and Kunioka, M. Biodegradation of Polycaprolactone Powders Proposed as Reference Test Materials for International Standard of Biodegradation Evaluation Method. *Journal of Polymers and the Environment.* 2006, **15**(1), pp.7-17.

Chinaglia, S., Tosin, M. and Degli-Innocenti, F. Biodegradation rate of biodegradable plastics at molecular level. *Polymer Degradation and Stability.* 2018, **147**, pp.237-244.

Gartiser, S. Manometric respiration tests according to OECD 301F with the OxiTop®Control measuring system under GLP conditions.

Adhikari, D., Mukai, M., Kubota, K., Kai, T., Kaneko, N., Araki, K.S. and Kubo, M. Degradation of Bioplastics in Soil and Their Degradation Effects on Environmental Microorganisms. *Journal of Agricultural Chemistry and Environment.* 2016, **05**(01), pp.23-34.

Fang, Z., Gao, Y., Wu, X., Xu, X., Sarmah, A.K., Bolan, N., Gao, B., Shaheen, S.M., Rinklebe, J., Ok, Y.S., Xu, S. and Wang, H. A critical review on remediation of bisphenol S (BPS) contaminated water: Efficacy and mechanisms. *Critical Reviews in Environmental Science and Technology.* 2020, **50**(5), pp.476-522.

Oh, Y.-R., Jang, Y.-A., Song, J.K. and Eom, G.T. Efficient enzymatic depolymerization of polycaprolactone into 6-hydroxyhexanoic acid by optimizing reaction conditions and microbial conversion of 6-hydroxyhexanoic acid into adipic acid for eco-friendly upcycling of polycaprolactone. *Biochemical Engineering Journal.* 2022, **185**.

Pastorino, L., Pioli, F., Zilli, M., Converti, A. and Nicolini, C. Lipase-catalyzed degradation of poly(ε-caprolactone). *Enzyme and Microbial Technology.* 2004, **35**(4), pp.321-326.

Nam, H.C. and Park, W.H. Aliphatic Polyester-Based Biodegradable Microbeads for Sustainable Cosmetics. *Acs Biomaterials Science & Engineering.* 2020, **6**(4), pp.2440-2449.

Tosin, M., Pischedda, A. and Degli-Innocenti, F. Biodegradation kinetics in soil of a multi-constituent biodegradable plastic. *Polymer Degradation and Stability.* 2019, **166**, pp.213-218.

Rosato, A., Barone, M., Negroni, A., Brigidi, P., Fava, F., Xu, P., Candela, M. and Zanaroli, G. Microbial colonization of different microplastic types and biotransformation of sorbed PCBs by a marine anaerobic bacterial community. *Science of the Total Environment.* 2020, **705**.

Chapter 5 Effect of varying surface area of PCL PMPs biodegradation Biodegradation

5.1 Introduction

In **Chapter 3**, three different batches of polycaprolactone microparticles (PCL PMPs) of varying particle size were prepared using the solvent extraction process. Increasing the surface area of PCL PMPs was achieved by increasing the homogenisation speed during the emulsion preparation stage, which resulted in the reduction of emulsion droplet size and the corresponding particle size (Katou et al., 2008; Makadia and Siegel, 2011; Staff et al., 2013a; Staff et al., 2013b). The homogenisation speeds used to prepare emulsion droplets were 4000 rpm, 8000 rpm and 12000 rpm resulting in specific surface areas of 0.54, 0.99 and 3.01 m^2/g respectively.

The purpose of measuring the surface area of PMPs was that the ratio of surface area to particle volume is a significant factor to determine the rate of degradation (Chinaglia et al., 2018). The hypothesis is that the larger the surface area, the faster the biodegradation kinetics as more of the polymer is made available for interaction with the components of the system initiating the degradation (i.e. enzymes in this case) (Chinaglia et al., 2018). While the idea that surface area is a relevant factor in biodegradation of microparticles is very common, few studies on the effect of this factor on biodegradation rates are available (Chen et al., 1999; Modelli et al., 1999; Funabashi et al., 2006; Yang, L. et al., 2015; Chinaglia et al., 2018). In a study by (Yang, H.-S. et al., 2005), the effect of the surface area of different plastics on their biodegradation behaviour has been investigated under controlled composting conditions at laboratory scale. In this study, the authors compared the biodegradation (produced CO_2) of polycaprolactone (PCL), poly (butylene succinate-co-adipate) (PBSA), poly(L-lactic acid) (PLLA) and poly(butylene succinate) (PBS) in film and ground particles form. The films were ~72 µm thickness and were cut into square pieces measuring approximately 2 x 2 cm, 1 x 1 cm, and 0.3 x 0.3 cm. The polymer pellets were ground into particles of 200 µm diameter. They found that at the early stage of the biodegradation, the polymers having a larger surface area, i.e. the ground particles, were degraded faster than the same mass of polymer in film

form. However, at the later stage of the degradation process, the biodegradation rate slowed down for both film and ground particle forms. This confirmed the hypothesis that the specific surface area of the polymer affects the biodegradation rate because of the different contact area between microbes or enzymes and the available surface area of the polymer (Yang, H.-S. et al., 2005). Chen et al. (1999) compared the degradation rates of PCL film and microparticles (PMPs) and found that despite PMPs having a much larger specific surface area (67 times more), the degradation rate of PCL film was not significantly different from that of PMPs (Chen et al., 1999). This is concordant with our observations that the surface area in the final stages of degradation (stage 3 – assimilation) does not play a significant role compared to stage 2 of the biodegradation process (explained in the literature review **(Chapter 2, section 2.32.3**) where fragmentation occurs at the surface of the PMP or film and the ester bonds of the polymer are cleaved to produce acid monomer units (Modelli et al., 1999; Chinaglia et al., 2018; Kjelsden et al., 2019). Chinaglia et al. (2018) compared the degradation rate (by monitoring CO_2 production) of different physical forms of polybutylene sebacate (PBS) and found that smaller particle sizes have a faster degradation rate as more surface area for a given mass is available for enzymatic activity. Pellets of the polymer were obtained and ground into powders to obtain three particle diameter size ranges: 50−75 μm, 200−355 μm, and 500−700 μm. Biodegradation of the three powders and the pellets was determined in an agricultural soil enriched with compost. All the powder forms achieved >89% degradation based on the amount of carbon dioxide produced compared to the theoretical maximum i.e. the amount of CO_2 expected in case of total oxidation of the carbon present in the polymer sample. The 50− 75 μm and 200−355 μm powder fractions exhibited similar degradation rates, while the 500−700 μm powder fraction degraded at a slower rate. However, the polymer was milled resulting in different size and shapes of microparticles. This adds complication and interference in the study such as inadequate representation of real life microparticles found in the environment, where their breakdown into micro and nanometer-sized fragments differ if the microparticles are milled, thus, leading to potential inaccurate representation of the real biodegradation process in the natural environment. More importantly, a measure of the size of non-spherical nanoparticles is often based on spherical equivalence as was the case here, then a calculation of the particle surface area (what actually matters here instead of

particle size) is not entirely accurate. The authors measured the particle size using specific surface area and Image J analysis of non-spherical particles. This is supported by Sintim and Flury (2017) who were concerned that grinding the primary constituents of a polymer into a powder would not be adequate for assessing the degradation potential of a final plastic product as this would not be comparable to real life scenarios. Modelli et al. (1999) evaluated the biodegradation using the same mass (about 0.5 g) of poly(3-hydroxybutyrate) (PHB) either as a film (with a thickness of 0.2–0.3 mm) or as a powder (≥100 μm) in soil. The degradation rate of PHB film was about 90 times slower than the initial rate measured with the PHB powder. The polymer films had a slow constant biodegradation rate, attributed to the effectively constant available surface area between the polymer and the microorganisms present in the soil (Modelli et al., 1999). The authors reported that the powdered polymers had a very high initial degradation rate but slowed down rapidly because the small particles degrade faster, but then leave behind the larger particles in mixtures with many sizes. When conducting surface area calculations based on the particle size distribution, it is important to consider the entire population rather than just relying on an average particle size. The average particle size can be influenced by the distribution of sizes within the population. For example, two populations may have the same average size diameter but differ in the distribution of particle sizes. A population with a broad distribution, including both small and large particles, will degrade faster due to the increased surface area provided by the smaller particles. Even if two populations have the same surface area based on calculations, their different distributions can impact degradation time. Smaller particles will degrade more quickly, affecting the kinetics of degradation.

The studies discussed either compare films with powders or compare polymer pellets ground to different degrees which is not very controllable. Thus this study to our knowledge is the first to look into microparticles specifically produced to mimic particles that are components of formulated products

In this study, the effect of biodegradation of engineered PCL PMPs at varying surface areas was investigated using the degradation methods described in **Chapter 4**. In **Chapter 4** the maximum efficiency of PCL PMPs to lipase mass ratio was found to be 0.040 where a biodegradation rate of 22% per h was observed. Furthermore, the maximum degradation rate measured via the production of carbon dioxide (CO_2) was also with a ratio of 0.040 PCL PMPs:

lipase, where 2.73% CO_2 production per day was observed. Consequently, this PCL PMPs: lipase ratio was used to evaluate the degradation (acid release and CO_2 production) of PCL PMPs with different surface area/particle size (**Chapter 3, Table 3:4**).

5.2 Materials and Methods

5.2.1 Materials

Lipase from *Pseudomonas cepacia* with measured enzymatic activity of 27.6 to 43.1 U/mg (CAS#: 9001-62-1), polycaprolactone (PCL**,** CAS # 24980-41-4 45 kDa), HEPES buffer (7.4), N-(2-Hydroxyethyl) piperazine-N′-(2-ethanesulfonic acid), CAS# 7364-45-9, mw = 238.31 g/mol and sodium hydroxide pellets (CAS # 1310-73-2) were all purchased from Sigma Aldrich, Dorset, UK. The polycaptolactone microparticles (PCL PMPs) were prepared as previously described in Chapter 3. OxiTop©-IDS wireless measuring head was purchased from Xylem (Germany) with Bluetooth© LE technology for operation with Multi 3620 IDS or Multi 3630 IDS and was used to monitor changes in pressure. All solutions were prepared using ultrapure water which was purified by a Milli-Q apparatus (Millipore Corp., Bedford, MA, USA) with a resistivity of 18.2 MΩ·cm at 25°C.

5.2.2 Free fatty acid release

The free fatty acids (FFAs) released from the depolymerisation of PCL were measured using an automatic pH-stat titration unit (TIM 856 titration manager, Titralab, Radiometer analytical) as previously described in **Chapter 4**.

5.2.3 Pressure measurement

The biodegradation of PCL PMPs was investigated by measuring the pressure difference. The pressure difference is turned into a calculation of how much carbon dioxide (CO_2) is removed by the NaOH in the instrument sleeve (Garcia-Depraect et al., 2022). The PCL PMPs were degraded as described previously in **Chapter 4**.

5.2.4 Statistical Analysis

Significant differences between samples were determined by one-way ANOVA and the significant difference between samples were considered when $p < 0.05$ using Tukey test was performed using Minitab Software (Minitab statistics software, version 19) and the level of confidence was 95%. Experiments were conducted at least in triplicate before carrying out the statistical analysis. Results in tables are expressed as mean ± standard deviation. Error bars in figures represent standard deviation.

5.3 Results and Discussion

5.3.1 Effect of varying surface area of PCL PMPs biodegradation – Acid release

The aim of this experiment was to understand the influence of varying surface area of PCL PMPs on their degradation rate. The rate and degree of free fatty acid (FFA – in this case 6-hydroxycaproic acid (6-HCA) released upon the initial steps in the degradation process of PCL were measured by using an automatic pH-stat titration unit (TIM 856 titration manager, Titralab, Radiometer analytical) (Tan et al., 2020). As previously described in **Chapter 4**, during the course of the experiment, the volume of NaOH (mL) required to maintain a constant pH is recorded as a function of time (hrs). As the pH decreases due to release of FFAs, NaOH is delivered by the instrument to keep the pH constant at a pre-determined endpoint value. Knowledge of base addition rate to the system allows for calculating the rate of acid production in the sample **(Figure 5:1)**. The statistical analysis shown in **Table 5:1** shows the mean %FFA of the three PMPs of different surface area. The Tukey method is used to identify significant differences by analysing multiple comparisons in which a set of group means are ranked from smallest to largest with letters to indicate significant differences and 95% confidence limit.

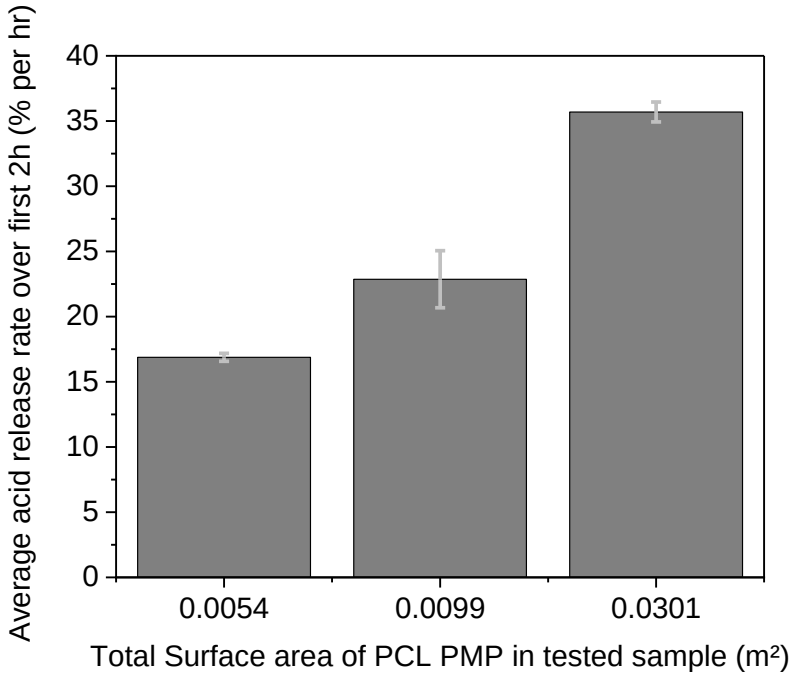


Figure 5:1- Enzymatic degradation of PCL PMPs at 37°C and pH 7.4 for varying initial total particle surface area. 6-hydroxycaproic acid (6-HCA) released (% rate acid release) after 2 h of exposure to lipase enzyme. Data presented are given as the mean of three independent experiments with the corresponding standard deviation. The quoted surface area of particles is calculated based on mass (10 mg PCL PMPs)/250 units lipase = 0.040 ratio (PCL PMPs:lipase mg/unit)

Table 5:1 – Effect of surface area of PCL PMPs on the rate of biodegradation - statistical analysis using the Tukey Method and 95% Confidence

Surface area (m^2)	**N**	**Rate acid release (% h^{-1})**	**Standard deviation**	CLD
0.0054	61	16.87	0.30	b
0.0099	61	22.87	2.19	b
0.0301	61	35.97	0.76	a

Compact Letter Display (CLD) - Means that do not share a letter are significantly different (level of significance) *p<0.05.*

The rate of acid release is presented in **Figure 5:1** and shows that the amount of 6-hydroxycaproic acid (6-HCA) released is proportional to the surface area of the particles. The trend is in agreement with many authors (Modelli et al., 1999; Funabashi et al., 2006; Kunioka et al., 2009; Chinaglia et al., 2018; Accinelli et al., 2019) and the aforementioned hypothesis that the polymer particle surface area/volume ratio plays a critical role in determining the degradation rate of polymer microparticles (PMPs). The results suggests that the 6-HCA released from the degradation of PMPs with the largest surface area of 0.031 m^2 is significantly different to that for PMPs of lower surface area (0.0054 and 0.0090 m^2) (**Table 5:1**)**.** The rate of degradation of PCL PMPs with the lowest total surface area present in the sample tested (0.0054 m^2) is 16.9% per h, and, in comparison, the degradation rate for the particle sample with highest total surface area present in the sample tested evaluated (0.0301 m^2) was 36.0% per h which is significantly different ($p<0.05$) (**Table 5:1**). These results suggest that there was more efficient interaction with the enzyme and available surface area of the PMPs for the larger surface area sample, which is expected. The reduced surface area of the PCL PMPs prevented efficient access to the ester bonds for the lipase. During the 2^{nd} stage of degradation (fragmentation), the biodegradation behaviour in the initial stage of the degradation reaction is well described by a linear relationship (Pearson correlation coefficient 0.981) (Chinaglia et al., 2018). Linear regressions describe the biodegradation curves in the first part of the reaction. This is an indication that the reaction rates are obeying a pseudo-zero order (Chinaglia et al., 2018). Although the pH stat is widely used for digestion studies (Mat et al., 2016), it is not used/seldom used in measuring biodegradability. Here, we have identified a method to monitor the initial stages of biodegradation of PCL PMPs and relate it to the biodegradation rate as a function time.

In the next section, we study the increase in production of CO_2 during the degradation process using pressure measurements to understand the secondary products of the biodegradation process, representing the final stage 3 of biodegradation i.e. the conversion of PCL into CO_2, water and biomass (Emadian et al., 2017).

5.3.2 Effect of varying surface area of PCL PMPs biodegradation - Production CO_2

The aim of this experiment was to degrade PCL PMPs using lipase enzyme to evaluate the influence of the surface area on the rate and degree of CO_2 production (3rd stage of degradation) (Kjelsden et al., 2019). This was accomplished by degrading PCL PMPs of varying the particle size using lipase, in order to estimate the degradation kinetics from the CO_2 production rate shown in **Figure 5:2**. The statistical analysis shown in **Table 5:2** shows the percentage of carbon in the sample that has produced into CO_2 during the degradation process over the first 2 days of the three PMPs of different surface areas.

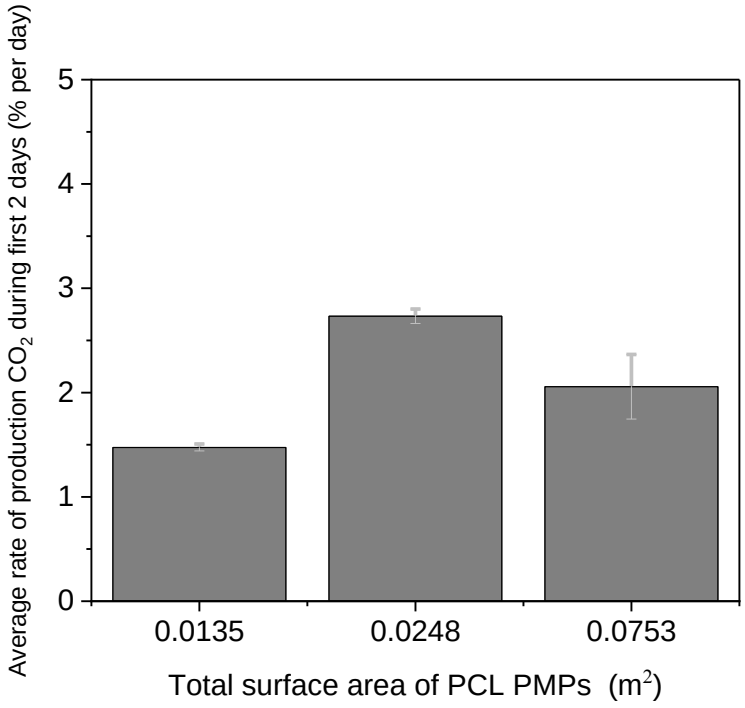


Figure 5:2 - CO_2 production rate resulting from the biodegradation of PCL PMPs of varying total surface areas (tested in each sample). Experiments are conducted at pH 7.4 in 30 mM HEPES buffer (N-(2-Hydroxyethyl)piperazine-N′-(2-ethanesulfonic acid). The reason for using a buffer system to maintain the pH at 7.4 is to avoid changes in hydrogen ion concentrations Pastorino et al. (2004); (Adhikari et al., 2016; Fang et al., 2020; Oh et al., 2022). When the enzyme attacks the surface of the PCL PMP, acid is released and therefore a pH decrease is observed which results in the denaturing of the enzyme, leading to insufficient degradation capacity and inaccurate data and a PCL/lipase ratio of 0.040. The biodegradation percentage is the ratio between the measured CO_2 and the total possible CO_2 i.e. the amount of CO_2 expected in case of total oxidation of the carbon present in the PCL PMPs introduced in the vessel. (Ahn et al., 2011; Gómez and Michel, 2013; Chinaglia et al., 2018). Error bars are standard deviation for three independent readings for triplicate samples (n = 3).

A linear regression analysis was performed on the data of CO_2 in the first biodegradation phase over 2 days of each sample in order to determine the initial biodegradation rate k. The results of the linear regression analysis are shown in **Table 5:2**. The slope constants k are the degradation rates (CO_2 production day^{-1}). The statistical analysis presented in **Table 5:2** shows the percentage of carbon in the sample that has produced into CO_2 during the degradation process over the first 2 of the three PMPs of different surface areas with letters to indicate significant differences using Tukey method and 95% confidence limit. The Tukey method is used to identify significant differences by analysing multiple comparisons in which a set of group means are ranked from smallest to largest with letters to indicate significant differences and 95% confidence limit.

Table 5:2 - The influence of surface area of PCL PMPs on the degree and rate of CO_2 production - statistical analysis using the Tukey Method and 95% Confidence

Surface area (m^2)	N	Rate CO_2 production (% day^{-1})	Standard deviation	CLD
0.0135	323	1.47	0.03	b
0.0248	323	2.73	0.07	a
0.0753	239	2.06	0.31	b

Compact Letter Display (CLD) - Means that do not share a letter are significantly different (level of significance) *p<0.05.*

In **Figure 5:2**, increasing the available surface area does not appear to have a significant impact on the rate of degradation (production of CO_2). It is important to mention that this conclusion is based on only three data points. The limited number of data points is due to time constraints during the PhD experiments, so the results may not be definitive. The error bars from statistical analysis show significant differences between samples, but the lowest and highest surface areas tested cannot be distinguished, even though they are not consecutive. It should be noted that the surface area calculations are determined by a spherical equivalent measurement of particle size, which may overlook specific details of particle shape. For example, if one of the second or third samples is significantly non-spherical, it could result in an inaccurate surface calculation. Chinaglia et al. (2018) and Modelli et al. (1999) observed that the biodegradation happening at the surface of PMPs is very fast (stage 2 of the biodegradation process) but the overall CO_2 production (stage 3 of the biodegradation process) has no influence on the available surface area at this stage. The rate of the degradation process may initially be limited by the surface area, but once the polymer chains have been broken down into smaller dissolvable molecules (acids) into solution, the rate of CO_2 production exerts its own influence in the final stages. They explained that biodegradation of solid microplastics (either film or ground pellets) is a heterogeneous reaction because it happens at the solid/liquid interface, where the enzymes in the liquid phase interact with the polymer chains that are available for chain scissions at the surface of the solid plastic sample subjected to biodegradation thus, the surface area plays a crucial role in this process (Pagga et al., 2000; Wolf-Ru¨ diger Mu¨ ller*, 2004; Abid et al., 2019; Grundy et al., 2021). The polymer chains in the inner parts of the sample are not involved in the reaction, as they are not ‘available’. As the polymer degrades, biomass is formed which further implicates the determination of CO_2 production as the degradation is calculated based on the theoretical total carbon (CO_2 or P/ThCO_2 or P **Figure 5:2**). The theoretical carbon dioxide (ThCO_2) is the expected amount of carbon dioxide to be produced from a polymer as a result of biodegradation based on the stoichiometry and theoretical yield calculations. Full degradation is difficult to reach, as a certain amount of carbon will be converted into microbial biomass (Ruka et al., 2015).

The rate of degradation of a surface area of 0.0135 m^2 is 1.5% per day, 0.0248 m^2 is 2.7% per day and 0.0753 m^2 is 2.0% per day (**Figure 5:2**, **Table 5:2**). When comparing these values to literature, there is strong agreement in terms of the magnitude of CO_2 production where Modelli et al. (1999) observed 2.28% CO_2 production of PCL ground pellets per day (100 µm diameter, 0.5 g), however, the surface area that was available was not specified for comparison.

The authors tested PHB as both film and PHB PMPs form to test the hypothesis. The empirical formula of the PHB repeating unit is $C_4H_6O_2$, with a carbon content of 55.8% ($\frac{48}{86}$) by weight. Complete degradation of the 0.5 g of polymer used in each test is thus expected to give rise to 23.25 m mols of CO_2. They observed a linear trend showing the initial rate as 2.60 m moles day^{-1} (averaged over the three tests), corresponding to 11.2% of the initial amount of polymer per day. They also tested the same mass of PHB polymer in a film form where the surface area is much smaller and they observed a best fit linear regression, with a slope (degradation rate) of 0.029 m moles day, (0.12% per day), about 90 times smaller than the initial rate measured with the same mass of polymer in the PHB powder.

5.4 Conclusion

It was found that the rate of hydrolysis of PCL PMPs was dependent on the surface area of the polymer exposed to hydrolysis during the surface degradation stage of the biodegradation process. The amount of 6-hydroxycaproic acid (6-HCA) produced from the degradation of the PCL PMPs with smaller particle size is increased as the surface area is increased. Surface degradation occurs during hydrolysis and proceeds to the inner part of the material (Gebauer and Jendrossek, 2006). Fragmentation of the PCL PMPs into oligomers of smaller molecular weights results in larger surface to volume ratio for the enzymes to act upon. Enzymatic depolymerisation of the polymers releases oligomers and/or monomers that can be easily assimilated by the microorganisms as a carbon source resulting to increase in microbial biomass (Kumar, G.A. et al., 2020). The breakdown of solid microplastics (such as film or ground pellets) through biodegradation is a heterogeneous process. This is because it occurs at the interface between the solid and liquid phases, where enzymes in the liquid phase interact with polymer chains that are accessible for breaking down on the surface of the solid plastic sample undergoing biodegradation. Therefore, the surface area of the plastic sample is essential in facilitating this process. In the next chapter, comparable degradation experiments will be carried out on PLGA and PHB PMPs using identical methods to examine how different polymers impact the degradation of particles.

5.5 References

Abid, Z., Dalskov Mosgaard, M., Manfroni, G., Singh Petersen, R., Hagner Nielsen, L., Mullertz, A., Boisen, A. and Sylvest Keller, S. 2019. Investigation of Mucoadhesion and Degradation of PCL and PLGA Microcontainers for Oral Drug Delivery. *Polymers (Basel).* **11**(11).

Accinelli, C., Abbas, H.K., Shier, W.T., Vicari, A., Little, N.S., Aloise, M.R. and Giacomini, S. 2019. Degradation of microplastic seed film-coating fragments in soil. *Chemosphere.* **226**, pp.645-650.

Adhikari, D., Mukai, M., Kubota, K., Kai, T., Kaneko, N., Araki, K.S. and Kubo, M. 2016. Degradation of Bioplastics in Soil and Their Degradation Effects on Environmental Microorganisms. *Journal of Agricultural Chemistry and Environment.* **05**(01), pp.23-34.

Ahn, H.K., Huda, M.S., Smith, M.C., Mulbry, W., Schmidt, W.F. and Reeves, J.B., 3rd. 2011. Biodegradability of injection molded bioplastic pots containing polylactic acid and poultry feather fiber. *Bioresour Technol.* **102**(7), pp.4930-4933.

Chen, D.R., Bei, J.Z. and Wang, S.G. 1999. Polycaprolactone microparticles and their biodegradation. *Polymer Degradation and Stability.* **67**, pp.455-459.
Chinaglia, S., Tosin, M. and Degli-Innocenti, F. 2018. Biodegradation rate of biodegradable plastics at molecular level. *Polymer Degradation and Stability.* **147**, pp.237-244.

Emadian, S.M., Onay, T.T. and Demirel, B. 2017. Biodegradation of bioplastics in natural environments. *Waste Manag.* **59**, pp.526-536.

Fang, Z., Gao, Y., Wu, X., Xu, X., Sarmah, A.K., Bolan, N., Gao, B., Shaheen, S.M., Rinklebe, J., Ok, Y.S., Xu, S. and Wang, H. 2020. A critical review on remediation of bisphenol S (BPS) contaminated water: Efficacy and mechanisms. *Critical Reviews in Environmental Science and Technology.* **50**(5), pp.476-522.

Funabashi, M., Ninomiya, F. and Kunioka, M. 2006. Biodegradation of Polycaprolactone Powders Proposed as Reference Test Materials for International Standard of Biodegradation Evaluation Method. *Journal of Polymers and the Environment.* **15**(1), pp.7-17.

Garcia-Depraect, O., Lebrero, R., Rodriguez-Vega, S., Bordel, S., Santos-Beneit, F., Martinez-Mendoza, L.J., Aragao Borner, R., Borner, T. and Munoz, R. 2022. Biodegradation of bioplastics under aerobic and anaerobic aqueous conditions: Kinetics, carbon fate and particle size effect. *Bioresource Technology.* **344**, pp.126-265.

Gebauer, B. and Jendrossek, D. 2006. Assay of poly(3-hydroxybutyrate) depolymerase activity and product determination. *Appl Environ Microbiol.* **72**(9), pp.6094-6100.

Gómez, E.F. and Michel, F.C. 2013. Biodegradability of conventional and bio-based plastics and natural fiber composites during composting, anaerobic digestion and long-term soil incubation. *Polymer Degradation and Stability.* **98**(12), pp.2583-2591.

Grundy, M.M.L., Abrahamse, E., Almgren, A., Alminger, M., Andres, A., Ariëns, R.M.C., Bastiaan-Net, S., Bourlieu-Lacanal, C., Brodkorb, A., Bronze, M.R., Comi, I., Couëdelo, L., Dupont, D., Durand, A., El, S.N., Grauwet, T., Heerup, C., Heredia, A., Infantes Garcia, M.R., Jungnickel, C., Kłosowska-Chomiczewska, I.E., Létisse, M., Macierzanka, A., Mackie, A.R., McClements, D.J., Menard, O., Meynier, A., Michalski, M.-C., Mulet-Cabero, A.-I., Mullertz, A., Payeras Perelló, F.M., Peinado, I., Robert, M., Secouard, S., Serra, A.T., Silva, S.D., Thomassen, G., Tullberg, C., Undeland, I., Vaysse, C., Vegarud, G.E., Verkempinck, S.H.E., Viau, M., Zahir, M., Zhang, R. and Carrière, F. 2021. INFOGEST inter-laboratory recommendations for assaying gastric and pancreatic lipases activities prior to in vitro digestion studies. *Journal of Functional Foods.* **82**.

Katou, H., Wandrey, A.J. and Gander, B. 2008. Kinetics of solvent extraction/evaporation process for PLGA microparticle fabrication. *Int J Pharm.* **364**(1), pp.45-53.

Kjelsden, A.P., M. Lilley, C. Guznicak, E. Archer, I. 2019. A Review of Standards for Biodegradable Plastics. *Industrial Biotechnology Innovation Centre.*

Kumar, G.A., Anjana, K., Hinduja, M., Sujitha, K. and Dharani, G. 2020. Review on plastic wastes in marine environment – Biodegradation and biotechnological solutions. *Marine Pollution Bulletin.* **150**, article no: 110733 [no pagination].

Kunioka, M., Ninomiya, F. and Funabashi, M. 2009. Biodegradation of poly(butylene succinate) powder in a controlled compost at 58 degrees C evaluated by naturally-occurring carbon 14 amounts in evolved CO(2) based on the ISO 14855-2 method. *Int J Mol Sci.* **10**(10), pp.4267-4283.

Makadia, H.K. and Siegel, S.J. 2011. Poly Lactic-co-Glycolic Acid (PLGA) as Biodegradable Controlled Drug Delivery Carrier. *Polymers (Basel).* **3**(3), pp.1377-1397.

Mat, D.J.L., Le Feunteun, S., Michon, C. and Souchon, I. 2016. In vitro digestion of foods using pH-stat and the INFOGEST protocol: Impact of matrix structure on digestion kinetics of macronutrients, proteins and lipids. *Food Research International.* **88**, pp.226-233.

Modelli, A., Calcagno, B. and Scandola, M. 1999. Kinetics of Aerobic Polymer Degradation in Soil by Means of the ASTM D 5988-96 Standard Method. *Journal of Environmental Polymer Degradation.* **7**(2), pp.109-116.

Oh, Y.-R., Jang, Y.-A., Song, J.K. and Eom, G.T. 2022. Efficient enzymatic depolymerization of polycaprolactone into 6-hydroxyhexanoic acid by optimizing reaction conditions and microbial conversion of 6-hydroxyhexanoic acid into adipic acid for eco-friendly upcycling of polycaprolactone. *Biochemical Engineering Journal.* **185**.

Pagga, U., Schafer, A., Muller, R.J. and Pantke, M. 2000. Determination of the aerobic biodegradability of polymeric material in aquatic batch tests. *Chemosphere.* **42**, pp.319-331.

Pastorino, L., Pioli, F., Zilli, M., Converti, A. and Nicolini, C. 2004. Lipase-catalyzed degradation of poly(ε-caprolactone). *Enzyme and Microbial Technology.* **35**(4), pp.321-326.

Ruka, D.R., Sangwan, P., Garvey, C.J., Simon, G.P. and Dean, K.M. 2015. Biodegradability of Poly-3-hydroxybutyrate/Bacterial Cellulose Composites under Aerobic Conditions, Measured via Evolution of Carbon Dioxide and Spectroscopic and Diffraction Methods. *Environ Sci Technol.* **49**(16), pp.9979-9986.

Sintim, H.Y. and Flury, M. 2017. Is Biodegradable Plastic Mulch the Solution to Agriculture's Plastic Problem? *Environ Sci Technol.* **51**(3), pp.1068-1069.
Staff, R.H., Schaeffel, D., Turshatov, A., Donadio, D., Butt, H.J., Landfester, K., Koynov, K. and Crespy, D. 2013. Particle formation in the emulsion-solvent evaporation process. *Small.* **9**(20), pp.3514-3522.

Wolf-Ru¨ diger Mu¨ ller*, I.F.R.J.r. 2004. Standardized methods for anaerobic biodegradability testing. *Reviews in Environmental Science and Bio/Technology 3: 141–158, 2004.* **3**, pp.141-158.

Yang, H.-S., Yoon, J.-S. and Kim, M.-N. 2005. Dependence of biodegradability of plastics in compost on the shape of specimens. *Polymer Degradation and Stability.* **87**(1), pp.131-135.

Yang, L., Li, J., Jin, Y., Li, M. and Gu, Z. 2015. In vitro enzymatic degradation of the cross-linked poly(ε-caprolactone) implants. *Polymer Degradation and Stability.* **112**, pp.10-19.

Yunbing. Tan, Z.Z., Hualu. Zhou, Hang. Xiao, and David. Julian. McClements,. 2020. Factors impacting lipid digestion and β-carotene bioaccessibility assessed by standardized gastrointestinal model (INFOGEST): Oil droplet concentration. *Food & Function.*

Chapter 6 Biodegradation effect of PCL, PLGA and PHB PMPs

6.1 Introduction

In **Chapter 3**, we successfully produced polymeric PMPs using three types of biodegradable polymers: polycaprolactone (PCL), poly (D, L-lactide-co-glycolide) (75:25) – (PLGA), and poly[(R)-3-hydroxybutyric acid] – (PHB). These particles were all prepared using the solvent extraction process with the same method preparation conditions. The biodegradation of PCL PMPs are described in Chapter 4, where the maximum PCL to lipase concentration ratio was found to be 0.040 and the rate of degradation at stage 2 of the biodegradation was 22% per h 6-HCA and the rate of produced CO_2 was 2.73% per day. In this chapter, equivalent degradation studies of PLGA and PHB PMPs are conducted using the same techniques so that the effect of various polymers on the degradation of particles is investigated.

Studies have shown that the extracellular enzyme polyhydroxybutyrate (PHB) depolymerase act on material surface first, and then hydrolysis occurs at the amorphous region and subsequently at the crystal region (Banerjee et al., 2014; Iwata, 2015; Zhang, S. et al., 2019). **Table 6:1** describes some of the degradation studies. As highlighted in the literature review, varying factors affect the rate of biodegradation including the polymer type, available surface area, residuals from polymer like additives and by products, and environmental factors such as exposure (heat, light, air), and interactions with microorganisms. Interestingly, PHB, PHBV (8–12% HV) and PH4B (47% 4HB) biodegrade beyond 80% in 100 days irrespective of the polymer type (Thellen et al., 2008), whilst similar polymer in powder form, under non-standard test method and a different source of environment, also report a similar biodegradation value by Deroiné et al. (2015). Again highlighting the complications and reliability with standardised test methods where, some samples were tested for their biodegradability in simulated environments while others were tested in sea water with varying pH and temperature conditions making it difficult to compare the biodegradation kinetics between various polymers and testing methodologies. Gebauer and Jendrossek (2006) investigated the degradation of poly(3-hydroxybutyrate) (PHB) (size not given) using a pH stat monitoring the NaOH consumption to

neutralise 3-hyroxybutaric acid (3HB). The paper discusses methods for determining PHB depolymerase activity, the importance of PHAs in biodegradability, and the specificity of enzymes for different forms of PHB, with a focus on understanding substrate specificities and product composition. They reported a hydrolysis rate for the depolymerisation of PHB in to 3HB as 4.3 nmol released acid min^{-1} mg^{-1} at 37ºCat pH 8.5. This is relevant to the studies conducted herein where the pH stat is used to monitor the acid release of PHB PMPs.

PLGA has been proposed to degrade primarily through hydrolytic degradation, but it has also been suggested that enzymatic degradation may play a role in the process (Abid et al., 2019). Lactic acid enters the tricarboxylic acid cycle and is metabolised and subsequently eliminated from the body as carbon dioxide and water (Mohamed and van der Walle, 2008; Makadia and Siegel, 2011). Regarding the difference between PLGA (75:25) and PCL, it was expected that the degradation time would vary as different ratios of the monomers have a significant influence on hydrolysis and enzymatic degradation. PLGA 75:25 is expected to have a higher degradation rate compared to PCL, which typically is approximately twice as slow due to the higher content of hydrophobic group (Middleton and Tipton, 2000; Makadia and Siegel, 2011). In a study by Therin and Christel (1991) found a 12% rate of degradation over 8 weeks (Mw measurements). Bagheri et al. (2017) conducted a study aimed specifically at trying to determine if so-called biodegradable polymers can degrade in simulated seawater and freshwater. Five well known polymers that claim to be biodegradable were evaluated, the polymers evaluated were PGLA, PCL, PLA, Ecoflex (BASF, compostable polymer), PHB and a non-biodegradable polymer PET. Films of the polymers were fabricated by hot punching with an average thickness of 320 +/- 20µm and dimensions of 1.2 x 1.2cm. These were placed in vials with holes in the cap and 3ml of either seawater (from aquarium) or freshwater (collected rainwater) was added and placed in an incubator under controlled conditions at 25ºC. The water was refreshed every 2 weeks. The mass loss of polymers at different time intervals were recorded. In the work, only amorphous PLGA shows 100% degradation as determined by weight loss **(Table 6:2)**, change in molar mass with time, NMR, electron microscopy, and high-performance liquid chromatography. This confirms the uncertainty of biodegradability claims of polymers (Bagheri et al., 2017). The lack of

biodegradation studies for PLGA PMPs further highlights the knowledge gap where much of the existing literature focuses on polymer films rather than particles, creating a need to explore model systems and gain a better understanding of the basic degradation process.

Table 6:1 - Biodegradation of Poly[(R)-3-hydroxybutyric acid] – (PHB) in different environments

PHA (co-monomer %)	Protocol and source	Conditions	Form	Days	Result	Ref
PHB	Non-ASTM, Eutrophic reservoir	18–25 °C	Film (5.50 µm thickness)	42	43.5% mass loss	(Volova et al., 2007)
PHB	Non-ASTM, South China sea	27–30 °C	Solid (10 mm diameter, 0.5 cm high)	160	62% mass loss	(Volova et al., 2011)
			Film (30 mm diameter, 0.1 mm thickness)		58% mass loss	(Volova et al., 2011)
PHBV (11% HV)	Non-ASTM, South China sea	27–30 °C	Solid (10 mm diameter, 0.5 cm high)	160	87% mass loss	(Volova et al., 2011)
			Film (30 mm diameter, 0.1 mm thickness)		54% mass loss	(Volova et al., 2011)
PHB	ASTM D6691, Woods Hole Harbor water	30 °C	Film (152 to 190 µm)	100	90% mass loss	(Thellen et al., 2008)
PH4B (44% 4HB)	ASTM D6691, Woods Hole Harbor water	30 °C	Film (152 to 190 µm)	100	80% biodegradation	(Thellen et al., 2008)
PH4B (47% 4HB)					82% biodegradation	(Thellen et al., 2008)
PHBV (8% HV)	ASTM D6691, Woods Hole Harbor water	30 °C	Film (152 to 190 µm)	100	85% biodegradation	(Thellen et al., 2008)
PHBV (12% HV)					100% biodegradation	(Thellen et al., 2008)
PHBV (8% HV)	Non-ASTM, Lorient Harbour	25 °C	Film (200 µm thickness, 200 x 120 mm)	180	36% mass loss	(Deroiné et al., 2015)
PHBV (8% HV)	Non-ASTM, Lorient Harbour water + Foreshore sand	25 °C	Powder (not specified)	210	90% biodegradation	(Deroiné et al., 2015)

PHA = polyhyroxyalkanoate; PHB = polyhydroxybutyrate; PHBV = poly(3-hyroxybutyrate-co-3-hydroxyvalerate);

Table 6:2 - Biodegradation of poly (D, L-lactide-co-glycolide) – (PLGA) in different environments

Polymer	**Form**	**Environment type and conditions**	**Biodegradability (%), production of CO_2** **days / months**	**Reference**
PLA	films	compost, simulated seawater 25-58°C, aerobic	10 – 53 upto 3 months average	(Ahn et al., 2011), (Nam and Park, 2020), (Massardier-Nageotte et al., 2006)
PLGA	Nanoparticles films	acidic pH range seawater 50°C, 25°C	100 10-270 days	(Ferrari et al., 2013; Bagheri et al., 2017; Abid et al., 2019)

6.2 Materials and Methods

6.2.1 Materials

Lipase from *Pseudomonas cepacia* with measured enzymatic activity of 27.6 to 43.1 U/mg was purchased from Sigma Aldrich, Dorset, UK (CAS#: 9001-62-1). PLGA – poly (D, L-lactide-co-glycolide) (75:25), mol wt 66 k Da – 107 k Da, no data for polydispersity and PHB - Poly [(R)-3-hydroxybutyric acid], natural origin, was purchased from Sigma Aldrich, Dorset UK. Polymeric microparticles (PMPs) were prepared as previously described in Chapter 3. HEPES buffer, N-(2-Hydroxyethyl) piperazine-N′-(2-ethanesulfonic acid), CAS# 7364-45-9, mw = 238.31 g/mol was purchased from Sigma Aldrich, Dorset, UK. Sodium hydroxide pellets (CAS # 1310-73-2) were purchased from Sigma Aldrich, Dorset, UK. All solutions used were prepared using Milli-Q water which was purified by a Milli-Q apparatus (Millipore Crop., Bedford, MA, USA) with water purity of 18.2 MΩ·cm at 25°C.

6.2.2 Free fatty acid release

The free fatty acids (FFAs) released from the depolymerisation of PCL were measured using an automatic pH-stat titration unit (TIM 856 titration manager, Titralab, Radiometer analytical) as previously described in Chapter 4.

6.2.3 Pressure measurement

In this work, the biodegradation of PMPs was investigated by measuring the pressure change in a sealed vessel as carbon dioxide (CO_2) is produced when the PMPs are degraded by the lipase (Garcia-Depraect et al., 2022). The PMPs' degradation was conducted in a controlled environment as described previously in **Chapter 4**.

The molecular weight of acid (g/mol) and the theoretical n number of carbons CO_2 is described in **Table 6:3** of the three different polymers, these values are then used to calculate the % degradation using equation **4:6**. The biodegradation percentage is the ratio between the produced CO_2 (or pressure decrease) and the theoretical CO_2 ($ThCO_2$/pressure) i.e. the amount of CO_2 expected in case of total oxidation of the carbon present in the polymer sample (Cpolymer) introduced in the vessel (Chinaglia et al., 2018; Gartiser, 2018b). The theoretical carbon dioxide ($ThCO_2$) is the expected amount of carbon dioxide to be produced from a polymer as a result of biodegradation based on the stoichiometry and theoretical yield calculations.

The biodegradation of PCL, PLGA and PHB PMPs were investigated by measuring the carbon dioxide (CO_2) production when they are degraded by enzyme (Garcia-Depraect et al., 2022). The PMPs were degraded as described previously in **Chapter 4**. The degradation mechanism of the three polymers (PCL, PLGA and PHB) into their monomer products are described by their relative stoichiometry equations (**6:1**, **6:2**, **6:3**) as the carbon present in the polymer sample is equal to the amount of consumed oxygen or CO_2 produced from the degradation of the polymer into their respective monomer.

$$C_6H_{10}O_2 + 6O_2 \longrightarrow 6CO_2 + XH_2O \qquad \textbf{6:1}$$

$C_6H_{10}O_2$ represents the chemical composition of caprolactone (Islam Mozumder et al., 2015; Chinaglia et al., 2018; Gartiser, 2018b)

$$C_5H_8O_5 + 5O_2 \longrightarrow 5CO_2 + XH_2O \qquad \textbf{6:2}$$

$C_5H_8O_5$ represents the chemical composition of (lactic-co-glycolic acid) (Ferrari et al., 2013; Gentile et al., 2014; Mahar et al., 2023)

$$C_4H_6O_2 + 4O_2 \longrightarrow 4CO_2 + XH_2O \qquad \textbf{6:3}$$

$C_4H_6O_2$ represents the chemical composition of [(R)-3-hydroxybutyric acid] (Wang, Y.-W. et al., 2004; Gebauer and Jendrossek, 2006; Arrieta et al., 2014; Islam Mozumder et al., 2015; Garcia-Depraect et al., 2022)

Table 6:3 – depolymerisation of polymer and molecular weight used to calculate FFA and CO_2 production

Polymer	Free fatty acid	Molecular weight of acid (g/mol)	Theoretical n number of carbons CO_2	Moles NaOH to neutralise equal moles acid
PCL	6-Hydroxylcaproic acid	114.14	6	1
PLGA (75:25)	lactic acid, glycolic acid	166.13	5	1
PHB	3-hyroxybutaric acid	104.1	4	1

6.3 Results and Discussion

6.3.1 Biodegradation effect of PCL, PLGA and PHB PMPs - Acid release

The aim of this experiment was to understand the influence of the polymer type on the initial rate of degradation in terms of acid release for PMPs made from PCL, PLGA and PHB, respectively. The rate and degree of free fatty acid (FFA) released upon the degradation of the different PMPs while keeping the mass constant (10 mg) in the system is discussed. Here, three different particle suspensions made from different polymers were degraded with lipase at 37ºC in water and the pH stat instrument was used to maintain the pH constant at 7.4 throughout. The quantity of base added is recorded in the process so that the quantity of acid produced in the degradation reactions can be calculated. These data are then processed to extract a rate of degradation over the first 2h of exposure of the particles to the enzyme at these environmental conditions. These values of acid release rates are plotted in **Figure 6:1.**

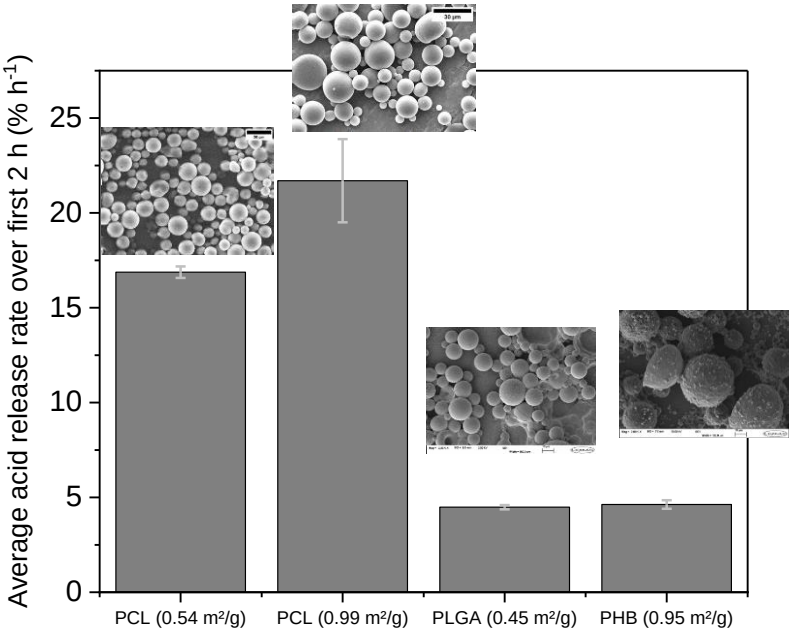


Figure 6:1- Effect of the polymer type on the initial rate of acid release from enzymatic degradation of PCL, PLGA and PHB PMPs at 37°C and pH 7.4 (mean ± SD, n=3 from independent experiments). The rate of acid release is calculated using over the first 2 h of exposure to lipase enzyme in a pH stat instrument. Data presented are the mean rate over the 2h with standard deviation of three independent experiments (**Figure C 1** and **Figure C 2**). The mass of particle was kept constant (10 mg). 250 units lipase = 0.040 ratio (PMPs:lipase mg/unit). Inset: (images of PMPs before degradation), highlighting the variations in particle size and surface texture).

Table 6:4 – Biodegradation effect of PCL, PLGA and PHB PMPs – rate acid release

Polymer PMPs	Rate acid release (% h^{-1})	Standard deviation
PCL (0.54 m²/g)	16.9	0.30
PCL (0.99 m²/g)	22.9	2.19
PLGA (0.45 m²/g)	4.5	0.16
PHB (0.95 m²/g)	4.6	0.27

The graph above (**Figure 6:1**) illustrates variations in degradation, but the reasons behind these differences are unclear due to numerous variables such as polymer type, polydispersity, surface porosity/texture, and particle size (inset: scanning microscopy images). For comparison, PMPs with similar surface areas have been included. Two PMPs (PLGA and PHB) yield similar rate of biodegradation (4.5 and 4.6 % h^{-1} respectively) despite significant differences in particle size, prompting further investigation into whether degradation would be the same with PMPs of similar particle sizes. However, the results show that while the outcomes are practically the same, the differences in particle size and surface texture prevent any definitive conclusions. Furthermore, the span obtained from the particle size distribution for each PMP, described in **Table C 1** indicate the variations in the PMPs. To enhance the study, focusing on a single polymer and varying particle sizes, as done with PCL, could provide more insightful results. Additionally, exploring other enzymes and maintaining a constant particle size in future experiments may yield more conclusive findings. Comparing PCL PMPs (0.99 m^2) and PHB PMPs (0.95 m^2) reveals stark differences due to variations in surface texture and particle size. Similarly, comparing PCL PMPs (0.54 m^2) and PLGA PMPs (0.45 m^2) shows differences in polydispersity and particle distortion, with PLGA PMPs appearing more spherical than PCL PMPs.

6.3.2 Biodegradation effect of PCL, PLGA and PHB PMPs – Production CO_2

The aim of this experiment was to degrade PLGA and PHB PMPs and compare the biodegradation rate and degree of CO_2 production (3rd stage of degradation) with PCL PMPs as described previously in Chapter 4 (Kjelsden et al., 2019). In this experiment, three different particle suspensions consisting of various polymers were treated with lipase at 37ºC in HEPES buffer to maintain a constant pH of 7.4. Pressure measurements were taken to track the increase in CO_2 production during the degradation process, providing insight into the secondary products of biodegradation (3rd stage). The mass of the particle suspension remained constant at 25 mg. By recording the difference in pressure, the amount of CO_2 generated in the degradation reactions could be determined. These results were analysed to calculate the rate of degradation over the initial 2 days of exposure to the enzyme under these specific environmental conditions. The acid release rates obtained from this analysis are presented in **Figure 6:2**

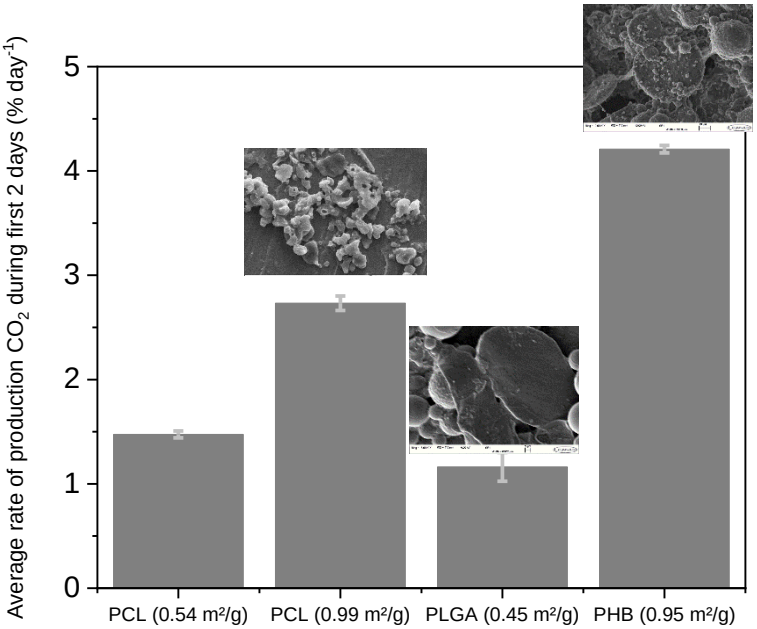


Figure 6:2 – Effect of the polymer type on the rate of production CO_2 during the first 2 days from enzymatic degradation of PCL, PLGA and PHB PMPs at 37°C and pH 7.4). The CO_2 production was calculated as described previously in equation **4:6**. Data presented are the mean rate over 2 days with standard deviation of three independent experiments. The mass of particle was kept constant (25 mg). 625 units lipase = 0.040 ratio (PMPs:lipase mg/unit). Inset: (images of PMPs after degradation, highlighting the variations in particle size and surface texture). Individual experiment can be found in the Appendix, **Figure C 3** (PLGA) and **Figure C 4** (PHB).

Table 6:5 - Biodegradation effect of PCL, PLGA and PHB PMPs – rate CO_2 production (% day^{-1})

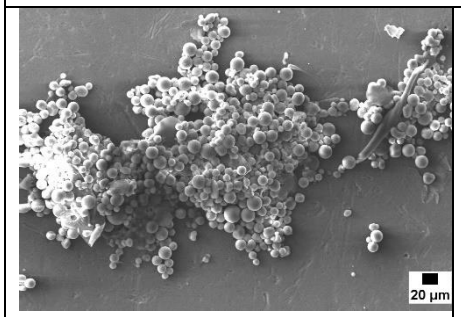
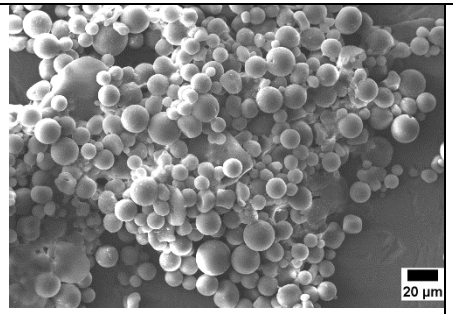
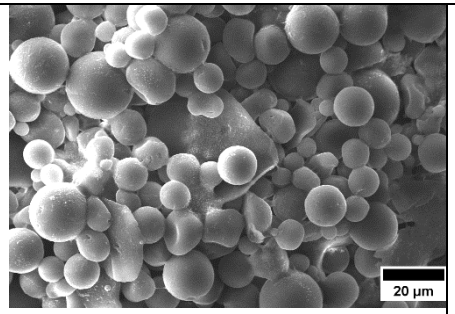
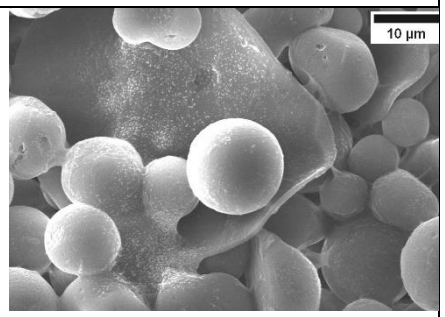
Polymer PMPs	Rate CO_2 production (% day^{-1})	Standard deviation
PCL (0.54 m²/g)	1.47	0.03
PCL (0.99 m²/g)	2.73	0.07
PLGA (0.45 m²/g)	1.16	0.14
PHB (0.95 m²/g)	4.20	0.04

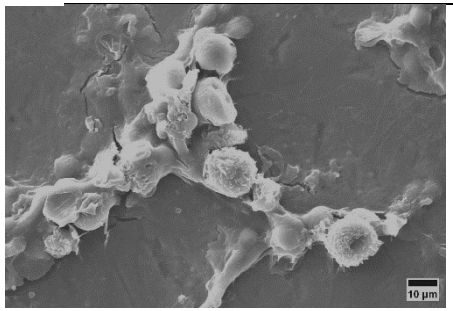
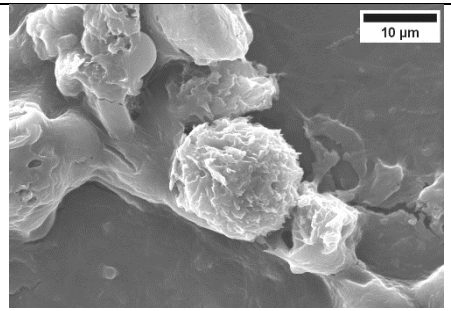
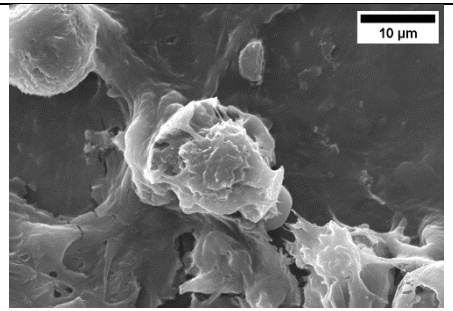
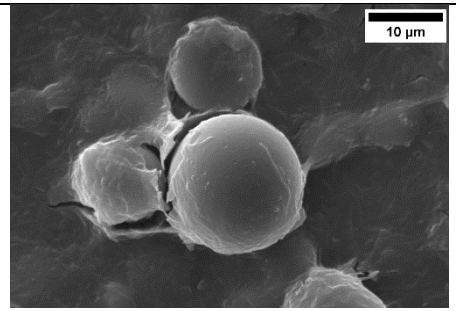
Chapter 5 highlights the importance of surface area in the second stage of biodegradation, where the polymer backbone of PMPs is cleaved (acid release) by enzymes at the surface. Various studies (Yu et al., 2005; Funabashi et al., 2006; Gebauer and Jendrossek, 2006; Ariffin et al., 2010; Ferrari et al., 2013; Gentile et al., 2014; Bartnikowski et al., 2019) have explored this phenomenon. At the third stage of biodegradation (further breakdown of the monomer into CO_2), the surface area is irrelevant. The results in **Figure 6:2** and **Table 6:5** suggests that there may be additional reactions happening simultaneously, complicating the interpretation of results. These findings are similar to those seen in Chapter 5, where the influence of surface area on biodegradation (CO_2 production, **Figure 5:2**) of PCL PMPs was evaluated, where increasing the available surface area did not appear to have a significant impact on the rate of degradation (production of CO_2). The theory behind this is that once the polymer chains have been broken down into smaller dissolvable molecules (acids) into solution, the rate of CO_2 production exerts its own influence in the final stages (Modelli et al., 1999; Chinaglia et al., 2018). On the other hand, the lower particle size PMPs seems to produce more CO_2. PCL PMPs (0.99 m^2) and PHB PMPs (0.95 m^2) show (significantly) higher CO_2 production. However, comparable production of CO_2 with PCL PMPs and PLGA PMPs at 0.54 m^2 and 0.45 m^2 respectively is observed. This raises a question, what if the surface area was increased, would the degradation (production of CO_2) be higher? Another hypothesis for the variations and inconstancy is that the difference in polymer backbone for each polymer is different resulting in each monomer unit cleavage occurring at varying rates (Middleton and Tipton, 2000; Makadia and Siegel, 2011). It should be noted that the same lipase (lipase from *pseudomonas cepacia*) was used for these experiments. However, it is well documented that not the same enzyme can be used for different polyester polymers. Polyesters are formed by bonding monomers with ester linkages. Enzymes that break down this polymer are found widely in living organisms (Leja and Lewandowicz, 2010). For example, Abid et al. (2019) used pancreatin enzymes for PLGA degradation studies. Ashton et al. (2011) used amino lipase from Pseudomonas fluorescens for PCL degradation studies. Gebauer and Jendrossek (2006) reported that enzymes that break down PHB typically target either nPHB/aPHB or dPHB forms specifically. For instance,

extracellular PHB depolymerases are specialised in breaking down dPHB, whereas intracellular PHB depolymerases target nPHB and potentially aPHB.

6.3.3 Scanning electron Microscopy

The morphological properties of PMPs were characterised using Zeiss Evo10 Environmental Scanning Electron Microscope (SEM) at 20 kV at varying magnifications. The SEM images of PMPs after degradation were used to compare the (size and shape), surface structure, roughness, and porosity of the particles, which has a significant effect on biodegradation. Visual observation during biodegradation as a function of time can be compared to the PMPs before degradation. As seen in Chapter 4, the PCL PMPs (**Figure 6:3 a,b and c)** show the deterioration of the initial mostly spherical particles with a smooth surface **Figure 6:3 a**, into noticeably non-spherical structures when degraded with enzyme (**Figure 6:3 b and c)**. Furthermore, PMPs prepared using biodegradable polymers Poly(D, L-lactide-co-glycolide) (75:25) (PLGA) and Poly [(R)-3-hydroxybutyric acid] (PHB) also show signs of degradation shown in **Figure 6:4 b and c** and **Figure 6:5 b and c** respectively. The SEM images of PLGA PMPs shown in **Figure 6:4 a** are the PMPs before degradation and show mostly spherical particles with a smooth surface. In comparison, no significant change is observed with PLGA PMPs after degradation using the pH stat **Figure 6:4 b.** This corresponds with the low rate of degradation (acid release) at 4.5 $\%hr^{-1}$ seen in **Figure 6:1**. On the other hand, the SEM images for PHB PMPs shown in **Figure 6:5 b** appear to show a higher degree of degradation with comparable rate of degradation (acid release) at 4.6 $\%hr^{-1}$. Upon examination of the SEM images of PLGA and PHB PMPs following degradation in a closed respirometer (with pressure measurements to monitor CO_2 production) as depicted in **Figure 6:4 c and Figure 6:5 c**, it is evident that the PMPs exhibit distinct morphological changes compared to their pre-degradation SEM images.

a	PCL PMP Blank, no lipase (after pH stat run)		
			
500 x	1000 x	2000 x	5000 x

b	Ratio 0.040 - PCL (45 kDa) + Lipase (10 mg: 249 units) – Acid release		
			
2000 x	5000 x	5000 x	5000 x

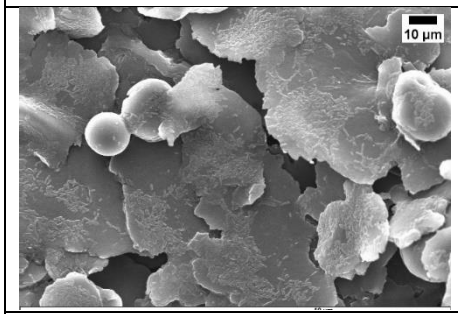
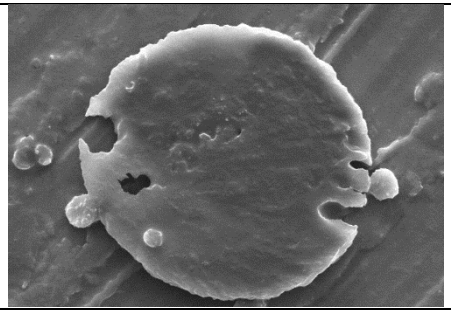
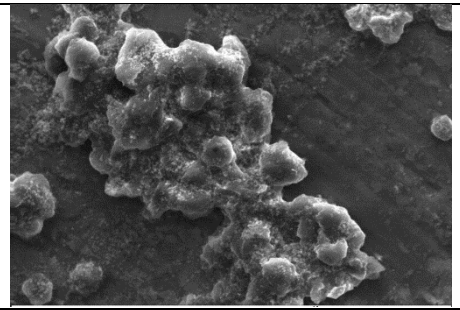
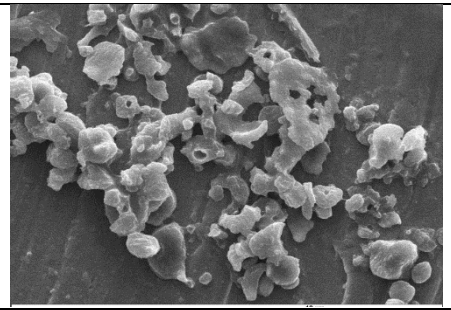
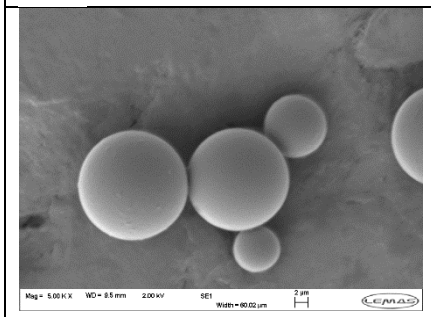
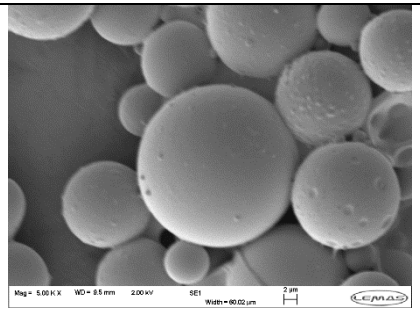
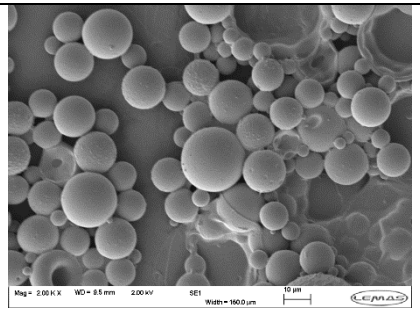
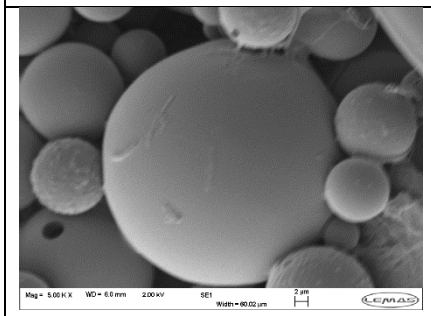
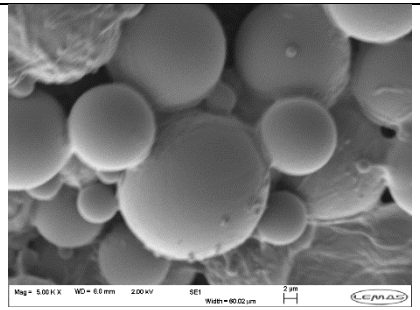
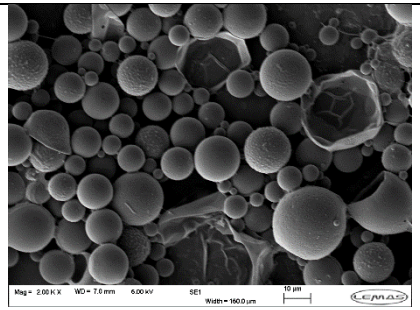
c	Ratio 0.040 - PCL (45 kDa) + Lipase (25 mg: 625 units) – CO_2 production		
			
A) HEPES + PCL only	B) 1 hr HEPES + PCL + lipase (0.040)	C) 2 hr HEPES + PCL + lipase (0.040)	D) Overnight HEPES + PCL + lipase (0.040)

Figure 6:3 - Scanning electron microscopy of PCL PMPs after degradation using pH stat and pressure measurements at Ratio 0.040 - PCL PMP (45 kDa) + Lipase. Showing significant differences in the morphology of the particles compared to the control (no lipase), **a)** Blank, no lipase (after pH stat run), **b)** Ratio 0.040 - PCL (45 kDa) + Lipase (10 mg: 249 units) – experiment conducted in pH stat to monitor acid release, **c)** Ratio 0.040 - PCL (45 kDa) + Lipase (25 mg: 625 units) – experiment conducted in closed respiromter (pressure measrements) to monitor CO_2 production. All images at 10 µm scalebar.

a	PLGA PMP Blank, no lipase	
		
5000 x	5000 x	2000 x

b	PLGA PMP after pH stat run Ratio 0.040 – PLGA PMP + Lipase (10 mg: 249 units)	
		
5000 x	5000 x	2000 x

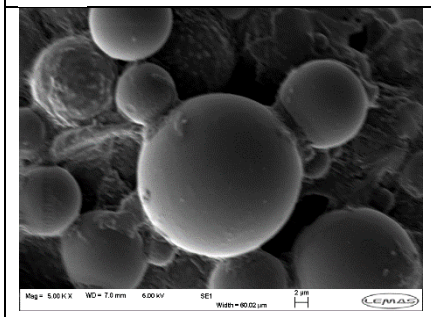
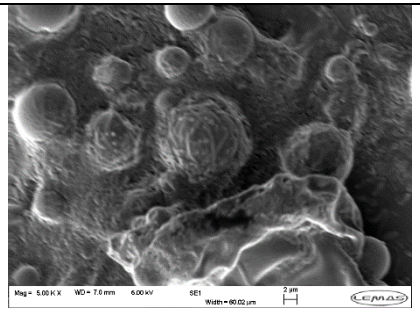
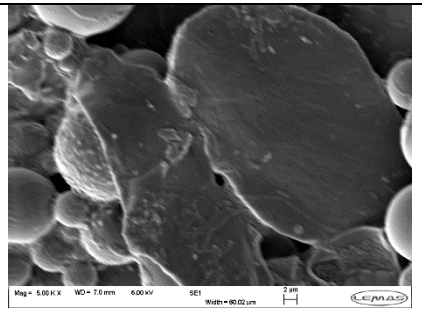
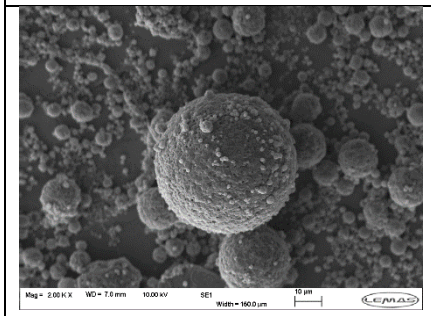
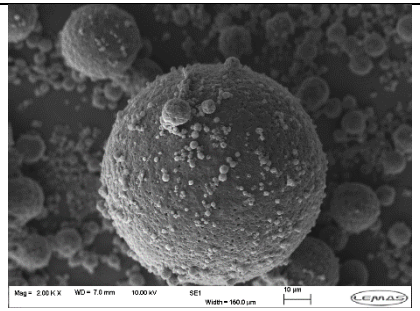
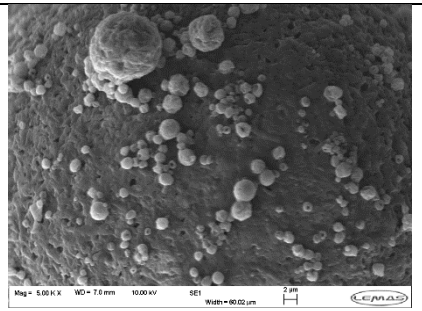
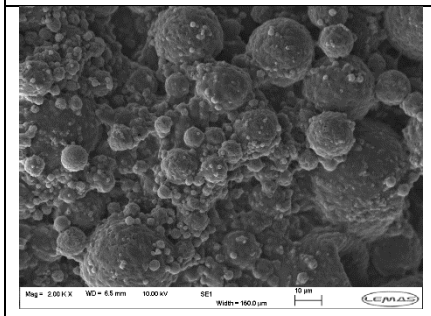
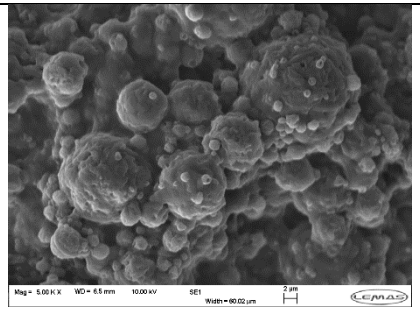
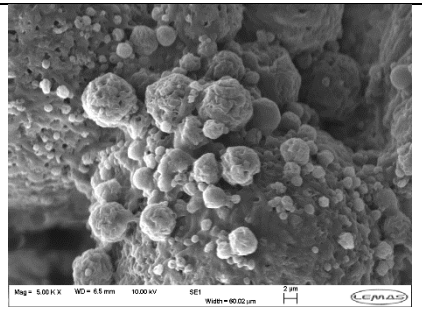
c	PLGA PMP after 10 days HEPES + PLGA PMP + lipase (0.040)	
		
5000 x	5000 x	5000 x

Figure 6:4 - Scanning electron microscopy of PLGA PMPs after degradation using pH stat and pressure measurements at Ratio 0.040 – PLGA PMP + Lipase. Showing significant differences in the morphology of the particles compared to the control (no lipase), **a)** Blank, before degradation, **b)** Ratio 0.040 – PLGA PMP + Lipase (10 mg: 249 units) – experiment conducted in pH stat to monitor acid release, **c)** Ratio 0.040 – PLGA PMP + Lipase (25 mg: 625 units) – experiment conducted in closed respiromter (pressure measurements) to monitor CO_2 production

a	PHB PMP Blank, no lipase	
		
2000 x	2000 x	5000 x

b	PHB PMP after pH stat run Ratio 0.040 – PHB PMP + Lipase (10 mg: 249 units)	
		
2000 x	5000 x	5000 x

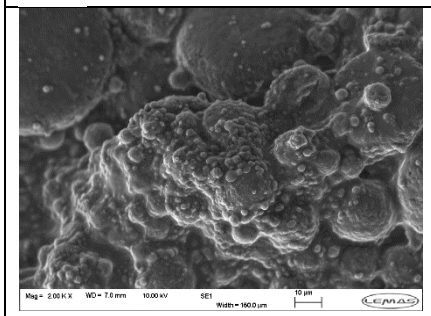
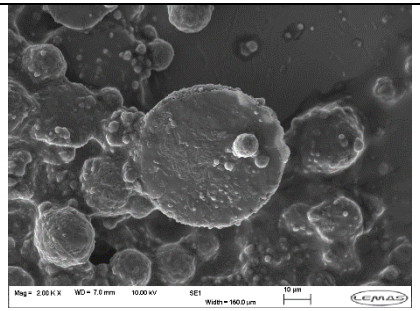
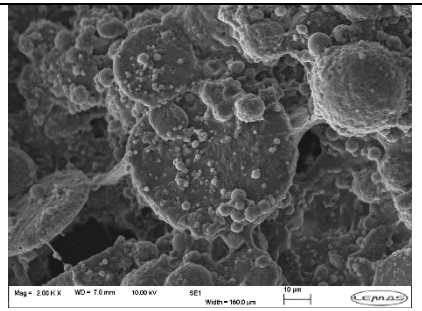
c	PHB PMP after 10 days HEPES + PHB PMP + lipase (0.040)	
		
2000 x	2000 x	2000 x

Figure 6:5 - Scanning electron microscopy of PHB PMPs after degradation using pH stat and pressure measurements at Ratio 0.040 – PHB PMP + Lipase. Showing significant differences in the morphology of the particles compared to the control (no lipase), **a)** Blank, before degradation, **b)** Ratio 0.040 – PHB PMP + Lipase (10 mg: 249 units) – experiment conducted in pH stat to monitor acid release, **c)** Ratio 0.040 – PHB PMP + Lipase (25 mg: 625 units) – experiment conducted in closed respiromter (pressure measrements) to monitor CO_2 production

6.4 Conclusion

The experiment aimed to determine how the type of polymer used in PMPs affects the initial rate of degradation in terms of acid release and the final stages of degradation in terms of production of CO_2. PCL, PLGA, and PHB PMPs were studied, with constant mass and enzyme concentration of each polymer being degraded with lipase at 37ºC and pH 7.4. In terms of the initial rate of degradation monitoring acid release, variations are seen in degradation rates of different polymer microparticles (PMPs), with factors such as polymer type, polydispersity, surface texture, and particle size influencing the results. Despite differences in particle size, PLGA and PHB PMPs exhibit similar rates of biodegradation. Further investigation into the effects of particle size on degradation is needed. Focusing on a single polymer and varying particle sizes, as seen with PCL, could provide more conclusive results. Exploring different enzymes and maintaining consistent particle sizes in future experiments may also lead to more definitive findings. Comparisons between PCL and PHB PMPs, as well as between PCL and PLGA PMPs, highlight the impact of surface texture, particle size, polydispersity, and particle distortion on degradation rates. In terms of the rate of degradation at the final stages (CO_2 production), the results suggest that there may be additional reactions happening simultaneously, complicating the interpretation of results. Increasing surface area did not significantly impact the rate of degradation of PCL PMPs, with smaller particle sizes producing more CO_2. Different polymer backbones may result in varying rates of degradation. The use of the same lipase for experiments raises questions about enzyme specificity for different polyester polymers. Overall, biodegradability of PMPs is thus affected by both their chemical and physical properties such as polymer type, particle size molecular weight, crystallinity, melting temperature, as well as environmental factors such as pH, enzymatic activity and temperature.

6.5 References

Abbott, S. 2018. *Solubility Science Principles and Practice.* 1.0.1.3 ed.

Abid, Z., Dalskov Mosgaard, M., Manfroni, G., Singh Petersen, R., Hagner Nielsen, L., Mullertz, A., Boisen, A. and Sylvest Keller, S. 2019. Investigation of Mucoadhesion and Degradation of PCL and PLGA Microcontainers for Oral Drug Delivery. *Polymers (Basel).* **11**(11).

Accinelli, C., Abbas, H.K., Shier, W.T., Vicari, A., Little, N.S., Aloise, M.R. and Giacomini, S. 2019. Degradation of microplastic seed film-coating fragments in soil. *Chemosphere.* **226**, pp.645-650.

Adhikari, D., Mukai, M., Kubota, K., Kai, T., Kaneko, N., Araki, K.S. and Kubo, M. 2016. Degradation of Bioplastics in Soil and Their Degradation Effects on Environmental Microorganisms. *Journal of Agricultural Chemistry and Environment.* **05**(01), pp.23-34.

Agarwal, S. 2020. Biodegradable Polymers: Present Opportunities and Challenges in Providing a Microplastic-Free Environment. *Macromolecular Chemistry and Physics.* **221**(6), article no: 2000017 [no pagination].

Ahn, H.K., Huda, M.S., Smith, M.C., Mulbry, W., Schmidt, W.F. and Reeves, J.B., 3rd. 2011. Biodegradability of injection molded bioplastic pots containing polylactic acid and poultry feather fiber. *Bioresour Technol.* **102**(7), pp.4930-4933.

Ahn, H.K., Richard, T.L. and Glanville, T.D. 2008. Optimum moisture levels for biodegradation of mortality composting envelope materials. *Waste Manag.* **28**(8), pp.1411-1416.

Albright, V.C., 3rd and Chai, Y. 2021. Knowledge Gaps in Polymer Biodegradation Research. *Environ Sci Technol.* **55**(17), pp.11476-11488.

Amelinckx, S., Dyck, D., Landuyt, V.J. and Tendeloo, V.G. 2008. *Electron microscopy: principles and fundamentals.* [Online]. John Wiley & Sons.

Ammala, A. 2013. Biodegradable polymers as encapsulation materials for cosmetics and personal care markets. *Int J Cosmet Sci.* **35**(2), pp.113-124.
Andrady, A.L. 2015. Persistence of Plastic Litter in the Oceans. *Marine Anthropogenic Litter.* pp.57-72.

Anstey, A., Muniyasamy, S., Reddy, M.M., Misra, M. and Mohanty, A. 2014. Processability and Biodegradability Evaluation of Composites from Poly(butylene succinate) (PBS) Bioplastic and Biofuel Co-products from Ontario. *Journal of Polymers and the Environment.* **22**(2), pp.209-218.

Arcos-Hernandez, M.V., Laycock, B., Pratt, S., Donose, B.C., Nikolić, M.A.L., Luckman, P., Werker, A. and Lant, P.A. 2012. Biodegradation in a soil environment of activated sludge derived polyhydroxyalkanoate (PHBV). *Polymer Degradation and Stability.* **97**(11), pp.2301-2312.

Ariffin, H., Nishida, H., Shirai, Y. and Hassan, M.A. 2010. Highly selective transformation of poly[(R)-3-hydroxybutyric acid] into trans-crotonic acid by catalytic thermal degradation. *Polymer Degradation and Stability.* **95**(8), pp.1375-1381.

Arrieta, M.P., López, J., Rayón, E. and Jiménez, A. 2014. Disintegrability under composting conditions of plasticized PLA–PHB blends. *Polymer Degradation and Stability.* **108**, pp.307-318.

Ashton, J.H., Mertz, J.A., Harper, J.L., Slepian, M.J., Mills, J.L., McGrath, D.V. and Vande Geest, J.P. 2011. Polymeric endoaortic paving: Mechanical, thermoforming, and degradation properties of polycaprolactone/polyurethane blends for cardiovascular applications. *Acta Biomater.* **7**(1), pp.287-294.

Bae, S.B., Nam, H.C. and Park, W.H. 2019. Electrospraying of environmentally sustainable alginate microbeads for cosmetic additives. *International Journal of Biological Macromolecules.* **133**, pp.278-283.

Bagheri, A.R., Laforsch, C., Greiner, A. and Agarwal, S. 2017. Fate of So-Called Biodegradable Polymers in Seawater and Freshwater. *Glob Chall.* **1**(4), p1700048.

Banerjee, A., Chatterjee, K. and Madras, G. 2014. Enzymatic degradation of polymers: a brief review. *Materials Science and Technology.* **30**(5), pp.567-573.
Barrowclough, D. and Birkbeck, C. 2022. Transforming the Global Plastics Economy: The Role of Economic Policies in the Global Governance of Plastic Pollution. *Social Sciences.* **11**(1).

Bartnikowski, M., Dargaville, T.R., Ivanovski, S. and Hutmacher, D.W. 2019. Degradation mechanisms of polycaprolactone in the context of chemistry, geometry and environment. *Progress in Polymer Science.* **96**, pp.1-20.

Baudonnet, L., Pere, D., Michaud, P., Grossiord, J.L. and Rodriguez, F. 2002. Effect of Dispersion Stirring Speed on the Particle Size Distribution and Rheological Properties of Carbomer Dispersions and Gels. *Journal of Dispersion Science and Technology.* **23**(4), pp.499-510.

Blackwell, C.J., Haernvall, K., Guebitz, G.M., Groombridge, M., Gonzales, D. and Khosravi, E. 2018. Enzymatic Degradation of Star Poly(epsilon-Caprolactone) with Different Central Units. *Polymers (Basel).* **10**(11).

Borthakur, L.J., Jana, T. and Dolui, S.K. 2010. Preparation of core–shell latex particles by emulsion co-polymerization of styrene and butyl acrylate, and evaluation of their pigment properties in emulsion paints. *Journal of Coatings Technology and Research.* **7**(6), pp.765-772.

Boyandin, A.N., Prudnikova, S.V., Karpov, V.A., Ivonin, V.N., Đỗ, N.L., Nguyễn, T.H., Lê, T.M.H., Filichev, N.L., Levin, A.L., Filipenko, M.L., Volova, T.G. and Gitelson, I.I. 2013. Microbial degradation of polyhydroxyalkanoates in tropical soils. *International Biodeterioration & Biodegradation.* **83**, pp.77-84.

BUCHI. downloaded Nov 2023. *Spray Drying Basic theory applications, BUCHI,* [Exhibition catalogue]. BUCHI UK Ltd, Unit 6, Goodwin Business Park, Willie Snaith Road, Newmarket Suffolk, CB8 7SQ.

Cao, J., Dang, G., Li, H., Li, T., Yue, Z., Li, N., Liu, Y., Liu, S. and Chen, L. 2015. Identification and Characterization of Lipase Activity and Immunogenicity of LipL from Mycobacterium tuberculosis. *PLoS One.* **10**(9), pe0138151.

Carriere, F., Barrowman, J.A., Verger, R. and Laugier, R. 1993. Secretion and Contribution to Lipolysis of Gastric and Pancreatic Lipases During a Test Meal in Humans. *SECRETION OF DIGESTIVE LIPASES AND LIPOLYSIS.* **105**, pp.876-888.

Castilla-Cortázar, I., Más-Estellés, J., Meseguer-Dueñas, J.M., Escobar Ivirico, J.L., Marí, B. and Vidaurre, A. 2012. Hydrolytic and enzymatic degradation of a poly(ε-caprolactone) network. *Polymer Degradation and Stability.* **97**(8), pp.1241-1248.

Charcosset, C., Limayem, I. and Fessi, H. 2004. The membrane emulsification process—a review. *Journal of Chemical Technology & Biotechnology.* **79**(3), pp.209-218.

Chen, D.R., Bei, J.Z. and Wang, S.G. 1999. Polycaprolactone microparticles and their biodegradation. *Polymer Degradation and Stability.* **67**, pp.455-459.

Chern, C.S. 2006. Emulsion polymerization mechanisms and kinetics. *Progress in Polymer Science.* **31**(5), pp.443-486.

Chinaglia, S., Tosin, M. and Degli-Innocenti, F. 2018. Biodegradation rate of biodegradable plastics at molecular level. *Polymer Degradation and Stability.* **147**, pp.237-244.

Ciuffreda, P., Casati, S., Loseto, A. and Santaniello, E. 2009. Spectrophotometric Assay of Lipase Activity: A New 4-nitrophenyl Ester of a Dialkylglycerol Suitable as a Chromogenic Substrate of Pseudomonas cepacia Lipase. *Biocatalysis and Biotransformation.* **21**(3), pp.123-127.

Corrêa-Filho, L., Moldão-Martins, M. and Alves, V. 2019. Advances in the Application of Microcapsules as Carriers of Functional Compounds for Food Products. *Applied Sciences.* **9**(3).

Dalgleish, D., West, J.S. and Hallett, F.R. 1996. The characterization of small emulsion droplets made from milk proteins and trigyceride oil. *Colloids and Surfaces.* pp.145-153.

Deroiné, M., César, G., Le Duigou, A., Davies, P. and Bruzaud, S. 2015. Natural Degradation and Biodegradation of Poly(3-Hydroxybutyrate-co-3-

Hydroxyvalerate) in Liquid and Solid Marine Environments. *Journal of Polymers and the Environment.* **23**(4), pp.493-505.

Dey, T.K., Uddin, M.E. and Jamal, M. 2021. Detection and removal of microplastics in wastewater: evolution and impact. *Environ Sci Pollut Res Int.* **28**(14), pp.16925-16947.

Eghbal, N. and Choudhary, R. 2018. Complex coacervation: coacervation: Encapsulation and controlled release of active agents in food systems. *Lwt-Food Science and Technology.* **90**, pp.254-264.

Eldsater, C., Erlandsson, B., Renstad, R., Albertsson, A.-C. and Karlsson, S. 2000. The biodegradation of amorphous and crystalline regions in film-blown poly(e-caprolactone). *Polymer.* **41**, pp.1297-1304.

Ellis, B. and Smith, M.C. 2009. *Polymers: A Property Database, Second Edition.* 2nd ed. US: Taylor & Francis.

Emadian, S.M., Onay, T.T. and Demirel, B. 2017. Biodegradation of bioplastics in natural environments. *Waste Manag.* **59**, pp.526-536.
Erlanson, C. and Borgström, B. 2020. Tributyrine as a Substrate for Determination of Lipase Activity of Pancreatic Juice and Small Intestinal Content. *Scandinavian Journal of Gastroenterology.* **5**(4), pp.293-295.

European Union. 2019. *European Chemicals Agency.* [Online]. [Accessed 19/07/2019]. Available from: https://echa.europa.eu/

Fang, Z., Gao, Y., Wu, X., Xu, X., Sarmah, A.K., Bolan, N., Gao, B., Shaheen, S.M., Rinklebe, J., Ok, Y.S., Xu, S. and Wang, H. 2020. A critical review on remediation of bisphenol S (BPS) contaminated water: Efficacy and mechanisms. *Critical Reviews in Environmental Science and Technology.* **50**(5), pp.476-522.

Ferrari, R., Colombo, C., Dossi, M. and Moscatelli, D. 2013. Tunable PLGA-Based Nanoparticles Synthesized Through Free-Radical Polymerization. *Macromolecular Materials and Engineering.* **298**(7), pp.730-739.

Freitas, S., Merkle, H.P. and Gander, B. 2005. Microencapsulation by solvent extraction/evaporation: reviewing the state of the art of microsphere preparation process technology. *J Control Release.* **102**(2), pp.313-332.

Funabashi, M., Ninomiya, F. and Kunioka, M. 2006. Biodegradation of Polycaprolactone Powders Proposed as Reference Test Materials for International Standard of Biodegradation Evaluation Method. *Journal of Polymers and the Environment.* **15**(1), pp.7-17.

Gadzinski, P., Froelich, A., Jadach, B., Wojtylko, M., Tatarek, A., Bialek, A., Krysztofiak, J., Gackowski, M., Otto, F. and Osmalek, T. 2022. Ionotropic Gelation and Chemical Crosslinking as Methods for Fabrication of Modified-Release Gellan Gum-Based Drug Delivery Systems. *Pharmaceutics.* **15**(1).

Garcia-Depraect, O., Lebrero, R., Rodriguez-Vega, S., Bordel, S., Santos-Beneit, F., Martinez-Mendoza, L.J., Aragao Borner, R., Borner, T. and Munoz, R. 2022.

Biodegradation of bioplastics under aerobic and anaerobic aqueous conditions: Kinetics, carbon fate and particle size effect. *Bioresource Technology.* **344**, pp.126-265.

Gartiser, S. 2018a. Manometric respiration tests according to OECD 301F with the OxiTop® Control measuring system under GLP conditions. **WTW Field Report**.

Gartiser, S. 2018b. Manometric respiration tests according to OECD 301F with the OxiTop®Control measuring system under GLP conditions.

Gebauer, B. and Jendrossek, D. 2006. Assay of poly(3-hydroxybutyrate) depolymerase activity and product determination. *Appl Environ Microbiol.* **72**(9), pp.6094-6100.

Gentile, P., Chiono, V., Carmagnola, I. and Hatton, P.V. 2014. An overview of poly(lactic-co-glycolic) acid (PLGA)-based biomaterials for bone tissue engineering. *Int J Mol Sci.* **15**(3), pp.3640-3659.

Geyer. R, Jambeck. R and Law. K.L. 2017. Production, use, and fate of all plastics ever made. *Science Advances.*

Ghimire, S., Flury, M., Scheenstra, E.J. and Miles, C.A. 2020. Sampling and degradation of biodegradable plastic and paper mulches in field after tillage incorporation. *Science of the Total Environment.* **703**, article no: 135577 [no pagination].

Gómez, E.F. and Michel, F.C. 2013. Biodegradability of conventional and bio-based plastics and natural fiber composites during composting, anaerobic digestion and long-term soil incubation. *Polymer Degradation and Stability.* **98**(12), pp.2583-2591.

Gonzalez-Pleiter, M., Tamayo-Belda, M., Pulido-Reyes, G., Amariei, G., Leganes, F., Rosal, R. and Fernandez-Pinas, F. 2019. Secondary nanoplastics released from a biodegradable microplastic severely impact freshwater environments. *Environmental Science-Nano.* **6**(5), pp.1382-1392.

Gouin, S. 2004. Microencapsulation. *Trends in Food Science & Technology.* **15**(7-8), pp.330-347.

Govindasamy, S., Syafiq, I.M., Amirul, A.A.A., Amin, R.M. and Bhubalan, K. 2019. Dataset on controlled production of polyhydroxyalkanoate-based microbead using double emulsion solvent evaporation technique. *Data in Brief.* **23**, article no: 103675 [no pagination].

Grundy, M.M.L., Abrahamse, E., Almgren, A., Alminger, M., Andres, A., Ariëns, R.M.C., Bastiaan-Net, S., Bourlieu-Lacanal, C., Brodkorb, A., Bronze, M.R., Comi, I., Couëdelo, L., Dupont, D., Durand, A., El, S.N., Grauwet, T., Heerup, C., Heredia, A., Infantes Garcia, M.R., Jungnickel, C., Kłosowska-Chomiczewska, I.E., Létisse, M., Macierzanka, A., Mackie, A.R., McClements, D.J., Menard, O., Meynier, A., Michalski, M.-C., Mulet-Cabero, A.-I., Mullertz, A., Payeras Perelló, F.M., Peinado, I., Robert, M., Secouard, S., Serra, A.T., Silva, S.D., Thomassen,

G., Tullberg, C., Undeland, I., Vaysse, C., Vegarud, G.E., Verkempinck, S.H.E., Viau, M., Zahir, M., Zhang, R. and Carrière, F. 2021. INFOGEST inter-laboratory recommendations for assaying gastric and pancreatic lipases activities prior to in vitro digestion studies. *Journal of Functional Foods.* **82**.

Hann, S.S., C. Jamieson, O. Hickman, H. 2018. *Investigating options for reducing releases in the aquatic environment of microplastics emitted by (but not intentionally added in) products.* Eunomia Research & Consulting Ltd.

Harmaen, A.S., Khalina, A., Azowa, I., Hassan, M.A., Tarmian, A. and Jawaid, M. 2014. Thermal and biodegradation properties of poly(lactic acid)/fertilizer/oil palm fibers blends biocomposites. *Polymer Composites.* **36**(3), pp.576-583.

Harrison, J.P., Boardman, C., O'Callaghan, K., Delort, A.M. and Song, J. 2018. Biodegradability standards for carrier bags and plastic films in aquatic environments: a critical review. *R Soc Open Sci.* **5**(5), p171792.

Harrison, J.P., Sapp, M., Schratzberger, M. and Mark Osborn, A. 2011. Interactions between Microorganisms and marine micro plastics: A call for research. *Marine Technology Society Journal.* **45**(2), pp.12-20.

Hartmann, N.B., Huffer, T., Thompson, R.C., Hassellov, M., Verschoor, A., Daugaard, A.E., Rist, S., Karlsson, T., Brennholt, N., Cole, M., Herrling, M.P., Hess, M.C., Ivleva, N.P., Lusher, A.L. and Wagner, M. 2019. Are We Speaking the Same Language? Recommendations for a Definition and Categorization Framework for Plastic Debris. *Environ Sci Technol.* **53**(3), pp.1039-1047.

Hashimoto, K., Sudo, M., Ohta, K., Sugimura, T., Yamada, H. and Aoki, T. 2002. Biodegradation of nylon4 and its blend with nylon6. *Journal of Applied Polymer Science.* **86**(9), pp.2307-2311.

Heiskanen, H., Denifl, P., Hurme, M., Pitkänen, P. and Oksman, M. 2012a. Effect of Physical Properties and Emulsification Conditions on the Microsphere Size Prepared Using a Solvent Extraction Process. *Journal of Dispersion Science and Technology.* **33**(2), pp.234-244.

Heiskanen, H., Denifl, P., Pitkänen, P. and Hurme, M. 2012b. Effect of concentration and temperature on the properties of the microspheres prepared using an emulsion–solvent extraction process. *Advanced Powder Technology.* **23**(6), pp.779-786.

Hochleitner, B., Schreiner, M., Drakopoulos, M., Snigireva, I. and Snivireg, A. 2003. Analysis of Paint Layers by Light Microscopy, Scanning Electron Microscopy and Synchrotron induced X-Ray Micro-Diffraction.

Ibraheem, D., Iqbal, M., Agusti, G., Fessi, H. and Elaissari, A. 2014. Effects of process parameters on the colloidal properties of polycaprolactone microparticles prepared by double emulsion like process. *Colloids and Surfaces A: Physicochemical and Engineering Aspects.* **445**, pp.79-91.

Islam Mozumder, M.S., Garcia-Gonzalez, L., Wever, H.D. and Volcke, E.I.P. 2015. Poly(3-hydroxybutyrate) (PHB) production from CO2: Model development and process optimization. *Biochemical Engineering Journal.* **98**, pp.107-116.

Iwata, T. 2015. Biodegradable and bio-based polymers: future prospects of eco-friendly plastics. *Angew Chem Int Ed Engl.* **54**(11), pp.3210-3215.

Jain, R. and Tiwari, A. 2015. Biosynthesis of planet friendly bioplastics using renewable carbon source. *J Environ Health Sci Eng.* **13**, p11.

Jaworek, A. 2006. Electrospray droplet sources for thin film deposition. *Journal of Materials Science.* **42**(1), pp.266-297.

Jenkins, M.J. and Harrison, K.L. 2008. The effect of crystalline morphology on the degradation of polycaprolactone in a solution of phosphate buffer and lipase. *Polymers for Advanced Technologies.* **19**(12), pp.1901-1906.

Jiang, S., Sudol, E.D., Dimonie, V.L. and El-Aasser, M.S. 2008. Kinetics of dispersion polymerization: Effect of medium composition. *Journal of Polymer Science Part A: Polymer Chemistry.* **46**(11), pp.3638-3647.

Kale, G., Auras, R., Singh, S.P. and Narayan, R. 2007. Biodegradability of polylactide bottles in real and simulated composting conditions. *Polymer Testing.* **26**(8), pp.1049-1061.

Karamanlioglu, M. and Robson, G.D. 2013. The influence of biotic and abiotic factors on the rate of degradation of poly(lactic) acid (PLA) coupons buried in compost and soil. *Polymer Degradation and Stability.* **98**(10), pp.2063-2071.

Katou, H., Wandrey, A.J. and Gander, B. 2008. Kinetics of solvent extraction/evaporation process for PLGA microparticle fabrication. *Int J Pharm.* **364**(1), pp.45-53.

Kim, M., Park, J.M., Um, H.J., Lee, D.H., Lee, K.H., Kobayashi, F., Iwasaka, Y., Hong, C.S., Min, J. and Kim, Y.H. 2010. Immobilization of cross-linked lipase aggregates onto magnetic beads for enzymatic degradation of polycaprolactone. *J Basic Microbiol.* **50**(3), pp.218-226.

Kjeldsen, A., Price, M., Lilley, C. and Guzniczak, E. 2019. A Review of Standards for Biodegradable Plastics. *IBioIC.*

Kjelsden, A.P., Lilley, M., Guznicak, C. and Archer, E.I. 2019. A Review of Standards for Biodegradable Plastics. *Industrial Biotechnology Innovation Centre.*

Kosvintsev, S.R., Gasparini, G. and Holdich, R.G. 2008. Membrane emulsification: Droplet size and uniformity in the absence of surface shear. *Journal of Membrane Science.* **313**(1-2), pp.182-189.

Kozlowska, J., Prus, W. and Stachowiak, N. 2019. Microparticles based on natural and synthetic polymers for cosmetic applications. *International Journal of Biological Macromolecules.* **129**, pp.952-956.

Kumar, A., Thakur, A. and Panesar, P.S. 2019. Recent developments on sustainable solvents for emulsion liquid membrane processes. *Journal of Cleaner Production.* **240**.

Kumar, G.A., Anjana, K., Hinduja, M., Sujitha, K. and Dharani, G. 2020. Review on plastic wastes in marine environment – Biodegradation and biotechnological solutions. *Marine Pollution Bulletin.* **150**, article no: 110733 [no pagination].

Kunioka, M., Ninomiya, F. and Funabashi, M. 2009. Biodegradation of poly(butylene succinate) powder in a controlled compost at 58 degrees C evaluated by naturally-occurring carbon 14 amounts in evolved CO(2) based on the ISO 14855-2 method. *Int J Mol Sci.* **10**(10), pp.4267-4283.

Labet, M. and Thielemans, W. 2009. Synthesis of polycaprolactone: a review. *Chem Soc Rev.* **38**(12), pp.3484-3504.

Laycock, B., Nikolić, M., Colwell, J.M., Gauthier, E., Halley, P., Bottle, S. and George, G. 2017. Lifetime prediction of biodegradable polymers. *Progress in Polymer Science.* **71**, pp.144-189.

Lee, J., Hill, A. and Kentish, S. 2013. Formation of a thick aromatic polyamide membrane by interfacial polymerisation. *Separation and Purification Technology.* **104**, pp.276-283.

Leja, K. and Lewandowicz, G. 2010. Polymer Biodegradation and Biodegradable Polymers – a Review. *Polish J. of Environ. Stud.* **Vol. 19**(2), pp.255-266.

Lengyel, M., Kállai-Szabó, N., Antal, V., Laki, A.J. and Antal, I. 2019. Microparticles, Microspheres, and Microcapsules for Advanced Drug Delivery. *Scientia Pharmaceutica.* **87**(3).

Leong, J.-Y., Lam, W.-H., Ho, K.-W., Voo, W.-P., Lee, M.F.-X., Lim, H.-P., Lim, S.-L., Tey, B.-T., Poncelet, D. and Chan, E.-S. 2016. Advances in fabricating spherical alginate hydrogels with controlled particle designs by ionotropic gelation as encapsulation systems. *Particuology.* **24**, pp.44-60.

Li, R.J., Liu, Y., Sheng, Y.F., Xiang, Q.Q., Zhou, Y. and Cizdziel, J.V. 2020. Effect of prothioconazole on the degradation of microplastics derived from mulching plastic film: Apparent change and interaction with heavy metals in soil. *Environmental Pollution.* **260**, article no: 113988 [no pagination].

M. T Stillwell, R. G Holdich, S. R Kosvintsev, G. Gasparini and I. W Cumming. 2007. Stirred Cell Membrane Emulsification and Factors Influencing Dispersion Drop. *Ind. Eng. Chem. Res. 2007, 46, 965-972.* **Ind. Eng. Chem. Res.**(46), pp.965-972.

Magni, S., Bonasoro, F., Della Torre, C., Parenti, C.C., Maggioni, D. and Binelli, A. 2020. Plastics and biodegradable plastics: ecotoxicity comparison between polyvinylchloride and Mater-Bi (R) micro-debris in a freshwater biological model. *Science of the Total Environment.* **720**, article no: 137602 [no pagination].

Mahar, R., Chakraborty, A., Nainwal, N., Bahuguna, R., Sajwan, M. and Jakhmola, V. 2023. Application of PLGA as a Biodegradable and Biocompatible Polymer for Pulmonary Delivery of Drugs. *AAPS PharmSciTech.* **24**(1), p39.

Makadia, H.K. and Siegel, S.J. 2011. Poly Lactic-co-Glycolic Acid (PLGA) as Biodegradable Controlled Drug Delivery Carrier. *Polymers (Basel).* **3**(3), pp.1377-1397.

Makio, T.R., H, Marchessault. 1999. Determination of solubility parameters for poly(3-hydroxyalkanoates). *International Journal of Biological Macromolecules.* **25**, pp.207-215.

Martin, A. 2022. Generation of biodegradability data on petroleum constituents using enhanced tests (OECD Guideline 301 F).

Massardier-Nageotte, V., Pestre, C., Cruard-Pradet, T. and Bayard, R. 2006. Aerobic and anaerobic biodegradability of polymer films and physico-chemical characterization. *Polymer Degradation and Stability.* **91**(3), pp.620-627.

Mat, D.J.L., Le Feunteun, S., Michon, C. and Souchon, I. 2016. In vitro digestion of foods using pH-stat and the INFOGEST protocol: Impact of matrix structure on digestion kinetics of macronutrients, proteins and lipids. *Food Research International.* **88**, pp.226-233.

Mauguet, M.C., Legrand, J., Brujes, L., Carnelle, G., Larre, C. and Popineau, Y. 2002. Gliadin matrices for microencapsulation processes by simple coacervation method. *J Microencapsul.* **19**(3), pp.377-384.

McClements, D.J. and Gumus, C.E. 2016. Natural emulsifiers - Biosurfactants, phospholipids, biopolymers, and colloidal particles: Molecular and physicochemical basis of functional performance. *Adv Colloid Interface Sci.* **234**, pp.3-26.

McDonough, K., Itrich, N., Casteel, K., Menzies, J., Williams, T., Krivos, K. and Price, J. 2017. Assessing the biodegradability of microparticles disposed down the drain. *Chemosphere.* **175**, pp.452-458.

Mezhuev, Y.O., Motyakin, M.V., Plyushchii, I.V., Alekperov, R.A., Luss, A.L., Kovarskii, A.L., Degtyarev, Y.N., Ionova, I.S., Dyatlov, V.A., Vorobev, I.Y., Vagramyan, T.A., Abrashov, A.A., Tsatsakis, A.M., Shtilman, M.I. and Korshak, Y.V. 2020. Interfacial oxidative polymerization of aniline on silica gel's surface. *Polymer.* **203**, p122808.

Middleton, J.C. and Tipton, A.J. 2000. Synthetic biodegradable polymers as orthopedic devices. *Biomaterials.* **21**, pp.2335-2346.

Mihai, M., Legros, N. and Alemdar, A. 2014. Formulation-properties versatility of wood fiber biocomposites based on polylactide and polylactide/thermoplastic starch blends. *Polymer Engineering & Science.* **54**(6), pp.1325-1340.

Miksch, L., Gutow, L. and Saborowski, R. 2021. pH-Stat Titration: A Rapid Assay for Enzymatic Degradability of Bio-Based Polymers. *Polymers (Basel).* **13**(6).

Modelli, A., Calcagno, B. and Scandola, M. 1999. Kinetics of Aerobic Polymer Degradation in Soil by Means of the ASTM D 5988-96 Standard Method. *Journal of Environmental Polymer Degradation.* **7**(2), pp.109-116.

Mohamed, F. and van der Walle, C.F. 2008. Engineering biodegradable polyester particles with specific drug targeting and drug release properties. *J Pharm Sci.* **97**(1), pp.71-87.

Mohee, R., Unmar, G.D., Mudhoo, A. and Khadoo, P. 2008. Biodegradability of biodegradable/degradable plastic materials under aerobic and anaerobic conditions. *Waste Manag.* **28**(9), pp.1624-1629.

Mostafa, N.A., Farag, A.A., Abo-dief, H.M. and Tayeb, A.M. 2018. Production of biodegradable plastic from agricultural wastes. *Arabian Journal of Chemistry.* **11**(4), pp.546-553.

Murueva, A.V., Shishatskaya, E.I., Kuzmina, A.M., Volova, T.G. and Sinskey, A.J. 2013. Microparticles prepared from biodegradable polyhydroxyalkanoates as matrix for encapsulation of cytostatic drug. *J Mater Sci Mater Med.* **24**(8), pp.1905-1915.

Nair, L.S. and Laurencin, C.T. 2007. Biodegradable polymers as biomaterials. *Progress in Polymer Science.* **32**(8-9), pp.762-798.

Nakasaki, K., Matsuura, H., Tanaka, H. and Sakai, T. 2006. Synergy of two thermophiles enables decomposition of poly-epsilon-caprolactone under composting conditions. *FEMS Microbiol Ecol.* **58**(3), pp.373-383.

Nam, H.C. and Park, W.H. 2020. Aliphatic Polyester-Based Biodegradable Microbeads for Sustainable Cosmetics. *Acs Biomaterials Science & Engineering.* **6**(4), pp.2440-2449.

Nguyen, T.V., Nguyen Tri, P., Nguyen, T.D., El Aidani, R., Trinh, V.T. and Decker, C. 2016. Accelerated degradation of water borne acrylic nanocomposites used in outdoor protective coatings. *Polymer Degradation and Stability.* **128**, pp.65-76.

O'Malley, L.P. 2006. Evaluation and Modification of the OECD 301F Respirometry Biodegradation Test Method with Regard to Test Substance Concentration and Inoculum. *Water, Air, and Soil Pollution.* **177**(1-4), pp.251-265.

Oh, Y.-R., Jang, Y.-A., Song, J.K. and Eom, G.T. 2022. Efficient enzymatic depolymerization of polycaprolactone into 6-hydroxyhexanoic acid by optimizing reaction conditions and microbial conversion of 6-hydroxyhexanoic acid into adipic acid for eco-friendly upcycling of polycaprolactone. *Biochemical Engineering Journal.* **185**.

Pabois, O., Antoine-Michard, A., Zhao, X., Omar, J., Ahmed, F., Alexis, F., Harvey, R.D., Grillo, I., Gerelli, Y., Grundy, M.M., Bajka, B., Wilde, P.J. and Dreiss, C.A. 2020. Interactions of bile salts with a dietary fibre, methylcellulose, and impact on lipolysis. *Carbohydr Polym.* **231**, p115741.

Pagga, U., Schafer, A., Muller, R.J. and Pantke, M. 2000. Determination of the aerobic biodegradability of polymeric material in aquatic batch tests. *Chemosphere.* **42**, pp.319-331.

Pastorino, L., Pioli, F., Zilli, M., Converti, A. and Nicolini, C. 2004. Lipase-catalyzed degradation of poly(ε-caprolactone). *Enzyme and Microbial Technology.* **35**(4), pp.321-326.

Pawlik, J., Łukowicz, K., Cholewa-Kowalska, K. and Osyczka, A.M. 2019. New insights into the PLGA and PCL blending: physico-mechanical properties and cell response. *Materials Research Express.* **6**(8).

Perignon, C., Ongmayeb, G., Neufeld, R., Frere, Y. and Poncelet, D. 2015. Microencapsulation by interfacial polymerisation: membrane formation and structure. *Journal of Microencapsulation.* **32**(1), pp.1-15.

Pranamuda, H., Tokiwa, Y. and Tanaka, H. 1997. Polylactide Degradation by an Amycolatopsis sp. *Applied and Environmental Micrbiology.* **63**, pp.1637-1640.

Qi, R., Jones, D.L., Li, Z., Liu, Q. and Yan, C. 2020. Behavior of microplastics and plastic film residues in the soil environment: A critical review. *Science of the Total Environment.* **703**, article no: 134722 [no pagination].

Qiao, T., Kim, S., Lee, W. and Lee, H. 2019. Biodegradable and Porous Poly(lactic-co-glycolic acid) Microbeads for In vitro Evaluation of Negatively Charged Fluorescent Bacteria. *Macromolecular Research.*

Qin, R., Su, C., Liu, W., Tang, L., Li, X., Deng, X., Wang, A. and Chen, Z. 2020. Effects of exposure to polyether sulfone microplastic on the nitrifying process and microbial community structure in aerobic granular sludge. *Bioresource Technology.* **302**, article no: 122827 [no pagination].

Ragusa, A., Svelato, A., Santacroce, C., Catalano, P., Notarstefano, V., Carnevali, O., Papa, F., Rongioletti, M.C.A., Baiocco, F., Draghi, S., D'Amore, E., Rinaldo, D., Matta, M. and Giorgini, E. 2021. Plasticenta: First evidence of microplastics in human placenta. *Environ Int.* **146**, p106274.

Reul, R., Renette, T., Bege, N. and Kissel, T. 2011. Nanoparticles for paclitaxel delivery: a comparative study of different types of dendritic polyesters and their degradation behavior. *Int J Pharm.* **407**(1-2), pp.190-196.

Rhodes, C.J. 2018. Plastic pollution and potential solutions. *Science progress.* **101**(3), pp.207-260.

Richez, A.P., Yow, H.N., Biggs, S. and Cayre, O.J. 2013. Dispersion polymerization in non-polar solvent: Evolution toward emerging applications. *Progress in Polymer Science.* **38**(6), pp.897-931.

Robinson, P.K. 2015. Enzymes: principles and biotechnological applications. *Essays Biochem.* **59**, pp.1-41.

Roppola, K., Kuokkanen, T., Ramo, J., Prokkola, H. and Heiska, E. 2007. Comparison Study of Different BOD Tests in the Determination of BOD(7) Evaluated in a Model Domestic Sewage. *J Autom Methods Manag Chem.* **2007**, p39761.

Rosato, A., Barone, M., Negroni, A., Brigidi, P., Fava, F., Xu, P., Candela, M. and Zanaroli, G. 2020. Microbial colonization of different microplastic types and biotransformation of sorbed PCBs by a marine anaerobic bacterial community. *Science of the Total Environment.* **705**, article no: 135790 [no pagination].

Ruka, D.R., Sangwan, P., Garvey, C.J., Simon, G.P. and Dean, K.M. 2015. Biodegradability of Poly-3-hydroxybutyrate/Bacterial Cellulose Composites under Aerobic Conditions, Measured via Evolution of Carbon Dioxide and Spectroscopic and Diffraction Methods. *Environ Sci Technol.* **49**(16), pp.9979-9986.

Samir, A., Ashour, F.H., Hakim, A.A.A. and Bassyouni, M. 2022. Recent advances in biodegradable polymers for sustainable applications. *npj Materials Degradation.* **6**(1).

Sanchez-Hernandez, J.C., Capowiez, Y. and Ro, K.S. 2020. Potential Use of Earthworms to Enhance Decaying of Biodegradable Plastics. *ACS Sustainable Chemistry and Engineering.* **8**(11), pp.4292-4316.

Sánchez, C. 2020. Fungal potential for the degradation of petroleum-based polymers: An overview of macro- and microplastics biodegradation. *Biotechnology Advances.* **40**, article no: 107501 [no pagination].

Sarasa, J., Gracia, J.M. and Javierre, C. 2009. Study of the biodisintegration of a bioplastic material waste. *Bioresour Technol.* **100**(15), pp.3764-3768.

Sarkar, A., Zhang, S., Holmes, M. and Ettelaie, R. 2019. Colloidal aspects of digestion of Pickering emulsions: Experiments and theoretical models of lipid digestion kinetics. *Adv Colloid Interface Sci.* **263**, pp.195-211.

Sarkar, A., Zhang, S., Murray, B., Russell, J.A. and Boxal, S. 2017. Modulating in vitro gastric digestion of emulsions using composite whey protein-cellulose nanocrystal interfaces. *Colloids Surf B Biointerfaces.* **158**, pp.137-146.

Schuck, P., Jeantet, R., Bhandari, B., Chen, X.D., Perrone, Í.T., de Carvalho, A.F., Fenelon, M. and Kelly, P. 2016. Recent advances in spray drying relevant to the dairy industry: A comprehensive critical review. *Drying Technology.* **34**(15), pp.1773-1790.

Scudo, A., Liebman, B., Corban, C., Tyrer, D., Kreissig, J. and Warrick, O. 2017. *Intentionally added microplastics in products.*

Shah, A.A., Hasan, F., Hameed, A. and Ahmed, S. 2008. Biological degradation of plastics: A comprehensive review. *Biotechnology Advances.* **26**(3), pp.246-265.

Sing, C.E. and Perry, S.L. 2020. Recent progress in the science of complex coacervation. *Soft Matter.* **16**(12), pp.2885-2914.

Sintim, H.Y. and Flury, M. 2017. Is Biodegradable Plastic Mulch the Solution to Agriculture's Plastic Problem? *Environ Sci Technol.* **51**(3), pp.1068-1069.

Siracusa, V. 2019. Microbial Degradation of Synthetic Biopolymers Waste. *Polymers (Basel).* **11**(6).

Sivalingam, G., Chattopadhyay, S. and Madras, G. 2002. Solvent effects on the lipase catalyzed biodegradation of poly (e-caprolactone) in solution. *Polymer Degradation and Stability.* **79**, pp.413-418.

Sivalingam, G., Chattopadhyay, S. and Madras, G. 2003. Enzymatic degradation of poly (ε-caprolactone), poly (vinyl acetate) and their blends by lipases. *Chemical Engineering Science.* **58**(13), pp.2911-2919.

Song, J.H., Murphy, R.J., Narayan, R. and Davies, G.B. 2009. Biodegradable and compostable alternatives to conventional plastics. *Philos Trans R Soc Lond B Biol Sci.* **364**(1526), pp.2127-2139.

Sridewi, N., Bhubalan, K. and Sudesh, K. 2006. Degradation of commercially important polyhydroxyalkanoates in tropical mangrove ecosystem. *Polymer Degradation and Stability.* **91**(12), pp.2931-2940.

Staff, R.H., Landfester, K. and Crespy, D. 2013a. Recent Advances in the Emulsion Solvent Evaporation Technique for the Preparation of Nanoparticles and Nanocapsules. *Hierarchical Macromolecular Structures: 60 Years after the Staudinger Nobel Prize II.* pp.329-344.

Staff, R.H., Schaeffel, D., Turshatov, A., Donadio, D., Butt, H.J., Landfester, K., Koynov, K. and Crespy, D. 2013b. Particle formation in the emulsion-solvent evaporation process. *Small.* **9**(20), pp.3514-3522.

Tabasi, R.Y. and Ajji, A. 2015. Selective degradation of biodegradable blends in simulated laboratory composting. *Polymer Degradation and Stability.* **120**, pp.435-442.

Tachibana, K., Urano, Y. and Numata, K. 2013. Biodegradability of nylon 4 film in a marine environment. *Polymer Degradation and Stability.* **98**(9), pp.1847-1851.

Tan, Y., Zhang, Z., Zhou, H., Xiao, H. and McClements, D.J. 2020. Factors impacting lipid digestion and β-carotene bioaccessibility assessed by standardized gastrointestinal model (INFOGEST): Oil droplet concentration. *Food & Function.*

Thellen, C., Coyne, M., Froio, D., Auerbach, M., Wirsen, C. and Ratto, J.A. 2008. A Processing, Characterization and Marine Biodegradation Study of Melt-Extruded Polyhydroxyalkanoate (PHA) Films. *Journal of Polymers and the Environment.* **16**(1), pp.1-11.

Therin, M. and Christel, P. 1991. In viva degradation of massive polyla-hydroxy acids): validation of in vitro findings. *Biomaterials 1992, Vol. 13 No. 9.* **13**(9).

Tokiwa, Y., Calabia, B.P., Ugwu, C.U. and Aiba, S. 2009. Biodegradability of plastics. *Int J Mol Sci.* **10**(9), pp.3722-3742.

Tokiwa, Y. and Suzuki, T. 2014. Hydrolysis of Polyesters byRhizopus delemarLipase. *Agricultural and Biological Chemistry.* **42**(5), pp.1071-1072.

Tosin, M., Pischedda, A. and Degli-Innocenti, F. 2019. Biodegradation kinetics in soil of a multi-constituent biodegradable plastic. *Polymer Degradation and Stability.* **166**, pp.213-218.

Valencia, G.A., Zare, E.N., Makvandi, P. and Gutiérrez, T.J. 2019. Self-Assembled Carbohydrate Polymers for Food Applications: A Review. *Comprehensive Reviews in Food Science and Food Safety.* **18**(6), pp.2009-2024. van den Oever, M., Molenveld, K., van der Zee, M. and Bos, H.t. 2017.

Vaverková, M. and Adamcová, D. 2015. Biodegrability of Bioplastic Materials in a Controlled Composting Environment. *Journal of Ecological Engineering.* **16**, pp.155-160.

Volova, T.G., Boyandin, A.N., Vasil'ev, A.D., Karpov, V.A., Kozhevnikov, I.V., Prudnikova, S.V., Rudnev, V.P., Xuån, B.B., Dũng, V.V. and Gitel'zon, I.I. 2011. Biodegradation of polyhydroxyalkanoates (PHAs) in the South China Sea and identification of PHA-degrading bacteria. *Microbiology.* **80**(2), pp.252-260.

Volova, T.G., Boyandin, A.N., Vasiliev, A.D., Karpov, V.A., Prudnikova, S.V., Mishukova, O.V., Boyarskikh, U.A., Filipenko, M.L., Rudnev, V.P., Bá Xuân, B., Việt Dũng, V. and Gitelson, I.I. 2010. Biodegradation of polyhydroxyalkanoates (PHAs) in tropical coastal waters and identification of PHA-degrading bacteria. *Polymer Degradation and Stability.* **95**(12), pp.2350-2359.

Volova, T.G., Gladyshev, M.I., Trusova, M.Y. and Zhila, N.O. 2007. Degradation of polyhydroxyalkanoates in eutrophic reservoir. *Polymer Degradation and Stability.* **92**(4), pp.580-586.

Wang, G.X., Huang, D., Ji, J.H., Völker, C. and Wurm, F.R. 2020. Seawater-Degradable Polymers—Fighting the Marine Plastic Pollution. *Advanced Science.* Wang, X., Shen, L.L. and An, Z.S. 2018. Dispersion polymerization in environmentally benign solvents via reversible deactivation radical polymerization. *Progress in Polymer Science.* **83**, pp.1-27.

Wang, Y.-W., Mo, W., Yao, H., Wu, Q., Chen, J. and Chen, G.-Q. 2004. Biodegradation studies of poly(3-hydroxybutyrate-co-3-hydroxyhexanoate). *Polymer Degradation and Stability.* **85**(2), pp.815-821.

Weng, Y.-X., Wang, X.-L. and Wang, Y.-Z. 2011. Biodegradation behavior of PHAs with different chemical structures under controlled composting conditions. *Polymer Testing.* **30**(4), pp.372-380.

Wolf-Ru¨ diger Mu¨ ller*, I.F.R.J.r. 2004. Standardized methods for anaerobic biodegradability testing. *Reviews in Environmental Science and Bio/Technology 3: 141–158, 2004.* **3**, pp.141-158.

Woolnough, C.A., Charlton, T., Yee, L.H., Sarris, M. and Foster, L.J.R. 2008. Surface changes in polyhydroxyalkanoate films during biodegradation and biofouling. *Polymer International.* **57**(9), pp.1042-1051.

Wu, C.-S. 2014. Preparation and Characterization of Polyhydroxyalkanoate Bioplastic-Based Green Renewable Composites from Rice Husk. *Journal of Polymers and the Environment.* **22**(3), pp.384-392.

Wu, C.S. 2011. Preparation, characterization, and biodegradability of renewable resource-based composites from recycled polylactide bioplastic and sisal fibers. *Journal of Applied Polymer Science.* **123**(1), pp.347-355.

Xiao, Z., Liu, W., Zhu, G., Zhou, R. and Niu, Y. 2014. A review of the preparation and application of flavour and essential oils microcapsules based on complex coacervation technology. *J Sci Food Agric.* **94**(8), pp.1482-1494.

Yang, H.-S., Yoon, J.-S. and Kim, M.-N. 2005. Dependence of biodegradability of plastics in compost on the shape of specimens. *Polymer Degradation and Stability.* **87**(1), pp.131-135.

Yang, L., Li, J., Jin, Y., Li, M. and Gu, Z. 2015. In vitro enzymatic degradation of the cross-linked poly(ε-caprolactone) implants. *Polymer Degradation and Stability.* **112**, pp.10-19.

Yang, X., Man, Y.B., Wong, M.H., Owen, R.B. and Chow, K.L. 2022. Environmental health impacts of microplastics exposure on structural organization levels in the human body. *Sci Total Environ.* **825**, p154025.
Ye, A., Cui, J., Zhu, X. and Singh, H. 2013. Effect of calcium on the kinetics of free fatty acid release during in vitro lipid digestion in model emulsions. *Food Chemistry.* **139**(1-4), pp.681-688.

Yu, J., Plackett, D. and Chen, L.X.L. 2005. Kinetics and mechanism of the monomeric products from abiotic hydrolysis of poly[(R)-3-hydroxybutyrate] under acidic and alkaline conditions. *Polymer Degradation and Stability.* **89**(2), pp.289-299.

Zhang, H., Wang, X., Wang, P., Liu, R., Hou, X., Cao, W., Zhong, R., Liu, X. and Zhang, Y. 2018. One-pot synthesis of biodegradable polydopamine-doped mesoporous silica nanocomposites (PMSNs) as pH-sensitive targeting drug nanocarriers for synergistic chemo-photothermal therapy. *RSC Advances.* **8**(65), pp.37433-37440.

Zhang, S., Wang, J., Liu, X., Qu, F., Wang, X., Wang, X., Li, Y. and Sun, Y. 2019. Microplastics in the environment: A review of analytical methods, distribution, and biological effects. *TrAC Trends in Analytical Chemistry.* **111**, pp.62-72.

Zhao, L., Su, C., Liu, W., Qin, R., Tang, L., Deng, X., Wu, S. and Chen, M. 2020. Exposure to polyamide 66 microplastic leads to effects performance and

microbial community structure of aerobic granular sludge. *Ecotoxicology and Environmental Safety.* **190**, article no: 110070 [no pagination].

Zhao, W.W. and Wang, Y.L. 2017. Coacervation with surfactants: From single-chain surfactants to gemini surfactants. *Advances in Colloid and Interface Science.* **239**, pp.199-212.

Zhong, F. and Pan, C.-Y. 2022. Dispersion Polymerization versus Emulsifier-Free Emulsion Polymerization for Nano-Object Fabrication: A Comprehensive Comparison. **43**(3), p2100566.

Zhu, J. and Wang, C. 2020. Recent advances in the analysis methodologies for microplastics in aquatic organisms: current knowledge and research challenges. *Anal Methods.* **12**(23), pp.2944-2957.

Zimmerman, D.W. and Zumbo, B.D. 1993. Relative Power of the Wilcoxon Test, the Friedman Test, and Repeated-Measures ANOVA on Ranks. *The Journal of Experimental Education.* **62**(1), pp.75-86.

Chapter 7

7.1 General discussion

Engineered model polymeric microparticles (PMPs) with a diameter of less than 5 mm are becoming a significant concern for both the environment and human health as they are increasingly found in our surroundings. Progress has been made in creating biodegradable polymers, such as polylactic acid (PLA), polybutylene succinate (PBS), and polycaprolactone (PCL), which are being utilised to produce PMPs. These polymers have demonstrated different rates and mechanisms of biodegradation in both simulated and real environments when used in film form. However, there have been few studies conducted on the degradation properties of polymers when converted into PMP. In this PhD, the overarching goal was to test these model particles for their degradation and extract the most influential parameters. In order to do this, polymer microparticles (PMPs) using a biodegradable polymers were engineered in a simple and efficient manner to mimic industry-produced particles. The solvent extraction method was selected for its simplicity and ability to produce particles of various sizes, similar to those used in industries such as personal care, foods, paints, and pharmaceuticals. Polycaprolactone (PCL), poly (D, L-lactide-co-glycolide) (PLGA), and poly [(R)-3-hydroxybutyric acid] (PHB) were chosen for biodegradation studies due to their widespread recognition as biodegradable polymers. An *in vitro* method was developed to accurately analyse the degradation of these model microparticles using an enzyme to identify key factors influencing degradation such as surface area/size and polymer type at varying stages of degradation.

As discussed in the literature review in **Chapter 2,** manufactured polymeric microparticles (PMPs) are an integral part of our life and will continue to serve a wide range of important functions in areas such as pharmaceuticals, cosmetics and personal/home care products where they provide significant improvement to our quality of life. To reduce their negative impact on the environment, a complete

shift to sustainable and biodegradable alternatives is imperative. However, it is challenging to maintain the current performance of the non-biodegradable PMPs in these products whilst improving the overall biodegradability. The review pointed out the shortcomings of PMP degradation studies conducted in simulated real-world systems that create gaps in the process, ultimately compromising the lifecycle and environmental impact of PMPs. For example, certain samples were evaluated for their ability to break down in simulated environments, while others were tested in seawater under different pH and temperature conditions. This made it challenging to compare the biodegradation rates of the various polymer-based structures and testing methods. In industry, standard test methods are utilised to determine the acceptability of formulations based on the results obtained. These regulations rely on the outcomes of these standards to assess the suitability of the formulations. The challenge of using standardised testing methods is significant, as they frequently yield varying results for identical samples based on the specific procedures used in conducting degradation tests resulting in false claims. The review further explored areas such as the mechanisms of biodegradation, factors that affect the biodegradation of PMPs and the scientific basis of current biodegradation test methods. Overall, it was found that biodegradation consists of multiple steps occurring in series, each with their exclusive kinetics. The kinetics of each biodegradation step is dependent on factors such as, available surface area, chemical composition (such as chemical cross-linking), microbial activity and environmental conditions (temperature, pH, salinity). It is well published that the biodegradability of polymers is influenced by their chemical and physical properties, such as molecular weight, crystallinity, melting temperature, particle size, as well as environmental factors like pH, enzymatic activity, temperature, and ionic strength. The inconsistencies and variations in biodegradation characterisation in the literature highlight the challenges in understanding industry standards. Environmental conditions and polymer particle characteristics show the limitations of relying solely on standard test methods for quantifying biodegradation. It is crucial to conduct basic tests to compare the degradation of different samples before trusting standards, taking into account the environments where engineered microparticles break down. These methods are not well-controlled, particularly in difficult environments like seawater or soil. Existing literature mainly focuses on polymer films rather than particles, emphasizing the need to study model systems and improve our

understanding of the degradation process. Currently, there is a lack of research on the degradation of PMPs, with limited *in vitro* studies using enzymes to investigate their biodegradation. By carefully examining the characteristics of PMPs before and during biodegradation, we can gain a better understanding of the chemical and physical changes that occur.

In **Chapter 3**, we successfully created model PMPs using three different biodegradable polymers (PCL, PLGA, and PHB) through the solvent extraction process with constant preparation conditions. The results showed that solvent extraction was a reliable and versatile method to produce PMPs of various polymers. While it was not crucial to use identical conditions for preparing the microparticles, the real challenge lay in ensuring that the structure and size of the particles remained consistent across various polymers. As anticipated, the solubility of the polymer in the emulsion core solvent had a significant impact on the final outcome when different polymers were used. The PMPs exhibited a range of polydipersity, with smaller particles measuring < 1 µm and larger particles >100 µm. Optical micrographs revealed that the PMPs were well dispersed in suspension, with no aggregation observed under optical light microscopy and scanning electron microscopy. By adjusting the stirring speed of the UltraTurrax for the preparation of the initial emulsion template, the particle size/total surface area was controlled. Next, extensive biodegradation studies were carried out in the following chapter on PCL PMPs to examine the impact of enzyme concentration on the biodegradation. Two instrumental methods were developed for this investigation.

In **Chapter 4**, the study aimed to develop *in vitro* biodegradation test methods for studying the degradation of PCL PMPs using an enzyme at varying concentrations. PCL was chosen due to existing data on the degradation of polymer films. The degradation of PCL PMPs was carried out by firstly, monitoring the increased amount of acid through the degradation process using a pH stat (related to stage 2 of the biodegradation process). It was found that a PCL PMPs to lipase mass ratio of 0.040 led to the highest degradation kinetics in the range of ratios explored, resulting in a biodegradation rate of 22% of acid release per hour. Secondly, we studied the carbon dioxide production using pressure measurements to understand the secondary products of the biodegradation process, representing the final stage 3 of biodegradation i.e. the conversion of

PCL into CO_2, water and biomass. Surprisingly, the maximum degradation rate, as indicated by the production of CO_2 was also achieved with a ratio of 0.040 PCL PMPs to lipase, leading to a CO_2 production rate of 2.73% per day. This ratio was then used to assess the degradation (acid release and CO_2 production) of PCL PMPs with varying surface area and particle size leading onto **Chapter 5**.

In **Chapter 5**, the influence of surface area on the rate of degradation of PCL PMPs was studied using the optimal substrate: enzyme ratio (0.040 ratio) identified in **Chapter 4**. It was found that biodegradation occurring on the surface of PMPs progresses rapidly (stage 2 of the biodegradation process), but the surface area has no impact on the overall CO_2 production (stage 3 of the biodegradation process) at this stage. This is because the surface area influences the two degradation steps separately. The rate of the degradation process may initially be limited by the surface area, but once the polymer chains have been broken down into smaller dissolvable molecules (acids) into solution, the rate of CO_2 production exerts its own influence in the final stages.

In **Chapter 6**, degradation experiments were carried out for PLGA and PHB PMPs using identical methods as in the previous chapter to examine how different polymers impact the degradation of microparticles. Differences in degradation rates of three PMPs were observed when monitoring the increase in acid release at the beginning of the degradation process. Interestingly, despite variations in particle size which in turn affects the total surface area and polymer chemistry, PLGA and PHB PMPs show comparable rates of biodegradation at the surface degradation stage measuring the increase amount of acid release. In terms of the rate of degradation during the final stage (CO_2 production), the results indicate that there may be additional reactions occurring during the final stages of degradation making it difficult to interpret the findings. It was discovered that utilising the same lipase in the degradation experiments is not ideal for its capacity to effectively target a range of polyester polymers. The differences and inconsistencies arise from the unique polymer backbone of each polymer, causing cleavage of each monomer unit to occur at different rates.

The purpose of the research was to assist the chemical industry in understanding the degradation process of polyester polymers and to develop a cost-effective and efficient screening test to determine if engineered microparticles are biodegradable and what factors affect biodegradation. The chemical industry is facing pressure to switch from non-biodegradable polymers to more environmentally friendly alternatives due to increasing demands and regulations from customers and consumers. This has led to job cuts and cost-saving measures within the chemical industries. Many industries lack expertise in biodegradation testing and therefore have to send their products externally for testing, resulting in time and money being spent. The results of these tests can vary depending on the testing environment, leading to inconsistencies in results. For example batch to batch variations in the testing media like soil, sludge or types of water. Having an internal screening test for biodegradation would be beneficial for industry. The research findings reported in this thesis suggest that measuring acid release and CO_2 production during biodegradation at different stages of the process, can provide quantifiable values to determine the percent degradation of polyester polymers. Comparisons can be made to identify factors affecting biodegradation, such as polymer type and particle size. Furthermore, the findings indicate that optimising the conditions for biodegradation testing, including temperature, pH, and microbial activity, can enhance the accuracy and reproducibility of biodegradation results.

Future direction

The work presented in this thesis has demonstrated that the properties of (PMPs) made from biodegradable polymers can be controlled by the characteristics of the solvent extraction method used for their production, in particular, the total surface area of the final particles can be manipulated by changing the mixing speed during the emulsion preparation stage. Furthermore, the PMPs can be degraded using an enzyme at optimal concentration to determine the rate of biodegradation. The main recommendations on further research that could be undertaken are summarised as follows:

- Maintaining consistent microparticle sizes with different polymer type in future experiments will lead to more definitive findings. For example, to produce monodisperse emulsion templates, using membrane emulsification would be an obvious next step (Charcosset et al., 2004; M. T Stillwell et al., 2007; Kosvintsev et al., 2008).

- There is a need for further in *vitro* studies using an enzyme on PMPs degradation using other polymers. Exploring different enzymes suited for specific polymers need to be determined for optimum degradation. For this, literature suggests that esterase and cutinase could be potential enzymes to investigate for PBS and PLGA (Kumar, G.A. et al., 2020; Miksch et al., 2021).

- It would be interesting to conduct a design of experiment to study the influence on the biodegradation rate by monitoring the increase in acid release at the beginning of the degradation process at varying particle size focusing on a single polymer, as performed with PCL PMPs, which could provide more conclusive results.

- The conclusions drawn from Chapter 5 & 6 study is based on a limited number of repeatable data points, specifically three. This

limitation is a result of time constraints during the PhD experiments, so the results may not be definitive. Thus, more than three measurements is required to ensure statistical validity and reproducibility as part of a given biodegradability standard.

Future studies should investigate additional aspects such as the characteristics of lipase enzymes, their stability, and inhibition kinetics. Research is also needed on bacterial metabolism of breakdown products that produce carbon dioxide, as well as the extension of the study to other types of polyesters. Exploring the environmental conditions present in marine and river sources of microplastics is also important for further research in this area.

Appendix A

Supporting information of Chapter 4

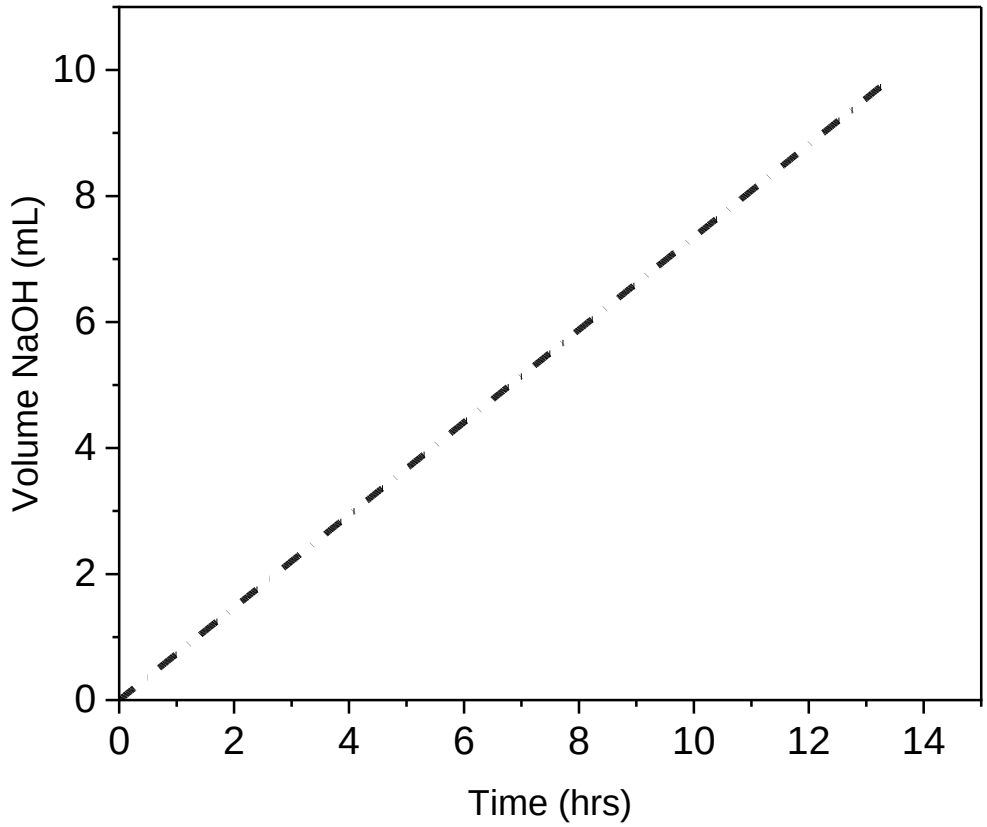


Figure A:0:1 – Enzyme activity standard curve showing the volume of NaOH added as function of using 50µL @ 1 mg/mL lipase enzyme solution. The hydrolysis reaction takes place between the enzyme and the surface ester-bonds of tributyrin. The free fatty acids released by the lipase are titrated at a constant pH by sodium hydroxide (NaOH, 0.1N) during the course of the hydrolysis.

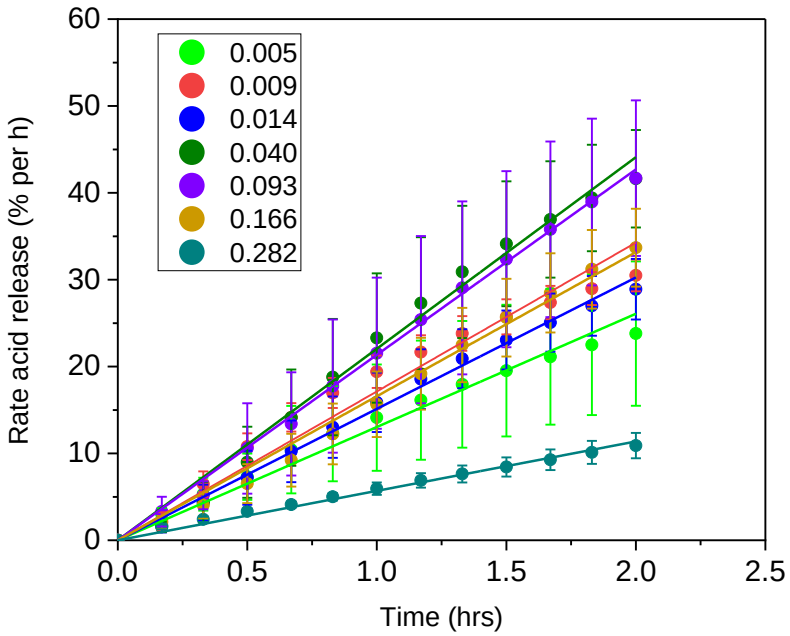


Figure A:0:2 - the initial rate of degradation – acid release as a function of time over 2 h can be determined by the gradient (rate constant *k*) for each of the lipase concentrations. The percent degradation is related to the free fatty acid released from the ester functional groups of polycaprolactone (6-hydroxylcaproic acid) as they are hydrolysed in the course of a lipase assay. Data presented are mean with standard deviation of three independent experiments All experiment with PCL PMPs 45 kDa molecular weight (10 mg particles) – Ratio of PCL: Lipase (mg per unit) (green – 0.005), (red – 0.009), (blue – 0.014), (olive – 0.040), (purple – 0.09), (yellow – 0.166), (dark cyan – 0.282).

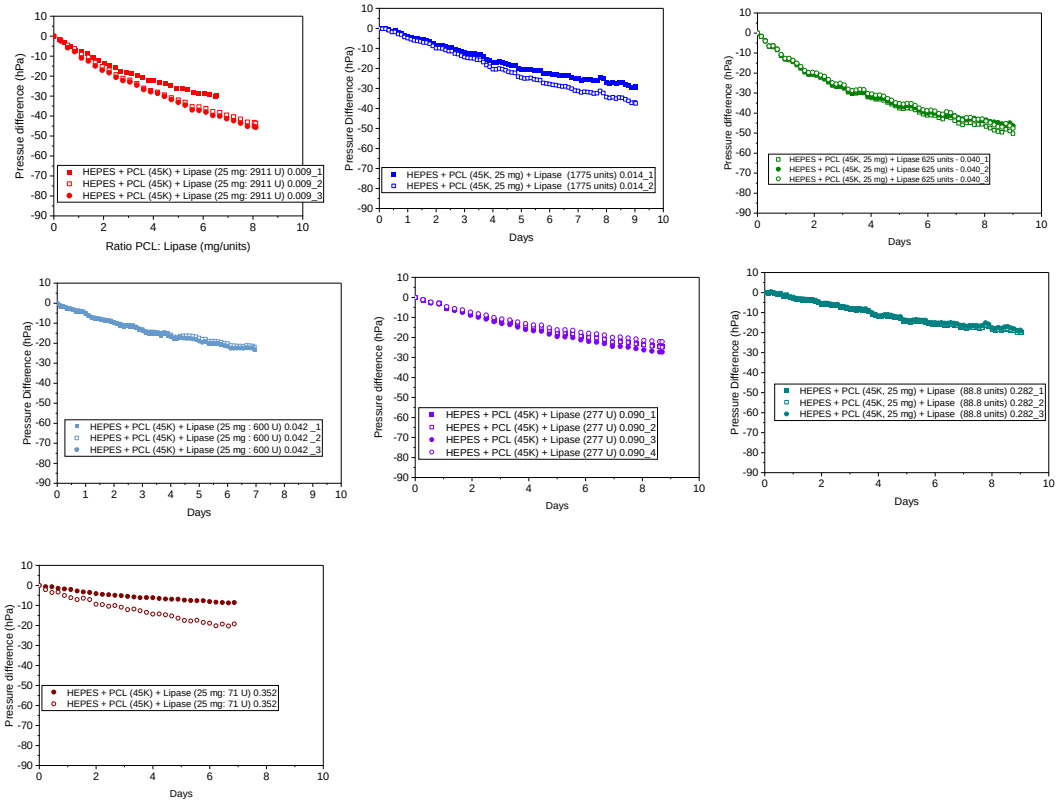


Figure A:0:3 – Normalised pressure difference as a function of time of PCL particles at varying ratio of PCL: Lipase (mg per unit). The carbon dioxide produced during degradation of PMPs is absorbed by the NaOH and is neutralised i.e. removes the carbon dioxide from the atmosphere and the pressure drops (as carbon dioxide forms, the pressure will decrease because the oxygen is being removed) resulting in less pressure (negative pressure). All experiment with polycaprolactone - 45 kDa molecular weight (25 mg particles) at pH 7.4, 37°C in HEPES buffer – Ratio of PCL: Lipase (mg per unit) - (red – 0.009), (blue – 0.014), (olive – 0.040), (teal – 0.042), (purple – 0.090), (cyan – 0.28), (wine – 0.352)

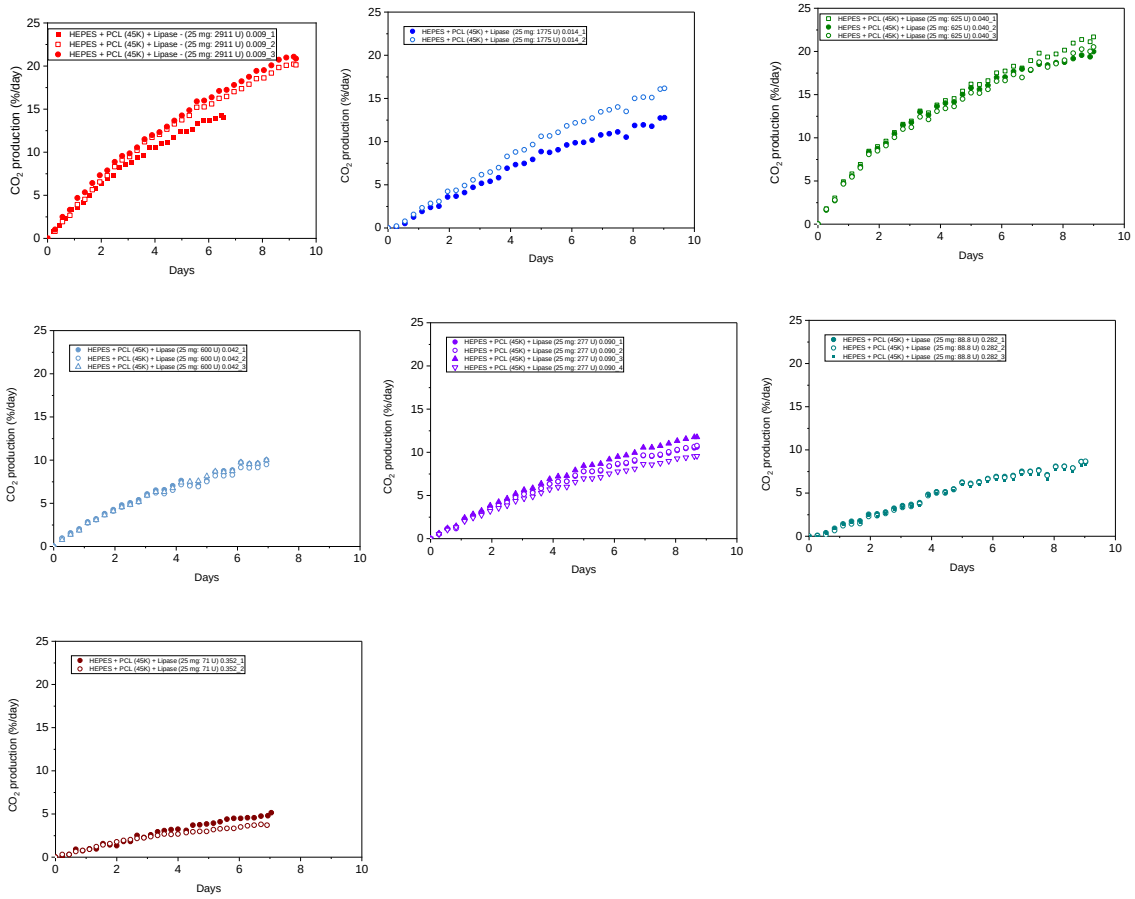


Figure A:0:4 – CO_2 production as a function of time of PCL particles at varying ratio of PCL: Lipase (mg per unit) in triplicates. All experiment with polycaprolactone - 45 kDa molecular weight (25 mg particles) at pH 7.4, 37°C in HEPES buffer – Ratio of PCL: Lipase (mg per unit) - (red – 0.009), (blue – 0.014), (olive – 0.040), (teal – 0.042), (purple – 0.090), (dark cyan – 0.28), (wine – 0.352)

Appendix B

Supporting information of Chapter 5

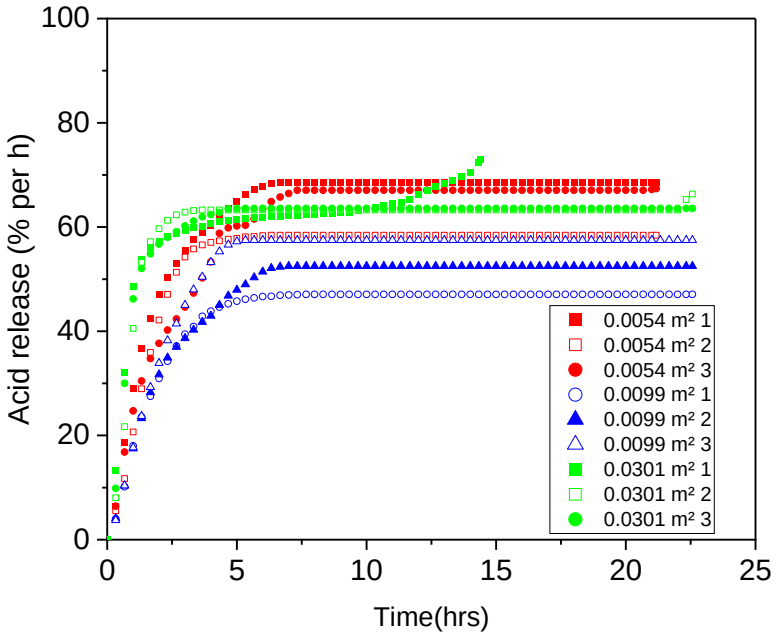


Figure B 1 Titration curve showing the % degradation of PCL PMPs with varying surface area at pH 7.4, 37°C at varying lipase dosages with a pH stat device. The percent degradation is related to the free fatty acid released from the ester functional groups of polycaprolactone (6-hydroxylcaproic acid) as they are hydrolysed in the course of a lipase assay. Data presented are of three independent experiments. All experiment with PCL PMPs 45 kDa molecular weight (10 mg particles) – Ratio of PCL: Lipase (mg per unit) at 0.040 (red – SA 0.0054 m^2), (blue – SA 0.099 m^2), (green – 0.0301 m^2)

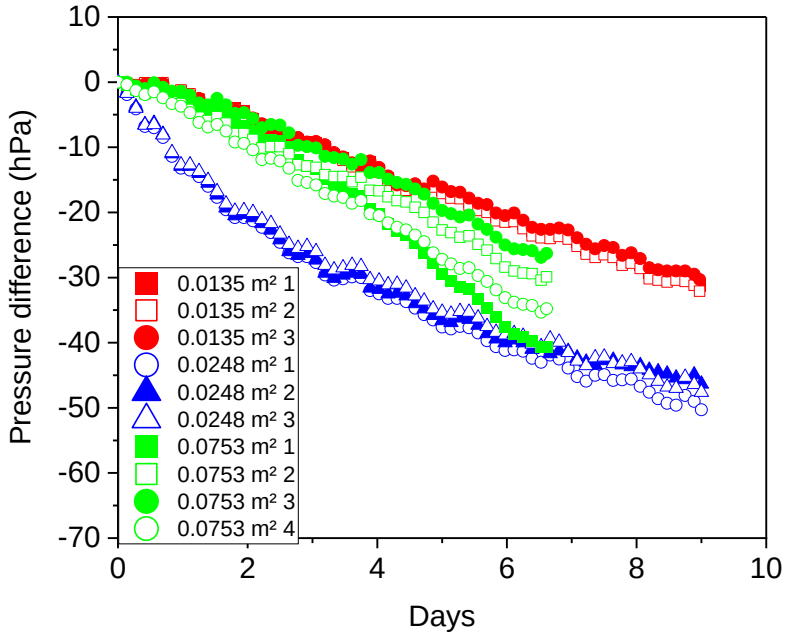


Figure B 2 Pressure difference as a function of time of enzymatic reaction during PCL PMPs degradation at varying surface at pH 7.4 and 37 °C in HEPES buffer. All experiment with PCL PMPs 45 kDa molecular weight (25 mg particles) – Ratio of PCL: Lipase (mg per unit) at 0.040 (red – SA 0.0135 m^2), (blue – SA 0.0248 m^2), (green – 0.0753 m^2)

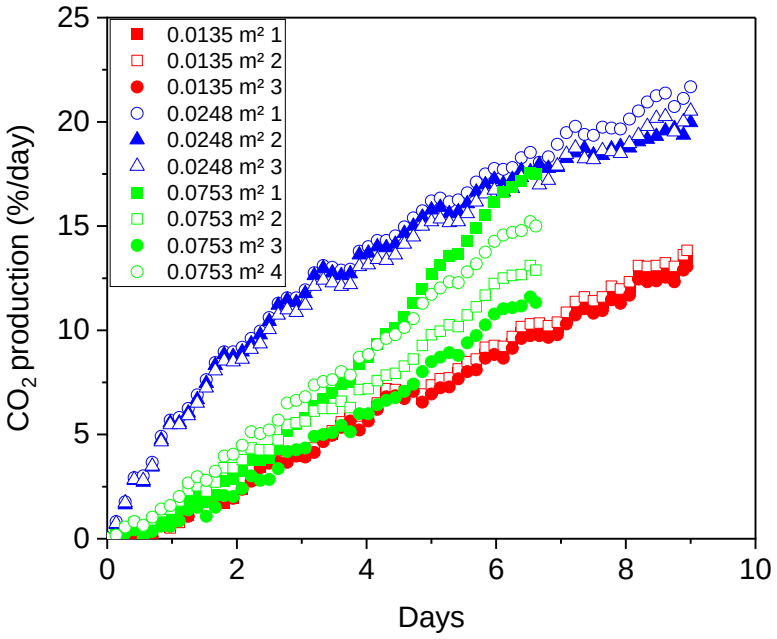


Figure B 3 CO_2 production as a function of time of enzymatic reaction during PCL PMPs degradation at varying surface area at pH 7.4 and 37 °C in HEPES buffer. The CO_2 production was calculated as described previously $\Delta \boldsymbol{p}\,(\boldsymbol{O_2}) \times \left[\frac{\boldsymbol{Vtot-V1}}{\boldsymbol{V1}}\right] = \boldsymbol{nRT}$ (Ahn et al., 2011; Gómez and Michel, 2013; Chinaglia et al., 2018). Three independent readings for each sample (n = 3). All experiment with PCL PMPs 45 kDa molecular weight (25 mg particles) – Ratio of PCL: Lipase (mg per unit) at 0.040 (red – SA 0.0135 m^2), (blue – SA 0.0248 m^2), (green – 0.0753 m^2)

Appendix C

Supporting information of Chapter 6

Table C 1- calculated surface area of PCL, PLGA and PHB PMPs based on the size distribution

Polymer	SA (m^2/g)	Total surface area (m^2)*	D_{10} (µm)	D_{50} (µm)	D_{90} (µm)	D_{32} (µm)	Span
PCL	0.54	0.27	12.4	26.8	75.8	12.9	2.40
PCL	0.99	0.50	5.0	13.4	84.0	8.1	2.36
PLGA	0.45	0.23	7.39	28.4	72.4	12.5	2.22
PHB	0.95	0.48	3.44	36.4	222	6.42	7.38

SA= surface area, polycaprolactone (PCL), poly (D, L-lactide-co-glycolide) (PLGA), poly(3-hydroxybutyrate) (PHB) *Total surface area = SA x mass (0.5 g)

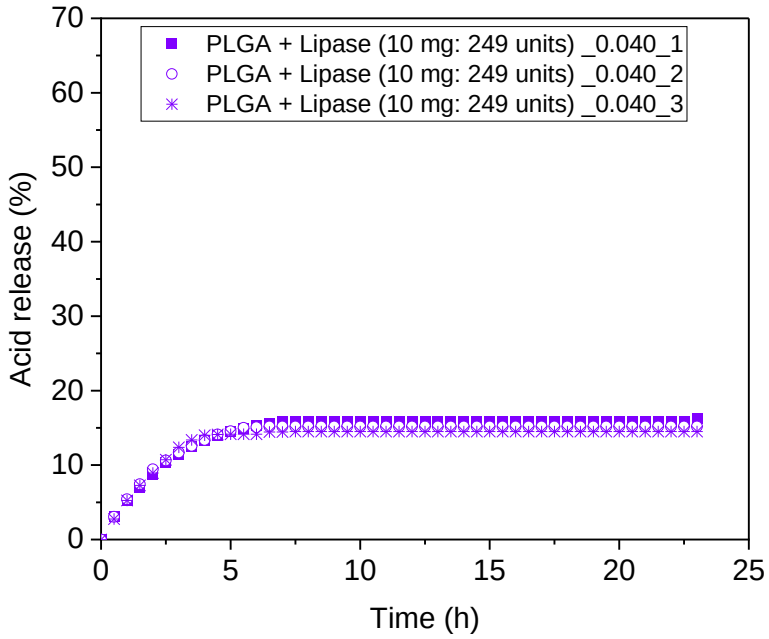


Figure C 1 Titration curve showing the % degradation i.e. acid release of PLGA PMPs at pH 7.4, 37°C at PLGA:lipase ratio 0.040 with a pH stat device. The percent degradation is related to the free fatty acid released from the ester functional groups of PLGA (lactic acid) as they are hydrolysed in the course of a lipase assay. Data presented are of three independent experiments. All experiment with PLGA PMPs 66-107 kDa molecular weight (10 mg particles)

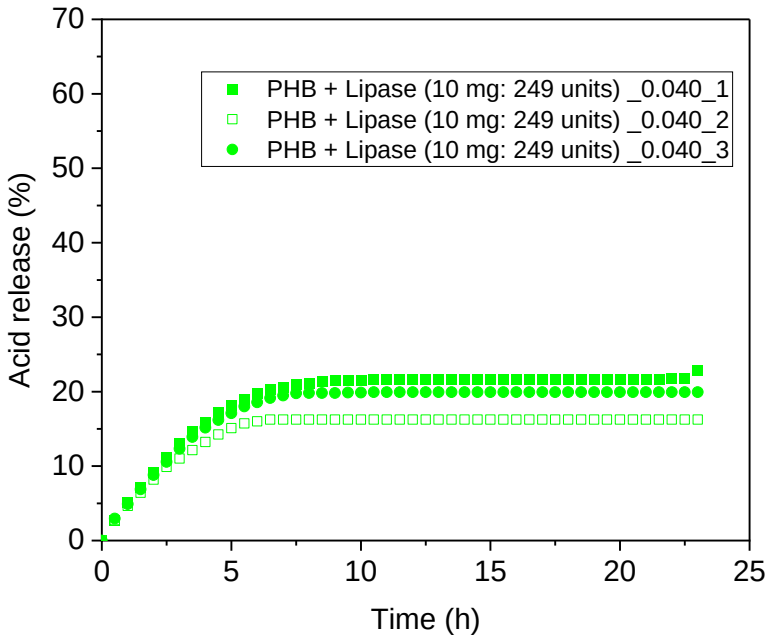


Figure C 2 Titration curve showing the % degradation i.e. acid release of PHB PMPs at pH 7.4, 37°C at PHB PMPs:lipase ratio 0.040 with a pH stat device. The percent degradation is related to the free fatty acid released from the ester functional groups of PHB (3-hyroxybutaric acid) as they are hydrolysed in the course of a lipase assay. Data presented are of three independent experiments. All experiment with PHB PMPs (10 mg particles)

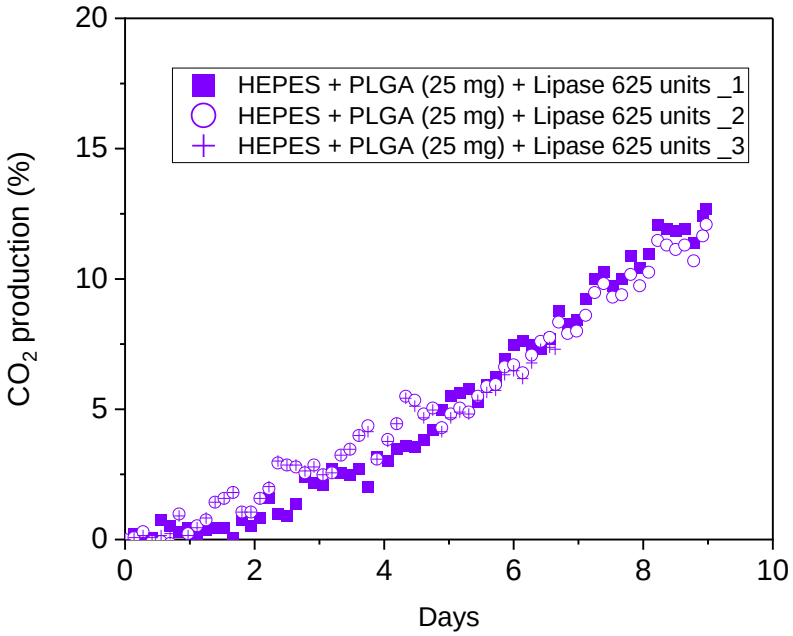


Figure C 3 CO_2 production as a function of time of enzymatic reaction during PLGA PMPs degradation at pH 7.4 and 37 °C in HEPES buffer. Three independent readings for triplicate samples (n = 3). The percent degradation is related to the conversion of organic carbon to CO_2 biomass (5 CO_2 for PLGA). Respirometer methods are normally used to record the quantitative formation of CO_2. Data presented are of three independent experiments. All experiment with PLGA PMPs (25 mg particles).

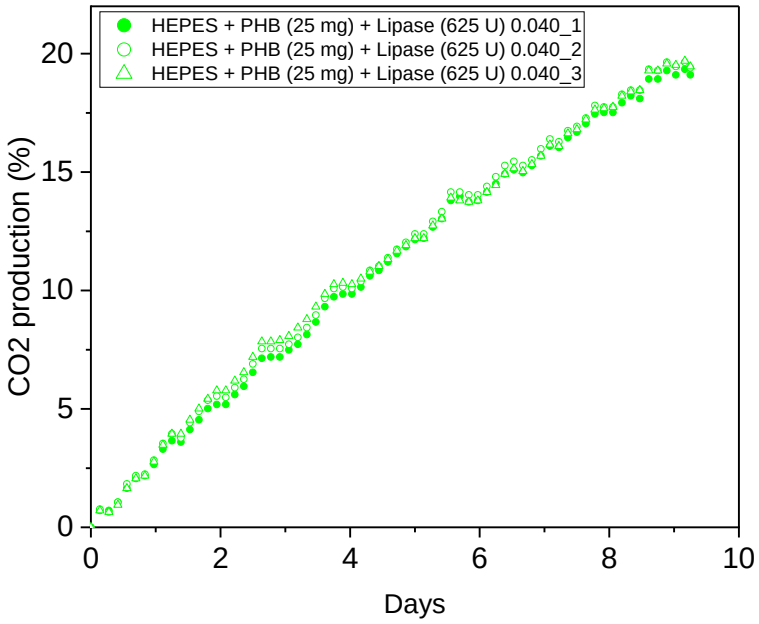


Figure C 4 CO_2 production as a function of time of enzymatic reaction during PHB PMPs degradation at pH 7.4 and 37 °C in HEPES buffer. Three independent readings for triplicate samples (n = 3). The percent degradation is related to the conversion of organic carbon to CO_2 (4 CO_2 for PHB). Respirometer methods are normally used to record the quantitative formation of CO_2. Data presented are of three independent experiments. All experiment with PHB PMPs (25 mg particles).